CRANFIELD UNIVERSITY

Mohammed Alsaadi

Unified Active and Reactive Power Dynamic Economic and Emission Dispatch of Microgrids

School of Water, Energy and Environment
Energy Division

PhD Thesis
Academic Year: 2013 - 2017

Supervisor: Prof. Patrick Chi-Kwong Luk
Dr. John Economou

September 2017

CRANFIELD UNIVERSITY

School of Water, Energy and Environment
Energy Division

PhD Thesis

Academic Year 2013-2017

Mohammed Alsaadi

Unified Active and Reactive Power Dynamic Economic and Emission Dispatch of Microgrids

Supervisor: Prof. Patrick Chi-Kwong Luk
Dr. John Economou

September 2017

ABSTRACT

The exchange of power among the microgrid (MG), electric vehicles (EVs), energy storages (batteries), and the utility grid is a great challenge in the formulation of the optimal scheduling of the MGs. Furthermore, considering the unit commitment (UC) with the uncertainties that derive from the fluctuations of the renewable generation, open market pricing (OMPs), demand side, and the EVs, result in a significantly complex optimisation problem. Optimised operation of the MGs can result in enormous economic benefits to both the users and the environment. Therefore, there are considerable interests to develop algorithms and approaches to formulate and solve the optimisation problems of the MGs efficiently.

In this research, a novel multi-period security-constrained unit commitment unified active and reactive dynamic economic and emission dispatch (SCUC-UARDEED) of the connected and isolated MG is presented. The formulation of the UC is developed and extended to accommodate both the active and reactive power of the distributed generators (DGs). The emission costs of the greenhouse gases in keeping with the emission level constraints are considered in the proposed optimisation problem to reduce the emission of the pollutant gases and achieve a low emission energy system. The overall formulation of the proposed SCUC-UARDEED of the MG takes into consideration the models of the reactive power production cost of the DGs, fuel cost, environmental costs, battery degradation cost, start-up and shutdown costs of the DGs, maintenance cost of the DGs, and the cost of the renewable power generation. The proposed optimisation of the MG is subjected to a comprehensive set of constraints, including active and reactive power security of supply for the connected and isolated MG and emission limit constraints. The impacts of the battery on the scheduling problem of the MG are determined by comparing scenarios with and without battery. Similarly, the impacts of the security of supply constraints are analysed. Uncertainties resulting from the fluctuations of the renewable generation and OMPs are modelled and incorporated into the scheduling

problem of the MG as a two-stage stochastic optimisation with taking into account the aforementioned models of the cost functions and constraints.

Integration of the active and reactive demand side management (DSM) with the SCUC-UARDEED of the connected and isolated MG is addressed. The DSM is considered as a separate appliance with an operation cycle, and it is considered as a decision variable within optimisation problems. Different types of the DSM techniques are applied to the various types of loads simultaneously under deterministic and stochastic environments. Accordingly, novel approaches and techniques are proposed in the thesis to allow the analysis and detailed investigation of the impacts of the DSM on the optimal scheduling of the MGs, the UC results, the exchanging active and reactive power with the utility grid, the system loads, the spinning reserve, and the secure supply of the MG. The uncertainties arising from both the generation and demand side are systematically modelled and incorporated into the optimisation problem in a two-stage stochastic approach with consideration given to the above cost functions and constraints, where the DSM is considered as a source of uncertainty.

A novel scheduling strategy is proposed to integrate the EVs with the SCUC-UARDEED of the connected and isolated MG. The EVs charging and discharging operations are considered as decision variables in the optimisation approaches. The EVs are incorporated with the grid as bidirectional, grid to vehicle (G2V) as energy storage and vehicle to grid (V2G) as energy source. This integration of the EVs with the scheduling problem of the MG that includes all aforementioned cost functions and constraints increases the complexity of the optimisation problem. Accordingly, the economic models involved in the integration of the EVs with MG are developed, and a variety of charging and discharging scenarios are conducted to analyse the impacts of the EVs on the optimal scheduling of the MGs. The uncertainties resulting from the availability of the EVs and fluctuation of the generation of the renewable energy resources are modelled and incorporated with SCUC-UARDEED into a two-stage stochastic optimisation approach.

ACKNOWLEDGEMENTS

Firstly, I would like to thank Iraqi people, particularly the Iraqi ministry of higher education and scientific research/University of Technology to provide me the opportunity to study the PhD at Cranfield University.

I would like to thank my supervisor Prof Patrick C. K. Luk for his invaluable supervision and guidance during the entire period of my PhD. He supports and guides me in a professional way throughout this work. He encourages and motivates me from the beginning of my PhD without these motivations I could not finish my PhD. I would like to thank my co-supervisor Dr John Economou for his supporting and helping.

Special thanks go to my colleagues and friends who studies and shares with me the same concerns of study. They always encourage and help me during the PhD.

Finally, my deepest gratitude goes to my family who supports and encourages me in different life aspects throughout my PhD.

TABLE OF CONTENTS

LIST OF FIGURES

LIST OF FIGURES IN APPENDICES

LIST OF TABLES

LIST OF TABLES IN APPENDICES

LIST OF MATHMATICAL SYMBOLS

Notation	Description	Unit
C	Consumption power per km	[kW]
C_b	Battery capital cost	[€]
C_d	Battery degradation cost	[€/kWh]
C_e	Emission cost	[€]
C_j	Price of emission of j^{th} Greenhouse gas	[€/kg]
C_t	Consumption power at time t read from the diversified consumption	[kW]
$C_{bo}(t)$	Battery operating cost	[€/h]
C_{EV}	EV battery capital cost	[€]
C_{EVd}	EV battery degradation cost	[€/kWh]
$C_{gP}(t)$	Cos of exchanging active power with the utility grid	[€/h]
$C_{QP}(t)$	Cos of exchanging reactive power with the utility grid	[€/h]
$C_{EV}^{Com}(t)$	Operating cost of the EVs that are connected to the commercial area	[€/h]
$C_{EV}^{Ind}(t)$	Operating cost of the EVs that are connected to the industrial area	[€/h]
$C_{EV}^{Res}(t)$	Operating cost of the EVs that are connected to the residential area	[€/h]
CP_{DG_i}	Fuel cost of the i^{th} DG	[€/h]
CQ_{DG_i}	Reactive power production cost of the i^{th} DG	[€/h]
$CP_{PV_{i2}}$	PV generation power cost of the $i2^{th}$ PV unit	[€/h]
$CP_{W_{i1}}$	WTs generation power cost of the $i1^{th}$ WT	[€/h]
COM_{DG_i}	Operating and maintenance cost of the i^{th} DG	[€/h]
$D(t)$	Driving distance	[km]
D_t	Number of devices that start their consumption at time t	[N]
DR_i	DGs ramping-up	[kW]
E_b	Rated energy capacity of the fixed battery	[kWh]
$E_b(t-1)$	State of charge of battery at previous time	[kWh]
$E_b(t)$	State of charge of battery at current time	[kWh]
E_{bmax}	Maximum state of charge of battery	[kWh]
E_{bmin}	Minimum state of charge of battery	[kWh]
$E_{EV}(t)$	State of charge of battery of the EV at current time	[kWh]
$E_{EV}(t-1)$	State of charge of battery of the EV at previous time	[kWh]
$E_{EV}(t_{last})$	State of charge of battery of the EV at last time before starting the first trip	[kWh]
E_{EVmax}	Maximum state of charge of battery of the EV	[kWh]
E_{EVmin}	Minimum state of charge of battery of the EV	[kWh]
$E_{EV}^{Trip}(t)$	Energy consumption during the trip at period t	[kWh]
$E_{j,i}$	Emission rate of the j^{th} greenhouse gas from i^{th} DG	[kg/kWh]
KOM_{DG_i}	Coefficient of the maintenance cost of the i^{th} DG	[€/kWh]
L_b	Real battery life	[kWh]

L_c	Battery cycle life	[N]
L_j	Allowable emission level of the greenhouse gas j in the MG	[kg/h]
N	Total number of DGs	[N]
$N1$	Total number of WTs units	[N]
$N2$	Total number of PV units	[N]
$N_{EV}^{Com}(t)$	Number of the EVs are connected to commercial area at each time interval	[N]
$N_{EV}^{Ind}(t)$	Number of the EVs are connected to industrial area at each time interval	[N]
$N_{EV}^{Res}(t)$	Number of the EVs are connected to residential area at each time interval	[N]
M	Total number of greenhouse gases	[N]
P	Active power	[kW]
P_b	Charging or discharging power of the battery	[kWh]
P_{bch}	Charging power of fixed battery	[kWh]
P_{bdis}	Discharging power of fixed battery	[kWh]
$P_{bchmax}(t)$	Maximum fixed battery charging power	[kW]
$P_{bchmin}(t)$	Minimum fixed battery charging power	[kW]
$P_{bdismax}(t)$	Maximum battery discharging power	[kW]
$P_{bdismin}(t)$	Minimum battery discharging power	[kW]
$P_{Dcom}(t)$	Commercial active power load	[kW]
$P_{Dcomshd}(t)$	Commercial active power load shedding	[kW]
$P_{Dcomcut}^{S}(t)$	Commercial active power load cutting at scenario s	[kW]
$P_{DG_i}(t)$	Output active power of i^{th} DG	[kWh]
$P_{DG_imax}(t)$	Maximum output active power of the i^{th} DG	[kW]
$P_{DG_imin}(t)$	Minimum output active power of the i^{th} DG	[kW]
$P_{DG_icut}^{S}(t)$	Generation active power cutting at scenario s	[kW]
$P_{Dind}(t)$	Industrial active power load	[kW]
$P_{Dindshd}(t)$	Industrial active power load shedding	[kW]
$P_{Dindcut}^{S}(t)$	Industrial active power load cutting at scenario s	[kW]
$P_{Dres}(t)$	Residential active power load	[kW]
$P_{Drescut}^{S}(t)$	Residential active power load cutting at scenario s	[kW]
$P_{Dres}^{DSM}(t)$	Residential load after applying DSM	[kW]
$P_{Dres}^{reco}(t)$	Residential recovered load	[kW]
$P_{Dres}^{shft}(t)$	Residential shifted load	[kW]
P_{EVch}	Charging power of the EV	[kWh]
$P_{EVcut}^{Com}(t)$	Unserved power to the EVs in the commercial area	[kW]
$P_{EVcut}^{Ind}(t)$	Unserved power to the EVs in the industrial area	[kW]
$P_{EVcut}^{Res}(t)$	Unserved power to the EVs in the residential area	[kW]
P_{EVdis}	Discharging power of EV battery	[kWh]
$P_{EVchmax}(t)$	Maximum charging power of battery of the EV	[kW]
$P_{EVchmin}(t)$	Minimum charging power of battery of the EV	[kW]
$P_{EVdismax}(t)$	Maximum discharging power of battery of the EV	[kW]
$P_{EVdismin}(t)$	Minimum charging power of battery of the EV	[kW]

P_{EVch}^{Com}	Charging power of the EVs in the commercial area	[kWh]
P_{EVch}^{Ind}	Charging power of the EVs in the industrial area	[kWh]
P_{EVch}^{Res}	Charging power of the EVs in the residential area	[kWh]
P_{EVdis}^{Com}	Discharging power of the EVs in the commercial area	[kWh]
P_{EVdis}^{Ind}	Discharging power of the EVs in the industrial area	[kWh]
P_{EVdis}^{Res}	Discharging power of the EVs in the residential area	[kWh]
$P_g(t)$	Exchanging active power with the utility grid	[kWh]
$P_{gpmax}(t)$	Maximum purchasing active power from the utility grid	[kW]
$P_{gpmin}(t)$	Minimum purchasing active power from the utility grid	[kW]
$P_{gsmax}(t)$	Maximum selling active power to the utility grid	[kW]
$P_{gsmin}(t)$	Minimum selling active power to the utility grid	[kW]
$P_{PV_{i2}}(t)$	Active power generation of $i2^{th}$ PV	[kW]
$P_{PV_{i2}cut}^{S}(t)$	PV active power cutting at scenario s	[kWh]
$\mathrm{P_{W-r}}$	Rated power of WT	[kW]
$P_{W_{i1}}(t)$	Active power generation of $i1^{th}$ WT	[kW]
$P_{W_{i1}cut}^{S}(t)$	WTs active power cutting at scenario s	[kW]
P_{1k}	Power consumption at time steps 1 of smart devices	[kW]
$P_{(1+l)k}$	Power consumption at time steps $(1+l)$ of smart devices	[kW]
$Q(t)$	Reactive power	[kVAr]
$Q_{Dcom}(t)$	Commercial reactive power load	[kVAr]
$Q_{Dcomshd}(t)$	Commercial reactive power load shedding	[kVArh]
$Q_{Dcomcut}^{S}(t)$	Commercial reactive power load cutting at scenario s	[kVArh]
$Q_{DG_i}(t)$	Output reactive power of i^{th} DG	[kVArh]
$Q_{DG_imax}(t)$	Maximum output reactive power of the i^{th} DG	[kVAr]
$Q_{DG_imin}(t)$	Minimum output reactive power of the i^{th} DG	[kVAr]
$Q_{Dind}(t)$	Industrial reactive power load	[kVAr]
$Q_{Dindshd}(t)$	Industrial reactive power load shedding	[kVAr]
$Q_{Dindcut}^{S}(t)$	Industrial reactive power load cutting at scenario s	[kVAr]
$Q_{Dres}(t)$	Residential reactive power load	[kVAr]
$Q_{Drescut}^{S}(t)$	Residential reactive power load cutting at scenario s	[kVAr]
$Q_{Dres}^{DSM}(t)$	Residential load after applying DSM	[kVAr]
$Q_{Dres}^{reco}(t)$	Residential recovered load	[kVAr]
$Q_{Dres}^{shft}(t)$	Residential shifted load	[kVAr]
$Q_g(t)$	Exchanging active power with the utility grid	[kVArh]
$Q_{gpmax}(t)$	Maximum purchasing reactive power from the utility grid	[kVAr]
$Q_{gpmin}(t)$	Minimum purchasing reactive power from the utility grid	[kVAr]
$Q_{gsmax}(t)$	Maximum selling reactive power to the utility grid	[kVAr]
$Q_{gsmin}(t)$	Minimum selling reactive power to the utility grid	[kVAr]
$R_p(t)$	Spinning reserve of the active power	[kW]
$R_q(t)$	Spinning reserve of the reactive power	[kW]

S	Maximum number of joint scenarios	[N]
Sc_i	Price of start-up cost	[€]
Sd_i	Price of shutdown cost	[€]
S_{sys}	Rated appearance power of the grid	[kVA]
$SD_{DG_i}(t)$	Shutdown cost	[€/h]
$SU_{DG_i}(t)$	Star-up cost	[€/h]
T^{down}	Minimum down time	[h]
T^{up}	Minimum up time	[h]
UR_i	DGs ramping-down	[kW]
X_{kft}	Number of devices of type k that are shifted from time f to t	[N]
$X_{kf(t-1)}$	Number of devices of type k that are shifted from time f to $t-1$	[N]
a_i	Coefficient of the fuel cost function of i^{th} DG	[€/h]
ar_i	Coefficient of reactive power cost function of i^{th} DG	[€/h]
b_i	Coefficient of the fuel cost function of i^{th} DG	[€/kWh]
$b_{PV_{i2}}$	Production costs of the PV	[€/kWh]
br_i	Coefficient of reactive power cost function of i^{th} DG	[€/kVArh]
$b_{W_{i1}}$	Production costs of the WT	[€/kWh]
c	Scale index of Weibull distribution equation	[N]
$c_{EVch}(t)$	Price of EVs charging	[€/kWh]
c_{EVcut}	Price of the unserved EVs charging power	[€/kW]
$c_{EVdis}(t)$	Price of the EV discharging	[€/kWh]
c_G	Price of active power cutting of the DGs	[€/kW]
$c_{gP}(t)$	Price of exchanging active power with utility grid	[€/kWh]
$c_{gQ}(t)$	Price of exchanging reactive power with utility grid	[€/kVArh]
c_i	Coefficient of the fuel cost function of i^{th} DG	[€/kW^{2}h]
$c_{isoP}(t)$	Price that is considered to sell active power to the consumers	[€/kWh]
$c_{isoQ}(t)$	Price that is considered to sell reactive power to the consumers	[€/kVArh]
$c_{Pcom}(t)$	Price of cutting active commercial load	[€/kWh]
$c_{Pind}(t)$	Price of cutting active industrial load	[€/kWh]
$c_{Pres}(t)$	Price of cutting active residential load	[€/kWh]
$c_{Pcomshd}(t)$	Price of shedding active commercial load	[€/kWh]
$c_{Pindshd}(t)$	Price of shedding active industrial load	[€/kWh]
$c_{Qcom}(t)$	Price of cutting reactive commercial load	[€/kVArh]
$c_{Qind}(t)$	Price of cutting reactive industrial load	[€/kVArh]
$c_{Qres}(t)$	Price of cutting reactive residential load	[€/kVArh]
$c_{Qcomshd}(t)$	Price of shedding reactive commercial load	[€/kVArh]
$c_{Qindshd}(t)$	Price of shedding reactive industrial load	[€/kVArh]
c_{ren}	Price of renewable power cutting	[€/kW]
cr_i	coefficient of reactive power cost function of i^{th} DG	[€/kVAr^{2}h]
$cos\theta$	Power factor	[N]
d	Whole duration of device consumption cycle	[N]

k_1	Shape index of Weibull distribution equation	[N]
n	Maximum number of reduced scenarios of WT generation	[N]
n_1	Number of devices types	[N]
n_2	Maximum delay of the devices	[N]
$n3$	Maximum number of the time steps	[N]
$m2$	Maximum number of reduced scenarios of WM	[N]
$m3$	Maximum number of reduced scenarios of EVs in the residential area	[N]
p_w	Device consumption at each time interval	[kW]
q	Maximum number of reduced scenarios of PV generation	[N]
r	Maximum number of reduced scenarios of OMP	[N]
$r1$	Maximum number of reduced scenarios of DW	[N]
$r2$	Maximum number of reduced scenarios of EVs in the commercial area	[N]
	Greek Symbol	
v	Wind speed	[m/s]
υ_{ci}	Cut in speed	[m/s]
υ_{co}	Cut out speed	[m/s]
υ_{cr}	Rated speed	[m/s]
η_{ch}	Charging efficiency of the battery	[N]
η_{dis}	Discharging efficiency of the battery	[N]
$\delta_{DG_i}(t)$	On/off state of i^{th} DG	[N]
$\delta_{gp}(t)$	Binary variable to control the purchasing active and reactive power from the utility grid	[N]
$\delta_{gs}(t)$	Binary variable to control the selling active and reactive power to the utility grid	[N]
$\delta_{bch}(t)$	Binary variable to control the charging of the battery	[N]
$\delta_{bdis}(t)$	Binary variable to control the discharging of the battery	[N]
$\delta_{EVch}(t)$	Binary variable to control the charging of batteries of the EVs	[N]
$\delta_{EVdis}(t)$	Binary variable to control the discharging of batteries of the EVs	[N]
$\delta_{ind}(t)$	Binary variable employed to accept or reject of industrial load shedding	[N]
$\delta_{com}(t)$	Binary variable employed to accept or reject of commercial load shedding	[N]
$\mu(t)^{PV}$	Random variable generated for the PV power at time t by using the normal distribution	[N]
$\mu(t)^{c_g}$	Random variable generated for the OMP at time t by using the normal distribution	[N]
$\mu(t)^{WM}$	Random variable generated for the WM at time t by using the normal distribution	[N]
$\mu(t)^{DW}$	Random variable generated for the DW at time t by using the normal distribution	[N]

$\mu(t)^{EV_{Res}}$	Random variable generated for the EVs in residential area at time t by using the normal distribution	[N]
$\mu(t)^{EV_{Com}}$	Random variable generated for the EVs in commercial area at time t by using the normal distribution	[N]
$\sigma(t)^{PV}$	Standard deviation of the PV power	[N]
$\sigma(t)^{c_g}$	Standard deviation of the OMP	[N]
$\sigma(t)^{WM}$	Standard deviation of the WM	[N]
$\sigma(t)^{DW}$	Standard deviation of the DW	[N]
$\sigma(t)^{EV_{Res}}$	Standard deviation of the EVs in the residential area	[N]
$\sigma(t)^{EV_{Com}}$	Standard deviation of the EVs in the commercial area	[N]
ρ^{W}	Probability happening of scenario of WT generation	[N]
ρ^{PV}	Probability happening of scenario of PV generation	[N]
ρ^{c_g}	Probability happening of scenario of OMP	[N]
ρ^{WM}	Probability happening of scenario WM	[N]
ρ^{DW}	Probability happening of scenario of DW	[N]
$\rho^{EV_{Res}}$	Probability happening of scenario EVs in the residential area	[N]
$\rho^{EV_{Com}}$	Probability happening of scenario EVs in the commercial area	[N]
λ_s	Probability of joint scenario	
Ψ	Tangent of angle θ	[N]
Δt	Sampling time	[h]
	Indices	
e	Index of generated scenarios of OMP	[N]
$e1$	Index of generated scenarios of DW	[N]
$e2$	Index of generated scenarios of EVs in the residential area	[N]
f	Index of time of shifted appliance	[N]
i	Index of DGs	[N]
$i1$	Index of WTs	[N]
$i2$	Index of PV panels	[N]
$i3$	Index of generated scenarios of WT generation	[N]
$i4$	Index of generated scenarios of PV generation	[N]
j	Index of greenhouse gases	[N]
$j1$	Index of recovered time of the smart appliances	[N]
k	Index of smart appliance	[N]
$k2$	Index of generated scenarios of WM	[N]
$k3$	Index of generated scenarios of EVs in the residential area	[N]
l	Index of consumption period of the smart appliances	[N]
s	Index of joint scenario	[N]
t	Time index	[N]
w	Index of duration cycle of smart appliances	[N]

LIST OF ABBREVIATIONS

CO_2	Carbon Dioxide
CPP	Critical Peak Pricing
CSA	Cross Sectional Area
EVs	Electric Vehicles
EDRP	Emergency Demand Response Programme
CAP	Capacity Market Programme
DBP	Demand Bidding Programme
DE	Diesel Engine
DED	Dynamic Economic Dispatch
DGs	Distributed Generators
DLC	Direct Load Control
DSM	Demand Side Management
DSR	Demand Side Response
DoD	Depth of Discharge
DWs	Dish Washers
ED	Economic Dispatch
EMS	Energy Management System
FC	Fuel Cell
G2V	Grid to Vehicle
HEVs	Hybrid Electric Vehicles
ILC	Indirect Load Control
LC	Local Controller
LP	Linear Programming
LV	Low Voltage
MG	Microgrid
MT	Microturbine
MO	Market Operator
MDT_i	Minimum Down Time
MUT_i	Minimum up Time
MGM	Microgrid Manager
MILP	Mixed Integer Liner Programming

MIQP	Mixed Quadratic Liner Programming
NO_x	Nitrogen Oxide
NLP	Non-Linear Programming
OMP	Open Market Price
OpenDSS	Open Distribution System Simulator
PM	Particulate Matter
PV	Photovoltaic
PCC	Point of Common Coupling
PSO	Practical Swarm Optimisation
RTP	Real Time Pricing
RDGs	Renewable Distributed Generators
SRCs	Spinning Reserve Constraints
SED	Static Economic Dispatch
SO_2	Sulphur Dioxide
SSSCs	Steady State Security Constraints
UC	Unit Commitment
SCUC-UARDEED	Security-Constrained Unit Commitment Unified Active and Reactive Dynamic Economic and Emission Dispatch
TOU	Time of Use
V2G	Vehicle to Grid
WMs	Washing Machines

1 Introduction

1.1 Chapter Summary

In this chapter, the MG concept and structure is introduced and presented. The motivations of this thesis are presented comprehensively. The aim and the objectives with the contribution to knowledge of this work are introduced. The thesis structure is also included. Finally, this chapter concludes with a list of publications.

1.2 Microgrids Concept

1.2.1 Microgrid Structure and Operation Modes

Recently, the renewable and environmentally friendly energy sources, such as wind turbines (WTs), photovoltaic panels (PV), and batteries have drawn greater attention because they help to mitigate the global warming and reduce dependency on fossil fuel. MG in particular is seen as promising technology to integrate these energy resources with the power system. The MG is a localised electric system comprising of several main components, which usually do not reside in the conventional power system. The MG is composed of uncontrollable generation resources such as WTs and PVs, controllable distributed generators (DGs), such as diesel generators (DEs), micro turbines (MTs), fuel cells (FCs), fixed batteries, and EVs. In addition, it has controllable loads that is cut or shifted to prevent the system from outages and to minimise the cost and potentially maximise the profit of the MG [1]. The MG operates either autonomously or connected to the utility grid via a point of common coupling (PCC) as shown in Figure 1-1 and it trades active and reactive power with the utility grid. The PCC is a point where the MG and the utility grid are connected. At the PCC, the active and reactive power flow between the utility grid and MG can be controlled. Generally, in both modes of operation, the MG must maintain power supply to its load.

The MG tackles the load growths by integration of the DGs locally and close to the loads. In addition, the MG relieves the global warming by integrating the

DGs, where these DGs have a low emission rate of greenhouse gases by producing clean energy [2], [3]. A useful feature of the MG is the bidirectional power flow between the MG and the loads and the utility grid when operating in the grid-connected mode. In this mode of operation, the MG sells and purchases active and reactive power to/from the utility grid, not only to balance the generation power with load demand but also to minimise the total cost or to maximise the profit. The economic dispatch of the system has been formulated either to minimise the total operation cost or to maximise the MG profit while meeting the load demand at a certain time and satisfying a set of realistic constraints. The economic dispatch of systems has been often called a static economic dispatch (SED) [4].

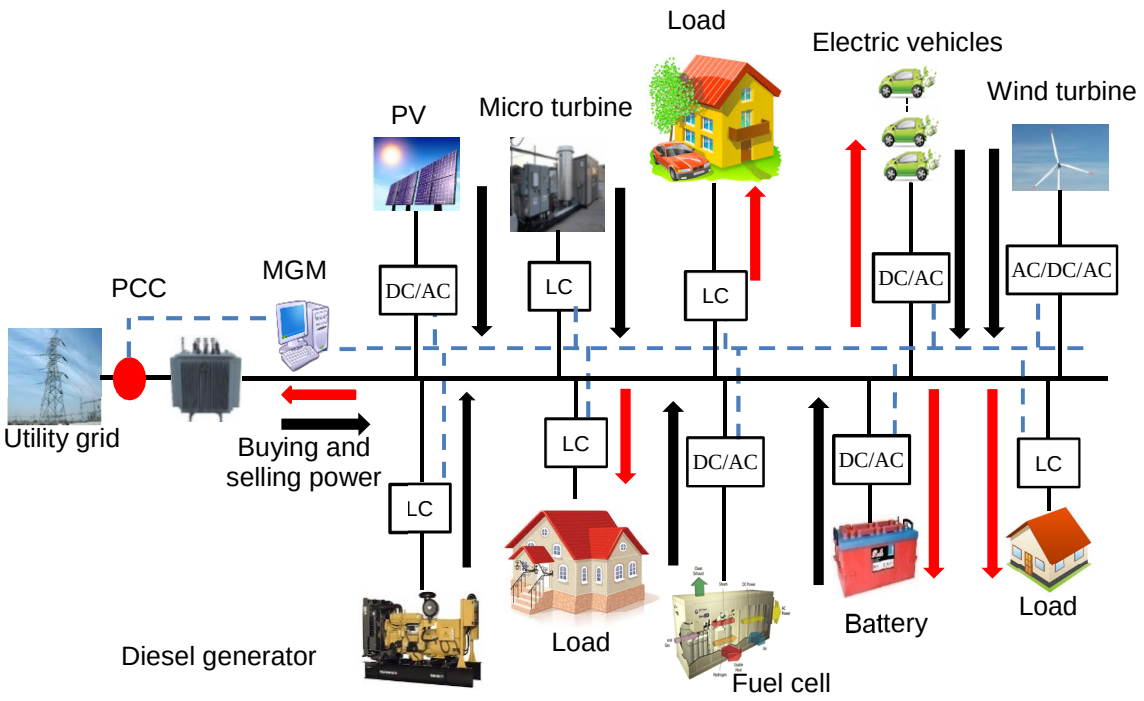

PCC (Point of common coupling), LC (Local controller)

Power line —— **Communication control line** - - -

Figure 1-1 Typical MG components

This type of economic dispatch is solved with one load level at a specific time, without taking into account the relations among different time intervals. Therefore, it may be improper to tackle large change in load and ramp rate constraints of generators. However, it is not capable of looking beyond load variation [5]. Therefore, it is necessary to explore dynamic economic dispatch (DED), because the scheduling of generator units when taking into account the ramp rate constraint can be considered when formulating and solving the optimisation problems. In addition, the load changed during the scheduling horizon can be taken into consideration when solving the optimisation problems [6], [7]. The bidirectional power flow between the MG and the fixed batteries, EVs, and the utility grid make the MG a significantly strong dynamic system. Therefore, the dynamic economic dispatch is more proper for formulating and solving the economic dispatch of the MG. The UC is a mature concept in the optimal operation of the conventional power system. The UC determines the on/off state of the generators during the scheduling horizon to minimise the total operating cost or to maximise the profit. Recently, the UC concept has been used with the connected and isolated MG. The UC is integrated with optimisation problems of the MG to minimise the total operating and emission costs or to maximise the profit. The integration of the UC with the economic dispatch of the MG is essential to the flexible operation of the MGs and to increase the penetration of the renewable energy resources [8].

1.2.2 Components of the Energy Management System of Microgrids

The function of the energy management system (EMS) of the MGs is to manage the active and reactive power flow between the generation resources and the load in the MG [9]. Figure 1-1 shows the main components of the EMS. The EMS provides interfacing between the MG and the main grid to manage the exchanging active and reactive power. The EMS of the MG generally consists of the following main components: local controllers (LCs) for each DG, load, and battery. The EMS also includes a manager (MGM) [10], [9]. The MGM determines the optimal scheduling of the MG and ensures the active and reactive load demands are met, while the constraints are satisfied at each time

interval. The interaction between the MGM and the main components of the MG is via bidirectional communication line [11], the discrete line in Figure 1-1.

The LCs of the DGs exchange data with MGM, such as the available generation, and the generation price, while the LCs for loads exchange data with MGM, such as the load that is shifted or curtailed and the price of the curtailed loads. Similarly, the LCs for the batteries exchange information of the state of charge at each time interval. The bidirectional communication between these main components and the MGM allow not only monitoring the operation of the MG but also optimising the operation of the MG securely. The MGM determines the active and reactive output power of each DG, the UC, the load cutting or shifting, the charging and discharging power of the battery and the batteries of the EVs, buying or selling active and reactive power from/to the utility grid. Then, the MGM sends back the data to the LC of each DG, each battery, and EV. The MGM also informs the consumers of accepting or rejecting their bids to cut their loads.

1.3 Motivation

The majority of researchers have studied the active power optimisation problems of MGs, whereas few have looked at optimisation, which involves both the active and reactive power. Ignoring the reactive power from the DGs at the scheduling problem of the MG may lead to increase in the investment cost. In addition, it may lead to reduce the security of supply particularly for the isolated MG. According to the literature, the consideration of the models involved in the cost of reactive power production, emission of greenhouse gases costs, renewable energy production cost, and battery degradation cost in a combined optimisation problem to minimise the total operating and emission costs or maximise the profit of the connected and isolated MG have not been investigated yet. In addition, previous works focused on a range of conservative formulations that had a limited set of constraints relating to reactive power optimisation. Further, they also overlooked the constraints such as the active and reactive power SSSCs and active and reactive power SRs, which make the

grid operate insecurly, and the emission of the greenhouse gases. The conservative assumptions in the existing works, such as not taking into consideration the models of the cost parameters and constraints, have a huge adverse impact on the credibility of the optimisation results under deterministic and stochastic environments. In this thesis, these assumptions are taken into consideration to make the optimisation approach more realistic.

In this research, the cohesive and synergistic duality of both the deterministic and stochastic environments is utilised in the optimisation approach. New optimisation approaches and strategies are proposed to accommodate the developed models of the optimal unified active and reactive power scheduling, with consideration also given to the models concerned with the costs of the emission of the greenhouse gases, battery degradation cost, maintenance cost of the DGs, the purchasing active and reactive power from the utility grid cost, start-up and shut down cost of the DGs, and the cost of the renewable generation. In addition, a realistic set of constraints, such as the ramp rate of the DGs, active and reactive generation limit of the DGs generation, the battery operation, the emission level limit of greenhouse gases, and time up/down of the DGs are incorporated with optimisation approaches. The security constraints for active and reactive power are also considered for the reliable and secure operation of MGs with regard to meet the demand. Further, the active and reactive SRs for the isolated MG are considered as well. Furthermore, the UC is developed to take into consideration both the active and reactive power of the DGs when solving the optimisation problems.

The integration of the DSM with optimisation problems of the MGs has not been fully investigated in the deterministic and stochastic environments. In the previous works the DSM was treated as an aggregated amount, instead of as a separate appliance. In addition, the DSM was considered as input to the optimisation algorithms. Further, they addressed the DSM of the active demand solely and they did not take into consideration the reactive load management. Furthermore, the DSM has not been considered as a stochastic variable in the previous works. The integration of the DSM as a shifting technique with the

isolated MG has not been explored yet. This work presents the novel optimisation approach and scheduling strategy to model and incorporate the active and reactive DSM with optimisation problems of the MG, consideration the model of all the proposed cost components and constraints in the previous paragraph. The DSM is considered as a decision variable in the proposed optimisation problem, in which the DSM is treated as a separate load with an operation cycle. Multi-techniques of the DSM are applied simultaneously to the different load types participating in the DSM programmes. This work considers the stochastic optimisation of both the generation and demand sides simultaneously to the proposed optimisation approach, where the DSM is considered as a source of uncertainty.

Many researches proposed the optimal integration of EVs with MGs. The majority studied the V2G or G2V integration. Few researchers have studied both V2G and G2V simultaneously. The previous publications that presented the impacts of the EVs on the total operating cost and the emission level of greenhouse gases did not consider many important issues, such as the models of the reactive power cost, emission cost, battery degradation cost, and production cost of the renewable generation. They also neglected active and reactive steady state security of supply constraints (SSSCs), active and reactive power spinning reserve constraints (SRCs), and emission of greenhouse gases constraints; and the UC was considered only the active power. In addition, the participations of the EVs on the deregulated market have not been fully studied under deterministic and stochastic environments. Previous optimisation approaches integrating the EVs consider either grid performance or consumers preference in the formulation of the optimisation approach. This work proposes a novel optimisation approach and scheduling strategy that take into consideration the integration of both V2G and G2V simultaneously with both deterministic and stochastic optimisation based on one of the following market policies: minimising the total operating and emission costs and maximising the MG profit.

1.4 Aim and Objectives

The aim is to develop optimisation approaches to minimise the total operating cost or to maximise the profit of the MG with protecting the environment and satisfying a set of realistic constraints.

The objectives below are conducted to achieve the aim of this research.

A. To develop comprehensive economic mathematical models of the subsystems of the MG and constraints.

B. To develop new optimisation approaches under deterministic and stochastic environments to formulate and solve the optimisation problem of the MG.

C. To analyse the impacts of the reactive power from the DGs, the storage battery, and security of supply constraints on the optimal operation of the MG.

D. To develop scheduling strategies to integrate the DSM techniques with optimisation problems of the MG.

E. To develop scheduling strategies to integrate the EVs with optimisation problems of the MG.

1.5 Thesis Contribution

The contribution of this work is divided for three main core areas. Firstly, a novel SCUC-UARDEED of the connected and isolated MG is presented. The optimisation problem involves the management of both the active and reactive power and considers the emission cost of greenhouse gases, battery degradation cost, and production cost of the renewable generation. According to the open literature, it appears that no study on the optimal scheduling of the MG has considered the models of above cost functions in a combined optimisation approach to minimise the total operating or maximises the profit. The UC is modified to take into account the active and reactive power generation of the DGs. In addition, new models of constraints are proposed, such as active and reactive security and reserve constraints, emission limits, the constraints relate to the reactive power, and the constraints for managing

the exchanging active and reactive power with the utility grid. Accordingly, new approaches and strategies are proposed to model and formulate the optimisation problem of the MG under deterministic and stochastic environments. The models of uncertainties that evolve from the fluctuation of renewable generation and OMPs are developed and incorporated with optimisation algorithms in a two-stage stochastic optimisation.

Secondly, novel scheduling strategies are presented to integrate the DSM techniques with the optimal scheduling of the connected and isolated MG. The DSM techniques are developed to apply to both the active and reactive load demands. The DSM is considered as decision variables in the optimisation approaches and the DSM is treated as a separate load with a specific operating cycle. All load demands are involved in the DSM techniques. In addition, different DSM techniques are applied to the various types of loads simultaneously. In stochastic environments, the estimated number of connected appliances is considered a source of uncertainty with the fluctuations of the renewable generation. The models of these uncertainties are developed and integrated with SCUC-UARDEED in a two-stage stochastic optimisation approach, where the DSM is considered as a stochastic variable.

Thirdly, a novel integration of the EVs with SCUC-UARDEED of the MG is proposed. The UC based on the active and reactive power with EVs are combined with the optimal scheduling of the MG to minimise the total operating cost or maximise the profit. The incorporating of the EVs in the deregulated market to maximise the profit has not been fully investigated under stochastic and deterministic environments. The optimisation approaches are developed to take into consideration both the grid performance and the owners of the EVs' requirements. A new pricing scheme is implemented to encourage the EVs' owners to participate in the optimal scheduling of the MG. The stochastic models of the EVs with the fluctuation of the renewable generation are developed and incorporated with the SCUC-UARDEED in a two-stage based-scenario stochastic optimisation approach.

1.6 Thesis Structure

Chapter 1 introduces and provides the background of the typical MG concept, subsystems, definition, and modes of operation. It also focuses on the aim, objectives, motivation, and the contribution of this research.

Chapter 2 presents a literature review of the strategies and approaches that have been proposed to formulate and solve the optimisation problem of MGs. It also provides models of each subsystem of the MG and the relevant constraints. The active and reactive optimal power flow is modelled and formulated to minimise the total operating and emission costs or maximise the MG profit. The optimisation approaches are applied to both the connected and isolated MG and the impacts of a storage battery and SSSCs constraints are explored. Published papers 1, 2, and 7 listed in the section 1.7 are extracted from this chapter.

Chapter 3 the stochastic optimisation problem is formulated, and the uncertainties occurring from the fluctuation of renewable generation and from forecasting errors of the OMPs and their constraints are modelled and the approaches tested on the connected and isolated MG. Published papers 5 and 8 listed in section 1.7 are extracted from this chapter.

Chapter 4 presents a literature review of the integration of the DSM with the optimal scheduling of the MG. The models of the smart appliances, shifting and curtailing DSM techniques and their constraints are incorporated with optimisation algorithm. The impacts of the DSM on the optimal operation of the MG are addressed through different realistic scenarios, where the different DSM techniques are applied to the different types of loads simultaneously. Published papers 3 and 6 listed in section 1.7 are extracted from this chapter.

Chapter 5 Introduces models of the uncertainties evolving from the renewable generation, and the estimated number of the smart devices. These models are integrated with optimisation approach in the two-stage optimisation based stochastic scenarios. The proposed stochastic optimisation approach is applied

to the connected and isolated MG to verify the robustness of the proposed approach and to determine the impacts of these uncertainties on the optimal scheduling of the MG.

Chapter 6 discusses the literature review of the integration of the EVs with optimisation of the MG, and the mathematical models of the bidirectional operation of the EVs with their constraints are introduced. The impacts of the EVs on the optimisation problem to minimise the operating costs or maximises the profit are demonstrated and the proposed approaches are validated through different charging and discharging scenarios. The uncertainties deriving from renewable generation and the behaviours of the EVs are modelled and incorporate with optimisation of the connected and isolated MG. Published paper 4 listed in section 1.7 is extracted from this chapter.

Chapter 7 presents a discussion of the thesis results, summarises the main conclusions of this research, and makes suggestions for future work that is related to the subject of this thesis.

1.7 Publications

1- Mohammed. K. Al-Saadi, Patrick C. K. Luk, Weizhong. Fei, A. Bati, “Security Constrained Active and Reactive Optimal Power Management of Microgrid in Different Market Policies,” in Proc. 11th International Conference on Control (CONTROL), Belfast, UK, 31st August-2nd September 2016.

2- Mohammed. K. Al-Saadi, Patrick C. K. Luk, Weizhong. Fei, “Impact of Unit Commitment on the Optimal Operation of Hybrid Microgrids,” in Proc. 11th International Conference on Control (CONTROL), Belfast, UK, 31st August-2nd September 2016.

3- Mohammed. K. Al-Saadi, Patrick C. K. Luk, J. Economou, “Integration of the Demand Side Management with Unified Active and Reactive Power Economic Dispatch of Microgrids,” accepted in International Conference on Life System Modeling and Simulation & Intelligent Computing for Sustainable Energy and Environment, Nanjing, China, 22-24 September 2017.

4- Mohammed. K. Al-Saadi, Patrick C. K. Luk, J. Economou, “Unit Commitment Dynamic Unified Active and Reactive Power Dispatch of Microgrids with Integration of Electric Vehicles,” accepted in International Conference on Life System Modeling and Simulation & Intelligent Computing for Sustainable Energy and Environment, Nanjing, China, 22-24 September 2017.

5- Mohammed. K. Al-Saadi, Patrick C. K. Luk, “Security-Constrained Two-Stage Stochastic Unified Active and Reactive Power Management System of the Mirogrids,” accepted in International Conference on Life System Modeling and Simulation & Intelligent Computing for Sustainable Energy and Environment, Nanjing, China, 22-24 September 2017.

6- Mohammed. K. Al-Saadi, Patrick C. K. Luk, J. Economou, “Microgrid Dynamic Economic and Environmental Dispatch with Consideration of Different Management Strategies of the Demand Side,” It is provisionally accepted in the Cognitive Computation journal.

7- Mohammed. K. Al-Saadi, Patrick C. K. Luk, J. Economou, Shatha Al Kubragyi, Hayder A. Abdulrahem, “Impacts of Storage Battery on the Economic Operation of the Microgrids with Considering the Battery Degradation Cost,” In Proceedings of the Conference of Cranfield Science for a Circular Economy. How to tackle the Water, Energy, Food nexus, Bedford, UK, 16 June 2017.

8- Mohammed. K. Al-Saadi, Patrick C. K. Luk, J. Economou, Shatha Al Kubragyi, “Multi-Period Scenario-Based Stochastic Combined Dynamic Economic Emission Dispatch of the Microgrids,” In Proceedings of the Conference of Cranfield Science for a Circular Economy. How to tackle the Water, Energy, Food nexus, Bedford, UK, 16 June 2017.

9- Shatha Al Kubragyi, Patrick C. K. Luk, J. Economou, Mohammed. K. Al-Saadi “Battery energy storage based on D-STATCOM device in distribution grid systems,” In Proceedings of the Conference of Cranfield Science for a Circular Economy. How to tackle the Water, Energy, Food nexus, Bedford, UK, 16 June 2017.

10- Shatha Al Kubragyi, Patrick C. K. Luk, J. Economou, Mohammed. K. Al-Saadi, “D-STATCOM Based on Energy Storage for Fault Ride through in Distribution Grids,” In Proceedings of the Conference of Cranfield Science for a Circular Economy. How to tackle the Water, Energy, Food nexus, Bedford, UK, 16 June 2017.

2 Dynamic Economic and Emission Dispatch of the MG

2.1 Chapter Summary

In this chapter, a comprehensive literature review is conducted for the approaches and strategies that are used to formulate and solve the optimisation problem of the MGs. A literature review of the incorporating of the storage batteries and reactive power management with optimisation algorithms is carried out. The comprehensive model of each subsystem of the MG and their constraints are developed and described. These proposed models of the subsystem of the MG are employed to formulate the optimisation problem, where the optimisation approaches are tested on the connected and isolated MG. Another goal of this chapter is to determine the impacts of the battery and the SSSCs constraints on the optimal operation of the MG, where the optimisation problem is formulated with and without the battery, or with and without the SSSCs.

2.2 Optimisation Problems of MGs

Optimisation problems are defined as problems of finding the best solution from all alternative feasible solutions [12]. The optimisation problem composes of these four main components [13]:

A. Objective function

B. Decision variables

C. Constraints

D. Parameters

The objective function is the mathematical equation that is needed to be optimised and it includes the decision variables with a number of coefficients. The decision variables control the value of the objective function, while the constraints restrict the values of the decision variables. The parameters are fixed known values. From the aforementioned definitions, it is deduced that the

aim of the optimisation is to find the optimal values of the variables that minimise or maximise the objective function.

In this thesis, the optimisation problem is formulated by the mixed integer quadratic programming (MIQP) because it involves continuous and discrete variables. The continuous variables involve the active and reactive output power of the DGs, the charging and discharging power of the battery and EVs, the exchanging active and reactive power with the utility grid, and shifting the active and reactive loads. The discrete variables are the on/off state of the DGs, the discrete variables that manage the charging and discharging operations of the battery and EVs, the exchanging active and reactive power with the utility grid, and the rejecting or accepting the bid of load shedding.

The optimisation problems of grids have two main parts: the economic dispatch (ED) and UC. The aim of the ED in this work is to determine the scheduling of the active and reactive power of the DGs, charging and discharging energy of batteries and batteries of the EVs, the selling and buying active and reactive power to/from the utility grid, and the load shifting and cutting. The UC determines the on/off state of the DGs based on the active and reactive power. Accordingly, some researchers proposed the optimisation problem as the ED only and some of them considered both the ED and UC. Reference [4] formulated the ED of a the conventional power system to minimise the total running cost and maintain the level of the emission of greenhouse gases. Reference [14] formulated the ED of the MG that included three DGs to minimise the operating cost.

Recently, researchers have extended the economic dispatch problems in MGs to involve the unit commitment, ramp rate of generators, minimum up and down constraints, and start up and shut down cost. These parameters increase the complexity of optimisation problems. These problems include both continuous decision variables such as output power of the generators and discrete decision variables, such as the UC. This leads to propose many approaches and methodologies to formulate and solve these optimisation problems.

It was suggested that in [15] the UC with the ED of the MG to minimise the operating cost with a set of constraints, such as ramp rate, minimum up and down and start-up and shutdown cost of generators. In [16] and [17], the UC optimisation approach was modelled and formulated to minimise the total operating cost of the MG including different types of DGs, renewable resources, and battery with different linear constraints. The optimisation problem was formulated by MILP and it was solved by software CPLEX. It was found that the proposed optimisation approach improved the solution equality and computational burden. Reference [18] pointed out the ED and UC to minimise the emission of carbon dioxide of the MG.

In contrast, the other aspects that make the optimisation problems more complex are the multi-objective optimisation and combined optimisation problems. The multi-objective optimisation to minimise both the operating cost and emission level of greenhouse gases were addressed in [19], [20], [21], [22], [23]. These papers applied the optimisation approaches to the conventional power system without renewable generation. Reference [24] presented the optimisation problem as a multi-objective optimisation problem with integration of the EVs. The optimisation problem was applied to the power system without renewable generation, while the same authors in [25] presented similar optimisation approach with the wind and solar renewable sources in their formulation of the optimisation problem. The optimisation problem in [26] was formulated as a multi-objective optimisation and the optimisation problem was applied to the smart distribution system with DGs and EVs. References [27], [28], [29], [30] proposed the optimisation problems to minimise both the operating and emission level of the greenhouse gases. The proposed optimisation approaches were applied to MGs, which included different types of the DGs, and renewable generation.

On the contrary, some researchers converted the emission of greenhouse gases to monetary cost and this cost was incorporated with objective function to minimise the combined total operating and emission costs [31], [32], [33]. In these papers, the optimisation problem was applied to the power system

without the renewable generation resources. Reference [34] presented the optimisation problem of the MG to minimise the operating and emission costs with renewable energy resources. However, the reactive power scheduling was overlooked in the optimisation approach. In addition, important cost components, such as reactive power production cost, the start-up\shutdown costs of the DGs, maintenance cost of the DGs, the production cost of the renewable energy resources, and the cost of purchasing both the active and reactive power from the utility grid were neglected in the formulation of the optimisation problem. Furthermore, essential constraints such as active and reactive security constraints, limit of the emission of the greenhouse gases, ramp rate constraints, and time up/down of the DGs were ignored. In addition, the battery model was not considered in the optimisation problem. The UC was not taken into account in the optimisation approach.

2.3 Storage Devices

Storage batteries play a vital role in the optimal management of power flow in the MGs. The batteries are utilized for different purposes in the optimal operation of the MGs. The batteries are used to minimise the total operating and emission cost by controlling the charging and discharging operations [35], [36], [37], [38], [39], [40]. The charging and discharging operations of the batteries are controlled to mitigate the fluctuation of the intermittent nature of the wind and solar energy generation to optimise the whole power consumption and balance the generation with load in MGs [8], [41], [42], [43], [44]. In addition, the batteries are employed to shave the peak load by discharging during peak load and charging during off peak load [45]. Solely [8] among the above publications has considered the degradation cost of the battery and in [46], [47], [48], [49] the battery degradation cost were considered as well. Ignoring the battery degradation cost in the formulation of the optimisation problem has significantly impacts on the charging and discharging operations of the batteries and this affects the results of the MG optimisation.

2.4 Maximising the MG Profit

All the aforementioned publications proposed the optimisation problems to minimise the operating cost, emission cost and both operating and emission cost. In contrast, some researchers addressed the optimisation problem of MGs in the deregulation market (competitive market) to maximise the profit of the MG [50], [51], [52], [53], [54], [55]. However, they did not consider the storage battery in their studies. A few researchers took into account the storage battery in the optimisation problem to maximise the profit [56], [57], [58], [59], although they did not consider the degradation cost of the storage battery. Quite a few researchers pointed out the degradation cost of the battery in the optimisation approach to maximise the MG profit [60]. The above papers tested the optimisation approaches on the connected MG solely, while in [53], the maximising profit was applied to the isolated MG without battery. The previous optimisation approaches to maximise the MG profit did not take into consideration the models of the reactive power and the emission costs of greenhouse gases. The maintenance cost of the DGs and the production cost of the renewable energy also were overlooked. In addition, important constraints such as the active and reactive power SSSCs and SRCs, and emission limit of greenhouse gases were neglected. Furthermore, some of these publications did not consider the constraints such as ramp rate, minimum up/down constraints of the DGs. Furthermore, the majority of the previous works ignored the UC.

2.5 Active and Reactive Power Economic Emission Dispatch of the MGs

Remarkably, the majority of researchers studied concern the optimisation problem of the active power flow solely, whereas relatively few look into unified optimisation problems involving both active and reactive power management in MGs. Reference [61] proposed an optimisation approach that included both active and reactive power to minimise the operating cost of a connected network consists of hybrid generation resources and energy storage. Reference

[62] reported stochastic optimisation approach to minimise the operating cost with consideration given to the reactive power, and the uncertainties that arose from the fluctuations of load and generation of renewable resources. However, these studies did not consider the reactive power production cost in their objective functions. In addition, important cost components models, such as reactive power production, battery degradation, the start-up\shutdown, maintenance cost of the DGs, the production cost of the renewable resources were overlooked. The model of the MG capability of exchanging both the reactive power with the utility grid was also neglected. Further, these studies neglected many essential constraints such as active and reactive SSSCs constraints of the connected MG, active and reactive SRCs for the isolated MGs, emission limit of the greenhouse gases, ramp rate constraints, and time up/down of the DGs. Furthermore, the environmental cost and the UC were not considered in [62], and solely the emission of the carbon dioxide was considered in [61] and the other pollutant gases were ignored.

Similarly, in [63], an optimisation approach was used to minimise the operating cost with the reactive power of the connected distribution MG. However, the reactive power production cost was not considered in the objective function. Important costs models were neglected, such as the maintenance cost of the DGs, the renewable energy production cost, environmental cost, battery degradation cost, and the purchasing reactive power from the utility grid in the formulation of the optimisation problems. It is also evident that many of the essential constraints such as active and reactive security constraints, emission limit of greenhouse gases, ramp rate limit of the DGs, minimum up/down constraints, and the limit of exchanging reactive power with utility grid have been largely omitted. The model of exchanging both the reactive power with the utility grid was overlooked.

From the above literature, it can be seen, that the optimisation problems were formulated to minimise the operating cost solely and the optimisation approaches were applied to the connected MG only. However, none of these publications addressed the optimisation problem to maximise the MG profit for

the connected and isolated MG. It appears that there is a justification for simplicity over fidelity when developing models that suffice to provide a credible system performance prediction. The inclusion the models of the proposed cost components in this work with constraints has made this study closer to a real-world scenario than any other previous studies. The high-fidelity model entails extending the optimisation problem to accommodate all cost components and constraints, as well as encompassing new approaches and strategies to formulate the novel proposed SCUC-UARDEED.

2.6 Mathematical Models of the System Components

It is necessary to model all components of the MG as accurate as possible to formulate the optimisation problem.

2.6.1 Fuel Cost of the DGs

The fuel cost of the i^{th} DG is modelled as a function of output active power at each time interval t as [21], [64], [65]:

$$CP_{DG_i}\left(P_{DG_i}(t)\right) = a_i + b_i.P_{DG_i}(t) + c_i.P_{DG_i}^2(t) \quad \textbf{(2.1)}$$

where a_i (€/h), b_i (€/kWh), and c_i (€/kW^{2}h) are the respective coefficients of the fuel cost function, and $P_{DG_i}(t)$ is the output active power of i^{th} DG.

2.6.2 Reactive Power Production Cost of the DGs

The corresponding production cost of the reactive power of i^{th} DG is calculated at each time interval as a quadratic function of reactive power as follows [66], [67], [68]:

$$CQ_{DG_i}(Q_{DG_i}(t)) = ar_i + br_i.Q_{DG_i}(t) + cr_i.Q_{DG_i}^2(t) \quad \textbf{(2.2)}$$

where ar_i (€/h), br_i (€/kVArh), and cr_i (€/kVAr^{2}h) are the respective coefficients of the reactive power cost function, and $Q_{DG_i}(t)$ is the output reactive power of i^{th} DG. It is considered that the WTs, the PVs, the battery, and the EVs do not provide reactive power, and only the DE, MTs, and FCs supply reactive power.

2.6.3 Operating and Maintenance Cost of the DGs Model

To prolong the life and to the proper operation of the DGs, the maintenance should be conducted regularly. The operating and maintenance cost of the DGs is assumed proportional to the produced power and it is calculated by the following equation:

$$COM_{DG_i}(P_{DG_i}(t)) = KOM_{DG_i}.P_{DG_i}(t) \quad \textbf{(2.3)}$$

where KOM_{DG_i} (€/kWh) is the coefficient of the maintenance cost of the i^{th} DG.

2.6.4 Wind Energy Model

The output power of the WTs depends on the wind speed. The relationship between the output power and the weather wind is expressed by the following equation [69], [70]. Figure 2-1 shows the effect of the wind speed on the output power of the WTs.

$$P_W = \begin{bmatrix} 0 & \upsilon \le \upsilon_{ci} \; or \; \upsilon \ge \upsilon_{co} \\ P_{W-r}\frac{\upsilon-\upsilon_{ci}}{\upsilon_r-\upsilon_{ci}} & \upsilon_{ci} \le \upsilon \le \upsilon_r \\ P_{W-r} & \upsilon_r \le \upsilon \le \upsilon_{co} \end{bmatrix} \quad \textbf{(2.4)}$$

where P_{W-r} is the rated power of WT, υ_{ci} , υ_{co} , and υ_r are cut in, cut out and rated wind speeds in(m/s).

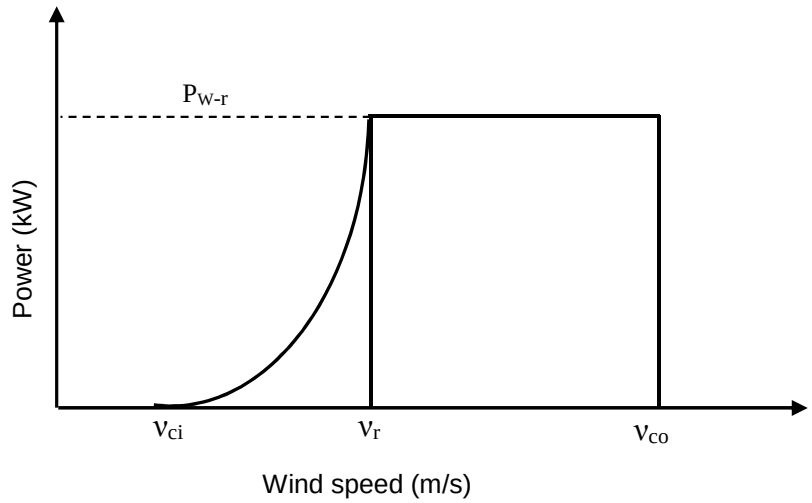

Figure 2-1 Wind turbine generation power curve

2.6.5 Renewable Sources Power Production Cost Model

The power production cost of the WTs and PV panels are determined for each kWh produced according to the yearly depreciation of the installation cost. Therefore, the production cost of the WT and PV should take into consideration in the formulation of the optimisation problems. Accordingly, the production costs of generation of the WT and PV are calculated as follows:

A. Production Cost of the WT

This cost is determined by the following equation

$$CP_{W_{i1}}(P_{W_{i1}}(t)) = \sum_{i1=1}^{N1} b_{W_{i1}}.P_{W_{i1}}(t) \quad \textbf{(2.5)}$$

where $P_{W_{i1}}(t)$ (kWh) is the active power generation of $i1^{th}$ WT, $b_{W_{i1}}$ (€/kWh) is the production cost of the WT, and $N1$ is the total number of the WTs.

B. Production Cost of the PV

The following equation is used to calculate the cost of the PV generation

$$CP_{PV_{i2}}(P_{PV_{i2}}(t)) = \sum_{i2=1}^{N2} b_{PV_{i2}}.P_{PV_{i2}}(t) \quad \textbf{(2.6)}$$

where $P_{PV_{i2}}(t)$ (kWh) is the active power generation of $i2^{th}$ PV, $b_{PV_{i2}}$ (€/kWh) is the production cost of the PV, and $N2$ is the total number of the PV units.

The $b_{W_{i1}}$ and $b_{PV_{i2}}$ are calculated by using the following equation:

$$b(t) = \left(\frac{r.(1+r)^n}{(1+r)^n - 1}\right)\left(\frac{Installation\ cost}{k.hours\ per\ year}\right) \quad \textbf{(2.7)}$$

where r is the interest rate, which is assumed to be 8 %. n is the depreciation period, which is considered 20 and 10 years for PV and WT respectively [71]. k is the capacity factor which is 40 % for WT, 3504 kWh/kW annual production, while for PV is 1300 kWh/kW yearly production [50].

2.6.6 Storage Batteries Model

Storage batteries have been modelled in several different ways. Criteria that have been adopted to choose the model depend on the details and the field of study. Accordingly, the linear discrete time state space model is commonly employed to model the storage batteries in the scope of the MG optimisation [35], [72]:

$$E_b(t) = E_b(t-1) - \left(\frac{P_{bdis}(t)}{\eta_{dis}}\right).\Delta t + P_{bch}(t).\eta_{ch}.\Delta t \quad \textbf{(2.8)}$$

where $E_b(t)$ and $E_b(t-1)$ are the state charge of the battery at current and previous time respectively, $P_{bch}(t)$ and $P_{bdis}(t)$ are the battery charging and discharging power respectively, while η_{ch} and η_{dis} are the corresponding charging and discharging efficiencies, and Δt is the sampling time (h).

The number of charging and discharging operations of the battery affects the battery life significantly. Therefore, the additional battery degradation cost added to the total MG cost to prolong the life of the battery. The degradation cost of the battery is formulated as follows [73], [74], [75]:

$$C_d = \frac{C_b}{L_b} \quad \textbf{(2.9)}$$

where C_d is the battery degradation cost (€/kWh), C_b is the battery capital cost (€), L_b is the real battery life (kWh), which is calculated as follows.

$$L_b = DoD.E_b.L_c \quad \textbf{(2.10)}$$

where DoD is the depth of discharge, E_b is rated energy capacity (kWh), L_c is the battery cycle life.

The battery operation cost (€) is determined as follows:

$$C_{bo}(t) = C_d\,.P_b(t).\Delta t \quad \textbf{(2.11)}$$

where $P_b(t)$ is either charging or discharging power of the battery. The battery operating cost helps the operators to involve the batteries into dynamic economic dispatch of the MG as energy sources.

2.6.7 Exchanging Active and Reactive Power with the Utility Grid Model

For connected MG, the MG can sell or purchases active and reactive power to/from the utility grid via PCC, where the models of the costs of the exchanging active and the reactive power with the main grid are proposed and developed in this section as follows:

$$C_{gP}(t) = c_{gP}(t).P_g(t) \quad \textbf{(2.12)}$$

$$C_{gQ}(t) = c_{gQ}(t).Q_g(t) \quad \textbf{(2.13)}$$

where $c_{gP}(t)$ (€/kWh) and $c_{gQ}(t)$ (€/kVArh) are the open market prices(OMPs) of selling and buying active and reactive power to/from the utility grid, $P_g(t)$ and $Q_g(t)$ are the active and reactive exchanging power with the utility grid, which they are positive for buying power from the utility grid and negative for selling power to the utility grid.

2.6.8 Emission Cost of Greenhouse Gases Model

The emission of carbon dioxide (CO_2), sulphur dioxide (SO_2), nitrogen oxide (NO_x) and particulate matter (PM) that are caused by burning the fossil fuel, which leads to environmental pollution. These greenhouse gases are considered in this work, where the emissions of the j^{th} greenhouse gases from i^{th} DG is converted to the corresponding expense by using this formula:

$$C_e((P_{DG_i}(t)) = \sum_{j=1}^{M}\sum_{i=1}^{N} E_{j\,i}\,.\,C_j.\,P_{DG_i}(t) \quad \textbf{(2.14)}$$

where C_j (€/kg) is a price of emission of j^{th} greenhouse gas, and $E_{j\,i}$ (kg/kWh) is the emission rate of the j^{th} greenhouse gas from i^{th} DG, M and N are the total number of the greenhouse gases and the DGs respectively.

2.6.9 Star-up and Shutdown Cost of the DGs Model

The behaviours of the generators start-up and shutdown are modelled in order to calculate the associated costs with these behaviours, where these costs affect the UC results of the DGs. The start-up and shutdown costs are calculated by the following equations [8]:

$$SU_{DG_i}(t) = Sc_i \,.\, (\delta_{DG_i}(t) - \delta_{DG_i}(t).\, \delta_{DG_i}(t-1)) \quad \textbf{(2.15)}$$

$$SD_{DG_i}(t) = Sd_i \,.\, (\delta_{DG_i}(t-1) - \delta_{DG_i}(t).\, \delta_{DG_i}(t-1)) \quad \textbf{(2.16)}$$

where $\delta_{DG_i}(t)$ is the state of i^{th} DG. Sc_i and Sd_i are the prices (€) of the start-up and shutdown cost of the i^{th} DG.

2.7 Modelling of Constraints

The optimisation problems are subjected to various equality and inequality constraints. These constraints should be satisfied and not violated when solving the optimisation problem. The proposed constraints are developed and presented in this section.

2.7.1 Power Balance the Constraints

The real-time balance of both the active and reactive power is essential for stable and secure operation of MGs, particularly for the MG that includes the renewable distributed generators (RDGs). These constraints are developed and expressed for connected and isolated MG as:

A. Active Power Balance

The real-time balance of active power generation with active load is presented as follows

$$\sum_{t=1}^{T}\{\sum_{i=1}^{N} \delta_{DG_i}(t).\, P_{DG_i}(t) + \sum_{i1=1}^{N1} P_{W_{i1}}(t) + \sum_{i2=1}^{N2} P_{PV_{i2}}(t) + P_b(t) + P_g(t) = P_{Dres}(t) + P_{Dind}(t) + P_{Dcom}(t)\} \quad \textbf{(2.17)}$$

where $P_{Dres}(t)$, $P_{Dcom}(t)$, and $P_{Dind}(t)$ are the residential, commercial and industrial active loads of the MG respectively.

For the isolated MG, the same equation is used with $P_g(t) = 0$, where the MG should meet active load demand from its energy resources.

B. Reactive Power Balance

The real-time balance of reactive power should be met at each time interval when solving the optimisation problem and it is formulated as follows:

$$\sum_{t=1}^{T}\{\sum_{i=1}^{N} \delta_{DG_i}(t).\, Q_{DG_i}(t) + Q_g(t) = Q_{Dres}(t) + Q_{Dind}(t) + Q_{Dcom}(t)\} \quad \textbf{(2.18)}$$

where $Q_{Dres}(t)$, $Q_{Dind}(t)$ and $Q_{Dcom}(t)$ are the residential, industrial, and commercial reactive loads of the MG respectively.

For isolated MG, the same equation is used with $Q_g(t) = 0$. The MG should meet the reactive load demand from its energy resources. Therefore, it is necessary to address the optimal scheduling of the reactive power as well.

2.7.2 Generators Operation Constraints

A. Ramp Rate Limit

It is inconvenient to increase or decreases the generation of any DG at a certain time interval ΔT more than or less than a specific value up–ramp limit (UR_i) or down-ramp limit (DR_i) in comparing to the previous generated level. This constraint should be met when the optimisation problem is solved and it is expressed as follows [76]:

$$-DR_i.\Delta t \leq P_{DG_i}(t+1) - P_{DG_i}(t) \leq UR_i.\Delta t \quad \textbf{(2.19)}$$

B. Generating Capacity

The DGs in the MG have minimum and maximum capacity limit for active and reactive power. These constraints should be satisfied at each time interval and they are formulated as

$$\delta_{DG_i}(t)\,.P_{DG_i min} \leq P_{DG_i}(t) \leq \delta_{DG_i}(t)\,.P_{DG_i max} \quad \textbf{(2.20)}$$

$$\delta_{DG_i}(t) \,.\, Q_{DG_i min} \leq Q_{DG_i}(t) \leq \delta_{DG_i}(t) \,.\, Q_{DG_i max} \quad \textbf{(2.21)}$$

where $P_{DG_i min}$ and $P_{DG_i max}$ are the minimum and maximum output active power of the i^{th} DG respectively, $Q_{DG_i min}$ and $Q_{DG_i max}$ are the respective minimum and maximum output reactive power.

C. Minimum up / Down Constraints

The generators have a minimum up/down (MUT_i /MDT_i) time constraint. The generator has to operate for a specific period after it switches on (T^{up})before it switches off. It also has to be off for a period (T^{down}) before it switches on again. These constraints are formulated as [8]

$$\delta_{DG_i}(t) - \delta_{DG_i}(t-1) \leq \delta_{DG_i}(\tau) \quad \text{(off/on switch)} \quad \textbf{(2.22)}$$

$$\delta_{DG_i}(t-1) - \delta_{DG_i}(t) \leq 1 - \delta_{DG_i}(\tau) \quad \text{(on/off switch)} \quad \textbf{(2.23)}$$

where in case of minimum up time

$$\tau = t+1 \ldots\ldots \min\left(t + T_i^{up} - 1, T\right) \quad \textbf{(2.24)}$$

Otherwise

$$\tau = t+1 \ldots\ldots \min\left(t + T_i^{down} - 1, T\right) \quad \textbf{(2.25)}$$

2.7.3 Exchanging Active and Reactive Power with the Utility Grid Management and Limit Models

The limits of exchanging active and reactive power with the utility grid are determined by the capacity of the line and the power electronic device that connect the utility grid with the MG. These limits should be satisfied for each time interval and these constraints are proposed and presented in this section. The exchanging active and reactive power with the utility grid at each period is normally either purchasing or selling active and reactive power. There are also possibilities that no exchanging power occurs between the MG and the utility grid at a certain period. Therefore, two binary variables $\delta_{gp}(t) \in \{0,1\}$

and $\delta_{gs}(t) \in \{0,1\}$, are assigned to represent this operation and the equation $\delta_{gp}(t) + \delta_{gs}(t) \leq 1$ is set to prevent buying and selling active and reactive power at the same time. With the minimum and maximum active and reactive power are selling to the utility grid, $P_{gsmin}(t)$, $P_{gsmax}(t)$, $Q_{gsmin}(t)$ and $Q_{gsmax}(t)$ together with the corresponding ones purchasing from the utility grid, $P_{gpmin}(t)$, $P_{gpmax}(t)$, $Q_{gpmin}(t)$, and $Q_{gpmax}(t)$. The exchanging operation constraints of the active and reactive power are accordingly formulated as:

$$\delta_{gp}(t) \,.\, P_{gpmin} \leq P_{gp}(t) \leq \delta_{gp}(t).\, P_{gpmax} \quad \textbf{(2.26)}$$

$$\delta_{gs}(t) \,.\, P_{gsmin} \leq P_{gs}(t) \leq \delta_{gs}(t).\, P_{gsmax} \quad \textbf{(2.27)}$$

$$\delta_{gp}(t) \,.\, Q_{gpmin} \leq Q_{gp}(t) \leq \delta_{gp}(t).\, Q_{gpmax} \quad \textbf{(2.28)}$$

$$\delta_{gs}(t) \,.\, Q_{gsmin} \leq Q_{gs}(t) \leq \delta_{gs}(t).\, Q_{gsmax} \quad \textbf{(2.29)}$$

2.7.4 Storage Batteries Constraints

The batteries normally have many operational constraints should be taken into consideration when formulating and solving the optimisation problem of the MG. The operating constraints of batteries normally are classified into two main categories as follows

A. State of Charge Constraints

To prolong the age of storage batteries, it is better to not be fully discharged. Therefore, the state of charge should keep between maximum and minimum values when the battery operates. This constraint is as follows:

$$E_{bmin} \leq E_b(t) \leq E_{bmax} \quad \textbf{(2.30)}$$

where E_{bmin}, E_{bmax} are the minimum and maximum state of charge respectively.

B. Charging and Discharging Power Constraints

The battery status of each sampling period can be described as three possible states: charging, discharging, and no exchanging power. Therefore, two binary

variables, $\delta_{bch} \in \{0,1\}$ and $\delta_{bdis} \in \{0,1\}$, are assigned to formulate the status of the battery operation and $\delta_{bch} + \delta_{bdis} \leq 1$ is set to prevent the battery from charging and discharging simultaneously during the optimisation. The charging and discharging operations constraints for storage battery are accordingly formulated as [37]:

$$\delta_{bch}(t).P_{bchmin} \leq P_{bch}(t) \leq \delta_{bch}(t).P_{bchmax} \quad \textbf{(2.31)}$$

$$\delta_{bdis}(t).P_{bdismin} \leq P_{bdis}(t) \leq \delta_{bdis}(t).P_{bdismax} \quad \textbf{(2.32)}$$

where P_{bchmin} and P_{bchmax} are the minimum and maximum charging power of the battery respectively, while $P_{bdismin}$ and $P_{bdismax}$ are the respective minimum and the maximum discharging power of the storage battery.

2.7.5 Emission of Greenhouse Gases Limits

The incorporation of emission cost and the emission limit of greenhouse gases constraints within optimisation problem are fitted with trending to reduce the environmental damage. The constraints of greenhouse gases in the area of the MG are expressed as:

$$\sum_{i=1}^{N} E_{j\,i}\,.P_{DG_i}(t) \leq L_j \quad \textbf{(2.33)}$$

where L_j (kg/h) is the allowable emission level of the greenhouse gas j in the MG, where $(j = 1, 2, 3 \ldots \ldots . M)$.

2.7.6 Active and Reactive Steady State Security Constraints

The active and reactive SSSCs are proposed and presented in this section. The SSSCs are essential for the reliable and secure operation of MGs and have to be satisfied at each time interval. The steady state secure operation of the MGs is examined in the sense of adequacy of supply. The most common contingency of the MGs is the loss of connection with the utility grid. In this case, the MG operates in isolated mode and it should supply its load from its energy resources. If the MG meets its load, this means that the MG operates in steady state secure otherwise it is considered insecure. The SSSCs guarantee

the secure operation of the MG when losing the connection with the utility grid and the SSSCs prevent the MG from resorting to the costly involuntary load curtailed. The active and reactive SSSCs are formulated as:

$$\sum_{i=1}^{T}\{\sum_{i=1}^{N}\delta_{DG_i}(t).P_{DG_imax}(t) \geq P_{Dres}(t) + P_{Dind}(t) + P_{Dcom}(t)\} \quad \textbf{(2.34)}$$

$$\sum_{i=1}^{T}\{\sum_{i=1}^{N}\delta_{DG_i}(t).Q_{DG_imax}(t) \geq Q_{Dres}(t) + Q_{Dind}(t) + Q_{Dcom}(t)\} \quad \textbf{(2.35)}$$

2.7.7 Spinning Reserve Constraints

Spinning reserve is important to protect the grid against unpredicted disturbance such as sudden load increasing, generation unit outage, fluctuation RDGs generation. The SRCs of the active and reactive power are proposed and incorporated with optimisation problems for reliable and secure operation of the isolated MG. These constraints need to be met at each time interval for reliable operation of the grid. The SRs for active and reactive power for grid-isolated mode are given by these proposed equations:

$$\sum_{t=1}^{T}\{\sum_{i=1}^{N}\delta_{DG_i}(t).P_{DG_imax}(t) \geq (P_{Dres}(t) + P_{Dind}(t) + P_{Dcom}(t)) + R_p(t)\} \quad \textbf{(2.36)}$$

$$\sum_{t=1}^{T}[\sum_{i=1}^{N}\delta_{DG_i}(t).Q_{DG_imax}(t) \geq (Q_{Dres}(t) + Q_{Dind}(t) + Q_{Dcom}(t)) + R_q(t)] \quad \textbf{(2.37)}$$

where $R_p(t)$ and $R_q(t)$ are the spinning reserves for the active and reactive power.

2.8 Proposed Deterministic Multi-Period SCUC-UARDEED

The proposed optimisation approach is formulated by MIQP under two market polices: either minimising the total operating and emission costs or maximising the profit. Figure 2-2 shows the essential step to formulate and solve the SCUC-UARDEED of the MG. The cost function of each components of the MG should be modelled then the equality and inequality constraints are modelled as well. These models are employed to formulate the objective functions. Finally, the optimisation problems are solved to determine at each time intervals, the total operating cost or the profit, the active and reactive power generation of the

DGs, the exchanging active and reactive power with the utility grid, exchanging active power with the battery, and the on/off state of the DGs.

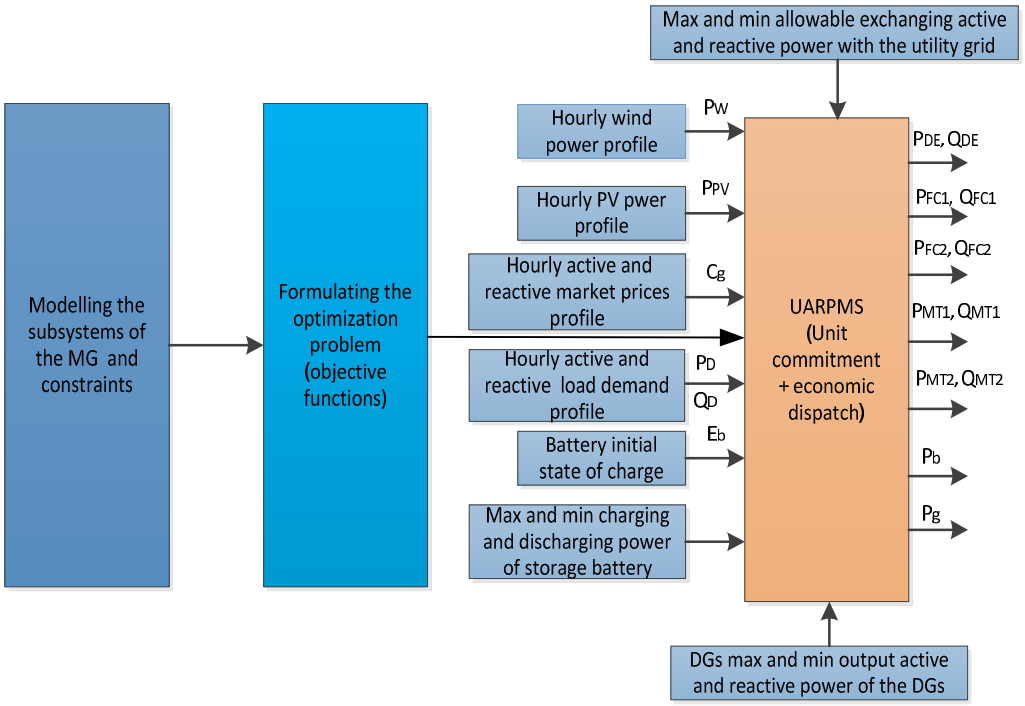

Figure 2-2 Proposed the SCUC-UARDEED structure

2.9 Proposed Deterministic Objective Functions

Two objective functions are proposed and developed as follows:

2.9.1 Minimisation the Total Operating Cost

The aim of this policy is to minimise the total operating and emission costs of the MG. The objective function of the connected MG includes the fuel cost of the DGs, reactive power production cost, start-up and shut down cost, maintenance cost of the DGs, environmental cost, battery degradation cost, purchasing active and reactive power from the utility grid cost, and power production cost of the WT and PV panels. In the isolated MG, the objective function includes the same cost components excluding the cost of exchanging power with the utility grid. The objective functions of the connected and isolated MG are formulated by employing the models of the MG components in the previous sections as follows:

A. Connected MG

The optimisation problem is formulated as

$$\min(F) \tag{2.38}$$

where the objective function F is

$$F = \sum_{t=1}^{T}\Big\{\sum_{i=1}^{N}[[CP_{DG_i}(P_{DG_i}(t)) + CQ_{DG_i}(Q_{DG_i}(t)) + COM_{DG_i}(P_{DG_i}(t))]\delta_{DG_i}(t) + SU_{DG_i}(t) + SD_{DG_i}(t)] + C_e(P_{DG_i}(t)) + C_{bo}(t) + C_{gP}(t) + C_{gQ}(t) + \sum_{i1=1}^{N1} CP_{W_{i1}}(P_{W_{i1}}(t)) + \sum_{i2=1}^{N2} CP_{PV_{i2}}(P_{PV_{i2}}(t))\Big\} \tag{2.39}$$

This is constructed using equations

(2.1), (2.2), (2.3), (2.15), (2.16), (2.14), (2.11), (2.12), (2.13), (2.5), and (2.6).

B. Isolated MG

Similarly, the optimisation problem of the isolated MG is formulated as

$$\min(F) \tag{2.40}$$

where the objective function F is

$$F = \sum_{t=1}^{T}\Big\{\sum_{i=1}^{N}[[CP_{DG_i}(P_{DG_i}(t)) + CQ_{DG_i}(Q_{DG_i}(t)) + COM_{DG_i}(P_{DG_i}(t))]\delta_{DG_i}(t) + SU_{DG_i}(t) + SD_{DG_i}(t)] + C_e(P_{DG_i}(t)) + C_{bo}(t) + \sum_{i1=1}^{N1} CP_{W_{i1}}(P_{W_{i1}}(t)) + \sum_{i2=1}^{N2} CP_{PV_{i2}}(P_{PV_{i2}}(t))\Big\} \tag{2.41}$$

This is constructed using equations

(2.1), (2.2), (2.3), (2.15), (2.16), (2.14), (2.11), (2.5), and (2.6).

2.9.2 Maximisation of the MG Profit

The goal of this policy is to generate the electricity with low cost and sell it with the maximum profit, meantime, keeping the environment safe by adding the constraints of the emission limits of the greenhouse gases. The revenue of the MG comes from selling active and reactive power to the consumers and trading active and reactive power with the utility grid. It is assumed that the MG sells power to the consumers and to the utility by OMPs in case of the connected

MG. In case of the isolated MG, the electricity is sold to the consumers with different price from the OMP. The maximising profit of the connected and isolated MG are driven as:

A. Connected MG

The optimisation problem is formulated as

$$\max(F) \tag{2.42}$$

where

$$F = (Revenue - Expense) \tag{2.43}$$

where revenue of the MG is calculated as

$$Revenue = \sum_{t=1}^{T}\{\sum_{i=1}^{N}[c_{gP}(t).P_{DG_i}(t) + c_{gQ}(t).Q_{DG_i}(t)]\delta_{DGi}(t) + c_{gP}(t).P_{bdis}(t).\Delta t + c_{gP}(t).\sum_{i2=1}^{N2}P_{PV_{i2}}(t) + c_{gP}(t).\sum_{i1=1}^{N1}P_{W_{i1}}(t) + c_{gP}(t).P_{gp}(t) + c_{gQ}(t).Q_{gp}(t)\} \tag{2.44}$$

and expense is

$$Expense = \sum_{t=1}^{T}\{\sum_{i=1}^{N}[[CP_{DG_i}(P_{DG_i}(t)) + CQ_{DG_i}(Q_{DG_i}(t)) + COM_{DG_i}(P_{DG_i}(t))]\delta_{DG_i}(t) + SU_{DG_i}(t) + SD_{DG_i}(t)] + C_e(P_{DG_i}(t)) + C_{bo}(t) + c_{gP}.P_{bch}(t).\Delta t + c_{gP}(t).P_{gp}(t) + c_{gQ}(t).Q_{gp}(t) + \sum_{i1=1}^{N1}CP_{W_{i1}}(P_{W_{i1}}(t)) + \sum_{i2=1}^{N2}CP_{PV_{i2}}(P_{PV_{i2}}(t))\} \tag{2.45}$$

giving

$$F = \sum_{t=1}^{T}\{\sum_{i=1}^{N}[c_{gP}(t).P_{DG_i}(t) + c_{gQ}(t).Q_{DG_i}(t)]\delta_{DG_i}(t) + c_{gP}(t).P_{bdis}(t).\Delta t + c_{gP}(t).\sum_{i2=1}^{N2}P_{PV_{i2}}(t) + c_{gP}(t).\sum_{i1=1}^{N1}P_{W_{i1}}(t)\} - \sum_{t=1}^{T}\{\sum_{i=1}^{N}[[CP_{DG_i}(P_{DG_i}(t)) + CQ_{DG_i}(Q_{DG_i}(t)) + COM_{DG_i}(P_{DG_i}(t))]\delta_{DG_i}(t) + SU_{DG_i}(t) + SD_{DG_i}(t)] + C_e(P_{DG_i}(t)) + C_{bo}(t) + c_{gP}.P_{bch}(t).\Delta t + \sum_{i1=1}^{N1}CP_{W_{i1}}(P_{W_{i1}}(t)) + \sum_{i2=1}^{N2}CP_{PV_{i2}}(P_{PV_{i2}}(t))\} \tag{2.46}$$

The revenue of the MG comes from selling the active and reactive power from the DGs, the discharging power of the battery, the power from the RDGs. The cost is constructed using equations

(2.1), (2.2), (2.3), (2.15), (2.16), (2.14), (2.11), (2.5), (2.6), and cost of charging the battery.

B. Isolated MG

For the isolated MG, the objective function is formulated as:

$$\max(F) \tag{2.47}$$

where the objective function F is

$$\begin{aligned} F = \sum_{t=1}^{T}\{\sum_{i=1}^{N}[c_{isoP}(t).P_{DG_i}(t) + c_{isoQ}(t).Q_{DG_i}(t)]\delta_{DG_i}(t) + \\ c_{isoP}(t).P_{bdis}(t).\Delta t + c_{isoP}(t).\sum_{i2=1}^{N2}P_{PV_{i2}}(t) + c_{isoP}(t).\sum_{i1=1}^{N1}P_{W_{i1}}(t)\} - \\ \sum_{t=1}^{T}\{\sum_{i=1}^{N}[[CP_{DG_i}(P_{DG_i}(t)) + CQ_{DG_i}(Q_{DG_i}(t)) + COM_{DG_i}(P_{DG_i}(t))]\delta_{DG_i}(t) + \\ SU_{DG_i}(t) + SD_{DG_i}(t)] + C_e(P_{DG_i}(t)) + C_{bo}(t) + c_{isoP}(t).P_{bch}(t).\Delta t + \\ \sum_{i1=1}^{N1}CP_{W_{i1}}(P_{W_{i1}}(t)) + \sum_{i2=1}^{N2}CP_{PV_{i2}}(P_{PV_{i2}}(t))\} \end{aligned} \tag{2.48}$$

where $c_{isoP}(t)$ in (€/kWh) and $c_{isoQ}(t)$ in (€/kVArh) are the prices that are considered to sell the active and reactive power to the consumers.

The revenue of the MG comes from selling the active and reactive power from the DGs, the discharging power of the battery, the power from the RDGs. The cost is constructed using equations

(2.1), (2.2), (2.3), (2.15), (2.16), (2.14), (2.11), (2.5), (2.6), and cost of charging the battery.

The objective functions of equations (2.39) and (2.46) are subjected to the constraints of equations (2.17) to (2.35), whereas the objective functions of equations (2.41) and (2.48) are subjected to the constraints of equations (2.17) to (2.25), (2.30) to (2.33), (2.36), and (2.37).

2.10 Case study

In this section, the proposed optimisation approaches are applied to the connected and isolated MG and different scenarios are carried out to verify the effectiveness of the proposed approaches. The impacts of the reactive power that is generated from GDs are analysed by comparison with the case of the reactive power that purchased from the utility grid solely. In addition, the quantifications of the impacts of the storage battery and the SSSCs on the optimal operation of the MG in the both market policies are carried out. Software package, ILOG CPLEX version 12.6 [77], [78], [79] which interfaced with Microsoft Excel is employed to solve the optimisation problems. While, OpenDSS (Open Distribution System Simulator) is employed to formulate and solve the power flow of the proposed MG to find the bus voltages [80]. The openDss is used either autonomously or driven by other software programmes. In this research, the OpenDss which is driven by MATLAB software is considered [81], [82].

2.11 Test System

The proposed optimisation approaches are validated by applying the optimisation problems on the multi-feeder hybrid MG as shown in Figure 2-3. The proposed MG is a hybrid modified and updated version of the MG which has been proposed in [83]. It is a LV distribution network, which it consists of nineteen bus bars and four feeders; where the line impedances are listed in Table A-1 [83], [84], [85]. Thereinto, the residential feeders supply 192 customers, where each one supplies 96 consumers, while the industrial and commercial feeders supplying the respective workshops and commercial loads. The typical aggregated daily load curves for each type are shown in Figure 2-4 [86], [83] . The maximum active loads of residential, Industrial and commercial areas are 192 kW, 60 kW and 130 kW respectively. The power factor is assumed 0.9 for the entire system. In addition, the MG includes different types of the DGs technology, such as a DE, two MTs, two FCs, two WTs, and four PV systems. The corresponding DGs technical parameters are listed in Table B-1

[8], [57], [87] [88], while the emission rate and the emission cost coefficients of the DGs are illustrated in Table B-2 and Table B-3 [87], [89], [90], [91], [92]. The wind Turbines data are presented in Table B-4 [86]. Moreover, the system includes a lithium ion storage battery, wherein the battery data are illustrated in the Table B-5.The hourly profiles of a typical day for wind, PV power generation for one system, OMPs [53], [86], and the total active and reactive loads are shown in Table B-6.

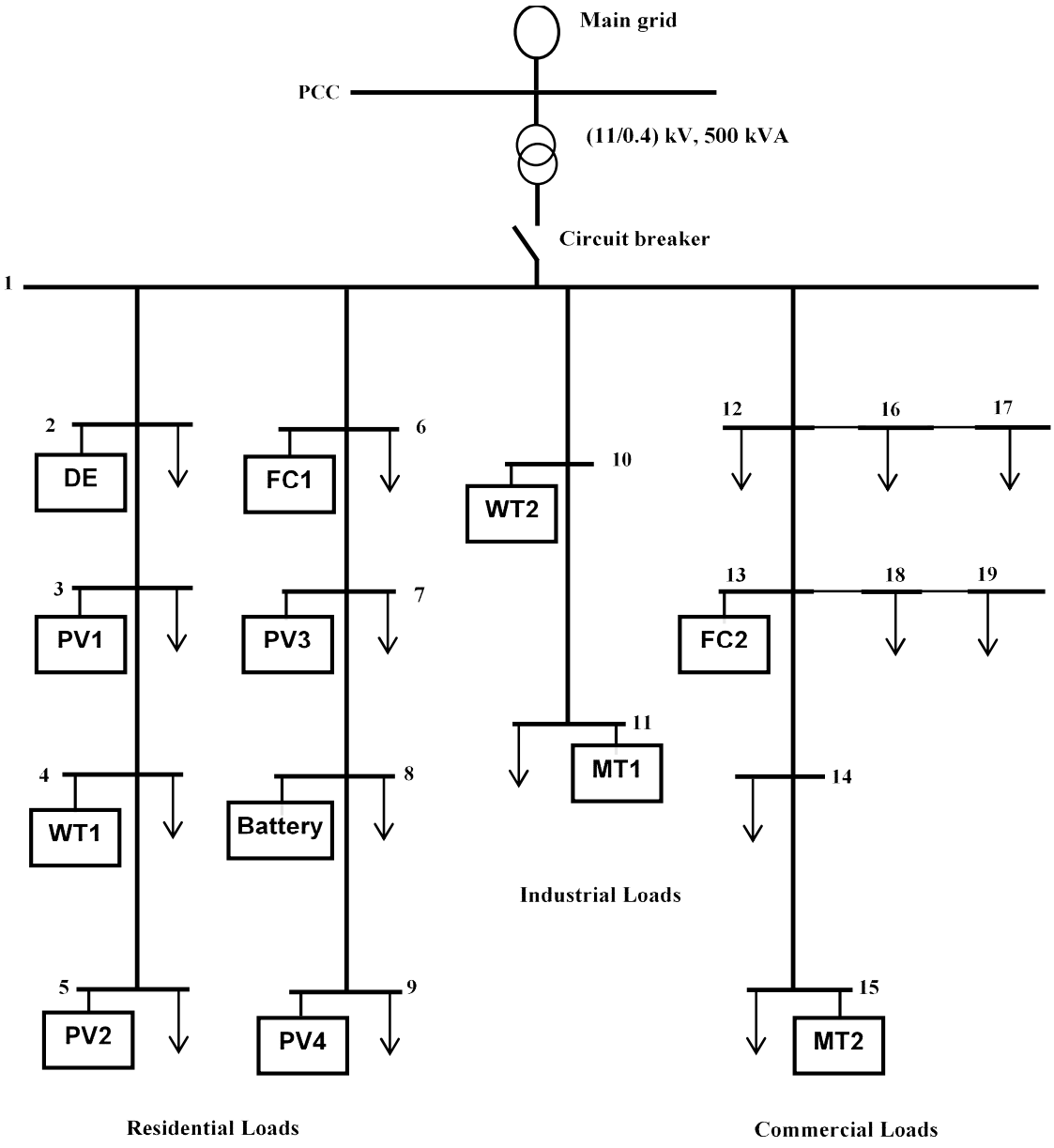

Figure 2-3 Structure of the multi-feeder MG test system

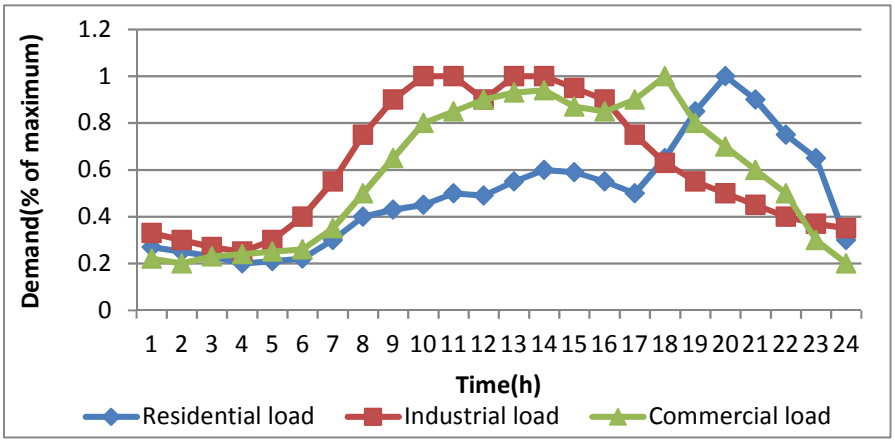

Figure 2-4 Daily load curves for the three loads types of the MG

2.12 Results of the SCUC-UARDEED of the MG

The proposed optimisation approach is applied to both the connected and isolated proposed MG. The results are obtained by running the simulation on the Inter (R) core (TM) i5 CPU, 2.6 GHz. The longest run for the connected MG took 3.6 s, while for isolated MG took 5.5 s.

2.12.1 Results of Minimising the Total Operating Cost

In this case, the DGs generate active and reactive power and the battery is assumed fully charge at the beginning and the end of the scheduling day.

A. Connected MG

Figure 2-5 and Figure 2-6 show the exchanging active and reactive power with the utility grid. It can be observed that the MG sells active and reactive power to the utility grid at hours 12, 13 and 16 to 21 when the OMPs have high values and exceed the cost of generation of the DGs in order to minimise the overall operating cost or maximises the profit. Exactly for the same purpose, the MG purchases active and reactive power from the utility grid at rest hours of the scheduling day when the OMPs reach low values. The DE is normally committed at hours 1 to 7 and 24 with minimum active and reactive power generation to satisfy the active and reactive SSSCs as shown in Figure 2-7. The DE is committed at hours 1 to 7, although the MT1 and FC1 have lower

operating cost than DE. This is because neither MT1 nor FC1 can satisfy the active and reactive SSSCs. In addition, Figure 2-8 shows that at hours 1 to 7 the reactive loads are supplied by purchasing power from the utility grid solely because the minimum output reactive power of the DE is equal to zero. Further, the DGs generate the highest active and reactive power at hours 13, 17, 19, and 21 to sell the highest active and reactive power to the utility grid to reduce the total operating cost or increase the profit because the OMPs have the highest values at these hours during the scheduling day.

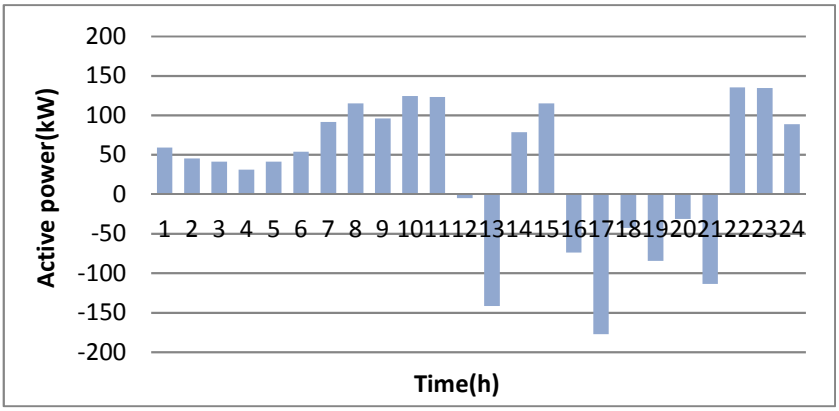

Figure 2-5 Optimal exchanging active power with the utility grid

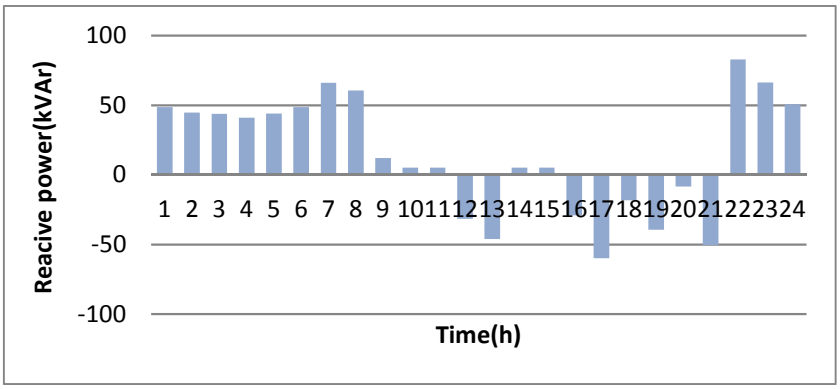

Figure 2-6 Optimal exchanging reactive power with the utility grid

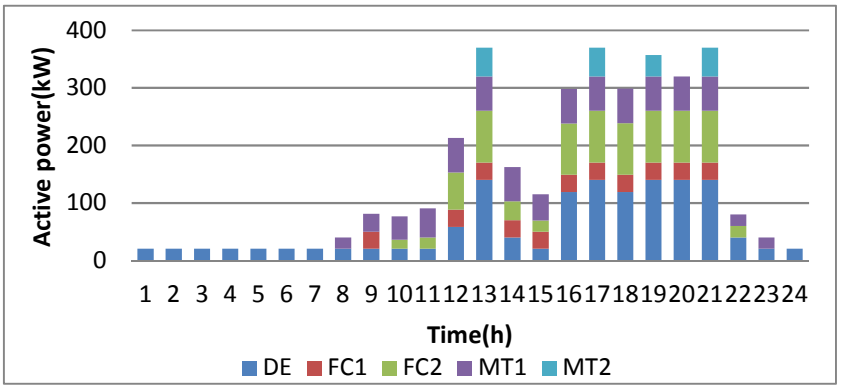

Figure 2-7 Optimal active power scheduling of the DGs

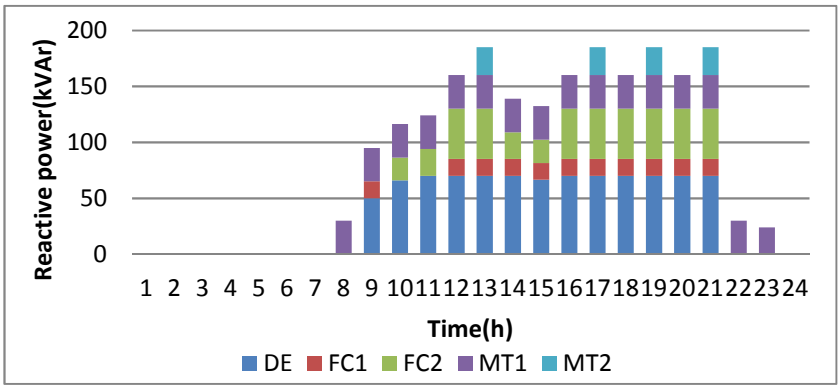

Figure 2-8 Optimal reactive power scheduling of the DGs

Furthermore, the storage battery is discharged its maximum active power at hour 17 when the OMP reaches the highest value, while it is charged at the low OMP as shown in Figure 2-9. Therefore, the storage battery charging and discharging operations are scheduled to effectively reduce the total operating cost or increase the MG profit.

Figure 2-10 shows the costs of active power, reactive power, emission, and total cost. This figure shows that at hour 17 the active and reactive power costs have negative values. This means that the MG gains revenue because the MG sells the highest active and reactive power to the utility grid at this hour and the OMPs have by far the highest value. The reactive power cost at hours 1 to 7 is significantly low because at these hours, the reactive power generation of the DGs is zero and the reactive OMP is very low at these hours. In addition, the emission cost at hours 13, 17, 19 and 21 has the highest values because the

DGs generate the highest power. Moreover, the highest total operating cost occurs at hour 20 because the active and reactive loads have the highest values at this hour.

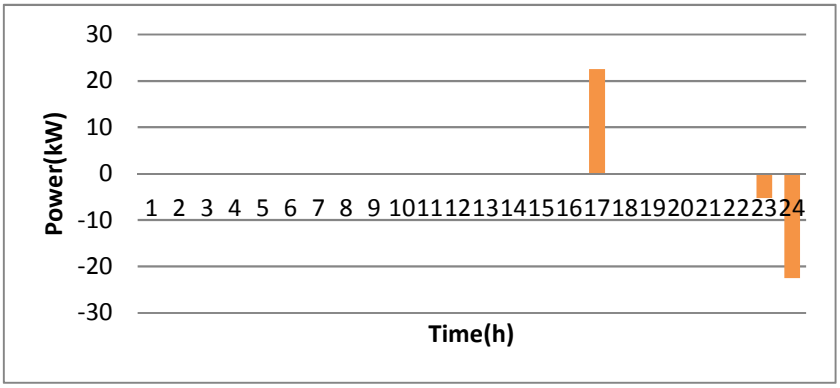

Figure 2-9 Optimal charging and discharging scheduling of the battery

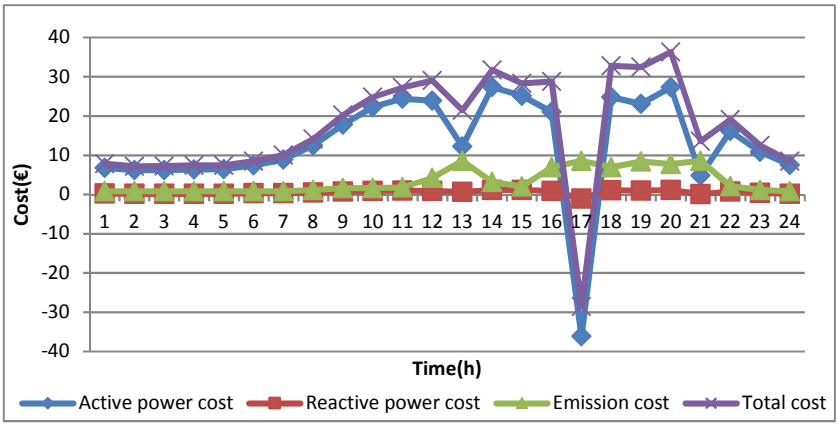

Figure 2-10 Optimal costs of active, reactive power, emission, and total

Table 2-1 shows the optimal on/off state of the DGs during the scheduling day. In this table, the cell with red colour means the corresponding generator is committed at that hour, while the one with green colour means the generator is uncommitted. On the other hand, the number one in the table means the corresponding generator is committed, while zero means the generator is uncommitted. This table shows that the DE is committed during the entire scheduling day to supply base load and to satisfy the active and reactive SSSCs constraints, whereas the MT2 is committed least hours among the DGs because it has the highest operating cost. Therefore, it is committed when the

OMPs have high values to sell highest active and reactive power to the utility grid. Overall, the total cost per scheduling day is 408.1 €.

Table 2-1 Optimal on/off state of the DGs of the connected MG

T(h)	1	2	3	4	5	6	7	8	9	10	11	12	13	14	15	16	17	18	19	20	21	22	23	24
DE	1	1	1	1	1	1	1	1	1	1	1	1	1	1	1	1	1	1	1	1	1	1	1	1
FC1	0	0	0	0	0	0	0	0	1	0	0	1	1	1	1	1	1	1	1	1	1	0	0	0
FC2	0	0	0	0	0	0	0	0	0	1	1	1	1	1	1	1	1	1	1	1	1	1	0	0
MT1	0	0	0	0	0	0	0	1	1	1	1	1	1	1	1	1	1	1	1	1	1	1	1	0
MT2	0	0	0	0	0	0	0	0	0	0	0	0	1	0	0	0	1	0	1	0	1	0	0	0

1 On state of the DG 0 Off state of the DG

The above discussion reveals that at some hours the DGs are committed with minimum output power to satisfy the SSSCs. Therefore, reducing the minimum characteristic output active power of the DGs to half reduces the total cost to 399.6 € and reduces the emission level of greenhouse gases by 6.2 %. This is an important finding of this research. Table 2-2 illustrates the components of the total cost per scheduling day. This table shows that the reduction of the minimum output active power of the DGs affects the cost components that they are corresponding to the active power generation.

Table 2-2 Components of the total cost of the connected MG

Components of the total cost	Cost (€/day)	Cost (€/day) for half minimum output
Active power cost	295.3	285.2
Active power cost of WTs	53.7	53.7
Active power cost of PVs	37.4	37.4
Reactive power cost	17.9	17.9
Maintenance cost	27.4	25.3
Start-up cost	1	1
Shutdown cost	1.6	1.6
Cost of exchanging active power with the utility grid	-105.6	-95.5
Cost of exchanging reactive power with the utility grid	-4.6	-4.6
Battery degradation cost	2.9	2.9
Emission cost	81.1	74.7
Total cost	408.1	399.6

B. Isolated MG

Figure 2-11 and Figure 2-12 depict the optimal active and reactive power scheduling respectively. It can be noticed that the MT1 and DE are committed at hours 1 to 6 to supply the active and the reactive load demand with RDGs. The DE is committed at these hours with the minimum output to satisfy the active and reactive SRCs, while the MT1 supplies the load with RDGs because it is cheaper than increasing the generation of the DE. It also is seen that the highest active and reactive power generation occurs at hour 20 because the load has the highest value, while the lowest value at hour 4 because the load reaches the lowest value during the scheduling day. Moreover, the DGs generate both active and reactive power for the entire scheduling day because there is no connection with the utility grid.

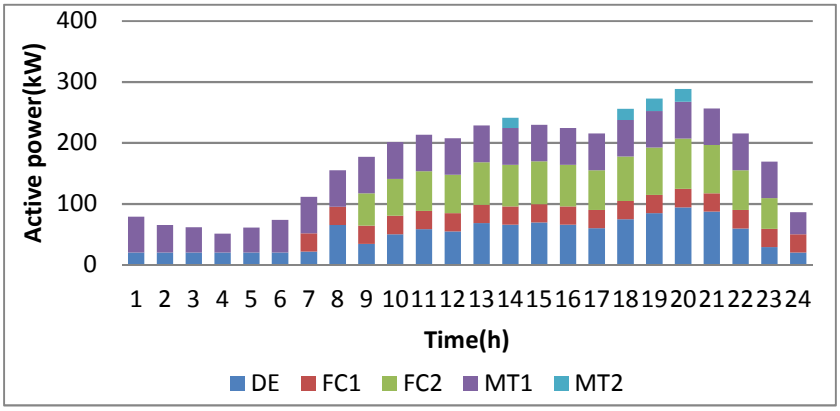

Figure 2-11 Optimal active power scheduling of the DGs

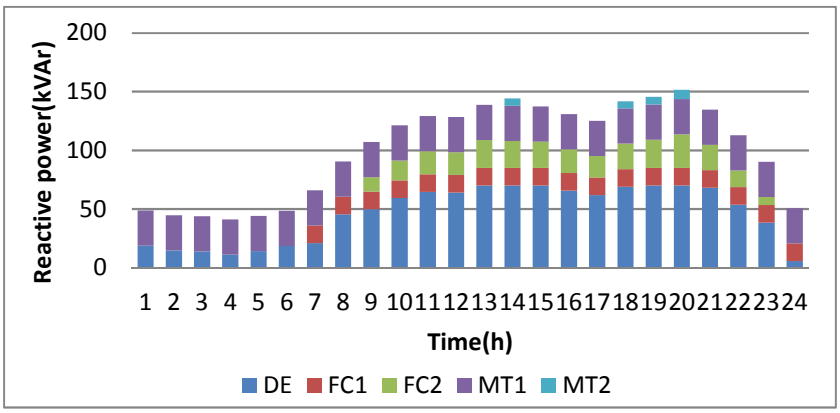

Figure 2-12 Optimal reactive power scheduling of the DGs

In addition, it is seen that the storage battery has no involvement in the entire scheduling period since it has high operating cost and there are no economic incentives for operating the battery. Furthermore, results show that the pattern of active and reactive power generation of the DGs almost close to the total load patterns, while in the case of connected MG is significantly different from the load pattern because the utility grid is involved in the supplying the loads. Figure 2-13 shows the hourly costs of active power, reactive power, emission, and the total. This figure reveals that the highest active, reactive and emission costs occur at hour 20 because the total loads have the highest value and the DGs generate the highest active and reactive power. The costs have only positive values because the MG operates in the isolated MG and no trading active and reactive power with the utility grid to gain revenue. Furthermore, the shapes of the total cost patterns are close to the generation pattern of the DGs because there is no exchanging power with the utility grid and the battery does not operate.

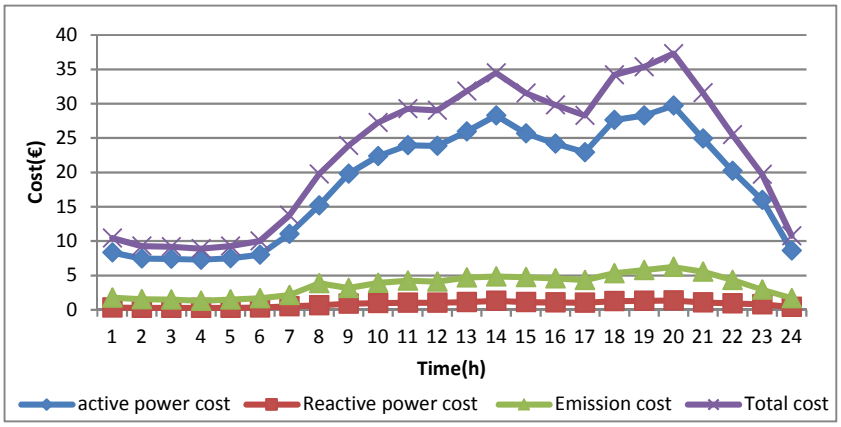

Figure 2-13 Optimal costs of active power, reactive power, emission, and total

Table 2-3 illustrates the optimal on/off state of the DGs in details. This table reveals that the MT1 is committed for the entire scheduling day because it has the lowest operating cost among the DGs. While, the MT2 is committed only for 4 hours to satisfy the active and reactive SRCs because it has the highest operating cost among the DGs. DE is committed for the entire scheduling period to supply the base load and satisfy the active and reactive SRCs, where DE is

committed with minimum output in some hours. The overall cost per scheduling day is 550.2 €. Table 2-4 illustrates the components of the overall cost per scheduling day in details.

Table 2-3 Optimal on/off state of the DGs of the isolated MG

T(h)	1	2	3	4	5	6	7	8	9	10	11	12	13	14	15	16	17	18	19	20	21	22	23	24
DE	1	1	1	1	1	1	1	1	1	1	1	1	1	1	1	1	1	1	1	1	1	1	1	1
FC1	0	0	0	0	0	0	1	1	1	1	1	1	1	1	1	1	1	1	1	1	1	1	1	1
FC2	0	0	0	0	0	0	0	0	1	1	1	1	1	1	1	1	1	1	1	1	1	1	1	0
MT1	1	1	1	1	1	1	1	1	1	1	1	1	1	1	1	1	1	1	1	1	1	1	1	1
MT2	0	0	0	0	0	0	0	0	0	0	0	0	0	1	0	0	0	1	1	1	0	0	0	0

1 On state of the DG 0 Off state of the DG

Table 2-4 Components of the operating cost of the isolated MG

Components of the total cost	Cost (€/day)
Active power cost	322.5
Active power cost of WTs	53.7
Active power cost of PVs	37.4
Reactive power cost	19.7
Maintenance cost	29.6
Start-up cost	0.6
Shutdown cost	0.9
Battery operating cost	0
Emission cost	85.8
Total cost	550.2

2.12.2 Results of Maximising the Profit of the MG

In this case, the optimisation approach is applied to the connected and isolated MG to maximise the profit of the MG.

A. Connected MG

The optimal scheduling of the active and reactive power of the DGs, the exchanging active, reactive power with the utility grid and the battery, and the on/off states of the DGs are the same in the case of minimising the total operating cost. The same discussion of minimising the operating cost can be considered for maximising the MG profit as well. Figure 2-14 shows the optimal revenue, expense, and profit. This figure shows that the highest value of the revenue and the profit occurs at hours 13, 17, 19 and 21 because the OMPs

have the highest values and the MG sells the highest active and reactive power to the utility grid at these hours. In addition, the highest expense occurs at hour 13, 17, 19, and 21 because the DGs generate the highest active and reactive power. Furthermore, the shape of the revenue pattern is quite close to the pattern shape of the OMP because the MG sells power to the consumers and trading power with the utility grid by the OMPs. It is found that the profit per scheduling day is 281.2 €, while the profit in case of reducing the minimum active power of the DGs to half is 289.7 €.

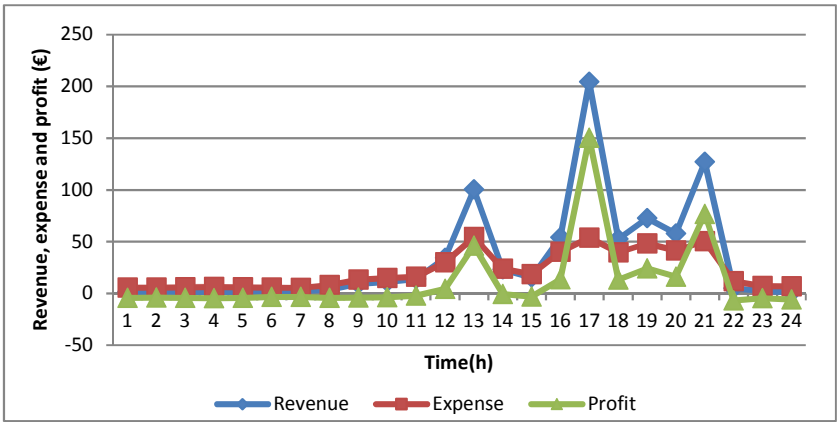

Figure 2-14 Optimal hourly revenue, expense and profit

Table 2-5 shows the profit components of the both cases. This table reveals that the reducing the minimum output active power of the DGs to half increase the profit by 3%. This is a new important finding for this work.

Table 2-5 Components of the MG profit of the connected MG

Components of the profit	Profit (€/day)	Profit (€/day) for half min output active power of the DGs
Revenue	800.3	790.2
Expense	519.1	500.5
Profit	281.2	289.7

B. Isolated MG

The optimal scheduling of the active and reactive power, the exchanging power with the battery, and the on/off states of the DGs are the same of the minimising

the operating cost. Figure 2-15 shows the hourly revenue, expense, and profit. This figure reveals that the highest profit is at hour 13, although the highest load is at hour 20 because at hour 20 the MT2 is committed to satisfy the SRCs comparing with hour 13. The patterns shape of the revenue and the profit are close to the generation pattern shape because there is no trading power with the utility grid and the prices of the selling active and reactive power to the consumers are fixed. It is found that the profit per scheduling day is 234 €. Table 2-6 illustrates the main components of the profit per scheduling day.

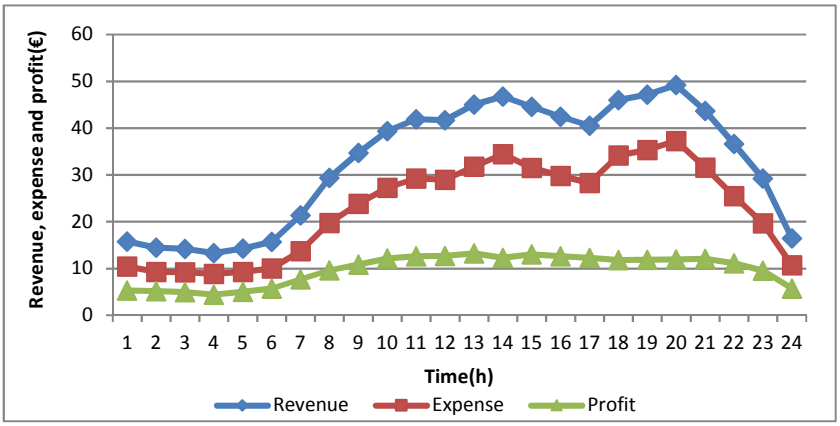

Figure 2-15 Hourly revenue, expense and profit

Table 2-6 Components of the MG profit of the isolated MG

Components of the profit (€/day)	Profit (€/day)
Revenue	784.2
Expense	550.2
Profit	234

In comparison between the connected and isolated MG, it can be deduced that in the connected MG, the lowest cost occurs at the same time with the highest profit and they occur when the OMPs have the highest value. The profit pattern has the same shape of the OMP, while for the isolated MG the profit and the cost have the close shape of the DGs. In addition, the profit and the total cost in case of the connected MG might have negative values, while in the isolated MG the total operating cost and profit always have positive values.

2.13 Reactive Power from the Utility Grid

In this section, a comparison between case the DGs give reactive power and the case when the reactive power is supplied from the utility grid solely. Two scenarios are considered as follows:

Sc1: the DGs generate active power only and the reactive power is delivered from the utility grid and the MG purchases active and reactive power from the utility grid and no selling active power to the utility grid.

Sc2: the DGs provide reactive power and the MG purchases active and reactive power from the utility grid and no selling active or reactive power to the utility grid.

The same constraints are considered to the both scenarios. The whole power factor is assumed 0.9 and the impedance data are presented in the Table A-1. The objective functions of minimising the overall cost and maximising the profit are slightly changed and they are formulated as

2.13.1 Minimising the Total Operating Cost

The problem is formulated as

$$\min(F) \tag{2.49}$$

where the objective function F for the Sc1 is

$$F = \sum_{t=1}^{T}\{\sum_{i=1}^{N}[[CP_{DG_i}(P_{DG_i}(t)) + COM_{DG_i}(P_{DG_i}(t))]\delta_{DG_i}(t) + SU_{DG_i}(t) + SD_{DG_i}(t)] + C_e(P_{DG_i}(t)) + C_{bo}(t) + C_{gP}(t) + C_{gQ}(t) + \sum_{i1=1}^{N1} CP_{W_{i1}}(P_{W_{i1}}(t)) + \sum_{i2=1}^{N2} CP_{PV_{i2}}(P_{PV_{i2}}(t))\} \tag{2.50}$$

This is constructed using equations

(2.1), (2.3), (2.15), (2.16), (2.14), (2.11), (2.12), (2.13), (2.5), and (2.6). With changing $P_g(t)$ to $P_{gp}(t)$ in equation (2.12) and $Q_g(t)$ to $Q_{gp}(t)$ in equation (2.13).

and the objective function F for the Sc2 is

$$F = \sum_{t=1}^{T}\{\sum_{i=1}^{N}[[CP_{DG_i}(P_{DG_i}(t)) + CQ_{DG_i}(Q_{DG_i}(t)) + COM_{DG_i}(P_{DG_i}(t))]\delta_{DG_i}(t) + SU_{DG_i}(t) + SD_{DG_i}(t)] + C_e(P_{DG_i}(t)) + C_{bo}(t) + C_{gP}(t) + C_{gQ}(t).Q_{gp}(t) + \sum_{i1=1}^{N1} CP_{W_{i1}}(P_{W_{i1}}(t)) + \sum_{i2=1}^{N2} CP_{PV_{i2}}(P_{PV_{i2}}(t))\} \quad \textbf{(2.51)}$$

This is constructed using equations

(2.1), (2.2), (2.3), (2.15), (2.16), (2.14), (2.11), (2.12), (2.13), (2.5), and (2.6). With changing $P_g(t)$ to $P_{gp}(t)$ in equation (2.12) and $Q_g(t)$ to $Q_{gp}(t)$ in equation (2.13).

2.13.2 Maximising the MG Profit

The problem is formulated as

$$\max(F) \quad \textbf{(2.52)}$$

where the objective function F for the Sc1 is

$$F = \sum_{t=1}^{T}\{\sum_{i=1}^{N} \delta_{DG_i}(t).c_{gP}(t).P_{DG_i}(t) + c_{gP}(t).P_{bdis}(t).\Delta t + c_{gP}(t).\sum_{i2=1}^{N2} P_{PV_{i2}}(t) + c_{gP}(t).\sum_{i1=1}^{N1} P_{W_{i1}}(t)\} - \sum_{i=1}^{T}\{\sum_{i=1}^{N}[[CP_{DG_i}(P_{DG_i}(t)) + COM_{DG_i}(P_{DG_i}(t))]\delta_{DG_i}(t) + SU_{DG_i}(t) + SD_{DG_i}(t)] + C_e(P_{DG_i}(t)) + C_{bo}(t) + c_{gP}(t).P_{bch}(t).\Delta t + \sum_{i1=1}^{N1} CP_{W_{i1}}(P_{W_{i1}}(t)) + \sum_{i2=1}^{N2} CP_{PV_{i2}}(P_{PV_{i2}}(t))\} \quad \textbf{(2.53)}$$

The revenue of the MG comes from selling the active power from the DGs, the discharging power of the battery, the power from the RDGs. The cost is constructed using equations

(2.1), (2.3), (2.15), (2.16), (2.14), (2.11), (2.5), (2.6), and cost of charging the battery.

For the Sc2, the objective function is the same of the equation (2.43).

The objective functions (2.50) and (2.53) are subjected to the constraints in equations

(2.17), (2.18), (2.19), (2.20), (2.22), (2.23), (2.24), (2.25), (2.26), (2.28), (2.30), (2.31), (2.32), (2.33).

The objective functions (2.50) is subjected to the constraints of equations

(2.17), (2.18), (2.19), (2.20), (2.21), (2.22), (2.23), (2.24), (2.25), (2.26), (2.28), (2.30), (2.31), (2.32), (2.33).

The balance constraint of the active power of equation (2.17) is changed slightly by changing the $P_g(t)$ to $P_{gp}(t)$, while the reactive power balance of equation (2.18) is changed as follows:

For the Sc1

$$\sum_{t=1}^{T}\{Q_{gp}(t) = Q_{Dres}(t) + Q_{Dind}(t) + Q_{Dcom}(t)\} \quad \textbf{(2.54)}$$

For the Sc2

$$\sum_{t=1}^{T}\{\sum_{i=1}^{N} \delta_{DG_i}(t).\, Q_{DG_i}(t) + Q_{gp}(t) = Q_{Dres}(t) + Q_{Dind}(t) + Q_{Dcom}(t)\} \quad \textbf{(2.55)}$$

By applying the above analysis, the following results are obtained. Figure 2-16 illustrates the optimal scheduling of the active power of the DGs and purchasing power from the utility grid for both minimizing the total operating cost and for maximizing the profit of the both scenarios. The figure shows that the storage battery is not operated over the entire scheduling horizon because there is no economic incentive for operating the battery. The MT2 is not committed because it has the highest operating and emission cost. In addition, the MG purchases active power from the utility grid when the price is low. Moreover, in the Sc2, the MG purchases reactive power from the utility grid when the OMP has low values and does not purchase when the price has high values as shown in Figure 2-17, whereas in the Sc1, the MG purchases the reactive power from the utility grid regardless of the price to meet the reactive loads as shown in Figure 2-18. Overall, the total operating cost and the profit per

scheduling day of the Sc1 are 473.6 € and 215.7 € respectively, while 458.6 € and 230.7 € per scheduling day of the Sc2.

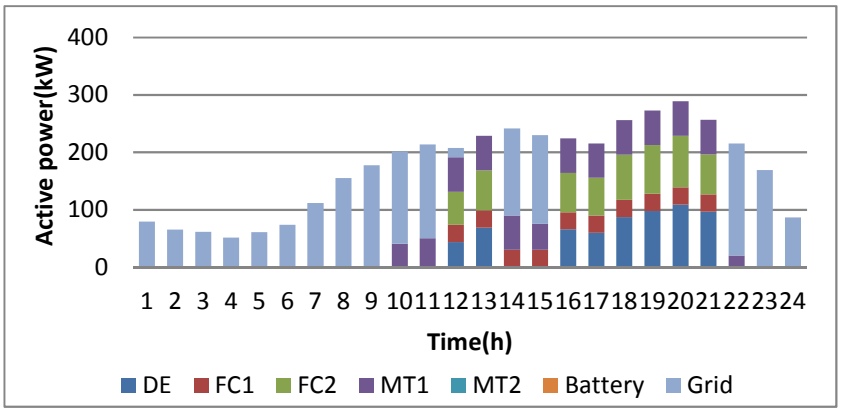

Figure 2-16 Optimal Scheduling of the active power of the DGs and purchasing power from the utility grid of Sc1 and Sc2

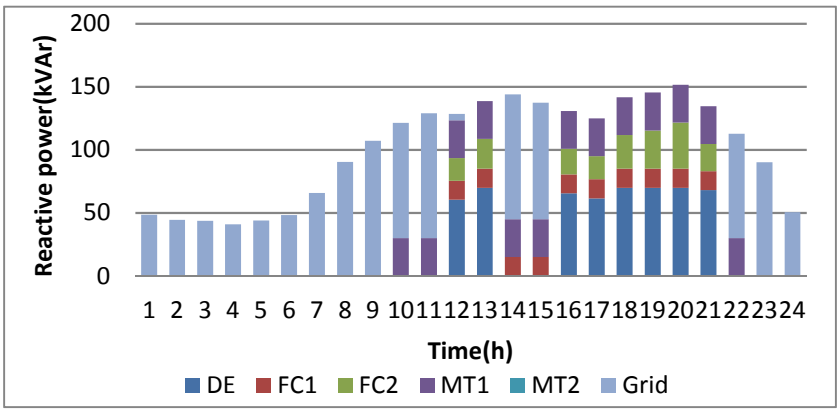

Figure 2-17 Optimal Scheduling of the reactive power of the DGs and purchasing power from the utility grid of the Sc2

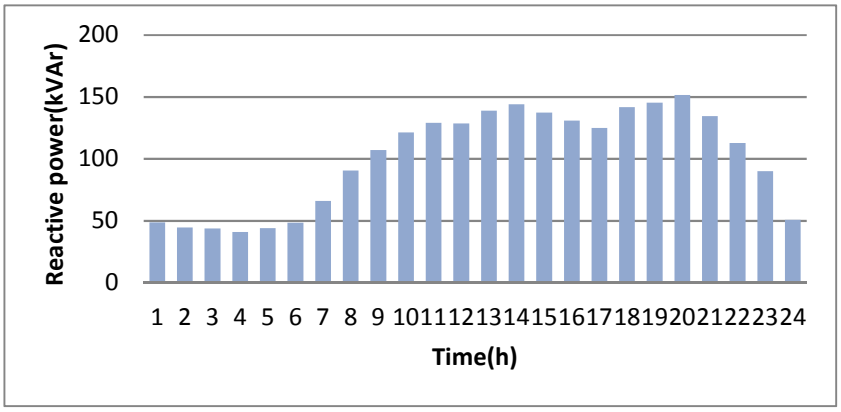

Figure 2-18 Optimal Scheduling of the reactive power of the Sc1

Table 2-7 illustrates the results of the two scenarios. It is seen that in the Sc2, the total operating cost is lower than in the Sc1 and the profit is higher in spite of consideration the production cost of the reactive power in the cost function. This is because the MG in the Sc1 should meet its reactive load from purchasing power from the utility grid, although the reactive OMP has high values.

Table 2-7 Cost and profit of the two scenarios

	Cost (€/day)	Profit (€/day)
Reactive from the utility grid only	473.6	215.7
DGs supply reactive power	458.6	230.7

Figure 2-19 to Figure 2-23 show the hourly voltage profiles of some MG buses for the two scenarios and for minimising the operating cost and maximising the profit. It can be seen that the voltage profiles for all buses are improved in the Sc2. In addition, the voltage values from hour 1 to 9 and hours 22 and 23 are the same because at these hours the MG meets its reactive load demand from purchasing power from the utility grid for both scenarios. Furthermore, the bus voltages are improved, although they do not have DGs.

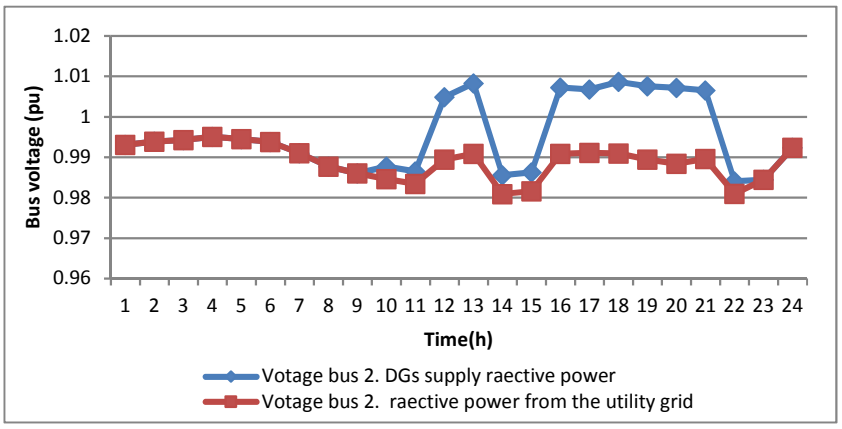

Figure 2-19 Voltage bus 2 of the both scenarios

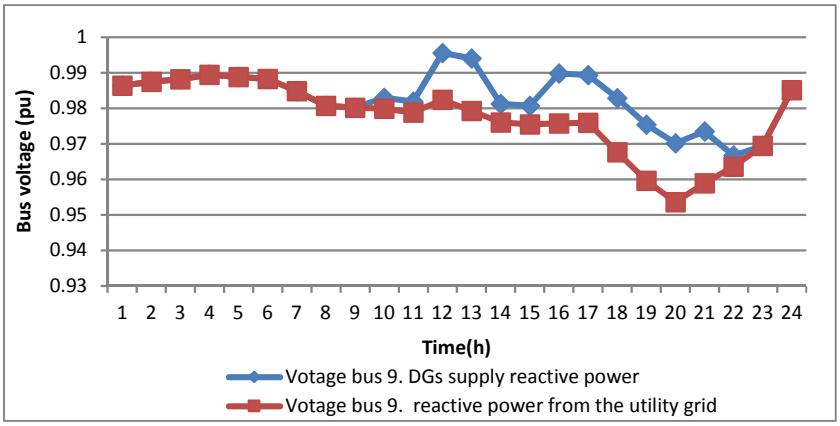

Figure 2-20 Voltage bus 9 of the both scenarios

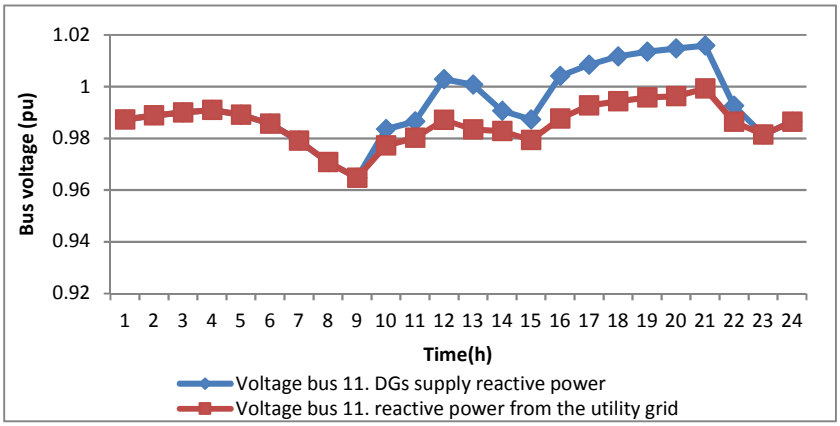

Figure 2-21 Voltage bus 11 of the both scenarios

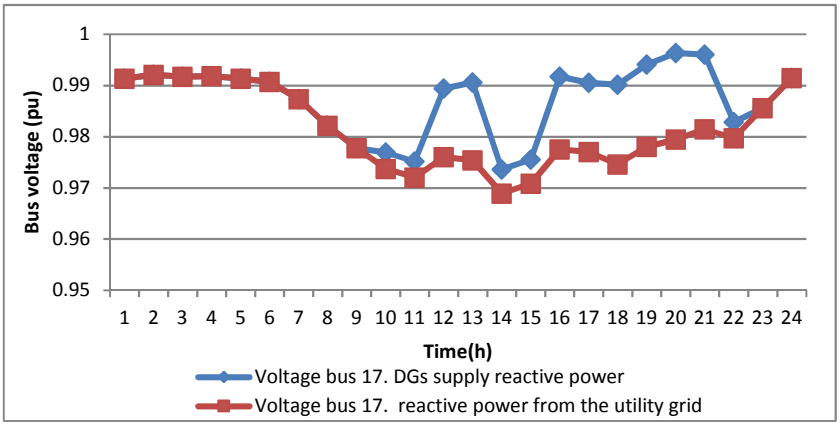

Figure 2-22 Voltage bus 17 of the both scenarios

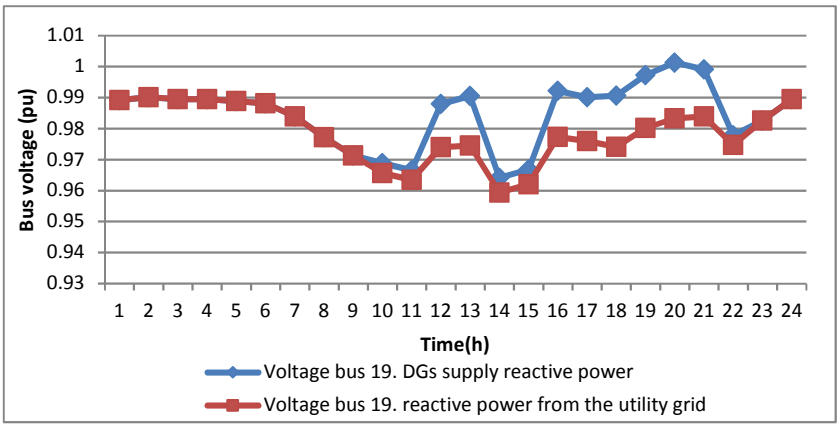

Figure 2-23 Voltage bus 19 of the both scenarios

2.14 Impacts of the Battery on the Optimal Scheduling of the MG

In this section, the impacts of the battery on the total operating cost, the profit and scheduling of the DGs are determined. The impacts are quantified by applying the proposed SCUC-UARDEED to the system with and without battery. The optimisation problems are applied to both the connected and isolated MG of the MG. Different scenarios of the storage battery state of charge are considered as follows

Sc1: the battery is fully charged at the beginning and at the end of the scheduling day.

Sc2: the battery is fully charged at the beginning and not strictly fully charged at the end of the scheduling day.

Sc3: the state of charge has a minimum value at the beginning and fully charge at the end of the scheduling day.

Sc4: without the battery.

The battery degradation cost is included in the cost function in all scenarios.

A. Connected MG

The results of the Sc1 of minimising the total cost and maximizing the profit are as in sections 2.12.1 and 2.12.2, while the active power scheduling of minimising the total operating cost or maximising the profit of the Sc2, Sc3, and Sc4 are shown in Figure 2-24, Figure 2-25 and Figure 2-26. The on/off state of the DGs is the same in the Sc1 because the battery affects the exchanging power with the utility grid. The optimal reactive power scheduling is as in the Sc1 because the storage battery is supplied or absorbed active power solely. In addition, these figures show that the storage battery is charged when the active OMP has the lowest values and is discharged when the price has the highest values for all scenarios. This reveals that the charging and discharging operations of the battery typically reduce the total operating cost and maximise the profit. Moreover, in case without he battery the selling power to the utility grid is reduced.

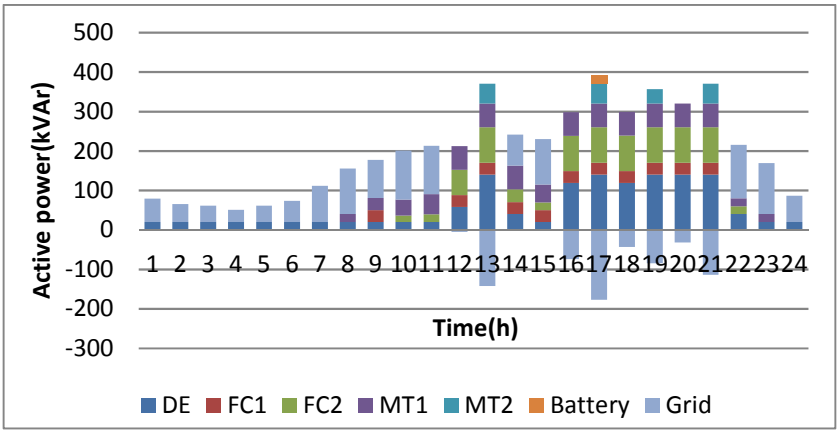

Figure 2-24 Optimal active power scheduling of the DGs and exchanging power with battery and the utility grid of Sc2

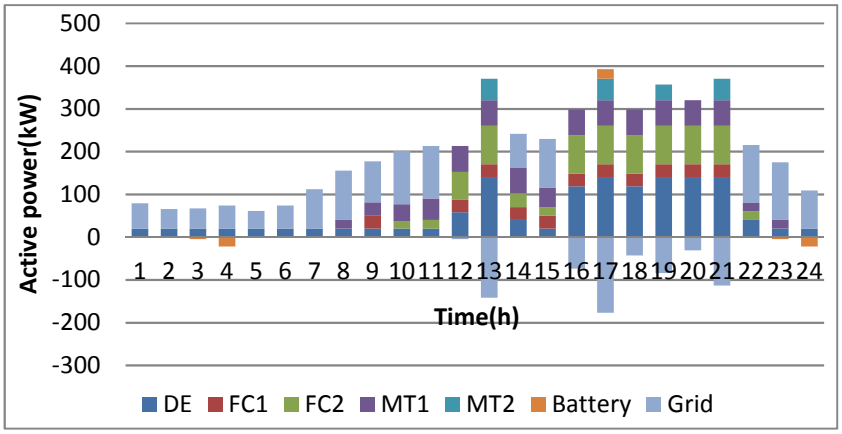

Figure 2-25 Optimal active power scheduling of the DGs and exchanging power with battery and the utility grid of Sc3

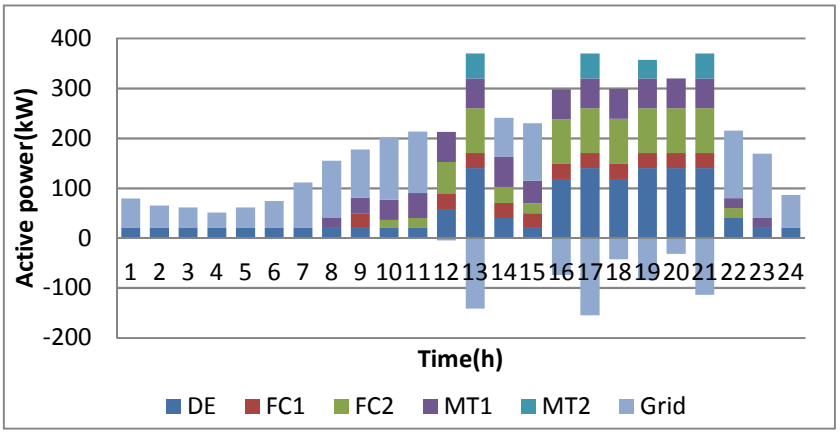

Figure 2-26 Optimal active power scheduling of the DGs and exchanging power with the utility grid of Sc4

Table 2-8 and Table 2-9 summarise the results of the four scenarios. The results in these tables show that the storage battery reduces the total operating cost and hence increases the profit despite consideration the battery degradation cost in the optimisation formulation for all scenarios. The results reveal that the battery affects the exchanging active power cost with the utility grid and the battery operating cost because the MG sells the charging power of the battery to the utility grid.

Table 2-8 Components of the cost of the four scenarios of the connected MG

Components of (€/day)	Sc1	Sc2	Sc3	Sc4
Active power cost	295.3	295.3	295.3	295.3
Active power cost of WTs	53.7	53.7	53.7	53.7
Active power cost of PVs	37.4	37.4	37.4	37.4
Reactive power cost	17.9	17.9	17.9	17.9
Maintenance cost	27.4	27.4	27.4	27.4
Start-up cost	1	1	1	1
Shutdown cost	1.6	1.6	1.6	1.6
Cost of exchanging active power with the utility grid	-105.6	-106.4	-104.8	-96.3
Cost of exchanging reactive power with the utility grid	-4.6	-4.6	-4.6	-4.6
Battery operating cost	2.9	1.3	4.5	0
Emission cost	81.1	81.1	81.1	81.1
Total cost	408.1	405.7	410.5	414.5

Table 2-9 Components of the profit of the four scenarios of the connected MG

Components of profit (€/day)	Sc1	Sc2	Sc3	Sc4
Revenue	800.3	800.3	800.3	790.2
Expense	519.1	516.7	521.5	515.4
Profit	281.2	283.6	278.8	274.8

B. Isolated MG

The results of the Sc1 of minimising the total cost and maximising the profit are in sections 2.12.1 and 2.12.2, whereas for the Sc2 and the Sc3, are shown in Figure 2-27, Figure 2-28 and for the Sc4 is the same of the Sc1. The optimal reactive power scheduling and the on/off state of the DGs are not changed and are the same in the Sc1. The battery in the Sc2 is discharged when the load reaches the highest values and when the P_{PV}=0, while in the Sc3 is charged when the load has the lowest values and MT1 affords the charging power because it has the lowest operating cost among the DGs. In the Sc3, the storage battery is operated in charge mode solely to full charge at the end of the scheduling day. The battery is operated as a load, so the total operating cost is

slightly higher and the profit is lower than other scenarios. This is the worst scenario to show the ultimate impacts of the battery on the economic operation of the isolated MG. In the Sc1, the battery is not involved in the operation of the MG and the Sc4 has the same results of the Sc1.

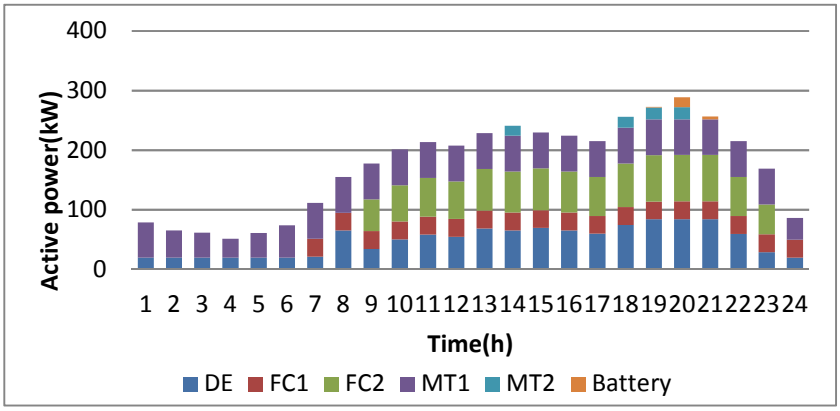

Figure 2-27 Optimal active power scheduling of the DGs and exchanging power with the battery of the Sc2

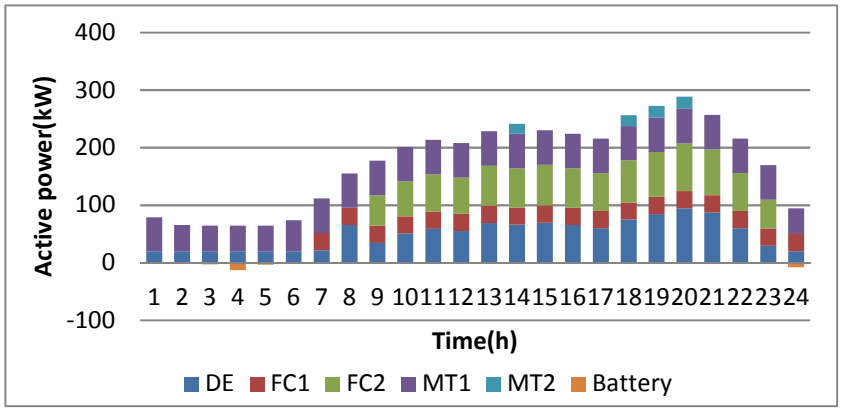

Figure 2-28 Hourly optimal active power scheduling of DGs and exchanging power with the battery of the Sc3

Table 2-10 and Table 2-11 show results of the four scenarios. These results reveal that the Sc2 has the lowest operating cost and the highest profit because the battery is discharged only and it is not strictly fully charged at the end of the scheduling horizon. In addition, the total cost and profit of the Sc1 and Sc4 are equal because in the Sc1 the battery is not operated. The battery operations affect the components of the costs that they are a function of the active

generation power, such as active power cost, maintenance and emission cost. This is because the battery operations affect the active power scheduling in the MG. Furthermore, the operations of the battery affect the revenue and the expense of the MG as shown in Table 2-11.

Table 2-10 Components of the cost of the four scenarios of the isolated MG

Components of overall cost (€/day)	Sc1	Sc2	Sc3	Sc4
Active power cost	322.5	320.2	324	322.5
Active power cost of WTs	53.7	53.7	53.7	53.7
Active power cost of PVs	37.4	37.4	37.4	37.4
Reactive power cost	19.7	19.7	19.7	19.7
Maintenance cost	29.6	29.4	29.8	29.6
Start-up cost	0.6	0.6	0.6	0.6
Shutdown cost	0.9	0.9	0.9	0.9
Battery operating cost	0	1.3	1.6	0
Emission cost	85.8	85.2	86.3	85.8
Total cost	550.2	548.4	554	550.2

Table 2-11 Components of the profit of the four scenarios of the isolated MG

Components of profit (€/day)	Sc1	Sc2	Sc3	Sc4
Revenue	784.2	784.2	788.4	784.2
Expense	550.2	548.4	558.1	550.2
Profit	234	235.8	230.3	234

2.15 Impacts of the Active and Reactive SSSCs on the UCSC-UARDEED of the MG

In this section, the impacts of active and reactive power SSSCs on the economic operation of the MG and the UC results are presented. Three scenarios are considered and comparisons between these scenarios are conducted to determine the impacts of the active and reactive power SSSCs on the optimal operation of the MG. These scenarios are as follows

Sc1: active and reactive power SSSCs for the full active and reactive loads.

Sc2: without the active and reactive power SSSCs.

Sc3: SSSCs for critical active and reactive load, where the critical active and reactive load is considered 70 % of the total load.

The results of the Sc1 are demonstrated in section 2.12.1 and 2.12.2, whereas Figure 2-29 and Figure 2-30 show the optimal scheduling of the active and reactive power of the minimising the total cost and maximising the profit of the Sc2. These figures reveal that at hours 1 to 9 and 23, 24 none of the DGs is committed because the MG purchases active and reactive power from the utility grid to supply its active and reactive load with renewable energy resources, where the purchasing power cost from the utility grid is lower than the generation cost of the DGs.

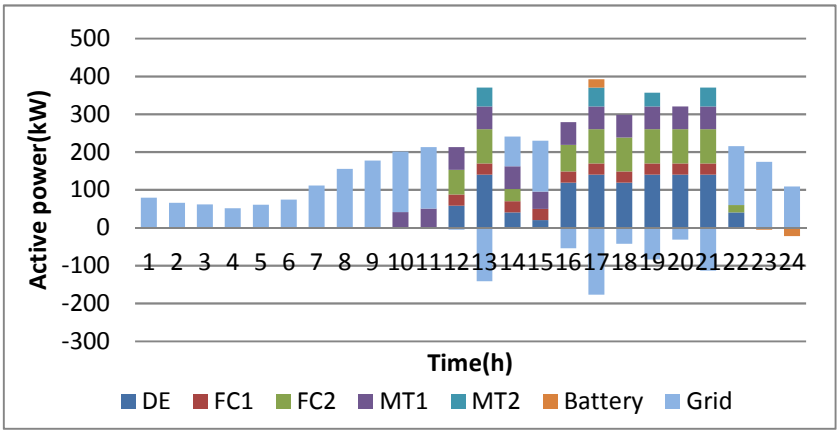

Figure 2-29 Optimal active power scheduling of the DGs and exchanging power with utility grid and the battery of the Sc2

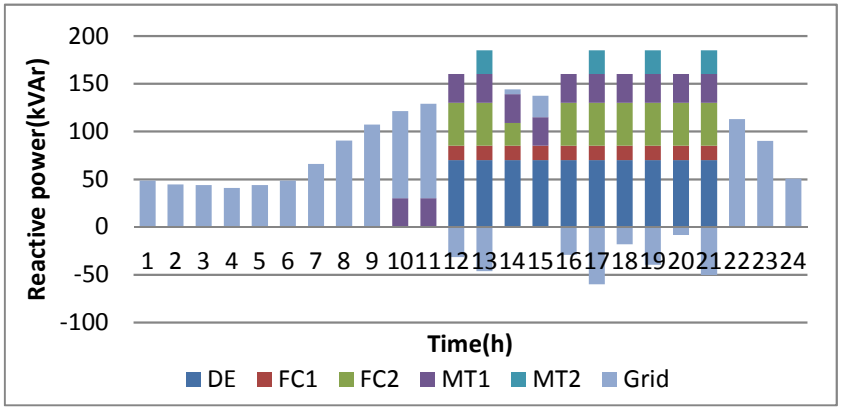

Figure 2-30 Optimal reactive power scheduling of the DGs and exchanging power with the utility grid of the Sc2

Figure 2-31 and Figure 2-32 show the hourly optimal scheduling of the active and reactive power for the minimising the total cost and maximising the profit of the Sc3. These figures show that the DGs are committed significantly different from the Sc1, wherein at hours 1 to 3 solely the FC2 is committed with minimum output power because it can satisfy the active and reactive power SSSCs for the critical loads. At hour 4 solely the MT1 is committed to satisfy the active and reactive SSSCs for critical loads. In the Sc1 the DE is committed over the entire horizon. The battery charging and discharging operations are the same of the Sc1.

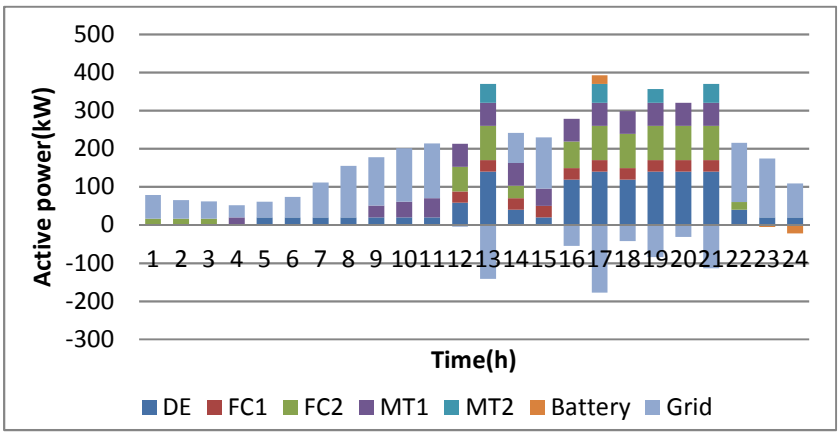

Figure 2-31 Optimal active power scheduling of the DGs and exchanging power with the utility grid and the battery of the Sc3

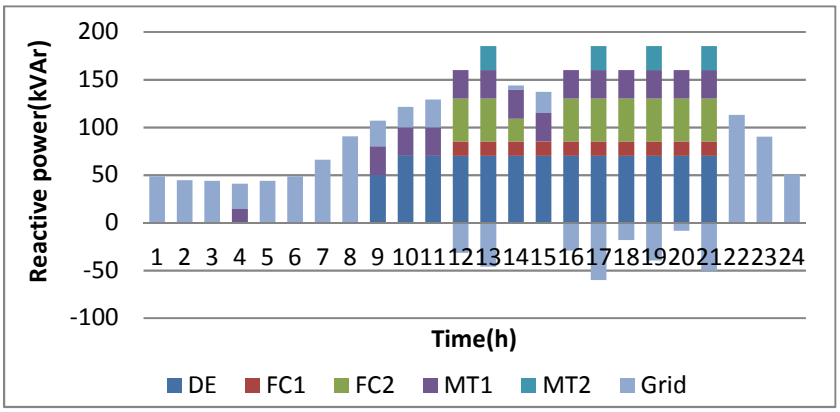

Figure 2-32 Optimal reactive power scheduling of the DGs of the Sc3

Table 2-12 and Table 2-13 show the optimal on/off state of the DGs of the Sc2 and the Sc3. These tables illustrate that in the Sc2, the majority of the DGs are operated fewer hours than the Sc1 and the Sc3 because the MG can supply it load demand by purchasing power from the utility grid and from RDGs. The yellow colour means the difference of committing of the DGs between the Sc2, the Sc3 versus the Sc1.

able 2-12 Optimal state of the DGs of the Sc2

T(h)	1	2	3	4	5	6	7	8	9	10	11	12	13	14	15	16	17	18	19	20	21	22	23	24
DE	0	0	0	0	0	0	0	0	0	0	0	1	1	1	1	1	1	1	1	1	1	1	0	0
FC1	0	0	0	0	0	0	0	0	0	0	0	1	1	1	1	1	1	1	1	1	1	0	0	0
FC2	0	0	0	0	0	0	0	0	0	0	0	1	1	1	0	1	1	1	1	1	1	1	0	0
MT1	0	0	0	0	0	0	0	0	0	1	1	1	1	1	1	1	1	1	1	1	1	0	0	0
MT2	0	0	0	0	0	0	0	0	0	0	0	0	1	0	0	0	1	0	1	0	1	0	0	0

1 On state of the DG 0 Off state of the DG Different state from the previous state

Table 2-13 Optimal state of the DGs of the Sc3

T(h)	1	2	3	4	5	6	7	8	9	10	11	12	13	14	15	16	17	18	19	20	21	22	23	24
DE	0	0	0	0	1	1	1	1	1	1	1	1	1	1	1	1	1	1	1	1	1	1	1	1
FC1	0	0	0	0	0	0	0	0	0	0	0	1	1	1	1	1	1	1	1	1	1	0	0	0
FC2	1	1	1	0	0	0	0	0	0	0	0	1	1	1	0	1	1	1	1	1	1	1	0	0
MT1	0	0	0	1	0	0	0	0	1	1	1	1	1	1	1	1	1	1	1	1	1	0	0	0
MT2	0	0	0	0	0	0	0	0	0	0	0	0	1	0	0	0	1	0	1	0	1	0	0	0

1 On state of the DG 0 Off state of the DG Different state from the previous state

Table 2-14 and Table 2-15 summarise the results of the three scenarios. By comparing the results of these scenarios, it is found that the take into account

the active and reactive power SSSCs in the optimisation of the MG for the whole load or for the critical load increases the operating cost and decreases the profit of the MG. Reducing the minimum output characteristics of the DGs reduces the increased cost that results from the active and reactive power SSSCs. However, the active and reactive power SSSCs lead to secure operation of the grid over the entire secluding day. The active and reactive power SSSCs prevents the system from resorting to the involuntary load shedding in case of losing the connection with the utility grid. In addition, the account of the active and reactive power SSSCs guarantees obtaining a feasible solution when the connection with the utility grid is lost. In case without the active and reactive power SSSCs, the MG operates the majority of day hours insecure and when any disturbance happens and leads to loss the connection with the utility grid, the MG cannot supply its load quickly because it needs time to start-up new DG to meet the active and reactive load demand. Therefore, The MG needs to run the involuntary load shed programmes and cuts involuntary load demands. This is inconvenient for the consumers and it is costly solution.

Table 2-14 Total cost components of the three scenarios

Components of total cost (€/day)	Sc1	Sc2	Sc3
Active power cost	295.3	256.5	281
Active power cost of WTs	53.7	53.7	53.7
Active power cost of PVs	37.4	37.4	37.4
Reactive power cost	17.9	14.4	16.8
Maintenance cost	27.4	23.2	25.9
Start-up cost	1	1.3	1.4
Shutdown cost	1.6	2.1	2
Cost of exchanging active power with the utility grid	-105.6	-78.7	-92.7
Cost of exchanging reactive power with the utility grid	-4.6	-1.9	-3.7
Battery operational cost	2.9	2.9	2.9
Emission cost	81.1	68.2	76.7
Total cost	408.1	379.1	401.4

Table 2-15 Profit components of the three scenarios

Components of overall cost (€ /day)	Sc1	Sc2	Sc3
Revenue	800.3	770.7	786.5
Expense	519.1	460.5	498.5
Profit	281.2	310.2	288

The hourly costs of the involuntary load interruption for residential, commercial and industrial consumers are 3 (€/kWh) [93]. For instance, if the MG loses the connection with the utility grid at hour 10 in case without the SSSCs, the MG should run the load shedding programme. At this hour only the MT1 is committed and the total load is 250.4 kW; therefore, the MT1 can supply only 60 kW and the other load should be cut. The cost of the load cutting for ten minutes is 95.2 € and the load cutting causes inconvenience for the consumers.

2.16 Chapter Conclusions

This chapter focuses on the formulating and solving the SCUC-UARDEED of the MG. The impacts of reactive power from the DGs, the battery, and the active and reactive SSSCs on the optimal scheduling of the MG are analysed. The results reveal that the reactive power from the DGs reduces the total operating cost, increases the profit, and boosts the buses voltage. In addition, the stationary battery reduces the total operating cost and increases the profit despite considering the battery degradation cost in the objective functions. Furthermore, the active and reactive SSSCs guarantee secure operation of the MG during the entire scheduling horizon, ensure continuous operation when the connection with utility grid is lost, avoid the system from resorting to involuntary load shed, increase the total operating cost, and decrease the profit.

3 Dynamic Economic and Emission Dispatch of the MG under Stochastic Environment

3.1 Chapter Summary

MGs have the varieties of the DGs and RDGs. The uncertainties evolving from different resources affect the optimal scheduling of the energy resources of the MG. If these uncertainties are ignored, this might lead to obtain infeasible solution or system outages. In this chapter, new approaches and methodologies are proposed to model the uncertainties and incorporate them with all the components of the cost and the constraints in chapter 2 in a two-stage stochastic based-scenario optimisation approach to minimise the total operating cost or to maximise the profit for the connected and isolated MG; however, the optimisation problems are maintained numerically tractable. The uncertainties of the fluctuation of the generation of the RDGs, and the OMP forecast error are considered as sources of the uncertainties, where the models of these uncertainties are presented in this chapter.

3.2 Stochastic Optimisation Problems of the MG

New approaches have been proposed to incorporate the uncertainties with optimisation problems and determine their impacts on the optimal operation of the MG. In [48]**,** stochastic optimisation was formulated as a probabilistic constrained approach. In this approach, the hard constraint on exact balance power was relaxed by introducing a probabilistic constraint, which contains renewable powers, and load demands as random variables. The power balance constraint was considered as a high probability, while a penalty was added to the cost function for violation of the constraint. On the other hand, a two-stage scenario-based stochastic optimisation was presented in the previous works. Reference [94] proposed a two-stage optimisation problem, where in the first stage the decision variables of the UC were taken, which could not be changed in the second stage. The second stage included the scheduling of the energy resources of the system with the realisation of the generation fluctuation of the RDGs. Reference [95] formulated the stochastic optimisation problem as a two-

stage, wherein the UC decisions were taken in the first stage, while the second stage contained the scheduling of the energy resources with consideration given to the uncertainties. In [96], the first stage of the objective function included the decisions of the UC and battery charging and discharging operations, which could not be changed in the second stage. The scheduling of the energy resources was included in the second stage with consideration given to the uncertainties. In [86] and [97], the first stage of the objective function included the UC and the day-ahead energy scheduling of DGs and other generation resources and the reserve and security costs of the each scenario were considered in the second stage. References [98], [99], [100] proposed the stochastic optimisation as a single-stage based on multi-scenarios stochastic optimisation, where the optimisation problem was solved for a set of generating scenarios of the uncertain variables. The two-stage is more accurate than a single stage [97]. The UC is defined at the first stage and the UC is not changed at the second stage. Therefore, the two-stage stochastic optimisation approach is more suitable for the real-time optimisation than the single-stage.

The above publications presented the optimisation problem for the connected MG, where quite a few researchers studied the optimisation problem in the isolated MG. Reference [93] proposed the optimisation problem for the isolated MG as a two-stage framework, where the first-stage decision was the UC and the second stage decisions were energy scheduling of the energy resources with the uncertainties from the wind generation. Reference [101] studied the optimisation in the isolated MG, where the optimisation problem formulated as a single stage. The wind and solar generation with uncertain load were considered as sources of the uncertainties.

The above works did not take into consideration the models of the reactive power production cost, the purchasing reactive power from the utility grid cost, the environmental cost, the maintenance cost of the DGs, and production cost of the RDGs. In addition, the limit of greenhouse gases emission constraints was overlooked. Furthermore, the active and reactive power SSSCs for the

connected MG and active and reactive power SRCs for the isolated MG were not considered.

All the above papers pointed out the stochastic optimisation to minimise the operating cost or to minimise both the cost and emission level. In contrast, quite a few researchers studied the impacts of the uncertainties on the maximising the MG profit. Reference [60] introduced a UC two-stage based stochastic scenario optimisation to maximise the profit of the connected MG. However, the models of the optimal management of reactive power, exchanging both active and reactive power with the utility grid were not considered. The models of the emission cost, maintenance cost of the DGs, and RDGs generation cost also were not taken into account. In addition, essential constraints were neglected, such as active and reactive SSSCs, limits of greenhouse gases emission, and the constraints related to the reactive power. The above literature review reveals that there is no study takes into account the models of the emission cost, production cost of the RDGs, and reactive power cost with cost components and constraints in previous Chapter in one combined optimisation approach under stochastic environment. The stochastic optimisation of maximising the profit of the isolated MG is not presented in the literature yet.

3.3 The Stochastic Model of the MG Components

The stochastic models of wind speed and PV generation, and the OMP are presented in this section.

3.3.1 Stochastic Model of the Wind Generation

The power generation of WT depends on the wind speed. Since the wind speed is an uncertain variable, the WT generation is also uncertain variable. Weibull distribution is used to formulate the stochastic nature of the wind speed [97], [102] and the following equation expressed the Weibull distribution.

$$f(v) = \frac{k_1}{c}\left(\frac{v}{c}\right)^{k_1-1} e^{-(v/c)^{k_1}} \quad \textbf{(3.1)}$$

where k_1 and c are shape index and scale index respectively. v is the wind speed(s/m). When $k_1 = 2$, the Weibull distribution is changed to Rayleigh distribution, which is quite similar to the distribution of the wind speed. The Rayleigh distribution as:

$$f(v) = (\frac{2v}{c^2})\, e^{-(v/c)^2} \quad \textbf{(3.2)}$$

The scale index is obtained from

$$c \cong 1.128 v_{mean} \quad \textbf{(3.3)}$$

where v_{mean} is the hourly forecasted wind speed. The power of the wind turbine is calculated by equation (2.4).

3.3.2 Stochastic Model of the PV Generation

The proposed stochastic model of the PV generation is developed and presented in this section. It is assumed that the fluctuation of the PV power generation follows the normal distribution, where the Monte Carlo simulation is used to obtain the stochastic PV power. The proposed stochastic PV power is as:

$$P_{PV}(t) = P_{PV}(t)^{mean} + \mu(t)^{PV}.\sigma(t)^{PV} \quad \textbf{(3.4)}$$

where $P_{PV}(t)^{mean}$ and $\sigma(t)^{PV}$ are the mean values of the PV power at hour t and the standard deviation of the PV power, $\mu(t)^{PV}$ is the random variable generated for the PV power at time t by using the normal distribution with a mean of zero and a standard deviation is one. $P_{PV}(t)^{mean}$ is from Table B-6.

3.3.3 Stochastic Model of the OMP

The stochastic model of the OMP is developed and explained in this section. The forecast error of the OMP follows a normal distribution and Monte Carlo simulation is used to obtain the stochastic OMP. The proposed stochastic behaviour of the OMP as follows.

$$c_g(t) = c_g(t)^{mean} + \mu(t)^{c_g}.\sigma(t)^{c_g} \quad \textbf{(3.5)}$$

where $c_g(t)^{mean}$ and $\sigma(t)^{c_g}$ are the mean OMP at hour t and its standard deviation of the OMP. $\mu(t)^{c_g}$ is a random variable generated for the OMP at time t by using normal distribution with the mean of zero and a standard deviation is one. $c_g(t)^{mean}$ is from Table B-6.

The generated scenarios are reduced by the reduction method, where the corresponding probability of the scenario of the wind and solar power, and the OMP are ρ^W, ρ^{PV}, and ρ^{c_g} respectively. Each scenario for each variable has a probability of happening as:

$$\rho_{i3}^W = [\rho_1^W\ ,\ \rho_2^W\ , \dots \rho_n^W]_{1\times n} \quad \textbf{(3.6)}$$

$$\rho_{i4}^{PV} = [\rho_1^{PV}\ ,\ \rho_2^{PV}\ , \dots \rho_q^{PV}]_{1\times q} \quad \textbf{(3.7)}$$

$$\rho_e^{c_g} = [\rho_1^{c_g}\ ,\quad \rho_2^{c_g}\ , \dots \rho_r^{c_g}]_{1\times r} \quad \textbf{(3.8)}$$

The summation probability of scenarios for each variable should equal 1 as follows.

$$\sum_{i3=1}^{n} \rho_{i3}^W = 1 \quad \textbf{(3.9)}$$

$$\sum_{i4=1}^{q} \rho_{i4}^{PV} = 1 \quad \textbf{(3.10)}$$

$$\sum_{e=1}^{r} \rho_e^{c_g} = 1 \quad \textbf{(3.11)}$$

The number of possible scenarios (S) is calculated as

$$S = n.q.r \quad \textbf{(3.12)}$$

The summation of the probability of joint scenarios is as follows

$$\sum_{s=1}^{S} \lambda_s = \sum_{i3=1}^{n} \sum_{i4=1}^{q} \sum_{e=1}^{r} \rho_{i3}^W\, \rho_{i4}^{PV} \rho_e^{c_g} = 1 \quad \textbf{(3.13)}$$

where λ_s is the probability of the joint scenario (s).

3.4 Formulation of the Proposed Two-stage Stochastic SCUC-UARDEED of the MG

A novel two-stage robust scenario-based stochastic optimisation of the MG combined with UC is proposed to formulate the stochastic optimisation problems of the MG either to minimise the overall operating and emission costs or maximise the profit. This stochastic approach consists of two stages. In the first stage, the day ahead scheduling based on forecasted data of the uncertain variables, while the second stage is mimicing the real-time operations by penetration the wind and solar generation variability, and OMP forecast error. Figure 3-1 shows the structure of the proposed stochastic optimisation approach. This figure reveals that the decisions that are taken in the first stage include the UC of the DGs before realisation of the uncertainties. In the second stage the output active and reactive power of the DGs, the exchanging active power with the battery and the exchanging active and reactive power with the utility grid are determined based on the realization of each scenario and the UC solution from the first stage. The decisions that are taken in the first stage should ensure a feasible solution of all expected scenarios in the second stage. A thousand scenarios are generated to represent the uncertainty of each variable, then a clustering technique is considered as a scenario reduction technique to reduce the number of the generated scenarios [47], [103] , [104], [105].

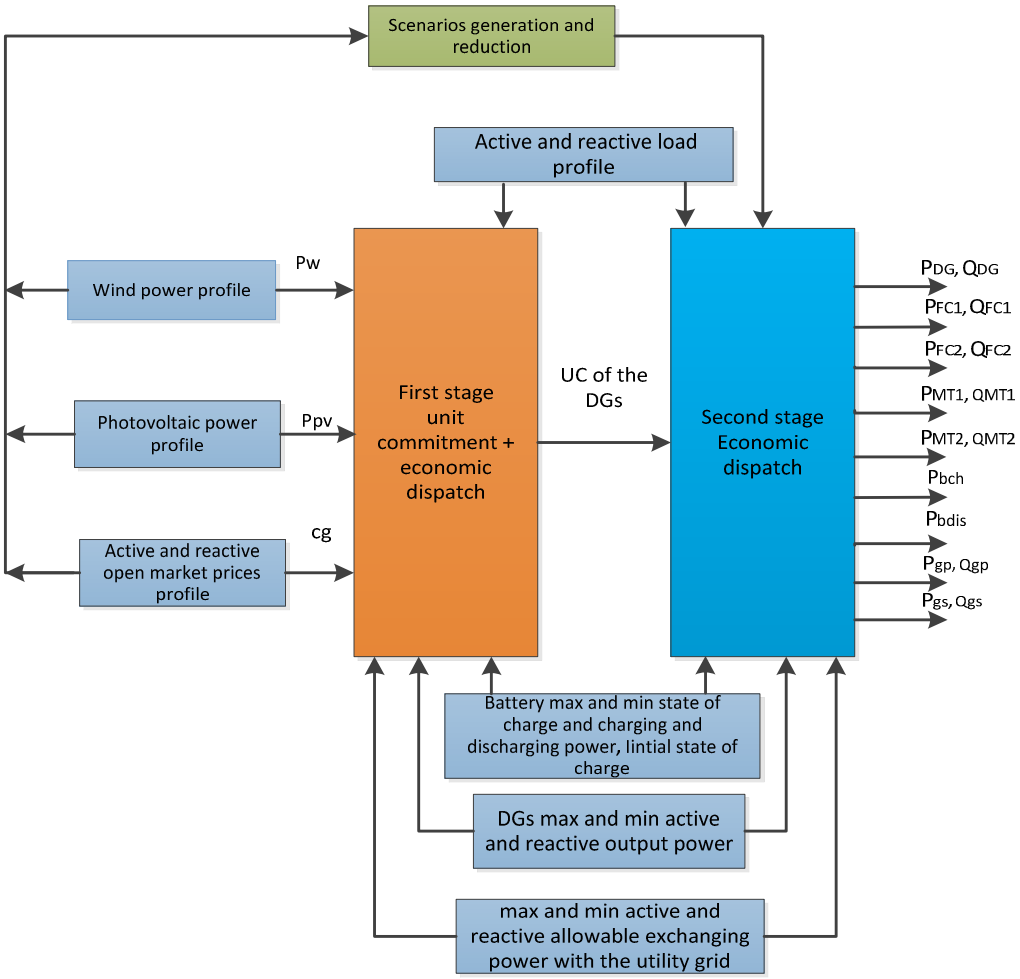

Figure 3-1 Proposed stochastic two-stage optimisation approach of the MG

3.5 Proposed Objective Functions

Two objective functions are considered. The first is the minimising the total operating cost and the second is the maximising the profit for both the connected and isolated MG.

3.5.1 Minimising the Total Operating Cost

The aim of this objective function is to minimise the overall operating cost of the MG over the scheduling day. All the decision variables are denoted by s are representing scenarios. The stochastic objective functions are formulated as follows:

A. Connected MG

The optimisation problem is formulated as

$$\min(F) \tag{3.14}$$

where the objective function F is

$$\begin{aligned} F = \sum_{t=1}^{T}\sum_{i=1}^{N}[SU_{DG_i}(t) + SD_{DG_i}(t)] + \sum_{s=1}^{S}\lambda_s \sum_{t=1}^{T}\{\sum_{i=1}^{N}[CP_{DG_i}(P_{DG_i}^{s}(t)) + \\ CQ_{DG_i}(Q_{DG_i}^{s}(t)) + COM_{DG_i}(P_{DG_i}^{s}(t))]\delta_{DG_i}(t) + C_e(P_{DG_i}^{s}(t)) + \\ C_{bo}^{s}(t) + c_{gP}^{s}(t) + c_{gQ}^{s}(t) + \sum_{i1=1}^{N1} CP_{W_{i1}}(P_{W_{i1}}^{s}(t)) + \sum_{i2=1}^{N2} CP_{PV_{i2}}(P_{PV_{i2}}^{s}(t)) + \\ c_{Pres}.P_{Drescut}^{s}(t) + c_{Qres}.Q_{Drescut}^{s}(t) + c_{Pind}.P_{Dindcut}^{s}(t) + \\ c_{Qind}.Q_{Dindcut}^{s}(t) + c_{Pcom}.P_{Dcomcut}^{s}(t) + c_{Qcom}.Q_{Dcomcut}^{s}(t)\} \end{aligned} \tag{3.15}$$

where $SU_{DG_i}(t)$, $SD_{DG_i}(t)$ and $\delta_{DG_i}(t)$ are calculated in the first stage. c_{Pres}, c_{Pind} and c_{Pcom} (€/kWh) are the cost of the active residential, industrial, and commercial involuntary loads cutting respectively. c_{Qres}, c_{Qind} and c_{Qcom} (€/kVArh) are the cost of the reactive residential, industrial, and commercial involuntary loads cutting respectively. $P_{Drescut}^{s}(t)$, $P_{Dindcut}^{s}(t)$ and $P_{Dcomcut}^{s}(t)$ are the active power cutting from residential, industrial and commercial loads, while $Q_{Drescut}^{s}(t)$, $Q_{Dindcut}^{s}(t)$ and $Q_{Dcomcut}^{s}(t)$ are the amount of cutting reactive power from residential, industrial and commercial loads for scenario ($s = 1, \ldots, S$).

This objective function is constructed using equations

(2.15), (2.16), (2.1), (2.2), (2.3), (2.14), (2.11), (2.12), (2.13), (2.5), (2.6), and the last six components which they are defined above.

B. Isolated MG

Similarly, the optimisation problem of the isolated MG is formulated as

$$\min(F) \tag{3.16}$$

where the objective function F is

$$F = \sum_{t=1}^{T}\sum_{i=1}^{N}[SU_{DG_i}(t) + SD_{DG_i}(t)] + \sum_{s=1}^{S}\lambda_s \sum_{t=1}^{T}\{\sum_{i=1}^{N}[CP_{DG_i}(P_{DG_i}^{s}(t)) + CQ_{DG_i}(Q_{DG_i}^{s}(t)) + COM_{DG_i}(P_{DG_i}^{s}(t))]\delta_{DG_i}(t) + C_e(P_{DG_i}^{s}(t)) + C_{bo}^{s}(t) + \sum_{i1=1}^{N1} CP_{W_{i1}}(P_{W_{i1}}^{s}(t)) + \sum_{i2=1}^{N2} CP_{PV_{i2}}(P_{PV_{i2}}^{s}(t)) + c_{Pres}.P_{Drescut}^{s}(t) + c_{Qres}.Q_{Drescut}^{s}(t) + c_{Pind}.P_{Dindcut}^{s}(t) + c_{Qind}.Q_{Dindcut}^{s}(t) + c_{Pcom}.P_{Dcomcut}^{s}(t) + c_{Qcom}.Q_{Dcomcut}^{s}(t) + \sum_{i=1}^{N} c_G.P_{DG_icut}^{s}(t) + \sum_{i1=1}^{N1} c_{ren}.P_{W_{i1}cut}^{s}(t) + \sum_{i2=1}^{N2} c_{ren}.P_{PV_{i2}cut}^{s}(t)\}\} \quad \textbf{(3.17)}$$

where c_G and c_{ren} (€/kWh) are the cost of the generated active power cutting of the DGs and RDGs respectively. $P_{DG_icut}^{s}(t)$, $P_{W_{i1}cut}^{s}(t)$, and $P_{PV_{i2}cut}^{s}(t)$ are the generated active power cutting from the i^{th} DG, $i1^{th}$ WT, and $i2^{th}$ PV for each scenario (s) respectively.

This objective function is constructed using equations

(2.15), (2.16), (2.1), (2.2), (2.3), (2.14), (2.11), (2.5), (2.6), and the last nine components which they are defined above.

The last six components in the equation (3.15) and the last nine terms in the equation (3.17(3.17) represent the active and reactive loads and generation cut are considered to provide more flexibility to the system operators to manage the loads and generation resources to prevent the system from outages and to get feasible solution in the second stage.

To supply electricity with high equality and to avoid resorting to load or generation cutting, the penalties of the load and generation cutting are considered significantly high. Accordingly, the penalties are taken 3 and 5 (€/kWh) [93] for the load and the generation cutting respectively. However, the load or the generation cutting is resorted when it is necessary and to avoid outage of the system.

3.5.2 The Proposed Maximising the Profit

A novel stochastic optimisation approach of maximising the profit of the connected and isolated MG is proposed in this section and it is formulated as follows:

A. Connected MG

The optimisation problem is formulated as

$$\max(F) \tag{3.18}$$

where the objective function F is

$$\begin{aligned} F = &- \sum_{t=1}^{T} \sum_{i=1}^{N} [SU_{DG_i}(t) + SD_{DG_i}(t)] + \\ &\sum_{s=1}^{S} \lambda_s \sum_{t=1}^{T} \{\sum_{i=1}^{N} [c_{gP}^{s}(t).P_{DG_i}^{s}(t) + c_{gQ}^{s}(t).Q_{DG_i}^{s}(t)]\delta_{DG_i}(t) + \\ &c_{gP}^{s}(t).P_{bdis}^{s}(t).\Delta t + c_{gP}^{s}(t).\sum_{i2=1}^{N2} P_{PV_{i2}}^{s}(t) + c_{gP}^{s}(t).\sum_{i1=1}^{N1} P_{W}^{s}(t)\} - \\ &\sum_{s=1}^{S} \lambda_s \sum_{i=1}^{T} \{\sum_{i=1}^{N} [CP_{DG_i}(P_{DG_i}^{s}(t)) + CQ_{DG_i}(Q_{DG_i}^{s}(t)) + \\ &COM_{DG_i}(P_{DG_i}^{s}(t))]\delta_{DG_i}(t) + C_e(P_{DG_i}^{s}(t)) + C_{bo}^{s}(t) + c_{gP}^{s}(t).P_{bch}^{s}(t).\Delta t + \\ &\sum_{i1=1}^{N1} CP_{W_{i1}}(P_{W_{i1}}^{s}(t)) + \sum_{i2=1}^{N2} CP_{PV_{i2}}(P_{PV_{i2}}^{s}(t)) + c_{Pres}.P_{Drescut}^{s}(t) + \\ &c_{Qres}.Q_{Drescut}^{s}(t) + c_{Pind}.P_{Dindcut}^{s}(t) + c_{Qind}.Q_{Dindcut}^{s}(t) + \\ &c_{Pcom}.P_{Dcomcut}^{s}(t)\} \end{aligned} \tag{3.19}$$

The revenue of the MG comes from selling the active and reactive power from the DGs, the discharging power of the battery, the power from the RDGs. The cost is constructed using equations

(2.15), (2.16), (2.1), (2.2), (2.3), (2.14), (2.11), (2.5), (2.6), cost of charging battery, and the last six components which they are defined above.

B. Isolated MG

The optimisation problem is formulated as

$$\max(F) \tag{3.20}$$

where the objective function F is

$$F = -\sum_{t=1}^{T}\sum_{i=1}^{N}[SU_{DG_i}(t) + SD_{DG_i}(t)] + \quad \textbf{(3.21)}$$
$$\sum_{s=1}^{S}\lambda_s \sum_{t=1}^{T}\{\sum_{i=1}^{N}[c_{isoP}(t).P_{DG_i}^{s}(t) + c_{isoQ}(t).Q_{DG_i}^{s}(t)]\delta_{DG_i}(t) +$$
$$c_{isoP}(t).P_{bdis}^{s}(t).\Delta t + c_{isoP}(t).\sum_{i2=1}^{N2}P_{PV_{i2}}^{s}(t) + c_{isoP}(t).\sum_{i1=1}^{N1}P_{W}^{s}(t)\} -$$
$$\sum_{s=1}^{S}\lambda_s \sum_{i=1}^{T}\{\sum_{i=1}^{N}[CP_{DG_i}(P_{DG_i}^{s}(t)) + CQ_{DG_i}(Q_{DG_i}^{s}(t)) +$$
$$COM_{DG_i}(P_{DG_i}^{s}(t))]\delta_{DG_i}(t) + C_e(P_{DG_i}^{s}(t)) + C_{bo}^{s}(t) + c_{isoP}(t).P_{bch}^{s}(t).\Delta t +$$
$$\sum_{i1=1}^{N1}CP_{Wi1}(P_{Wi1}^{s}(t)) + \sum_{i2=1}^{N2}CP_{PVi2}(P_{PVi2}^{s}) + c_{Pres}.P_{Drescut}^{s}(t) +$$
$$c_{Qres}.Q_{Drescut}^{s}(t) + c_{Pind}.P_{Dindcut}^{s}(t) + c_{Qind}.Q_{Dindcut}^{s}(t) +$$
$$c_{Pcom}.P_{Dcomcut}^{s}(t) + c_{Qcom}.Q_{Dcomcut}^{s}(t) + \sum_{i=1}^{N}c_G.P_{DG_icut}^{s}(t) +$$
$$\sum_{i1=1}^{N1}c_{ren}.P_{W_{i1}cut}^{s}(t) + \sum_{i2=1}^{N2}c_{ren}.P_{PV_{i1}cut}^{s}(t)\}$$

The revenue of the MG comes from selling the active and reactive power from the DGs, the discharging power of the battery, the power from the RDGs. The cost is constructed using equations

(2.15), (2.16), (2.1), (2.2), (2.3), (2.14), (2.11), (2.5), (2.6), cost of charging battery, and the last nine components which they are defined previously.

The solutions of the aforementioned objective functions produce a different solution for each possible $s = 1, \dots, S$. Each scenario has a respective probability of occurrence.

The first stage of the objective functions of equations (3.15) and (3.19) is subjected to the constraints of equations (2.17) to (2.35), whereas the first stage of the objective functions of equations (3.17) and (3.21) is subjected to the constraints of equations (2.17) to (2.25), (2.30) to (2.33), (2.36), and (2.37). The second stage of these objective functions is subjective to the same constraints of the first stage. However, the constraints in equations (2.17), (2.18), (2.34), (2.35), (2.36), and (2.37) are modified in the second stage to involve the uncertainties in the optimisation problems as in the following equations:

A. Active and reactive power balance constraints of the connected MG

For the connected MG

$$\sum_{t=1}^{T}\{\sum_{i=1}^{N}\delta_{DG_i}(t).P_{DG_i}^{S}(t)+\sum_{i1=1}^{N1}P_{W_{i1}}^{S}(t)+\sum_{i2=1}^{N2}P_{PV_{i2}}^{S}(t)+P_{b}^{S}(t)+ \quad (3.22)$$
$$P_{g}^{S}(t)=(P_{Dres}(t)-P_{Drescut}^{S}(t))+(P_{Dind}(t)-P_{Dindcut}^{S}(t))+$$
$$(P_{Dcom}(t)-P_{Dcomcut}^{S}(t))\}$$

$$\sum_{t=1}^{T}\{\sum_{i=1}^{N}\delta_{DG_i}(t).Q_{DG_i}^{S}(t)+Q_{g}^{S}(t)=(Q_{Dres}(t)-Q_{Drescut}^{S}(t))+ \quad (3.23)$$
$$(Q_{Dind}(t)-Q_{Dindcut}^{S}(t))+(Q_{Dcom}(t)-Q_{Dcomcut}^{S}(t))\}$$

For the isolated MG

$$\sum_{t=1}^{T}\{\sum_{i=1}^{N}\delta_{DG_i}(t).P_{DG_i}^{S}(t)+\sum_{i1=1}^{N1}P_{W_{i1}}^{S}(t)+\sum_{i2=1}^{N2}P_{PV_{i2}}^{S}(t)+P_{b}^{S}(t)- \quad (3.24)$$
$$\sum_{i=1}^{N}P_{DG_icut}^{S}(t)-\sum_{i1=1}^{N1}P_{W_{i1}cut}^{S}(t)-\sum_{i2=1}^{N2}P_{PV_{i1}cut}^{S}(t)=(P_{Dres}(t)-$$
$$P_{Drescut}^{S}(t))+(P_{Dind}(t)-P_{Dindcut}^{S}(t))+(P_{Dcom}(t)-P_{Dcomcut}^{S}(t))\}$$

$$\sum_{t=1}^{T}\{\sum_{i=1}^{N}\delta_{DG_i}(t).Q_{DG_i}^{S}(t)=(Q_{Dres}(t)-Q_{Drescut}^{S}(t))+(Q_{Dind}(t)- \quad (3.25)$$
$$Q_{Dindcut}^{S}(t))+(Q_{Dcom}(t)-Q_{Dcomcut}^{S}(t))\}$$

B. SSSCs

$$\sum_{i=1}^{T}\{\sum_{i=1}^{N}\delta_{DG_i}(t).P_{DG_imax}(t)\geq(P_{Dres}(t)-P_{Drescur}^{S}(t))+(P_{Dind}(t)- \quad (3.26)$$
$$P_{Dindcut}^{S}(t))+(P_{Dcom}(t)-P_{Dcomcut}^{S}(t))\}$$

$$\sum_{i=1}^{T}\{\sum_{i=1}^{N}\delta_{DG_i}(t).Q_{DG_imax}(t)\geq(Q_{Dres}(t)-Q_{Drescut}^{S}(t))+(Q_{Dind}(t)- \quad (3.27)$$
$$Q_{Dindcut}^{S}(t))+(Q_{Dcom}(t)-Q_{Dcomcut}^{S}(t))\}$$

C. SRCs

$$\sum_{i=1}^{T}\{\sum_{i=1}^{N}\delta_{DG_i}(t).P_{DG_imax}(t)\geq(P_{Dres}(t)-P_{Drescut}^{S}(t))+(P_{Dind}(t)- \quad (3.28)$$
$$P_{Dindcut}^{S}(t))+(P_{Dcom}(t)-P_{Dcomcut}^{S}(t))+R_{p}^{S}(t)\}$$

$$\sum_{i=1}^{T}\{\sum_{i=1}^{N}\delta_{DG_i}(t).Q_{DG_imax}(t)\geq(Q_{Dres}(t)-Q_{Drescut}^{S}(t))+(Q_{Dind}(t)- \quad (3.29)$$
$$Q_{Dindcut}^{S}(t))+(Q_{Dcom}(t)-Q_{Dcomcut}^{S}(t))+R_{q}^{S}(\mathrm{t})\}$$

3.6 Results of the Minimising the Total Operating Cost and Maximising the Profit of the MG

The proposed optimisation approaches are applied to the connected and isolated MG of the MG shown in Figure 2-3 and the DGs parameter data are presented in Table B-1, Table B-2, and Table B-3. The mean values of wind speed, PV generation, and OMPs are presented in Table B-6, whereas Figure C-1, Figure C-2, and Figure C-3 in appendix C show the generated scenarios for 24 hours for wind speed, PV generation, and OMP. These uncertainties resulting from the fluctuations of wind and solar generation and the OMP are considered to the connected MG, while wind and solar generation are adopted as sources of the uncertainties to the isolated MG.

A. Connected MG

Figure 3-2 and Figure 3-3 show the optimal scheduling of the active and reactive power generation of the five highest probability scenarios. It can be observed that the solely DE is committed from hours 1 to 7 with minimum output power to satisfy the SSSCs for the all five scenarios. At these hours, the active load demand is supplied from the DE, RDGs, and the rest loads are met by purchasing power from the utility grid because the purchasing power from the utility grid is lower than the DGs generation cost. The storage battery in the scenarios 1, 3 and 4 is discharged twice at hours 13 and 17 because the OMP has high values at these hours. Whereas, in the scenarios 2 and 5 the battery is discharged once at hour 17 when the price has the highest value because at hour 13 the OMP is lower than other scenarios. Therefore, there are no economic incentives for operating the battery at hour 13. Generally, the storage battery charging and discharging operations are scheduled to minimise the overall operating cost or maximise the MG profit. In addition, the MG at hours 4, 5, and 24 in the scenarios 3 and 5 purchases more active power from the utility grid than other scenarios because the wind and solar generation are equal to zero at hours 4 and 5 and quite low at hour 24. Further, the MG at hour 21 in the scenario 3 sells higher active power to the utility grid than other scenarios

because the renewable generation is higher than other scenarios. Furthermore, in the scenarios 1, 3, and 4 the MG at hour 13 sells higher active power to the utility grid than other scenarios because the battery is discharged at this hour for these scenarios.

Figure 3-3 reveals that in the scenarios 2 and 5 at hours 1 to 6 the reactive load is supplied by purchasing power from the utility grid because at these hours the reactive power generation cost of the DGs is higher than the purchasing power from the utility grid. While, in the scenarios 1, 3, and 4 at hour 6 the DE is committed to supply the load with the utility grid because the reactive OMP at hour 6 of the scenarios 1, 3 and 4 higher than the other two scenarios. In addition, the MG at hours 22 and 23 in the scenarios 2 and 5 purchases more reactive power from the utility grid than other scenarios because the reactive OMP is lower than other scenarios.

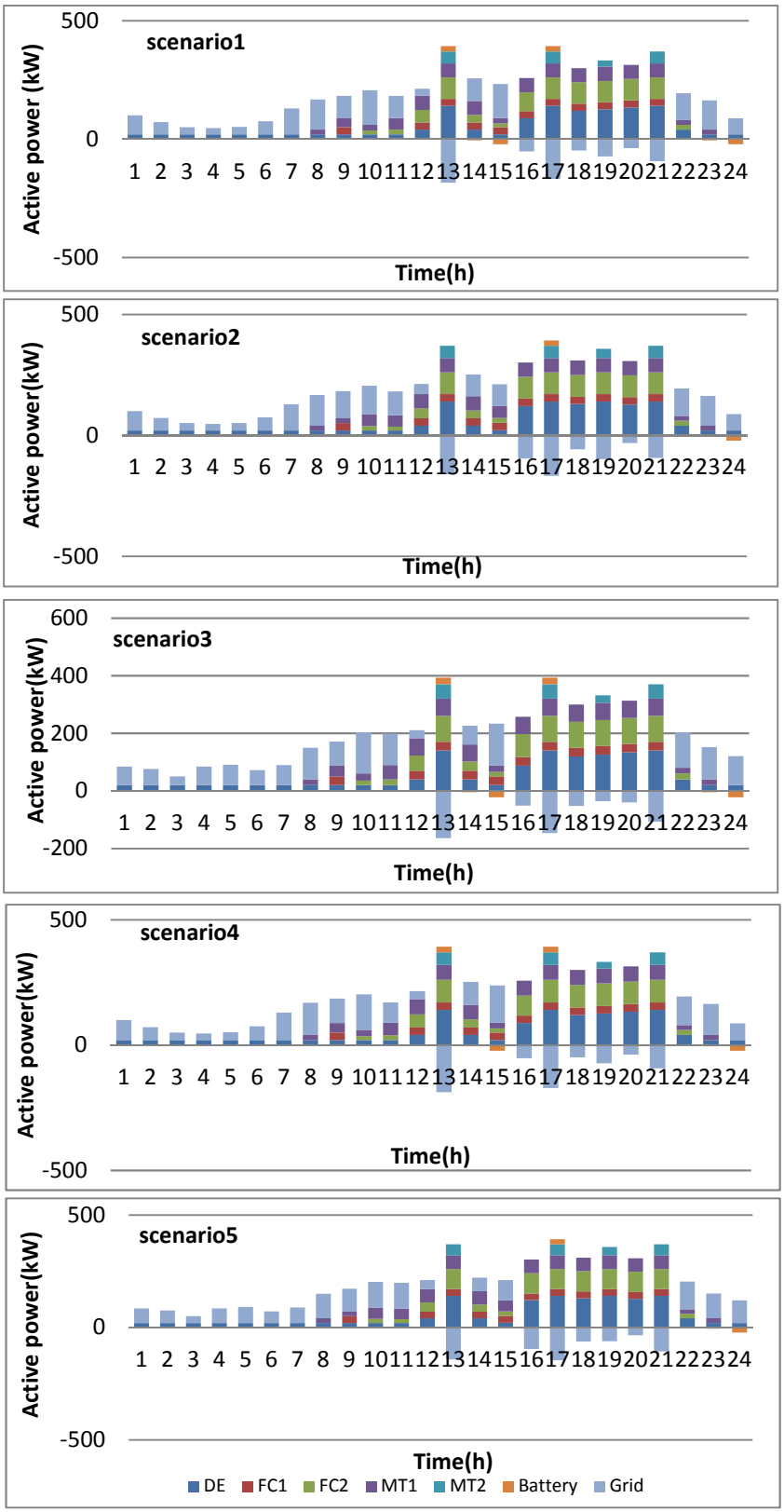

Figure 3-2 Optimal active power scheduling of the DGs and exchanging power with utility grid and the battery of the five highest probability scenarios

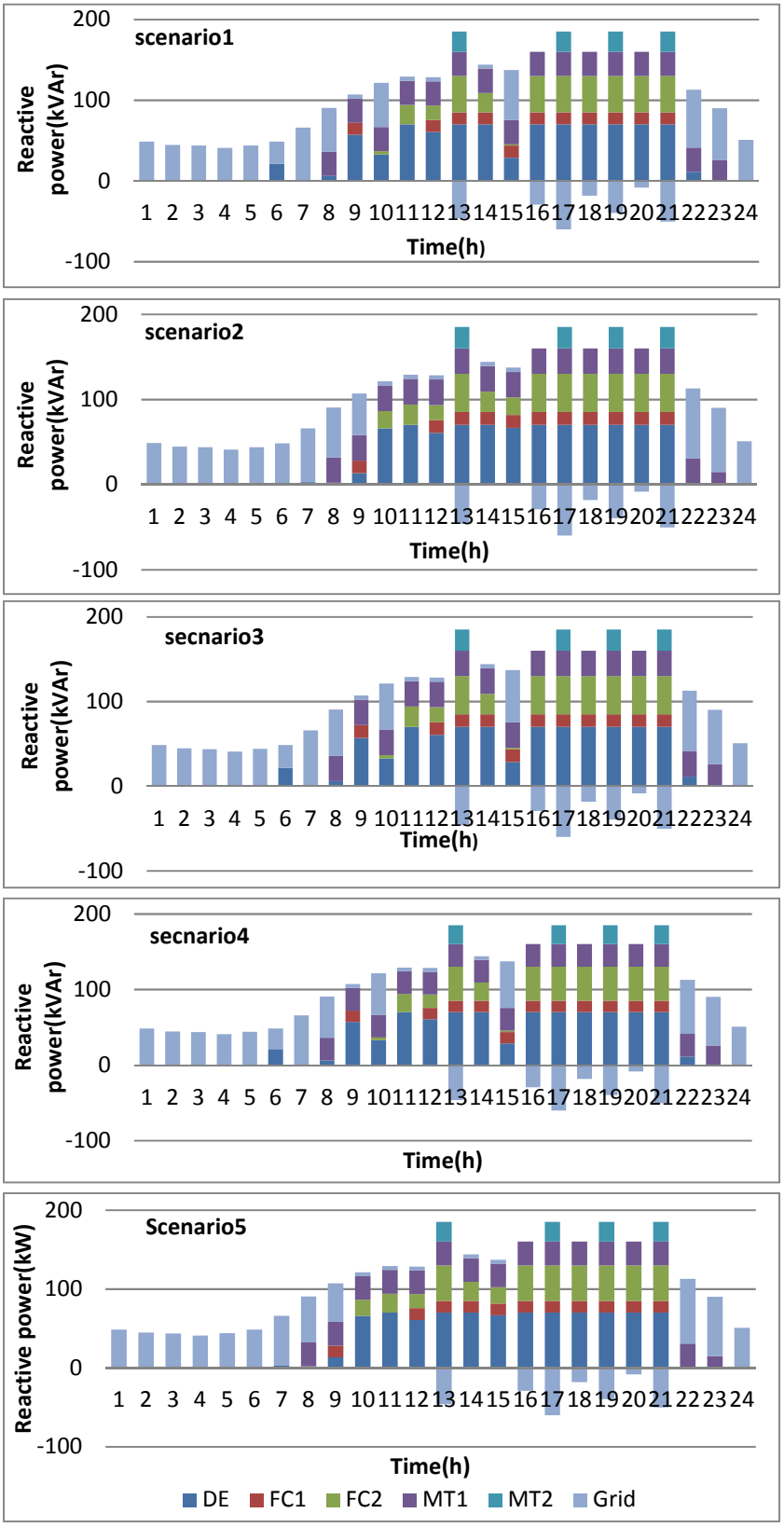

Figure 3-3 Optimal reactive power scheduling of the DGs and exchanging power with the utility grid of the five highest probability scenarios

Table 3-1 summarises the results of the five scenarios and Det. Case. The results demonstrate that the battery leads to reduce the overall cost and increases the profit despite including the battery degradation cost in the cost function for all scenarios.

Table 3-1 Results of the five scenarios and Det. Case of the connected MG

Scenarios	Sc1	Sc2	Sc3	Sc4	Sc5	Det. Case
Total cost (€/day)	410.7	418	416.9	409	424.5	408.1
Total cost (€/day) without battery	417.9	424	424.2	416.2	430.6	414.5
Profit (€/day)	253.8	243	247.6	255.5	236.5	281.2
Profit without battery (€/day)	246.6	237	240.3	248.3	230.5	274.8

Figure 3-4 and Figure 3-5 show the impacts of the uncertainties on the operating cost and the profit and Table C-1 and Table C-2 illustrate the hourly values of the operating cost and profit for the five scenarios and Det. Case. It can be seen that the lowest total cost is at hour 17 for all scenarios because at this hour the MG sells the highest active and reactive power to the utility grid and it also can be observed for the similar reasons that by far the highest profit of the MG is at hour 17 as well. It also can be seen that the costs of the of scenarios 1, 3, and 4 at hour 13 are lower than other scenarios because the MG sells higher power to the utility grid and the OMP has the values higher than other scenarios.

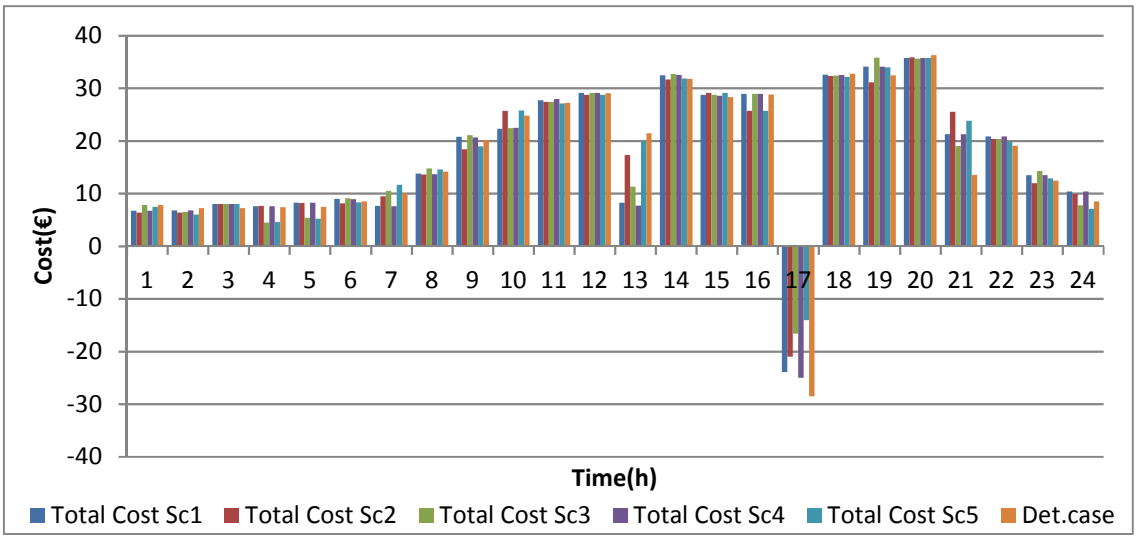

Figure 3-4 Total operating cost of the five highest probability and Det. Case of the connected MG

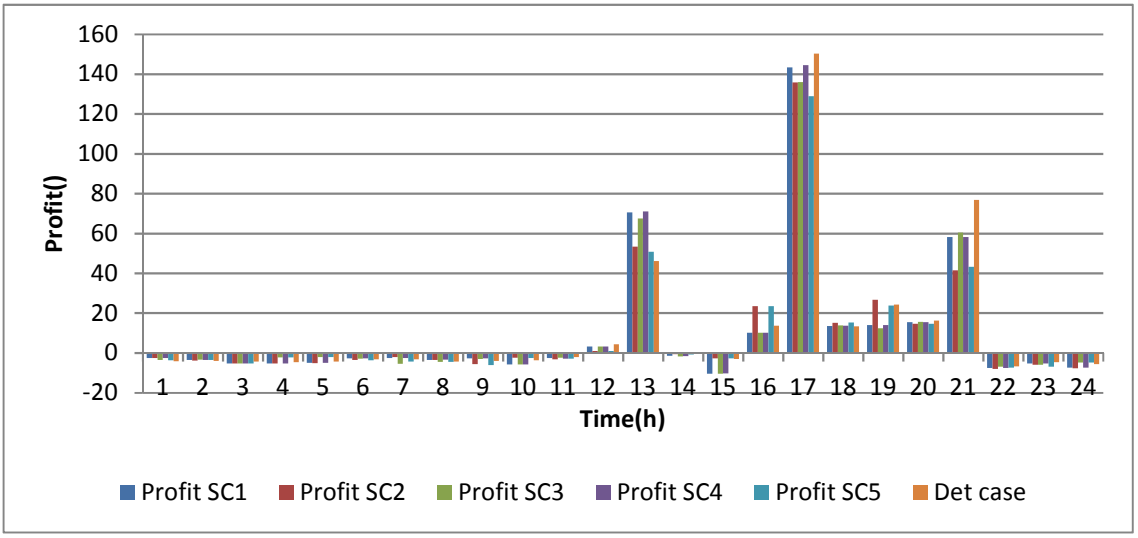

Figure 3-5 The MG profit of the five highest probability scenarios and Det. Case of the connected MG

From the aforementioned discussion, it is deduced that the scheduling of DGs active and reactive power and exchanging active and reactive power with the utility are altered with the fluctuation of the RDGs generation and the OMPs, whereas the battery charging and discharging operations are affected significantly by the OMP stochastic behaviour.

B. Isolated MG

Figure 3-6 shows the optimal scheduling of the active power of the five highest probability scenarios, while the reactive power scheduling of the five highest scenarios is the same of the Det. Case because the OMP is equal to zero, so there is no stochastic of the reactive variable in this case. It can be noticed that for the five stochastic scenarios at hours 1 to 6 only MT1 and DE are committed to satisfy the active and reactive SRs and meet the load with RDGs. The highest generation of the DGs of the Sc1, 3, 4, and 5 occurs at hour 20, whereas in the Sc2 occur at hour 19 because the wind generation is very low in this hour in comparing with other scenarios. In addition, this figure shows that the storage battery is not operated during the scheduling day of all the scenarios because there are not economic incentives from operating the battery. Further, in the Sc2 at hours 4, 5, and 24 the DGs generates more active

power than other scenarios because the renewable generation is equal to zero at hours 4 and 5 and it quite low at hour 24 comparing with other scenarios. In the Sc2, also the DGs generate less power at hour 14 than other scenarios. This is due to abundant renewable generation in comparing with other scenarios. Furthermore, the DGs in the Sc5 generate more active power at hour 22 than other scenarios because the renewable generation is very low at this hour. Table 3-2 shows the impacts of the uncertainties on the total cost and profit values per scheduling day for the five scenarios and Det. Case. Figure 3-7 and Figure 3-8 show the hourly total cost and profit of the MG of all the scenarios and Det. Case and Table C-3 and Table C-4 illustrate the hourly values of the operating cost and profit for the five scenarios and Det. Case. These figures reveal that the cost and profit have positive values over the entire scheduling day and the hourly values depend on the generation profile of the RDGs.

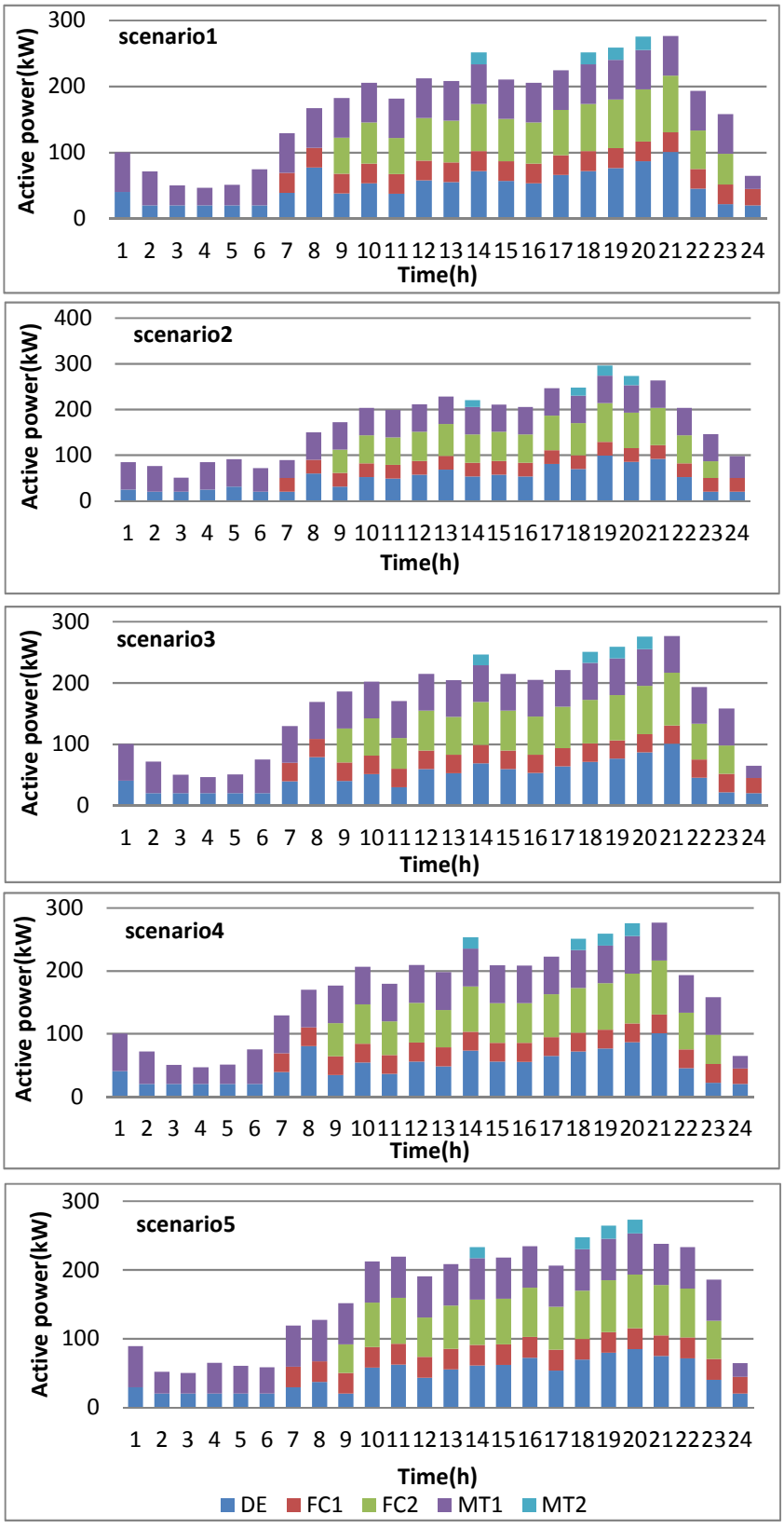

Figure 3-6 Optimal active power scheduling of the DGs of the five highest probability scenarios of the isolated MG

Table 3-2 Results of the five scenarios and Det. Case of the isolated MG

	Sc1	Sc2	Sc3	Sc4	Sc5	Det. Case
Total cost(€/day)	550.7	548.8	550.5	550.6	549.6	550.2
Profit (€/day)	233.5	235.4	233.7	233.6	234.6	234

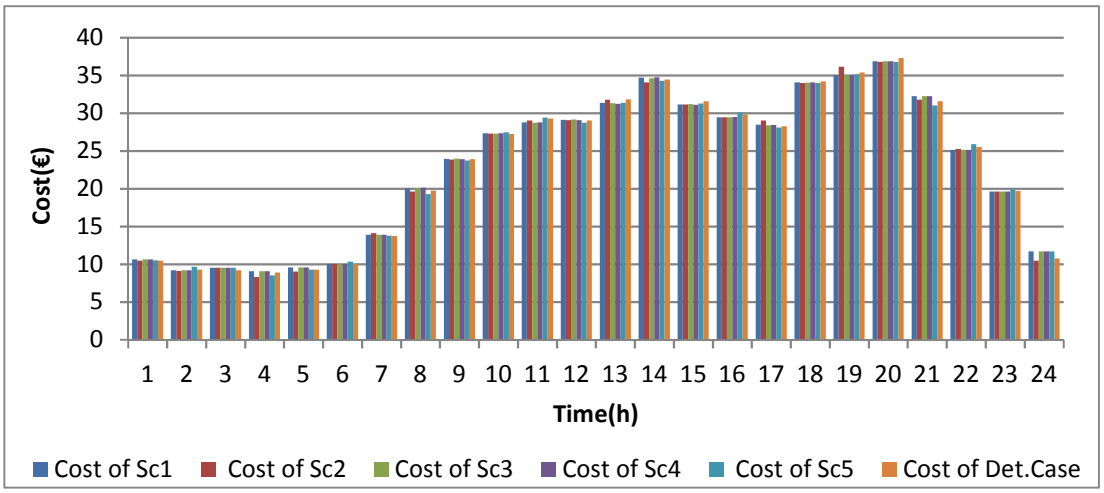

Figure 3-7 Total operating cost of the five highest probability and Det. Case of the isolated MG

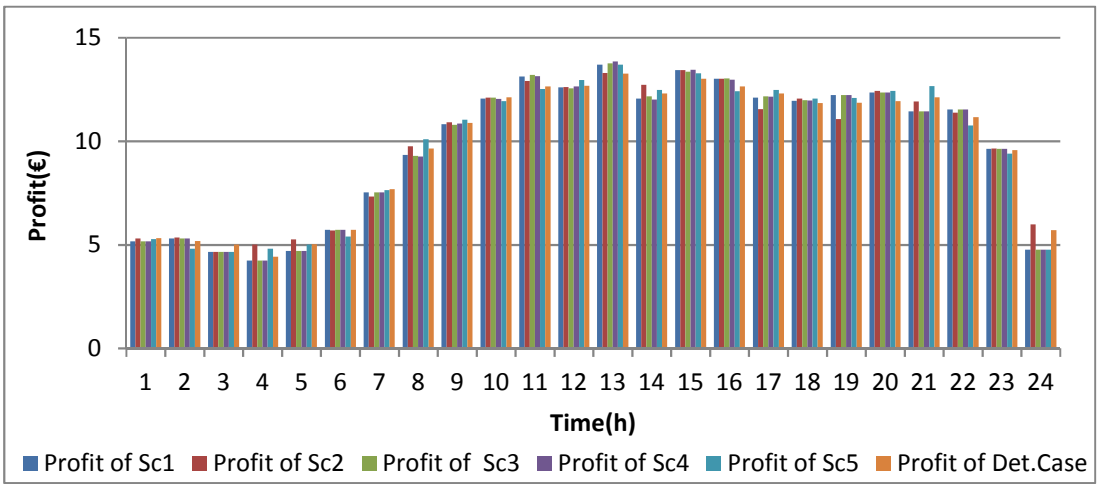

Figure 3-8 The MG profit of the five highest probability and Det. Case of the isolated MG

In comparison of the results of the connected and isolated MG, it can be seen that the impacts of the uncertainties on the generation of the DGs in the case of isolated MG are more obvious than the connected MG. This is because in the isolated MG solely the DGs compensate the fluctuations in the renewable

generation, whereas in the connected MG, the utility grid and the DGs can compensate the uncertainties.

3.7 Chapter Conclusions

This chapter presents a two-stage stochastic SCUC-UARDEED for the connected and isolated MG. It is concluded that the battery charging and discharging operations are affected by the OMP stochastic behaviour. The proposed approach can accommodate the uncertainties for connected and isolated mode. In addition, the scenario that has the highest renewable generation per scheduling day does not necessarily have the lowest cost or highest profit. This is because the power production cost of the renewable generation is included in the cost function.

4 Integration of the DSM with Optimal Scheduling of the MG

4.1 Chapter Summary

In this chapter, a novel integration of the DSM with SCUC-UARDEED of the MG is proposed. The impacts of the DSM on the total operating cost and the MG profit are presented. In addition, the impacts of the DSM on the active and reactive power optimal scheduling, the load profiles, the UC results, and the grid security of supply are demonstrated. In the proposed optimisation approach, all types of loads such as residential, industrial, and commercial are participated in the DSM. The DSM as load shifting technique [106] is applied to the residential consumers, whereas DBP is applied to the commercial and industrial loads. The models of the domestic appliances that operate in restricted cycles, such as washing machines (WMs) and dishwashers (DWs) are developed and the constraints relate to the DSM techniques are proposed and integrated with optimisation problem. The proposed optimisation approaches are applied to the connected and isolated MG and many scenarios are carried out to analyse the effectiveness of the proposed approaches.

4.2 Literature Review

The growth penetration of the RDGs with MGs makes the power balance and optimal scheduling of the MG generation resources more challenging. Therefore, the DSM becomes a key factor in the MG to help the grid operators to manage both the load and generation side to balance the power flow on the system. The DSM also has several potential benefits not only for the utilities but also to the customer. It reduces the total operating cost, increases the profit, improves security of supply, increases the penetration of the renewable generation, decreases the peak load, and saves the electricity bill for the consumer who participate in the DSM programmes [107], [108], [109]. Therefore, researchers have addressed the DSM and its impacts on the system operation. Reference [110] proposed load management strategies, such as peak clipping, valley filling, strategic conservation, and strategic load growth. It

was found that applying the DSM improved the system reliability. Reference [111] presented the impacts of load management as an interruptible load on the system reliability and cost. It was found that the DSM saved system costs. Reference [112] proposed DSM to improve security of the system. It was concluded that the proposed DSM Improved system stability and reliability. In [113], the impact of the DSM programmes on the unit commitment results was addressed. It was claimed that the DSM as peak clipping saved system cost and energy consumption. It was presented in [114] the benefits of the demand side response and energy storage on the postponement of the reinforcement of the existing distribution network, while the benefits of the DSM on the increasing the utilisation and penetration of wind energy were claimed in [115].

In contrast, in [16] and [8], the DSM as load cutting is incorporated with optimisation problems of the MG and it was determined the impacts of the DSM on the operating cost. These papers found that the DSM reduced the cost of the MG by the value depends on the penalty factor, while in [116], EMS of the MG with integration of the DSM was proposed. it was concluded that the DSM reduced the operating cost and the emission of the CO_2. Reference [17] incorporated the DSM as a shifting algorithm with an optimisation problem and it was claimed that the cost decreased when the load was shifted to the period when the renewable generation was available. The impacts of load cutting on the operating cost and the profit were determined in [50], [53]. It was stated that the load curtailed reduced the operating cost. References [117] and [118] proposed a shifting algorithm that was mathematically formulated to minimise the difference between the objective load curve and the actual load curve. This DSM programme was applied to the MG to study the impacts of the DSM on the loads and on the operating cost. It was concluded that the DSM reduced the operating cost; however, it was not explained how the DSM affects the operating cost mathematically and it was not stated the formulation of the optimisation problem to minimise the operating cost. Reference [57] incorporated the DSM with the profit of the MG. However, the DSM algorithms were considered as input to the optimisation algorithm and not as decisions

variable. It was demonstrated that the DSM as a shifting technique led to a reduction in the operating cost. The impacts of the DSM as load shifting to minimise both operating cost and the emission levels of greenhouse gases were suggested in [119]. It was found that the management of the LV load results in a significantly reduction of the cost.

The aforementioned previous works demonstrate that the majority of the proposed DSM techniques treated the load shifting as an aggregated amount, instead of as separate appliances with an operation cycle. In addition, in previous works that applied the DSM to separate appliances, the appliances are scheduled to bring the load consumption curve as close to objective load that had been previously determined. This means that the results of the DSM are treated as input to the optimisation algorithms not as decision variables. The previous papers considered the DSM as a shifting technique only and they did not consider other DSM techniques simultaneously; however, the reactive power management was overlooked and the DSM was applied to the active load solely. Furthermore, the previous papers did not take into consideration the environmental cost, battery degradation cost, RDGs production cost, reactive power cost, and purchasing reactive power from the utility grid in the formulating of the optimisation problems. The important constraints were neglected in the formulation of the optimisation problem in the previous works, such as active and reactive security constraints of the connected and isolated MG and limit of the greenhouse gases, and other constraints related to the reactive power management.

According to the literature, it appears that the integration of the DSM as a shifting strategy with the isolated MG to maximise the profit has not been addressed yet. This is addressed in this chapter.

4.3 Demand Side Management

The DSM changes the consumption electricity patterns of the consumers from the normal pattern in responding to change of the electricity price or to incentive payment programmes. The DSM techniques can be divided into two categories

depending on the time scaling and control approaches. These two groups are price or time and incentives based programmes [120]. In general, the time based programmes consist of three types, namely time of use (TOU), real time pricing (RTP) and critical peak pricing (CPP) [107]. The TOU has two or three-time blocks. Usually, this rate reflects the cost of electricity generation during different time intervals. RTP is a dynamic price reflects the change on the wholesale price on an hourly, half hour, quarter hour. CPP is a mix between TOU and RTP and it is difficult to implement. It is restricted to the extreme peak hours of a limited number of times during a year. The aforementioned price based programmes are indirect load control (ILC) where the load reduction has to be accomplished by consumer itself in responding to one of the above price schemes.

On the other hand, the incentives DSM programmes consist of six kinds, namely direct load control (DLC), interruptible/curtailed(I/C), emergency demand response (EDR), demand bedding (DB), capacity market (CA) and ancillary service (A/S) [121], [122]. DLC and EDRP are voluntary programmes and the consumers do not penalise, if they do not curtail their electricity consumption. I/C and CAP are compulsory programmes and enrolled consumers are subjected to penalize if they do not reduce their consumption. DBP encourages large consumers to offer load curtailment at a price that is willing to be curtailed. A/S allows to the consumer to bid in the electricity as an operating reserve [121]. More details about these strategies can be found in [123], [124].

4.4 DSM Objectives

Generally, the main objective of the DSM techniques is to reshape the load profile of the consumers. Accordingly, six load shapes are obtained [108], [125] namely peak clipping, valley filling, load shifting, strategic conservation, strategic load growth and flexible load shape. These six shapes are depicted in Figure 4-1. The peak clipping and valley filling aim to flatten the load curve and reduce the peak load. This increases the security of smart grid and reduces the

operating cost. Load shifting is the most famous DSM technique, which is widely used in load shaping of the distribution system. It reduces peak load and shift it to off peak hours if possible [126]. Strategic conservation focuses on reducing the demand not only during peak load but also at other times. This may reduce the overall cost [127]. Strategic load growth the utility encourages consumers to change the fossil fuel equipment or improve customer productivity or life quality. The load growth may include electrification such as EVs [124]. Flexible load is regarding to the power supply reliability, where the load can be controlled or curtailed.

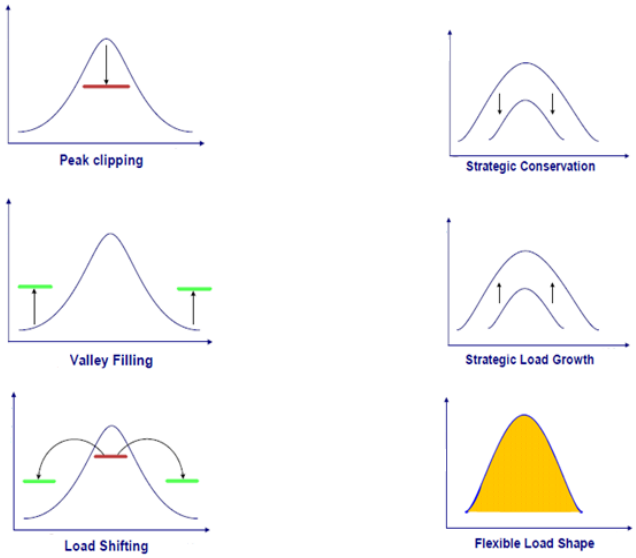

Figure4-1 Load shapes produced from applying the DSM techniques [127]

4.5 Proposed Models of the DSM

The loads in the power system is classified into three main groups, namely residential (R), commercial (C) and industrial (C) consumers. In this research, these three types of loads are considered. Different types of the DSM techniques are applied to these loads, where the DSM as shifting technique is applied to the residential load, while DBP is applied to the industrial and commercial loads. Each load has different profile and the total load is the summation of these three loads.

The proposed optimisation approach has two main functions: the first one is to schedule the starting time of each shift-able appliance type and the second is to accept or rejects the bids of the commercial and industrial consumers, where the DSM techniques are considered as decision variables in the optimisation algorithms. The choosing of WMs and DWs as shift-able appliances is for many reasons: their data availability, they used in all seasons during the year, a flexibility which is offered by consumer acceptance due to the less impact on the comfort of the consumers. The proposed approach is general and it can be applied to other appliances.

4.6 Proposed Load Shifting Technique

The load shifting technique is used to shift the connection time of household smart appliances (WMs, DWs), where the shifting decisions are taken by the MG optimiser depending on the optimisation problem either to minimise of the operating cost or maximises the profit. The input data for the optimisation algorithm is the number of devices at each time step of each device type and the control possibilities of each appliance.

4.6.1 Shifting Devices Data

A summary of the data of the WMs and DWs are illustrated in Table 4-1. Penetration factor means the percentages of domestic households having a specific type of these devices. These values are chosen based on the household survey data presented in reports [128], [129], [130], [131].

Table 4-1 Shifting devices data

	Operation cycle duration (h)	Penetration factor (%)	Energy consumption per cycle (Wh)
WMs	2	0.82	887.5
DWs	2	0.75	1192.5

Figure 4-2(a) and Figure 4-3(a) show the diversified consumption curves per 192 household of the WMs and DWs per 1h resolution respectively. Wide consumption of each appliance can be obtained by multiplying these diversified profiles by the number of households and by penetration factor. Diversified

consumption profile for a specific device gives the information about the device time of day use. For example, it can be observed from Figure 4-2 (a) that the WMs have two peaks in the morning and one in the evening and relatively there is low consumption during the night, while the DWs have one peak at night. The operation cycles of WMs and DWs per 1h resolution are given in Figure 4-2(b) and Figure 4-3(b) respectively [129], [131].

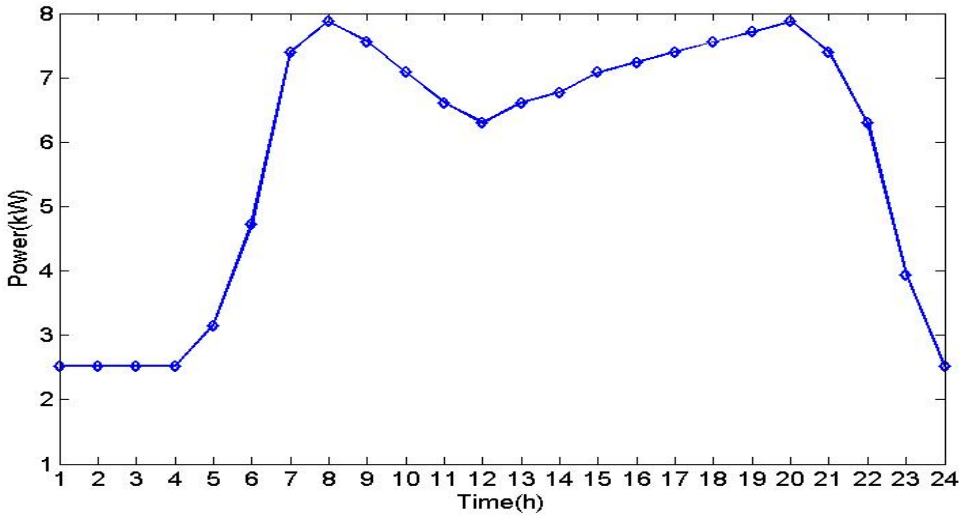

(a) Diversified profile of WM

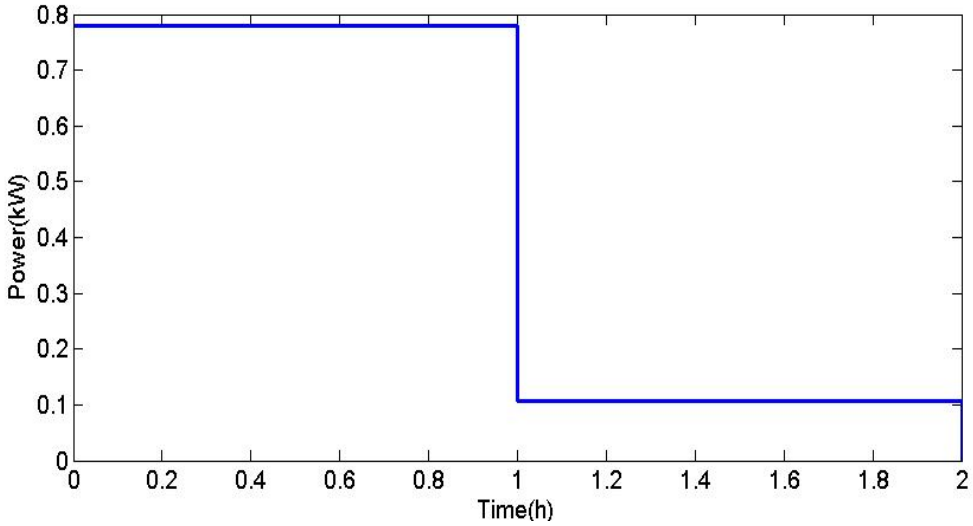

(b) Operation cycle of WM

Figure 4-2 WM diversified profile and operation cycles

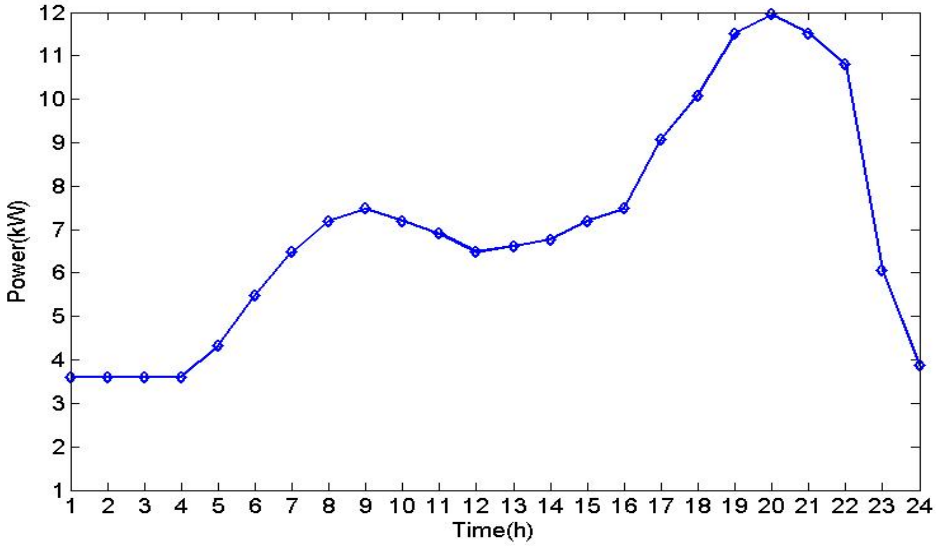

(a) Diversified profile of DW

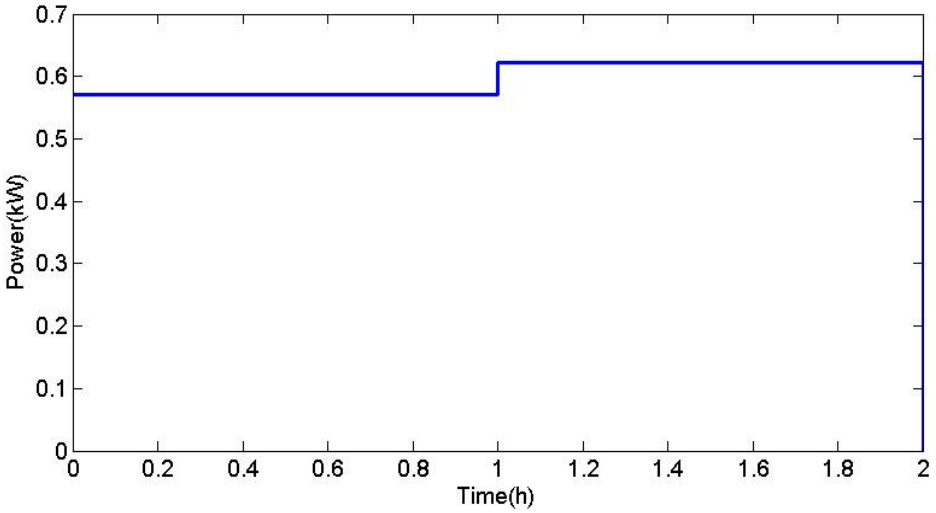

(b) Operation cycle of DW

Figure 4-3 DW diversified profile and operation cycles

4.6.2 Estimating Number of Smart Appliances Connected to the Grid at each Time Interval

The optimisation algorithm needs the number of devices that are connected to the grid at each time interval. This represents the diversified consumption curve for each device when no DSM activities are taken into consideration. The estimated number of each device is calculated by diversified curve disaggregation [109]

$$C_t = \sum_{w=1}^{d} D_{t-(w-1)} \cdot p_w \quad \textbf{(4.1)}$$

where D_t represents the number of devices that start their consumption time at t. C_t is the consumption power at time t read from the diversified consumption pattern. d is the duration of device consumption cycle and p_w is the device consumption at each time interval, $(w = 1,2 \dots d)$. Power C_t at each time step is composed of the consumption power of the devices that start their consumption at t and the devices that have already started their operation at the previous time interval.

There is an equation like equation 4.1 for each time step for each device. In general, the obtained number of connected appliances will not be an integer number. These numbers should be truncated to the closest integer number. The number of WMs and DWs in the UK for the 192 households are shown in Figure 4-4, which is calculated by using equation 4.1.

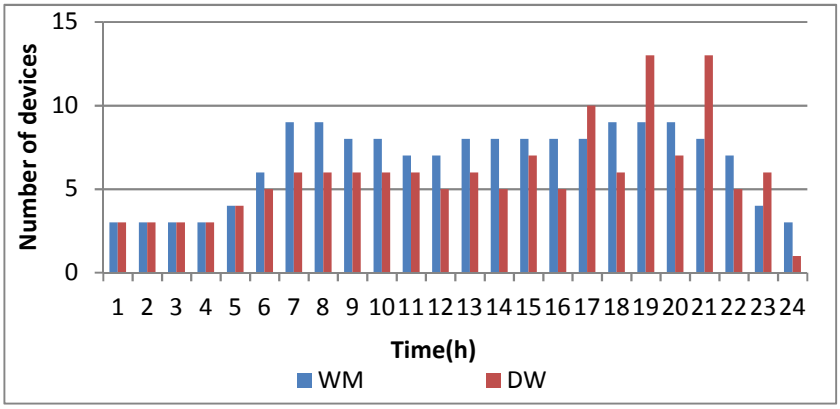

Figure 4-4 Expected number of appliances that are connected to the MG at each time step

4.6.3 Proposed Control Possibilities of the WMs and DWs

The control possibilities should satisfy a specific condition agreed between the customers and MG operator. Three scenarios are proposed to the possible control of the controllable devices, where the customers can choose one of them.

Sc1: The devices can be shifted every day at any time between hours 18 to 23.

Sc2: The devices can be shifted every day at any time between hours 10 and 16.

Sc3: The connection time of the devices can be delayed for maximum 4 hours.

These scenarios are compared with scenario without the DSM (base case). It is supposed that the scheduling day starts at 8.00 AM and finished at 8.00 AM next day as illustrated in Table D-1.

4.6.4 Proposed Mathematical Models of the Shifting Technique

Applying the shifting DSM technique to residential load will change the original load according to the demand shifted and recovered as follows [109]:

$$P_{Dres}^{DSM}(t) = P_{Dres}(t) - P_{Dres}^{shft}(t) + P_{Dres}^{reco}(t) \quad \textbf{(4.2)}$$

where $P_D^{DSM}(t)$ is the residential load after applying the DSM.

The recovered load is calculated as follows:

$$P_{Dres}^{reco}(t) = \sum_{f=1}^{t-1}\sum_{k=1}^{n_1} X_{kft}.P_{1k} + \sum_{l=1}^{d-1}\sum_{f=1}^{t-1}\sum_{k=1}^{n_1} X_{kf(t-1)}.P_{(1+l)k} \quad \textbf{(4.3)}$$

where X_{kft} is the number of devices of the type k that are shifted from time f to t, P_{1k} and $P_{(1+l)k}$ are the power consumption at time steps 1 and $(1+l)$, n_1 is the number of device types. d is the whole duration consumption of the device of type k. Obviously, the equation 4.3 shows that the connection load consists of two parts. Firstly, the increased load at time t due to the connection of devices shifted to time t, while the second is the increase of load at time t that comes from the connection of device at previous time step $t-1$.

Mathematical formulation of the shifting demand is formulated in a similar manner as above

$$P_{Dres}^{shft}(t) = \sum_{j1=t+1}^{t+n2}\sum_{k=1}^{n_1} X_{ktj1}.P_{1k} + \sum_{l=1}^{d-1}\sum_{j1=t+1}^{t+n2}\sum_{k=1}^{n_1} X_{k(t-1)j1}.P_{(1+l)k} \quad \textbf{(4.4)}$$

where $n2$ is the maximum dely. It can be observed from equation 4.4 that the disconnected loads that result from disconnected appliances consist of two parts. Firstly, the decrease in load due to postponing the connection time of the devices that were originally estimated to start their consumption at time step t and secondly the decrease of load due to the delay of devices that were supposed to start their consumption at a time $(t-1)$. It is assumed that the operating time of shift-able devices cannot be interrupted.

4.6.5 The Constraints of the Shifting DSM

The following constraints should be satisfied when solving the optimisation problem

A. The number of the shifting devices cannot be negative

$$X_{kft} \geq 0 \tag{4.5}$$

where $k = 1, \dots, n_1$.

B. The number of the devices that are shifted away at a time step is not be greater than the devices available for control at the time step i.

$$D_{kft} \geq \sum_{t=1}^{n3} X_{kft} \tag{4.6}$$

where D_{kft} is the expected number of the appliances that are calculated in section 4.6.2, $n3$ is the maximum number of time steps.

C. The appliances cannot be moved back in the past

$$X_{kft} = 0 \qquad if \;\; t < f \tag{4.7}$$

D. The shifted appliances should be recovered within the scheduling day

$$X_{kft} = 0 \qquad if \;\; t > T - (d-1) \tag{4.8}$$

4.7 Proposed DB Technique

The DBP encourages the heavy consumers like (industrial and commercial loads) to offer load reduction at a specific price. The DB technique is incorporated directly to the optimisation problems. The consumers send their bids of the load reduction in kW with prices that would be willing to curtail their loads and the MG has to send back the acceptance or reject the bids of the consumers on the day-ahead or hour-ahead. The MG accepts or rejects the bids according to the minimise the total cost or maximises the profit.

The cost of the commercial and industrial loads shedding is formulated as follows:

$$C_{Pindshd}(t) = \sum_{t=1}^{T} \delta_{ind}(t).P_{Dindshd}(t).c_{Pindshd}(t) \quad \textbf{(4.9)}$$

$$C_{Pcomshd}(t) = \sum_{t=1}^{T} \delta_{com}(t).P_{Dcomshd}(t).c_{Pcomshd}(t) \quad \textbf{(4.10)}$$

where $\delta_{ind}(t)$ and $\delta_{com}(t)$ are the binary variables are employed to accept or reject the load curtailments for the industrial and commercial loads respectively, $P_{Dindshd}(t)$ and $P_{Dcomshd}(t)$ are the curtailed loads that are offered by industrial and commercial consumers, $c_{Pindshd}(t)$ and $c_{Pcomshd}(t)$ are the prices of cutting the industrial and commercial loads.

4.8 Proposed Active and Reactive DSM

The reactive load shifting or shedding is not directly managed but it is estimated indirectly by using power factor ($cos\theta$). The reactive power is calculated by using $cos\theta$ [132] as follows:

$$PF = cos\theta = \frac{P}{S_{sys}} \quad \textbf{(4.11)}$$

where θ is the angle between voltage and current phasors, P (kW) is the active power and S_{sys} (kVA) is the apparent power. If the $cos\theta$ is known, it is straightforward to find $\Psi = tan\theta$ that represents the ratio between active power and the reactive power. Ψ is calculated as

$$tan\theta = \Psi = \frac{Q}{P} \quad \textbf{(4.12)}$$

If the power factor and active power are known, it is easy to compute the reactive power as follows:

$$Q(t) = \Psi.P(t) \quad \forall t \in T \quad \textbf{(4.13)}$$

By using equation 4.13 the shifting DSM technique for the reactive power is expressed by the following equations

$$Q_{Dres}^{DSM}(t) = Q_{Dres}(t) - Q_{Dres}^{shft}(t) + Q_{Dres}^{reco}(t) \quad \textbf{(4.14)}$$

$$Q_{Dres}^{shft}(t) = \Psi.P_{Dres}^{shft}(t) \quad \textbf{(4.15)}$$

$$Q_{Dres}^{reco}(t) = \Psi.P_{Dres}^{reco}(t) \quad \textbf{(4.16)}$$

while the reactive load for the DBP is formulated by the following equations:

$$C_{Qindshd}(t) = \sum_{t=1}^{T} \delta_{ind}(t).Q_{Dindshd}(t).c_{Qindshd}(t) \quad \textbf{(4.17)}$$

$$C_{Qcomshd}(t) = \sum_{t=1}^{T} \delta_{com}(t).Q_{Dcomshd}(t).c_{Qcomshd}(t) \quad \textbf{(4.18)}$$

$$Q_{Dindshd}(t) = \Psi.P_{Dindshd}(t) \quad \textbf{(4.19)}$$

$$Q_{Dcomshd}(t) = \Psi.P_{Dcomshd}(t) \quad \textbf{(4.20)}$$

where $c_{Qindshd}$ and $c_{Qcomshd}$ are the cost of the reactive industrial and commercial loads shed. The $cos\theta$ is assumed time independent and has only one value for the whole system; therefore, the reactive power is proportional to the active load. Accordingly, if the active load shedding or shifting equal zero, the reactive load shedding or shifting equal zero as well.

4.9 Formulation of the Proposed Optimisation Problem with Appling the Shifting DSM to the Residential Area

The same objective functions of equations (2.39) and ((2.412.41) are used for the connected and isolated MG respectively to minimise the total operating cost.

Similarly, equations (2.46) and (2.48) are used to the connected and isolated MG respectively to maximise the profit. These objective functions are subject to the constraints of equations (2.17) to (2.35) for the connected MG. In case of the isolated MG, the objective functions are subjected to the constraints of equations (2.17) to (2.25), (2.30) to (2.33), (2.36), and (2.37). These objective functions are subjected to the constraints of equations (4.5) to (4.8). However, the constraints of the equations (2.17), (2.18), (2.34), (2.35), (2.36), and (2.37) are modified to involve the DSM techniques as in the following equations:

A. Power balance constraints

The active and reactive power balance constraints for the connected MG are as

$$\sum_{t=1}^{T}\{\sum_{i=1}^{N}\delta_{DG_i}(t).P_{DG_i}(t)+\sum_{i1=1}^{N1}P_{W_{i1}}(t)+\sum_{i2=1}^{N2}P_{PV_{i2}}(t)+P_b(t)+ \quad \textbf{(4.21)}$$
$$P_g(t)=(P_{Dres}(t)-P_{Dres}^{shft}(t)+P_{Dres}^{reco}(t))+P_{Dind}(t)+P_{Dcom}(t)\}$$

$$\sum_{t=1}^{T}\{\sum_{i=1}^{N}\delta_{DG_i}(t).Q_{DG_i}(t)+Q_g(t)=(Q_{Dres}(t)-Q_{Dres}^{shft}(t)+Q_{Dres}^{reco}(t))+ \quad \textbf{(4.22)}$$
$$Q_{Dind}(t)+Q_{Dcom}(t)\}$$

The same equations are used for isolated MG with both the $P_g(t)$ and $Q_g(t)$ being equal to zero.

B. SSSCs

The active and reactive SSSCs of the connected MG are formulated as

$$\sum_{i=1}^{T}\{\sum_{i=1}^{N}\delta_{DG_i}(t).P_{DG_imax}(t)\geq(P_{Dres}(t)-P_{Dres}^{shft}(t)+P_{Dres}^{reco}(t))+ \quad \textbf{(4.23)}$$
$$P_{Dind}(t)+P_{Dcom}(t)\}$$

$$\sum_{i=1}^{T}\{\sum_{i=1}^{N}\delta_{DG_i}(t).P_{DG_imax}(t)\geq(Q_{Dres}(t)-Q_{Dres}^{shft}(t)+Q_{Dres}^{reco}(t))+ \quad \textbf{(4.24)}$$
$$Q_{Dind}(t)+Q_{Dcom}(t)\}$$

C. SRCs

The active and reactive SRCs of the isolated MG are formulated as

$$\sum_{t=1}^{T}[\sum_{i=1}^{N}\delta_{DG_i}(t).P_{DG_i max}(t) \geq (P_{Dres}(t) - P_{Dres}^{shft}(t) + P_{Dres}^{reco}(t)) + P_{Dind}(t) + P_{Dcom}(t) + R_p(t)] \quad \textbf{(4.25)}$$

$$\sum_{t=1}^{T}[\sum_{i=1}^{N}\delta_{DG_i}(t).Q_{DG_i max}(t) \geq (Q_{Dres}(t) - Q_{Dres}^{shft}(t) + Q_{Dres}^{reco}(t)) + Q_{Dind}(t) + Q_{Dcoms}(t) + R_q(t)] \quad \textbf{(4.26)}$$

4.10 Proposed Objective Functions of Applying the DBP to the Industrial and Commercial Loads

The objective functions of minimising the total operating cost and maximising the profit for the connected and isolated MG are modified as follows:

4.10.1 Minimising the Operating Cost

A. Connected MG

The optimisation problem is formulated as

$$\min(F) \quad \textbf{(4.27)}$$

where the objective function F is

$$F = \sum_{t=1}^{T}\{\sum_{i=1}^{N}[[CP_{DG_i}(P_{DG_i}(t)) + CQ_{DG_i}(Q_{DG_i}(t)) + COM_{DGi}(P_{DG_i}(t))]\delta_{DG_i}(t) + SU_{DG_i}(t) + SD_{DG_i}(t)] + C_e(P_{DG_i}(t)) + C_{bo}(t) + C_{gP}(t) + C_{gQ}(t) + \sum_{i1=1}^{N1} CP_{W_{i1}}(P_{W_{i1}}(t)) + \sum_{i2=1}^{N2} CP_{PV_{i2}}(P_{PV_{i2}}(t)) + C_{Pindshd}(t) + C_{Qindshd}(t) + C_{Pcomshd}(t) + C_{Qcomshd}(t)\} \quad \textbf{(4.28)}$$

This is constructed from the same equations that are constructed the objective function of the equation (2.39) with adding the equations of (4.9), (4.10), (4.17), and (4.18).

B. Isolated MG

The optimisation problem is formulated as

$$\min(F) \tag{4.29}$$

where the objective function F is

$$F = \sum_{t=1}^{T}\{\sum_{i=1}^{N}[[CP_{DG_i}(P_{DG_i}(t)) + CQ_{DG_i}(Q_{DG_i}(t)) + COM_{DGi}(P_{DG_i}(t))]\delta_{DG_i}(t) + SU_{DG_i}(t) + SD_{DG_i}(t)] + C_e(P_{DG_i}(t)) + C_{bo} + \sum_{i1=1}^{N1} CP_{W_{i1}}(P_{W_{i1}}(t)) + \sum_{i2=1}^{N2} CP_{PV_{i2}}(P_{PV_{i2}}(t)) + C_{Pindshd}(t) + C_{Qindshd}(t) + C_{Pcomshd}(t) + C_{Qcomshd}(t)\} \tag{4.30}$$

This is constructed from the same equations that are constructed the objective function of equation (2.41) with adding the equations of (4.9), (4.10), (4.17), and (4.18).

4.10.2 Maximising the MG profit

A. Connected MG

The optimisation problem is formulated as

$$\max(F) \tag{4.31}$$

where the objective function F is

$$F = \sum_{t=1}^{T}\{\sum_{i=1}^{N}[c_{gP}(t).P_{DG_i}(t) + c_{gQ}(t).Q_{DG_i}(t)]\delta_{DG_i}(t) + c_{gP}(t).P_{bdis}(t).\Delta t + c_{gP}(t).\sum_{i2=1}^{N2} P_{PV_{i2}}(t) + c_{gP}(t).\sum_{i1=1}^{N1} P_{W_{i1}}(t)\} - \sum_{t=1}^{T}\{\sum_{i=1}^{N}[[CP_{DG_i}(P_{DG_i}(t)) + CQ_{DG_i}(Q_{DG_i}(t)) + COM_{DG_i}(P_{DG_i}(t))]\delta_{DG_i}(t) + SU_{DG_i}(t) + SD_{DG_i}(t)] + C_e(P_{DG_i}(t)) + C_{bo} + c_{gP}.P_{bch}(t).\Delta t + \sum_{i1=1}^{N1} CP_{W_{i1}}(P_{W_{i1}}(t)) + \sum_{i2=1}^{N2} CP_{PV_{i2}}(P_{PV_{i2}}(t)) + C_{Pindshd}(t) + C_{Qindshd}(t) + C_{Pcomshd}(t) + C_{Qcomshd}(t)\} \tag{4.32}$$

This is constructed from the same equations that are constructed the objective function of equation (2.46) with adding the equations of (4.9), (4.10), (4.17), and (4.18).

B. Isolated MG

The optimisation problem is formulated as

$$\max(F) \tag{4.33}$$

where the objective function F is

$$\begin{aligned} F = \sum_{t=1}^{T}\{\sum_{i=1}^{N}[c_{isoP}(t).P_{DG_i}(t) + c_{isoQ}(t).Q_{DG_i}(t)]\delta_{DG_i}(t) + \\ c_{isoP}(t).P_{bdis}(t).\Delta t + c_{isoP}(t).\sum_{i2=1}^{N2}P_{PV_{i2}}(t) + c_{isoP}(t).\sum_{i1=1}^{N1}P_{W_{i1}}(t)\} - \\ \sum_{t=1}^{T}\{\sum_{i=1}^{N}[[CP_{DG_i}(P_{DG_i}(t)) + CQ_{DG_i}(Q_{DG_i}(t)) + COM_{DG_i}(P_{DG_i}(t))]\delta_{DG_i}(t) + \\ SU_{DG_i}(t) + SD_{DG_i}(t)] + C_e(P_{DG_i}(t)) + C_{bo}(t) + c_{isoP}.P_{bch}(t).\Delta t + \\ \sum_{i1=1}^{N1}CP_{W_{i1}}(P_{W_{i1}}(t)) + \sum_{i2=1}^{N2}CP_{PV_{i2}}(P_{PV_{i2}}(t)) + C_{Pindshd}(t) + \\ C_{Qindshd}(t) + C_{Pcomshd}(t) + C_{Qcomshd}(t)\} \end{aligned} \tag{4.34}$$

This is constructed from the same equations that are constructed the objective function of equation (2.48) with adding the equations of (4.9), (4.10), (4.17), and (4.18).

The objective functions of equations (4.28) and (4.32) are subjected to the constraints of equations (2.17) to (2.35), whereas the objective functions of equations (4.30) and (4.34) are subjected to the constraints of equations (2.17) to (2.25), (2.30) to (2.33), (2.36), and (2.37). However, the constraints of the equations (2.17), (2.18), (2.34), (2.35), (2.36), and (2.37) are modified to involve the DSM as in the following equations:

A. Active and reactive power balance constraints for the connected MG are as follows:

$$\begin{aligned} \sum_{t=1}^{T}\{\sum_{i=1}^{N}\delta_{DG_i}(t).P_{DG_i}(t) + \sum_{i1=1}^{N1}P_{W_{i1}}(t) + \sum_{i2=1}^{N2}P_{PV_{i2}}(t) + P_b(t) + \\ P_g(t) = P_{Dres}(t) + (P_{Dind}(t) - P_{Dindshd}(t)) + \big(P_{Dcom}(t) - P_{Dcomshd}(t)\big)\} \end{aligned} \tag{4.35}$$

$$\begin{aligned} \sum_{t=1}^{T}\{\sum_{i=1}^{N}\delta_{DG_i}(t).Q_{DG_i}(t) + Q_g(t) = Q_{Dres}(t) + (Q_{Dind}(t) - \\ Q_{Dindshd}(t)) + \big(Q_{Dcom}(t) - Q_{Dcomshd}(t)\big)\} \end{aligned} \tag{4.36}$$

The same equation is used for the isolated MG with both $P_g(t)$ and $Q_g(t)$ equal to zero.

B. SSSCs

The active and reactive SSSCs for the connected MG are formulated as

$$\sum_{i=1}^{T}\{\sum_{i=1}^{N}\delta_{DG_i}(t).P_{DG_i max}(t) \geq P_{Dres}(t) + (P_{Dind}(t) - P_{Dindshd}(t)) + \left(P_{Dcom}(t) - P_{Dcomshd}(t)\right)\} \quad \textbf{(4.37)}$$

$$\sum_{i=1}^{T}\{\sum_{i=1}^{N}\delta_{DG_i}(t).P_{DG_i max}(t) \geq Q_{Dres}(t) + \left(Q_{Dcom}(t) - Q_{Dcomshd}(t)\right) + (Q_{Dind}(t) - Q_{Dindshd}(t))\} \quad \textbf{(4.38)}$$

C. SRCs

The active and reactive SRs for the isolated MG solely are formulated as

$$\sum_{t=1}^{T}[\sum_{i=1}^{N}\delta_{DG_i}(t).P_{DG_i max}(t) \geq P_{Dres}(t) + \left(P_{Dcom}(t) - P_{Dcomshd}(t)\right) + (P_{Dind}(t) - P_{Dindshd}(t)) + R_p(t)] \quad \textbf{(4.39)}$$

$$\sum_{t=1}^{T}[\sum_{i=1}^{N}\delta_{DG_i}(t).Q_{DG_i max}(t) \geq Q_{Dres}(t) + (Q_{Dind}(t) - Q_{Dindshd}(t)) + \left(Q_{Dcom}(t) - Q_{Dcomshd}(t)\right) + R_q(t)] \quad \textbf{(4.40)}$$

4.11 Proposed Objective Function of Applying both shifting and DBP Simultaneously

The objective functions of applying both shifting and DB techniques simultaneously are the same of equations (4.28) and (4.30) to minimise the operating and emission costs of the connected and isolated MG respectively, while equations (4.32) and (4.34) to maximise the profit of the connected and isolated MG. These objective functions are subjected to the constraints of equations (2.17) to (2.35) for the connected MG. In case of the isolated MG, the objective functions are subjected to the constraints of equations (2.17) to (2.25), (2.30) to (2.33), (2.36), and (2.37). These objective functions are subjected to the constraints of equations 4.5 to 4.8. However, the constraints of the

equations (2.17), (2.18), (2.34), (2.35), (2.36), and (2.37) are modified to involve the DSM techniques as in the following equations:

A. Power balance constraints

The active and reactive power balance constraints are formulated for the connected MG as

$$\sum_{t=1}^{T}\{\sum_{i=1}^{N}\delta_{DG_i}(t).P_{DG_i}(t)+\sum_{i1=1}^{N1}P_{W_{i1}}(t)+\sum_{i2=1}^{N2}P_{PV_{i2}}(t)+P_b(t)+ \quad \textbf{(4.41)}$$
$$P_g(t)=(P_{Dres}(t)-P_{Dres}^{shft}(t)+P_{Dres}^{reco}(t))+(P_{Dcom}(t)-P_{Dcomshd}(t))+$$
$$(P_{Dind}(t)-P_{Dindshd}(t))\}$$

$$\sum_{t=1}^{T}\{\sum_{i=1}^{N}\delta_{DG_i}(t).Q_{DG_i}(t)+Q_g(t)=(Q_{Dres}(t)-Q_{Dres}^{shft}(t)+Q_{Dres}^{reco}(t))+ \quad \textbf{(4.42)}$$
$$(Q_{Dcom}(t)-Q_{Dcomshd}(t))+(Q_{Dind}(t)-Q_{Dindshd}(t))\}$$

The same equation is used for the isolated MG with both $P_g(t)$ and $Q_g(t)$ equal to zero

B. SSSCs

The active and reactive SSSCs for the connected MG are formulated as

$$\sum_{i=1}^{T}\{\sum_{i=1}^{N}\delta_{DG_i}(t).P_{DG_imax}(t)\geq(P_{Dres}(t)-P_{Dres}^{shft}(t)+P_{Dres}^{reco}(t))+ \quad \textbf{(4.43)}$$
$$(P_{Dind}(t)-P_{Dindshd}(t))+(P_{Dcom}(t)-P_{Dcomshd}(t))\}$$

$$\sum_{i=1}^{T}\{\sum_{i=1}^{N}\delta_{DG_i}(t).Q_{DG_imax}(t)\geq(Q_{Dres}(t)-Q_{Dres}^{shft}(t)+Q_{Dres}^{reco}(t))+ \quad \textbf{(4.44)}$$
$$(Q_{Dind}(t)-Q_{Dindshd}(t))+(Q_{Dcom}(t)-Q_{Dcomshd}(t))\}$$

C. SRCs

The active and reactive SRCs for the isolated MG are formulated as

$$\sum_{t=1}^{T}\{\sum_{i=1}^{N}\delta_{DG_i}(t).P_{DG_imax}(t)\geq(P_{Dres}(t)-P_{Dres}^{shft}(t)+P_{Dres}^{reco}(t))+ \quad \textbf{(4.45)}$$
$$(P_{Dind}(t)-P_{Dindshd}(t))+(P_{Dcom}(t)-P_{Dcomshd}(t))+R_p(t)\}$$

$$\sum_{t=1}^{T}\{\sum_{i=1}^{N}\delta_{DG_i}(t).Q_{DG_imax}(t)\geq(Q_{Dres}(t)-Q_{Dres}^{shft}(t)+Q_{Dres}^{reco}(t))+ \quad \textbf{(4.46)}$$
$$(Q_{Dind}(t)-Q_{Dindshd}(t))+(Q_{Dcom}(t)-Q_{Dcomshd}(t))+R_q(t)\}$$

4.12 Results without the DSM (Base Case)

In order to quantify the impacts of the DSM techniques on the optimal operation of the MG, the comparison with the base case is conducted. Figures 4-5 and 4-6 show the results of the base case for minimising the total operating cost and maximising the profit of the connected MG, while Figures 4-7 and 4-8 show the results of the isolated MG. The total operating cost and the profit are 407.8 € and 281.5 € per scheduling day respectively of the connected MG while for the isolated MG they are 549.7 € and 234.5 € per scheduling day respectively. Tables 4-2 and 4-3 illustrate the optimal on/off state of the DGs of the connected and isolated MG.

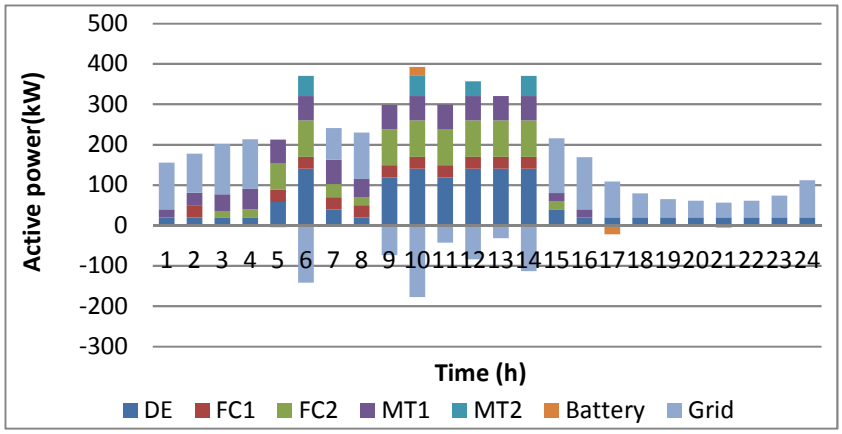

Figure 4-5 Optimal active power scheduling of the DGs and exchanging power with the battery and the utility grid of the connected MG without DSM

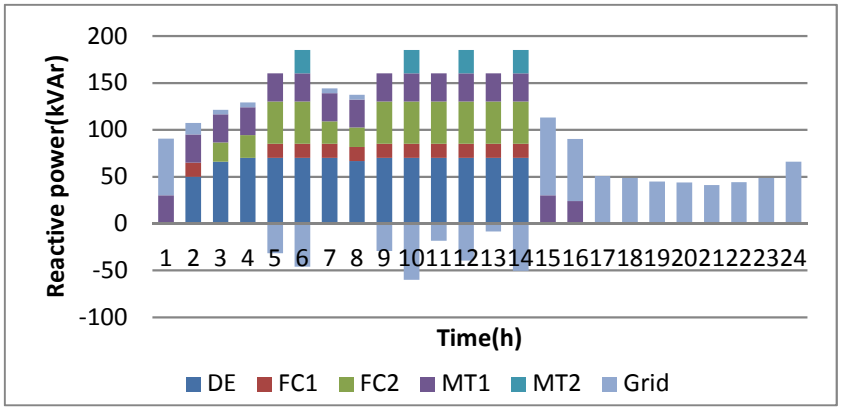

Figure 4-6 Optimal reactive power scheduling of the DGs and exchanging power with the utility grid of the connected MG without DSM

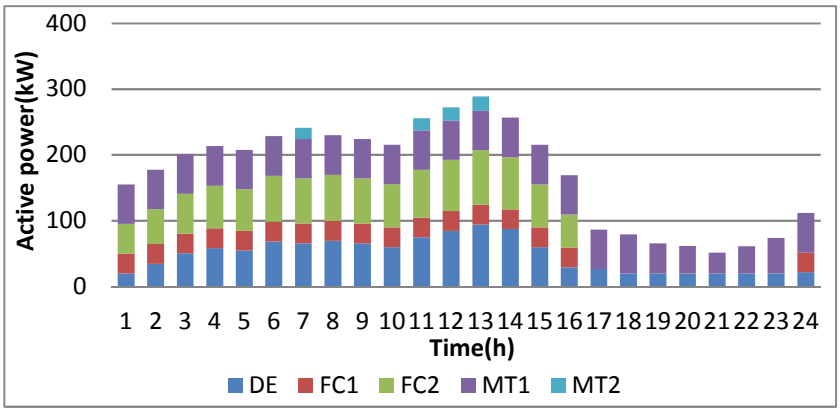

Figure 4-7 Optimal active power scheduling of the DGs of the isolated MG without DSM

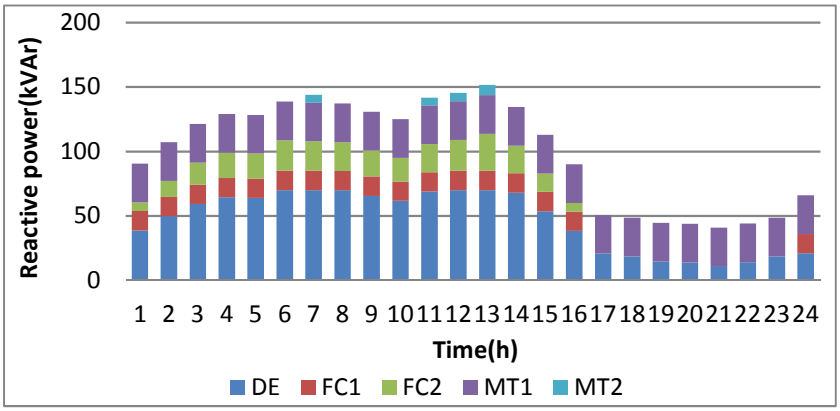

Figure 4-8 Optimal scheduling of the reactive power of the DGs of the isolated MG without DSM

Table 4-2 Optimal on/off state of the DGs of the connected MG without DSM

T(h)	1	2	3	4	5	6	7	8	9	10	11	12	13	14	15	16	17	18	19	20	21	22	23	24
DE	1	1	1	1	1	1	1	1	1	1	1	1	1	1	1	1	1	1	1	1	1	1	1	1
FC1	0	1	0	0	1	1	1	1	1	1	1	1	1	1	0	0	0	0	0	0	0	0	0	0
FC2	0	0	1	1	1	1	1	1	1	1	1	1	1	1	1	0	0	0	0	0	0	0	0	0
MT1	1	1	1	1	1	1	1	1	1	1	1	1	1	1	1	1	0	0	0	0	0	0	0	0
MT2	0	0	0	0	0	1	0	0	0	1	0	1	0	1	0	0	0	0	0	0	0	0	0	0

1 On state of the DG 0 Off state of the DG

Table 4-3 Optimal on/off state of the DGs of the isolated MG without DSM

T(h)	1	2	3	4	5	6	7	8	9	10	11	12	13	14	15	16	17	18	19	20	21	22	23	24
DE	1	1	1	1	1	1	1	1	1	1	1	1	1	1	1	1	1	1	1	1	1	1	1	1
FC1	1	1	1	1	1	1	1	1	1	1	1	1	1	1	1	1	0	0	0	0	0	0	0	1
FC2	1	1	1	1	1	1	1	1	1	1	1	1	1	1	1	1	0	0	0	0	0	0	0	0
MT1	1	1	1	1	1	1	1	1	1	1	1	1	1	1	1	1	1	1	1	1	1	1	1	1
MT2	0	0	0	0	0	0	1	0	0	0	1	1	1	0	0	0	0	0	0	0	0	0	0	0

1 On state of the DG 0 Off state of the DG

4.13 Results of Appling the DSM as shifting Technique to the Residential Area

The proposed approach is applied to the connected and isolated MG of the MG that is shown in Figure 2-3, where the DSM is applied to the residential loads. The hourly time series of the wind speed, PV generations, the open market price, and the total active and reactive loads are illustrated in the Table D-1. The load of each area is illustrated in the Table D-2. The control possibilities which they are in section 4.6.3 are considered.

4.13.1 Minimising the Total Operating Cost

A. Connected MG

The control possibilities are applied to smart appliances in the connected MG.

Scenario1

Figures 4-9 and 4-10 show the impacts of the proposed DSM on the residential and the total active and reactive loads. It can be noticed that the peak of the active and reactive total and residential loads is reduced because the peak of the total and residential loads occurs at the same time. The active and reactive loads are recovered between hours 19 to 22 because the OMPs have the lowest values at these hours. In addition, the proposed DSM reduces the peak of the active and reactive total and residential loads by 20.1 kW and 9.7 kVAr respectively or by 6.4 % with respect to the peak of the total base active and reactive loads. However, the peak of the active and reactive loads is still at hour 13. Furthermore, the proposed DSM improves the grid security because a

reduction of the total peak load leads to a reduction in the active and reactive generation capacity required to satisfy the active and reactive SSSCs.

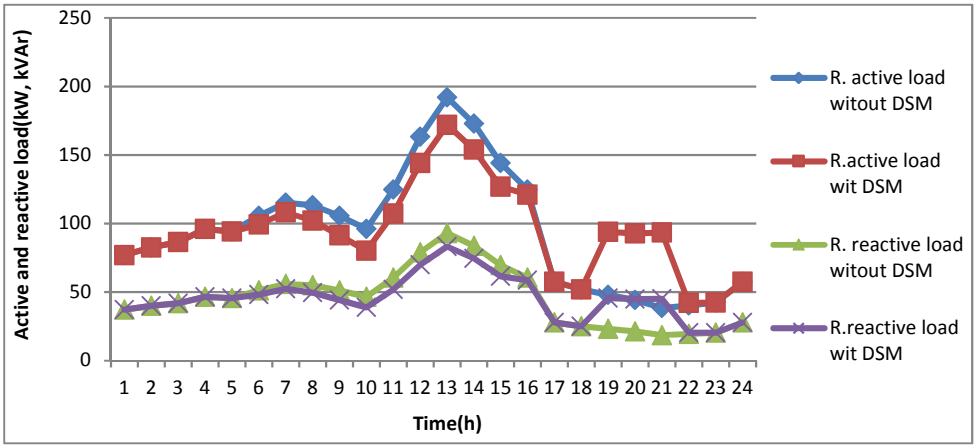

Figure 4-9 Impacts of the DSM on the active and reactive residential loads

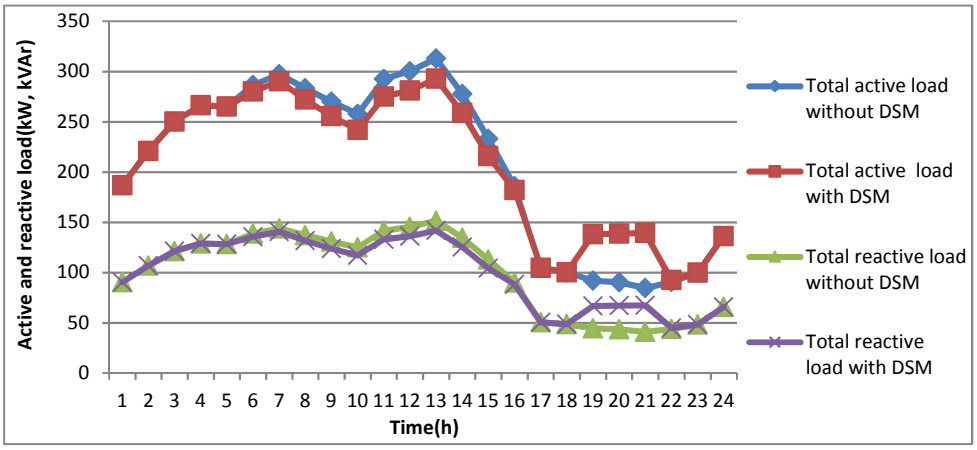

Figure 4-10 Impacts of the DSM on the active and reactive total loads

Figures 4-11 and 4-12 show the hourly optimal scheduling of the active and reactive power. These figures reveal that the MG sells active and reactive power to the utility grid when the OMPs reach the highest values, and purchases power when the OMPs reach the lowest values. In comparison with the base case, the MG sells more active and reactive power to the utility grid at hour 6 and between hours 9 and 14 by the same amount of the shifted loads to reduce its cost because the OMPs have the highest values at these hours. In contrast, the MG purchases more active and reactive power from the utility grid between hours 19 and 22 than the base case by an amount equal to the

recovered loads because the purchasing power from the utility grid is cheaper than increasing the generation of the DGs. It is found that the total operating cost is 382.4 € per scheduling day, where the proposed DSM reduces the total operating cost by 25.4 € or by 6.2 % per scheduling day.

Table 4-4 shows that at hour 15 the MG turns off the MT1 in comparison with the base case, because in the base case the total active and reactive loads are 233 kW and 112.84 kVAr respectively; therefore, the MG needs to commit DE, FC2 and MT1 to satisfy the SSSCs. While, in this scenario the total active and reactive loads are reduced to 215.7 kW and 104.5 kVAr, where the DE and FC2 are enough to satisfy the active and reactive SSSCs.

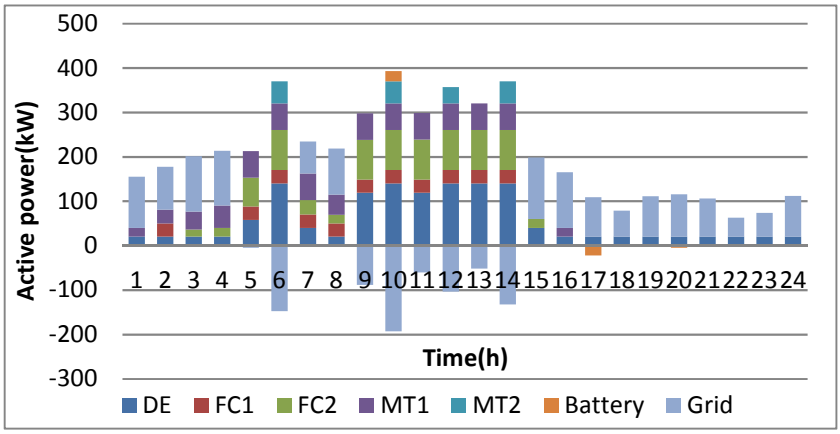

Figure 4-11 Optimal active power scheduling of the DGs and exchanging power with the battery and the utility grid

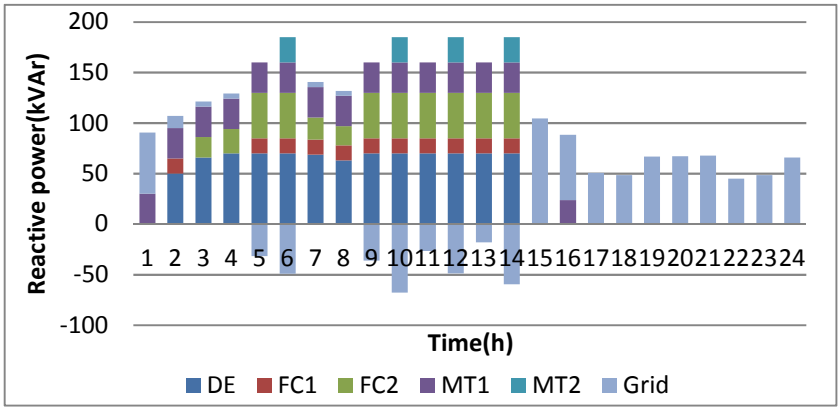

Figure 4-12 Optimal reactive power scheduling of the DGs and exchanging power with the utility grid

Table 4-4 Optimal on/off state of the DGs

T(h)	1	2	3	4	5	6	7	8	9	10	11	12	13	14	15	16	17	18	19	20	21	22	23	24
DE	1	1	1	1	1	1	1	1	1	1	1	1	1	1	1	1	1	1	1	1	1	1	1	1
FC1	0	1	0	0	1	1	1	1	1	1	1	1	1	1	0	0	0	0	0	0	0	0	0	0
FC2	0	0	1	1	1	1	1	1	1	1	1	1	1	1	1	0	0	0	0	0	0	0	0	0
MT1	1	1	1	1	1	1	1	1	1	1	1	1	1	1	0	1	0	0	0	0	0	0	0	0
MT2	0	0	0	0	0	1	0	0	0	1	0	1	0	1	0	0	0	0	0	0	0	0	0	0

1 On state of the DG 0 Off state of the DG Different state from the previous state

Scenario2

Figures 4-13 and 4-14 show the impacts of the proposed DSM on the active and reactive residential and total loads. It can be seen that the peak of the active and reactive residential and total loads is not reduced because the shifting load time is located before the peak hours. Therefore, in this scenario, there is no improvement in the grid security. In addition, the shifted active and reactive loads are recovered at hours 15 to 17 because the OMPs have the lowest values during the recovered period.

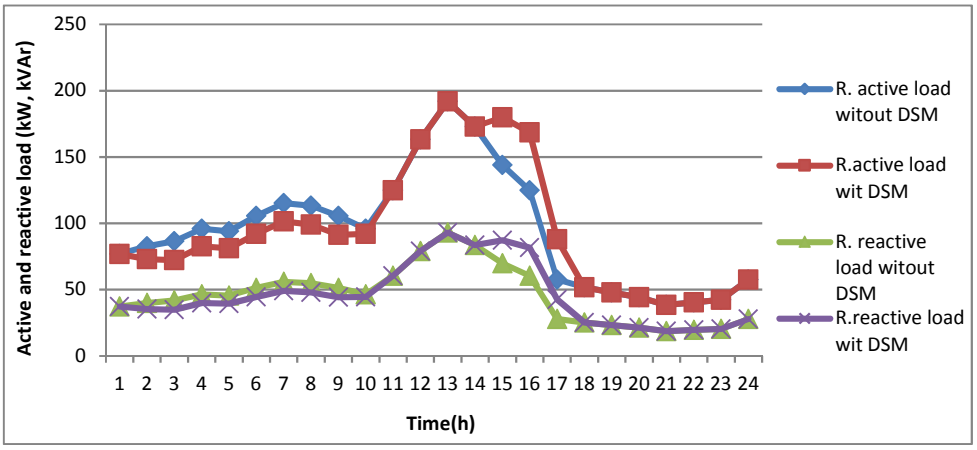

Figure 4-13 Impacts of the DSM on the active and reactive residential loads

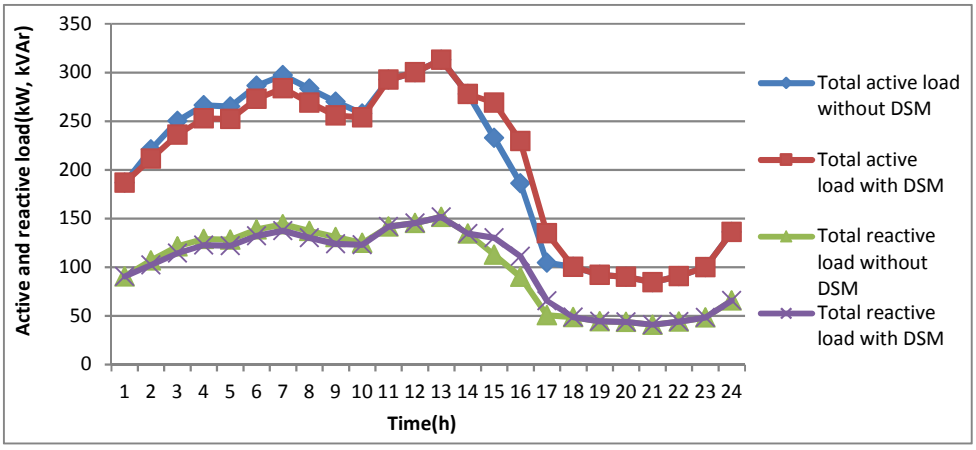

Figure 4-14 Impacts of the DSM on the active and reactive total loads

Figures 4-15 and 4-16 show the hourly optimal scheduling of the active and reactive power. It can be shown that the MG purchases less active power than in the base case at hours 2, 3, 4, 7 and 8 because the active load is shifted at these hours. The MG also purchases more active and reactive power than in the base case at hour 15, 16, 17 because at these hours the active and reactive loads are recovered and the OMPs have the lowest values. Moreover, the active and reactive shifted loads do not recover at hours from 10 to 14 because the OMPs have the highest values and the MG sells active and reactive power to the utility grid to reduce its cost.

Table 4-5 illustrates that at hour 16 the MG turns on the FC2 and switches off the MT1 in comparison with base case to meet the load and satisfy the active and reactive SSSCs. This is because in the base case the total active and reactive loads are 186 kW and 90.1 kVAr. Therefore, the DE and MT1 are enough to satisfy the SSSCs, while in this scenario the active and reactive loads are increased to 229.6 kW and 111.2 kVAr because the loads are recovered; therefore, the DE and MT1 are not adequate to satisfy the active and reactive SSSCs. Overall, the total cost is 398.6 € per scheduling day, where the proposed DSM reduces the total operating cost by 9.2 € or by 2.3 % per scheduling day.

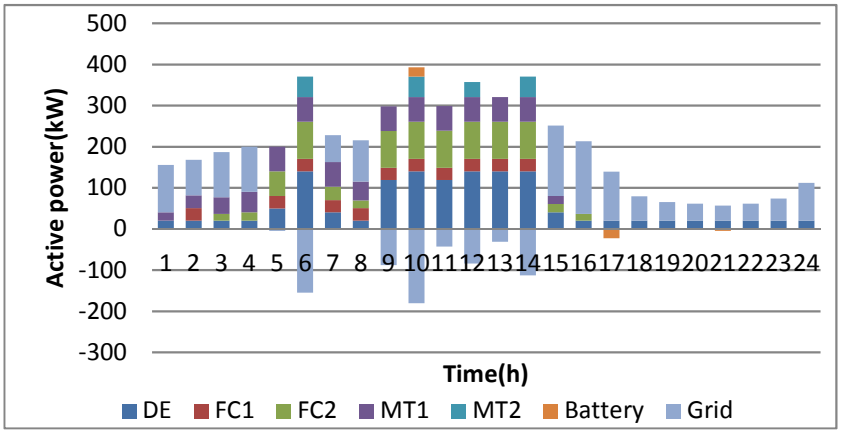

Figure 4-15 Optimal active power scheduling of the DGs and exchanging power with the battery and the utility grid

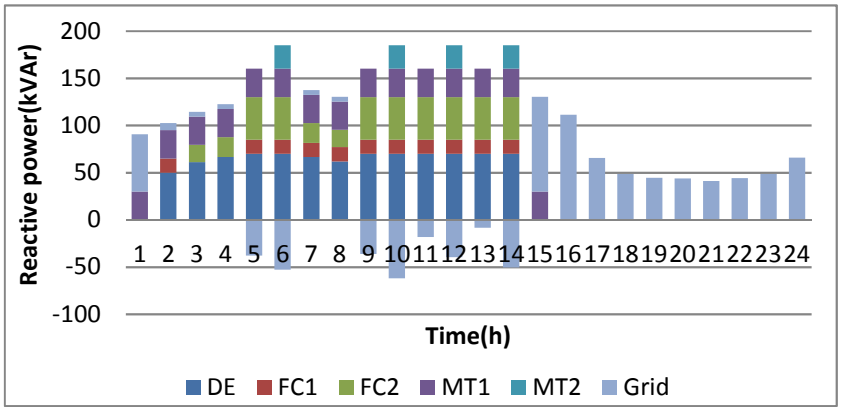

Figure 4-16 Optimal reactive power scheduling of the DGs and exchanging power the utility grid

Table 4-5 Optimal on/off state of the DGs

T(h)	1	2	3	4	5	6	7	8	9	10	11	12	13	14	15	16	17	18	19	20	21	22	23	24
DE	1	1	1	1	1	1	1	1	1	1	1	1	1	1	1	1	1	1	1	1	1	1	1	1
FC1	0	1	0	0	1	1	1	1	1	1	1	1	1	1	0	0	0	0	0	0	0	0	0	0
FC2	0	0	1	1	1	1	1	1	1	1	1	1	1	1	1	1	0	0	0	0	0	0	0	0
MT1	1	1	1	1	1	1	1	1	1	1	1	1	1	1	1	0	0	0	0	0	0	0	0	0
MT2	0	0	0	0	0	1	0	0	0	1	0	1	0	1	0	0	0	0	0	0	0	0	0	0

1 On state of the DG 0 Off state of the DG Different state from the previous state

Scenario3

Figures 4-17 and 4-18 show the impacts of the proposed DSM on the active and reactive residential and total loads. These figures reveal that the peak of the active and reactive residential and total loads is reduced for the same reason of the Sc1. The proposed DSM reduces the peak of the active and reactive total and residential loads by 7.8 kW and 3.8 kVAr respectively or by 2.5 % with respect to the total base load; however, the peak of the total active and reactive loads is still at hour 13. The proposed DSM improves the grid security by reducing the peak load.

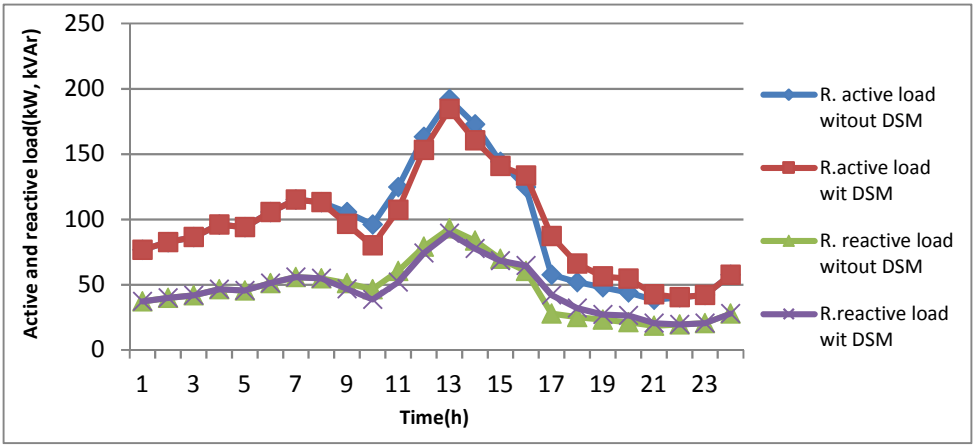

Figure 4-17 Impacts of the DSM on the active and reactive residential loads

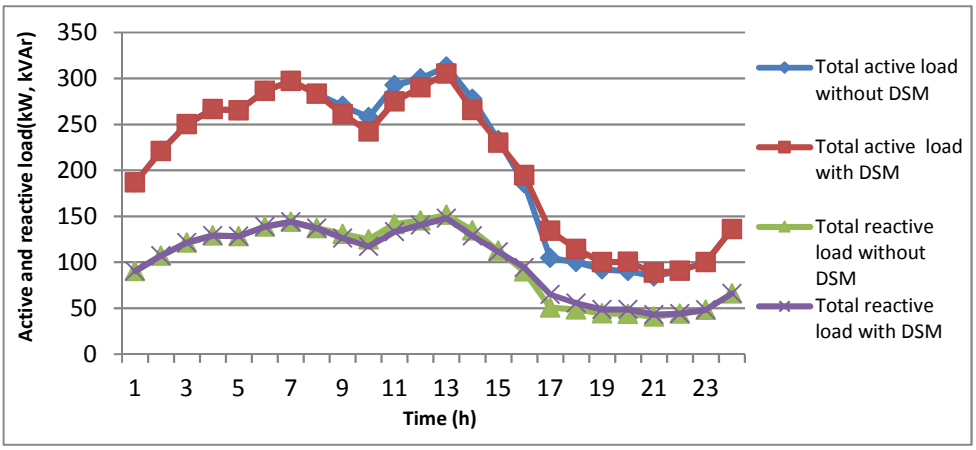

Figure 4-18 Impacts of the DSM on the active and reactive total loads

Figures 4-19 and 4-20 depict the optimal scheduling of active and reactive power. It can be seen that the MG sells more active and reactive power than in

the base case at hours 9 to 14 because the OMPs have by far the highest values at these hours and the total active and reactive loads are shifted from these hours. The on/off state of the DGs is the same of Sc1. Overall, the total cost is 390.8 € per scheduling day, where, the proposed DSM reduces the total operating cost by 17 € or by 4.2 % per scheduling day.

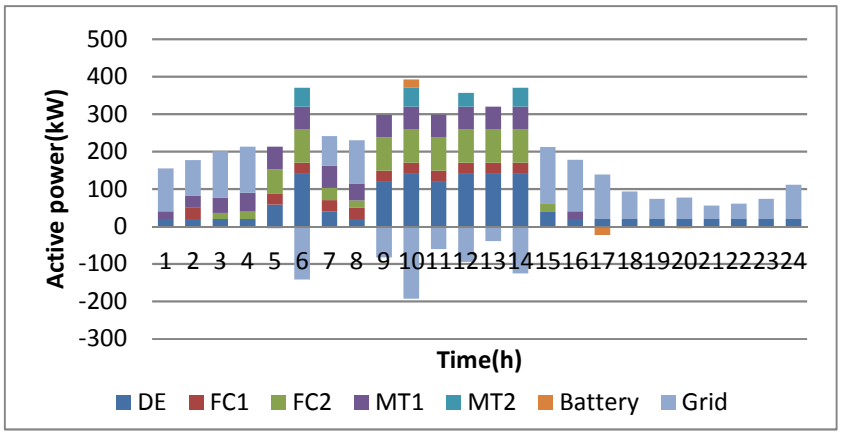

Figure 4-19 Optimal active power scheduling of the DGs and exchanging power with the battery and the utility grid

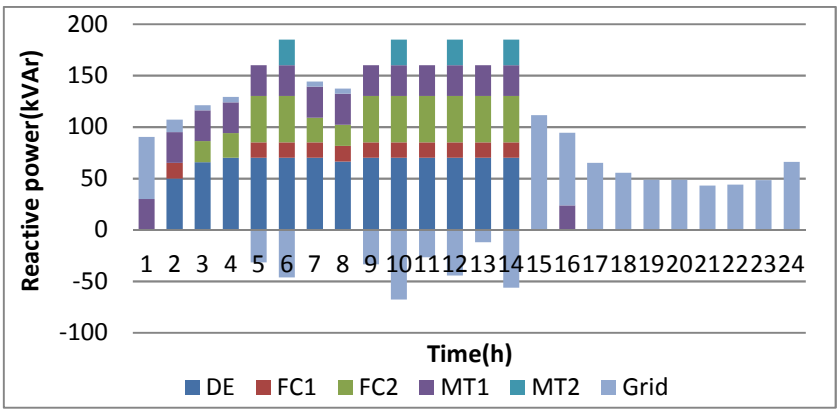

Figure 4-20 Optimal reactive power scheduling of the DGs and exchanging power with the utility grid

B. Isolated MG

Similarly, the proposed control possibilities are applied to the residential loads of the isolated MG.

Scenario 1

The proposed DSM reduces the peak of the active and reactive total and residential loads by 20.1 kW and 9.7 kVAr respectively or by 6.4 % with respect to the total base load as shown in Figures 4-21 and 4-22, although the peak of the total active and reactive loads is still at hour 13. These figures show that the active and reactive loads are shifted from peak hours to the off-peak hours. The proposed DSM reduces the active and reactive generating capacity necessary to satisfy the active and reactive SRCs by reducing the peak of the total load.

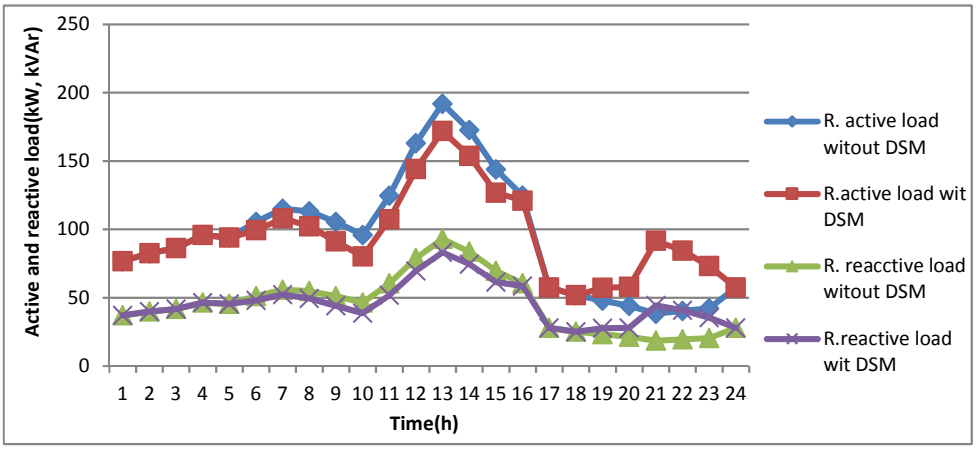

Figure 4-21 Impacts of the DSM on the active and reactive residential loads

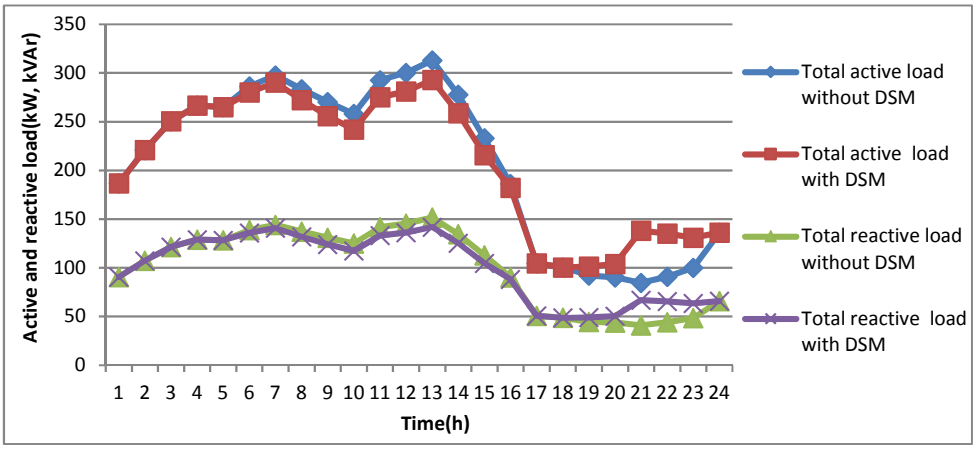

Figure 4-22 Impacts of the DSM on the active and reactive total loads

Figures 4-23 and 4-24 show the optimal scheduling of the active and reactive power. These figures and Table 4-6 reveal that the MG switches off the MT2 at hours 7, 11 and 12 in comparison with base case because the load is shifted at

these hours. In this scenario, the MT2 is committed solely at hour 13 to satisfy the active and reactive SRCs and meet the active and reactive loads. The MT2 is switched off because it has the highest operating cost among the DGs. The DGs generate more active and reactive power at hours 19 to 23 than in the base case to supply the recovered active and reactive loads. Similarly, the DGs generate less active and reactive power than in the base case at hours 6 to 16 because the loads are shifted at these hours. In addition, the MG switches on the FC1 at hours 21, 22 and 23 to meet the base and recovered loads rather than increasing the generation of the DE. This is more economical than increasing the generation of the DE because the FC1 has lower operating cost than the DE. It is found that the total cost is 540.3 € per scheduling day, where the proposed DSM reduces the total operating cost by 9.4 € or by 1.7 % per scheduling day.

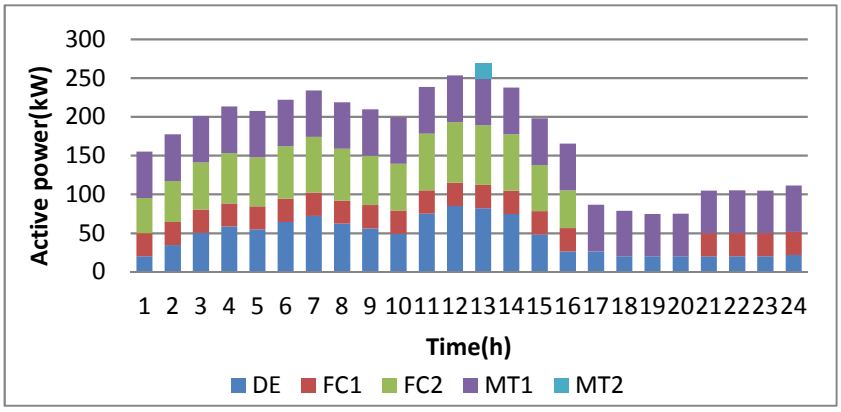

Figure 4-23 Optimal active power scheduling of the DGs

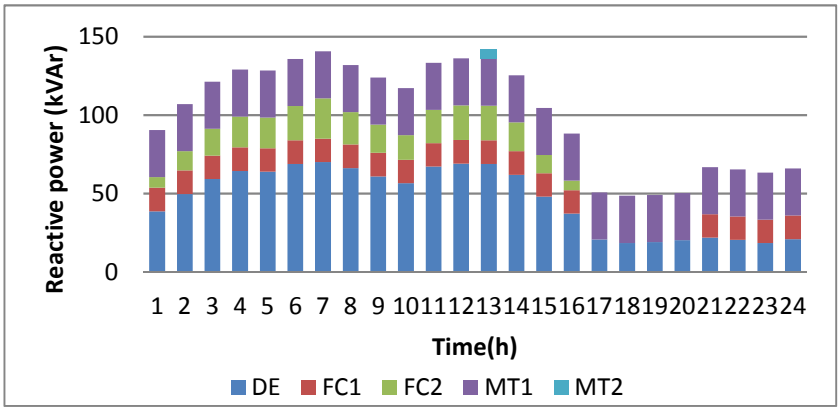

Figure 4-24 Optimal reactive power scheduling of the DGs

Table 4-6 Optimal on/off state of the DGs

T(h)	1	2	3	4	5	6	7	8	9	10	11	12	13	14	15	16	17	18	19	20	21	22	23	24
DE	1	1	1	1	1	1	1	1	1	1	1	1	1	1	1	1	1	1	1	1	1	1	1	1
FC1	1	1	1	1	1	1	1	1	1	1	1	1	1	1	1	1	0	0	0	0	1	1	1	1
FC2	1	1	1	1	1	1	1	1	1	1	1	1	1	1	1	1	0	0	0	0	0	0	0	0
MT1	1	1	1	1	1	1	1	1	1	1	1	1	1	1	1	1	1	1	1	1	1	1	1	1
MT2	0	0	0	0	0	0	0	0	0	0	0	0	1	0	0	0	0	0	0	0	0	0	0	0

1 On state of the DG 0 Off state of the DG Different state from the previous state

Scenario 2

It can be seen from Figures 4-25 and 4-26 that the proposed DSM does not affect the peak of the active and reactive residential and total loads for the same reasons of the connected MG. It also is obvious that the loads are recovered at hour 16 and 17 because the active and reactive loads have the lowest values during the recovering period.

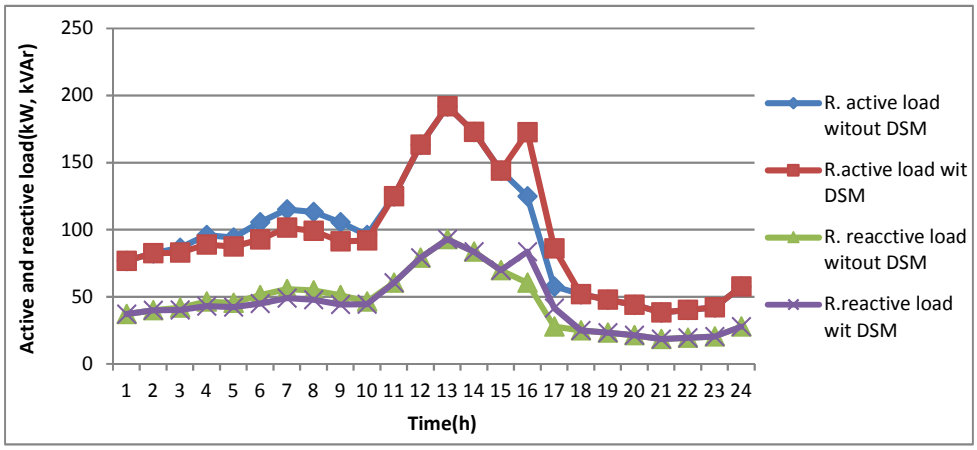

Figure 4-25 Impacts of the DSM on the active and reactive residential loads

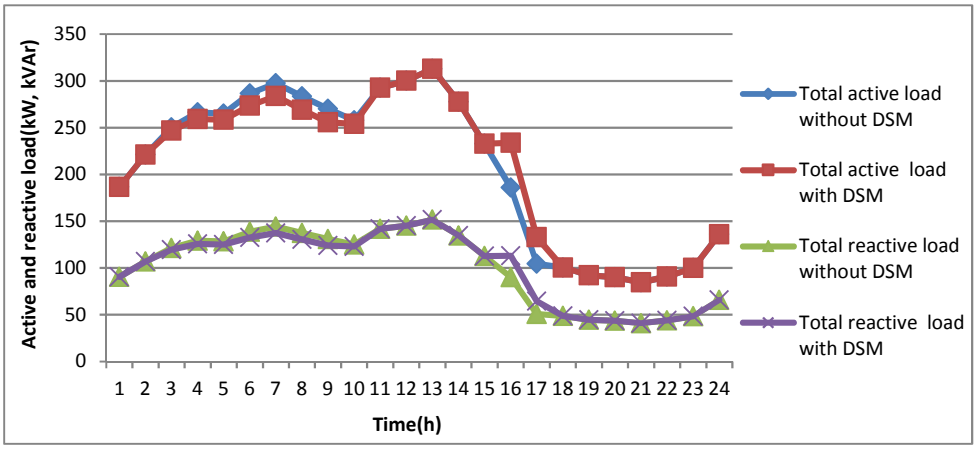

Figure 4-26 Impacts of the DSM on the active and reactive total loads

It can be seen from Figures 4-27 and 4-28 and Table 4-7 that at hour 7 the MT2 is switched off in comparison with the base case. This is because the total active and reactive loads are reduced to 283.715 kW and 137.403 kVAr, wherein the other DGs can satisfy the active and reactive SRCs and meet the total load. Moreover, the MG switches on the FC1 at hour 17 to meet the base and recovered loads in comparison with the base case because it is more economical than increasing the generation of the DE. Overall, the total cost is 547.1 € per scheduling day, where the proposed DSM reduces the total operating cost by 2.6 € or by 0.5 %.

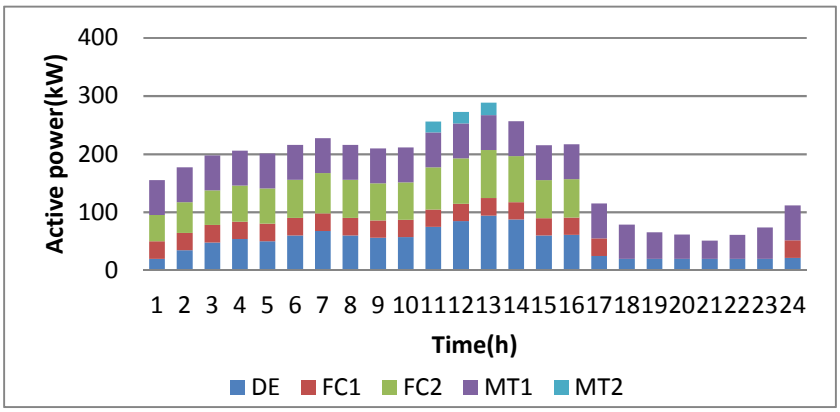

Figure 4-27 Optimal active power scheduling of the DGs

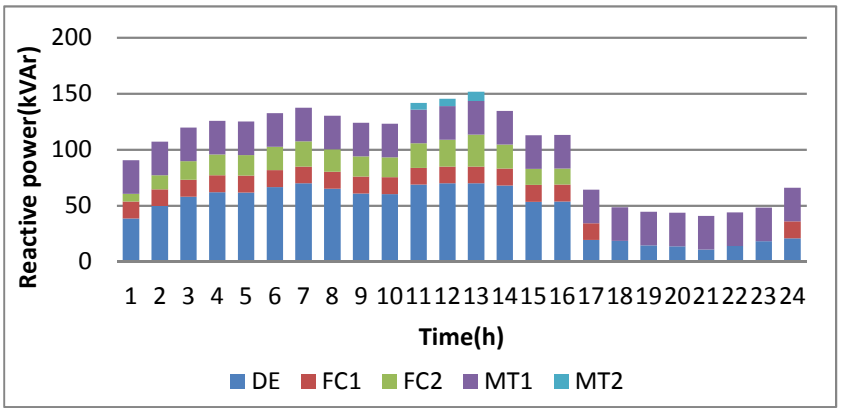

Figure 4-28 Optimal reactive power scheduling of the DGs

Table 4-7 Optimal on/off state of the DGs

T(h)	1	2	3	4	5	6	7	8	9	10	11	12	13	14	15	16	17	18	19	20	21	22	23	24
DE	1	1	1	1	1	1	1	1	1	1	1	1	1	1	1	1	1	1	1	1	1	1	1	1
FC1	1	1	1	1	1	1	1	1	1	1	1	1	1	1	1	1	1	0	0	0	0	0	0	1
FC2	1	1	1	1	1	1	1	1	1	1	1	1	1	1	1	1	0	0	0	0	0	0	0	0
MT1	1	1	1	1	1	1	1	1	1	1	1	1	1	1	1	1	1	1	1	1	1	1	1	1
MT2	0	0	0	0	0	0	0	0	0	0	1	1	1	0	0	0	0	0	0	0	0	0	0	0

1 On state of the DG 0 Off state of the DG Different state from the previous state

Scenario 3

Figures 4-29 and 4-30 reveal that the peak of the active and reactive total and residential loads is reduced because the peak of the active and reactive total loads occurs at the same time with the peak of the active and reactive residential load. The proposed DSM reduces the peak of the active and reactive total and residential loads by 20.1 kW and 9.7 kVAr respectively or by 6.4 % with respect of the total loads. Therefore, the proposed DSM improves the active and reactive spinning reserve by reducing the generating capacity to satisfy the SRCs.

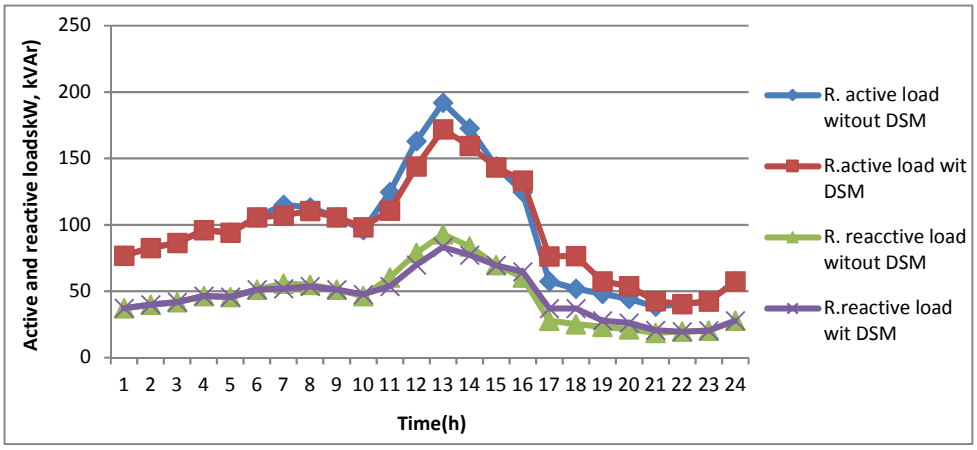

Figure 4-29 Effect of the DSM on the active and reactive residential loads

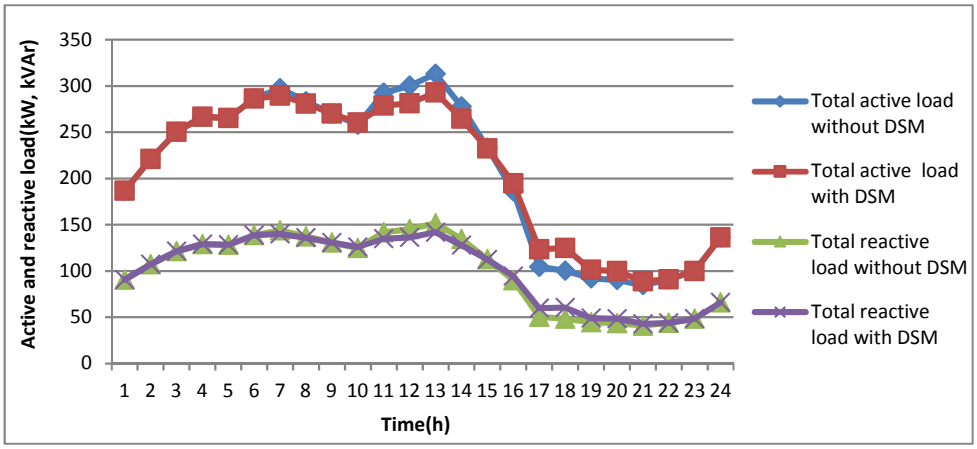

Figure 4-30 Effect of the DSM on the active and reactive total loads

Figures 4-31, 4-32 and Table 4-8 show that at hour 7, 11, and 12 the MG switches off the MT2 in comparison with the base case for the same reasons of the Sc1. In contrast, the MG switches on the FC1 at hours 17 and 18 to meet the base and recovered loads, where the highest recovered loads are at these hours. This is more economical than increasing the generation of the DE. Overall, the total cost is 543.2 € per scheduling day. It can be noticed that the proposed DSM reduces the total operating cost by 6.5 € or by 1.2 % per scheduling day.

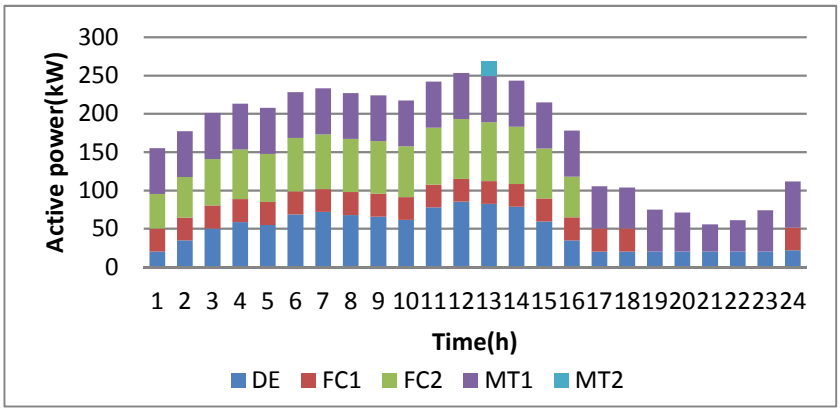

Figure 4-31 Optimal active power scheduling of the DGs

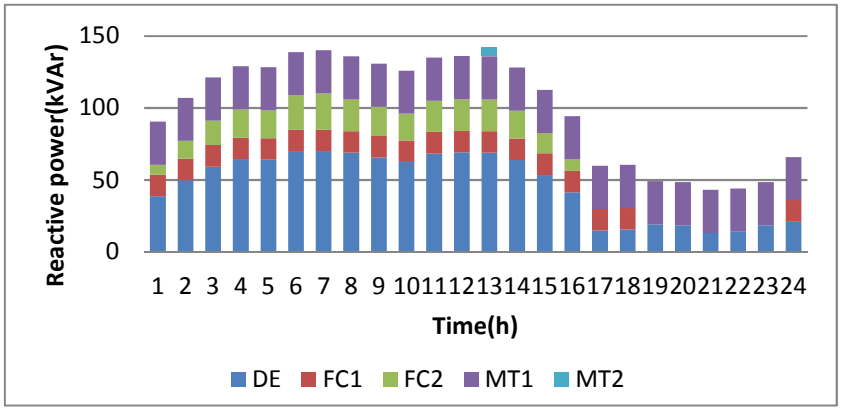

Figure 4-32 Optimal reactive power scheduling of the DGs

Table 4-8 Optimal on/off state of the DGs

T(h)	1	2	3	4	5	6	7	8	9	10	11	12	13	14	15	16	17	18	19	20	21	22	23	24
DE	1	1	1	1	1	1	1	1	1	1	1	1	1	1	1	1	1	1	1	1	1	1	1	1
FC1	1	1	1	1	1	1	1	1	1	1	1	1	1	1	1	1	1	1	0	0	0	0	0	1
FC2	1	1	1	1	1	1	1	1	1	1	1	1	1	1	1	1	0	0	0	0	0	0	0	0
MT1	1	1	1	1	1	1	1	1	1	1	1	1	1	1	1	1	1	1	1	1	1	1	1	1
MT2	0	0	0	0	0	0	0	0	0	0	0	0	1	0	0	0	0	0	0	0	0	0	0	0

1 On state of the DG 0 Off state of the DG Different state from the previous state

Tables 4-9 and 4-10 summarise the results of the three scenarios for the connected and isolated MG. It can be seen that the highest reduction of the total operating cost and the highest peak load reduction occur at Sc1 for both the connected and isolated MG. This is because the shifting time coincide with peak hours and the recovering load times occur during the off-peak hours.

While, the lowest cost reduction and no peak load reduction are in the Sc2 because the shifting load time are prior to the peak load for both the connected and isolated MG. In addition, the proposed DSM strategies reduce the total operating cost for all the scenarios with the amount depending on the control possibilities of the appliances.

Table 4-9 Results of the scenarios of the connected MG

	Cost with DSM (€/day)	Cost reduction %	Peak load reduction with DSM (kW)	Percentage reduction %	No. shifting WMs	No. shifting DWs
Sc1	382.4	6.2	20.1	6.4	82	66
Sc2	398.6	2.3	0	0	62	46
Sc3	390.8	4.2	7.8	2.5	62	65

Table 4-10 Results of the scenarios of the isolated MG

	Cost with DSM (€/day)	Cost reduction %	Peak load reduction with DSM (kW)	Percentage reduction %	No. shifting WMs	No. shifting DWs
Sc1	540.3	1.7	20.1	6.4	82	66
Sc2	547.1	0.5	0	0	32	40
Sc3	543.2	1.2	20.1	6.4	54	63

4.13.2 Maximising of the MG Profit

A. Connected MG

The control possibilities of the smart appliances are applied to the residential load of the connected MG to maximise the profit.

Scenario 1

Figures 4-33 and 4-34 reveal that the peak of the active and reactive total and residential loads is not changed in comparison with the minimising the operating cost because the MG sells and buys active and reactive power by the OMPs, where the OMPs have high values at hour of the peak load. Therefore, there are not economic incentives for shifting the peak load. Figures 4-35 and 4-36 show that the MG sells active and reactive power to the utility grid when the OMPs have the highest values and purchases active and reactive power when the prices reach the lowest values. In addition, the MG sells higher active and reactive power than the base case at hour 14 because the active and reactive

loads are shifted at this hour, while the MG buys higher active and reactive power than in the base case at hours 19, 20 because the loads are recovered at these hours. Overall, the profit is 281.9 € per scheduling day, where the proposed DSM slightly increases the profit. The on/off state of the DGs are the same of the Sc1 of minimising the cost and it is shown in Table 4-4.

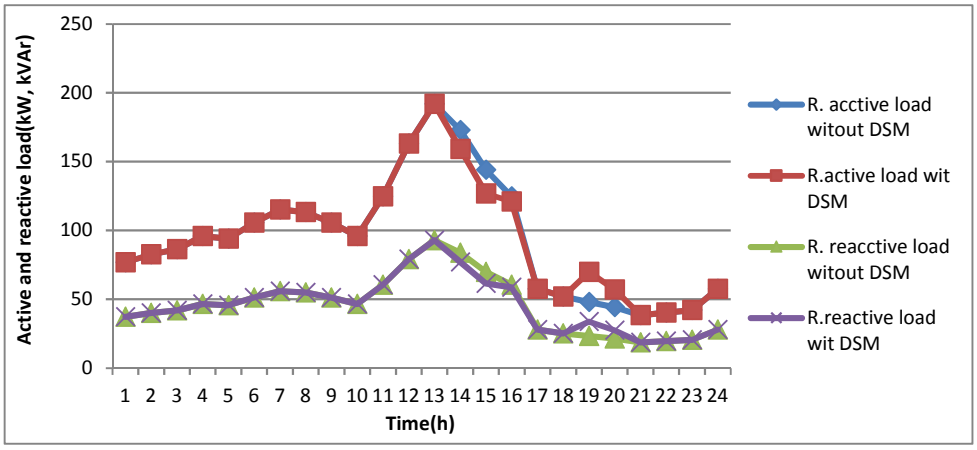

Figure 4-33 Impacts of the DSM on the active and reactive residential loads

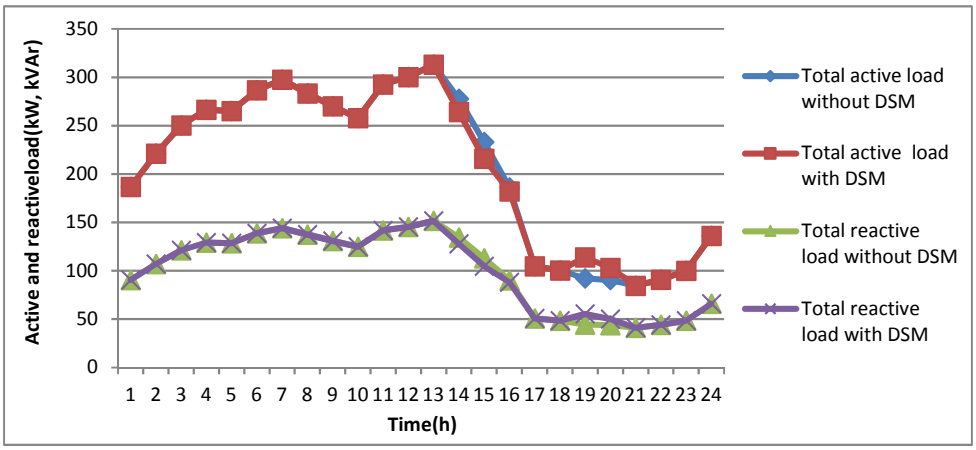

Figure 4-34 Impacts of the DSM on the active and reactive total loads

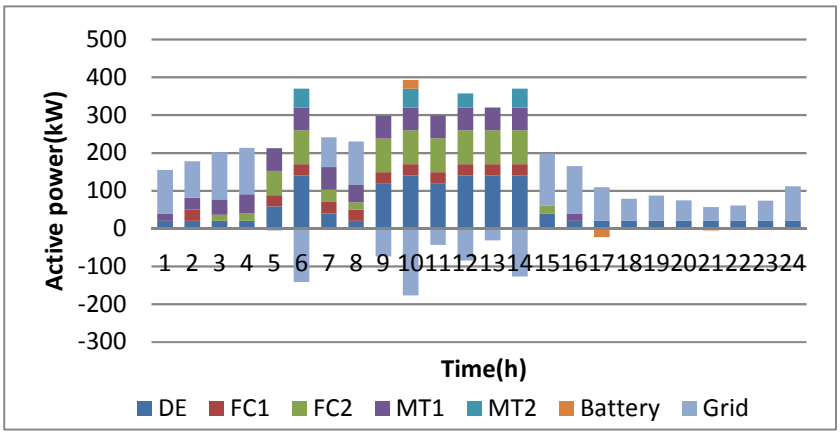

Figure 4-35 Optimal active power scheduling of the DGs and exchanging power with the battery and the utility grid

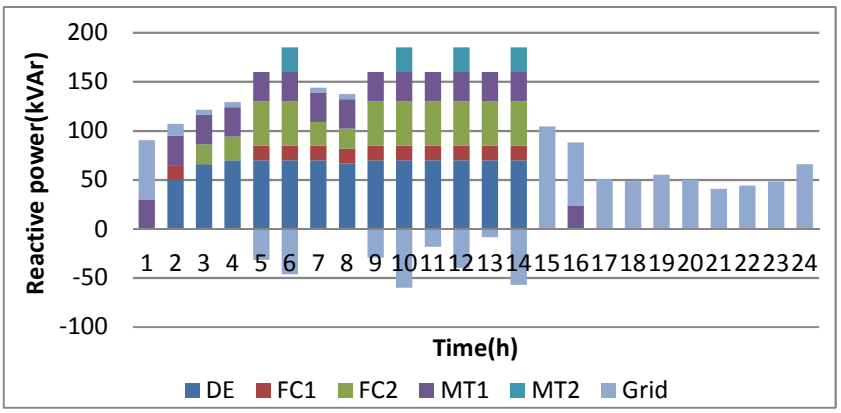

Figure 4-36 Optimal reactive power scheduling of the DGs and exchanging reactive power with the utility grid

Scenario 2

It can be seen from Figures 4-37 and 4-38 that the peak of the residential and total loads is increased. However, increasing the peak of the active and reactive total loads does not affect the value of the profit because the MG sells and buys the active and reactive power with the OMPs. The peak of the active and reactive loads is increased by 6.27 kW and 3.036 kVAr because the shifted load is recovered when the OMPs have higher values during the recovering period to increase the revenue of the MG. Figures 4-39 and 3-40 show that the MG sells less active and reactive power to the utility grid at hours 11 to 13 in comparison with base case because the active and reactive loads are recovered at these hours. Furthermore, the on/off state of the DGs is the same of the base case

and it is shown in Table 4-2. The profit is 281.5 €, where proposed DSM does not affect the profit.

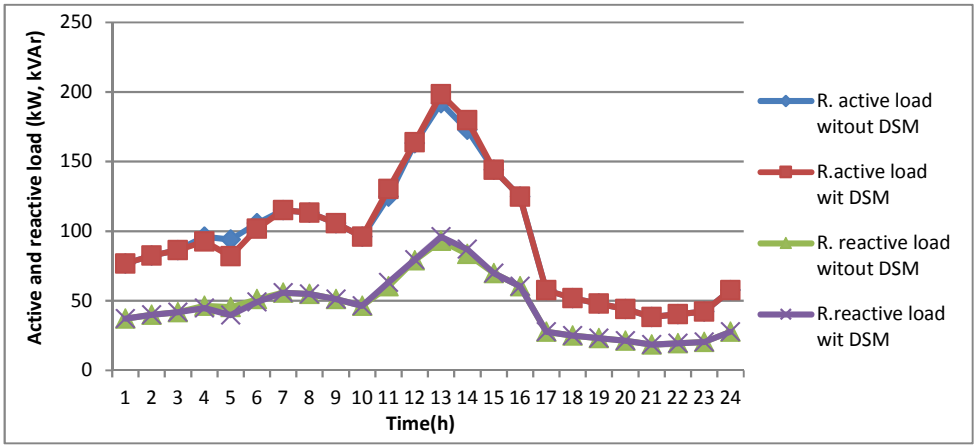

Figure 4-37 Impacts of the DSM on the active and reactive residential loads

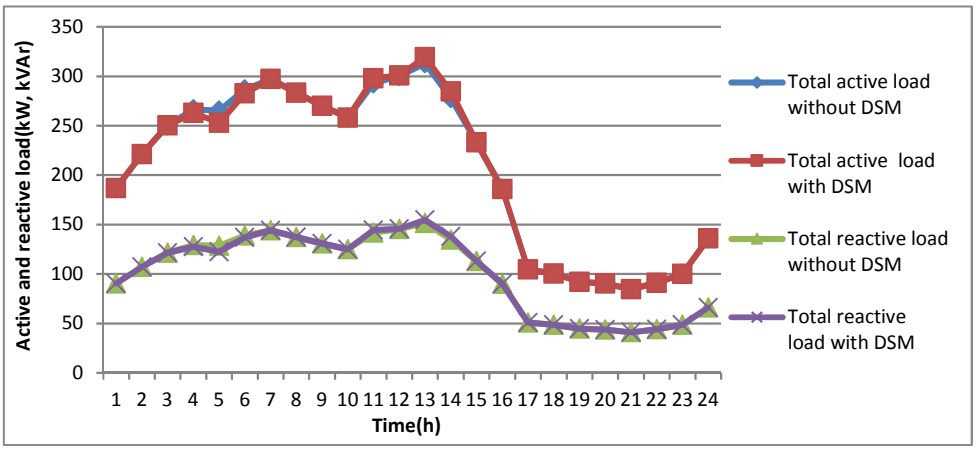

Figure 4-38 Impacts of the DSM on the active and reactive total loads

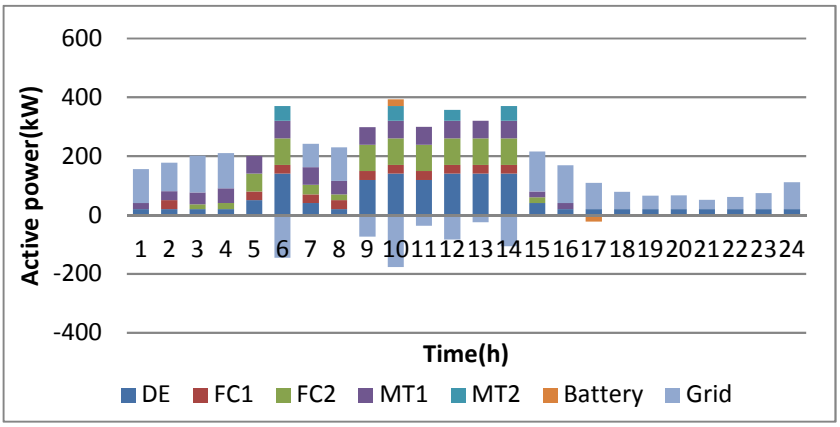

Figure 4-39 Optimal active power scheduling of the DGs and exchanging power with battery and the utility grid

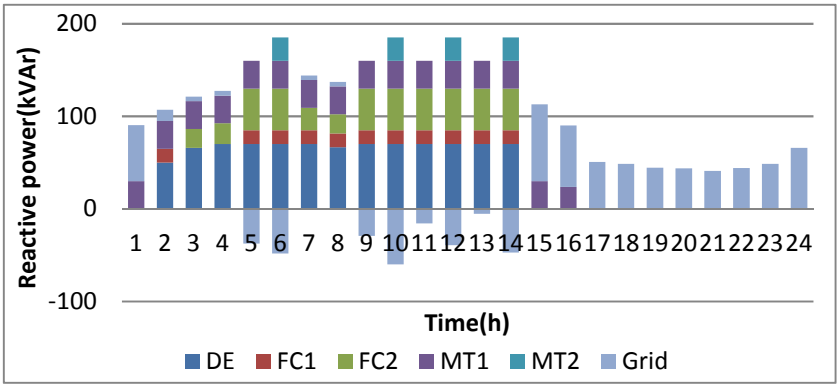

Figure 4-40 Optimal reactive power scheduling of the DGs and exchanging power with the utility grid

Scenario 3

It can be noticed from Figures 4-41 and 4-42 that the peak of the active and reactive total and residential loads is not changed for the same reasons of the Sc1.

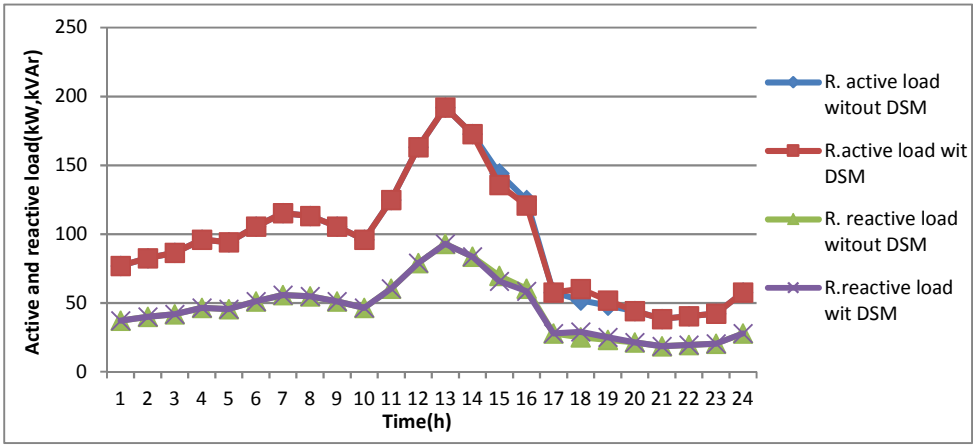

Figure 4-41 Impacts of the DSM on the active and reactive residential loads

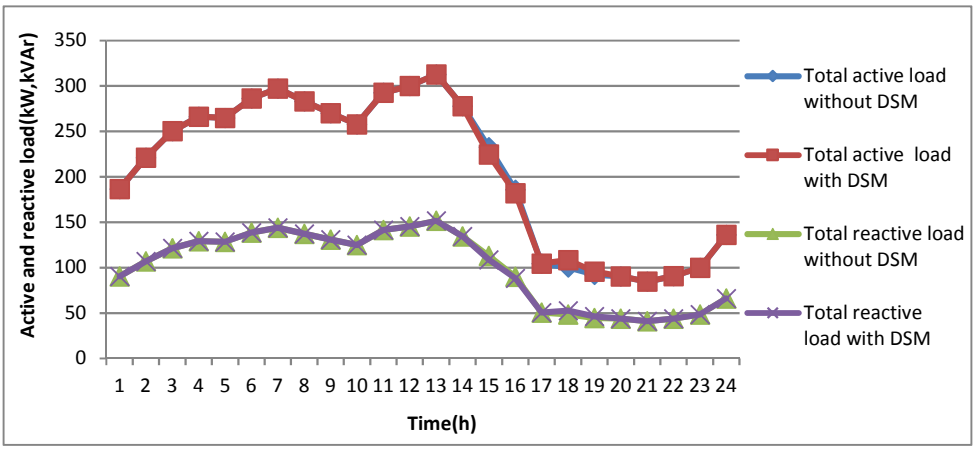

Figure 4-42 Impacts of the DSM on the active and reactive total loads

The on/off state of the DGs is the same of Sc1 of the minimising the operating cost and it is shown in Table 4-4. Figures 4-43 and 4-44 show the active and reactive power scheduling. The DGs active power scheduling is the same of the case of minimising the operating cost and the shifted or recovered loads are compensated from the utility grid. The profit is 281.9 € per scheduling day.

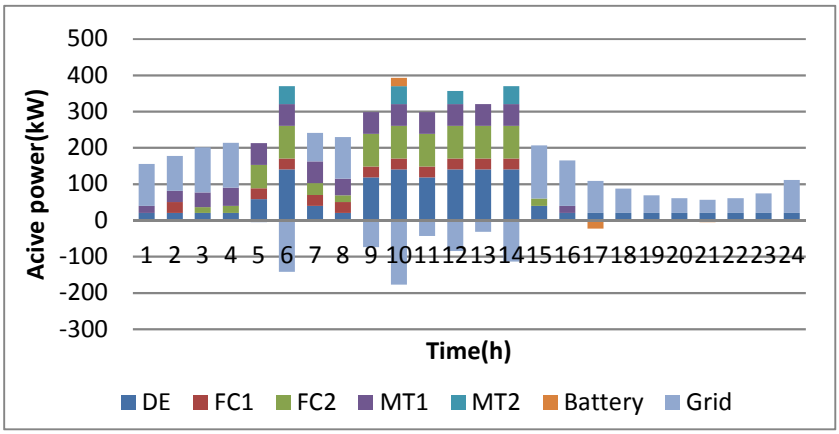

Figure 4-43 Optimal active power scheduling of the DGs and exchanging power with battery and the utility grid

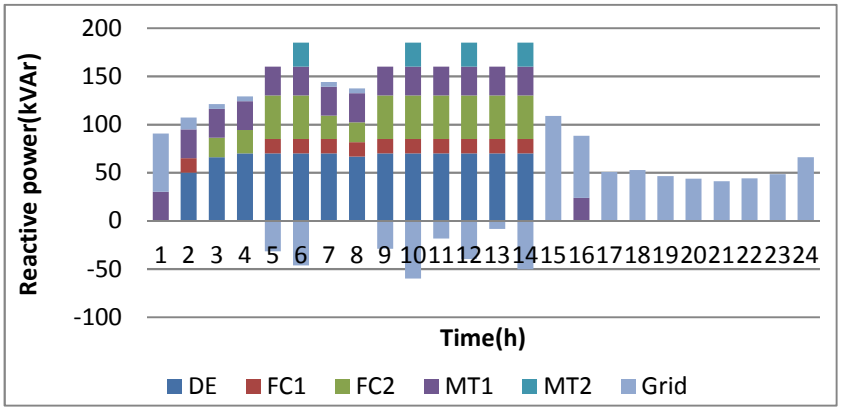

Figure 4-44 Optimal reactive power scheduling of the DGs and exchanging power with the utility grid

It can be concluded from the results that in case of maximising the profit of the connected MG the DSM as shifting technique have insignificantly impacts on the profit and the peak loads may be increased. This is an important finding for this work. In addition, there is no reduction in the peak loads. Therefore, there is no improvement to the spinning reserve.

B. Isolated MG

According to the literature, there appears no study proposed the impacts of the shifting DSM techniques on the profit of the isolated MG.

Scenario 1

The shifted and recovered loads and the optimal scheduling of the active and reactive power are the same as the Sc1 for minimising the cost of the isolated MG and they are shown in Figures 4-21, 4-22, 4-23 and 3-24. The on/off state of the DGs is the same as well and it is as in Table 4-6. It is found that the profit is 243.9 €, where the proposed DSM increases the profit by 9.4 € per scheduling day or by 4 %.

Scenario 2

The shifted and recovered loads and the optimal scheduling of the active and reactive power are the same as the Sc2 for minimising the cost of the isolated MG and they are shown in Figures 4-25, 4-26, 4-27 and 4-28. The on/off state of the DGs is as in Table 4-7. On the whole, the profit is 237.1 € per scheduling day, where the proposed DSM increases the profit by 2.6 € per scheduling day or by 1.1 %.

Scenario 3

The shifted and recovered loads and the optimal scheduling of the active and reactive power are the same as the Sc3 for minimizing the cost of isolated MG and they are shown in Figures 4-29, 4-30, 4-31 and 4-32. The on/off state of the DGs is as in Table 4-8. Overall, the profit is 241 €, where the proposed DSM increases the profit by 6.5 € per scheduling day or by 2.8 %.

Tables 4-11 and 4-12 summarise the results of the impacts of the proposed DSM on the maximising the profit of the connected and isolated MG. The results reveal that in the connected mode, there are insignificantly impacts on the profit of the MG and the peak reduction of the active and reactive loads is zero of the Sc1 and Sc3, whereas for Sc2 the peak load is increased. This is because the MG sells and buys the electricity by the OMPs and the OMPs have high values at hours of the peak load.

In case of the isolated MG, the profit is increased for all the scenarios. The peak active and reactive loads are reduced for the Sc1 and Sc3, while there is no load reduction for the Sc2.

Table 4-11 Results of the scenarios of connected MG

	Profit with DSM (€/day)	Profit increasing %	Peak load reduction with DSM (kW)	Percentage reduction %	No. shifting WMs	No. shifting DWs
Sc1	281.9	0.14	0	0	15	18
Sc2	281.5	0	-6.27	-2	7	11
Sc3	281.9	0.14	0	0	7	5

Table 4-12 Results of the scenarios of isolated MG

	Profit with DSM (€/day)	Profit increasing %	Peak load reduction with DSM (kW)	Percentage reduction %	No. shifting WMs	No. shifting DWs
Sc1	243.9	4	20.1	6.4	82	66
Sc2	237.1	1.1	0	0	32	40
Sc3	241	2.8	20.1	6.4	54	63

4.14 Results of Appling the DSM as curtailing Techniques to the Industrial and Commercial Loads

The industrial and commercial consumers offer active and reactive loads shedding at the peak hours of the total loads. The proposed approach is applied to the connected and isolated MG. The industrial and commercial consumers offer load shedding by 10 kW and 15 kW respectively at each hour from 11 to 13. The MG should accept of rejects the bids of the consumer and inform them day-ahead.

4.14.1 Minimising the Operating Cost

A. Connected MG

The MG accepts the load shedding bids of the both industrial and commercial consumers. It can be noticed from Figure 4-45 that the peak of the active and reactive industrial loads is not changed because the DSM is designed according to the peak of the active and reactive total loads, wherein the peak of the active and reactive industrial loads does not coincide with the peak of the active and reactive total load. Figure 4-46 shows that the peak of the active and reactive commercial loads is reduced because the peak of the active and reactive

commercial loads coincides with the peak of the active and reactive total loads. In addition, the peak of the active and reactive total loads is reduced by 25 kW and 12.12 kVAr respectively as shown in Figure 4-47. Furthermore, the peak of the active and reactive total loads is displaced to hour 7. The reduction of the peak of the total load decreases the generating capacity needs to satisfy the active and reactive SSSCs. This loads to improve the system security of supply.

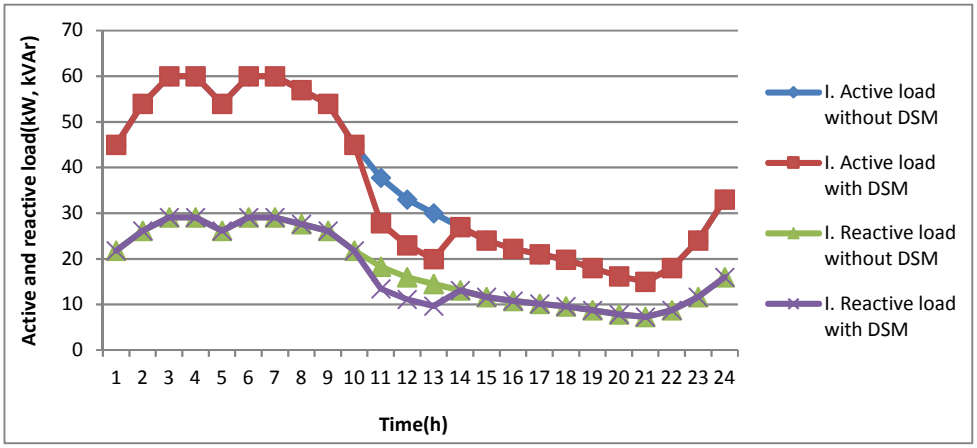

Figure 4-45 Impacts of the DSM on the active and reactive Industrial loads

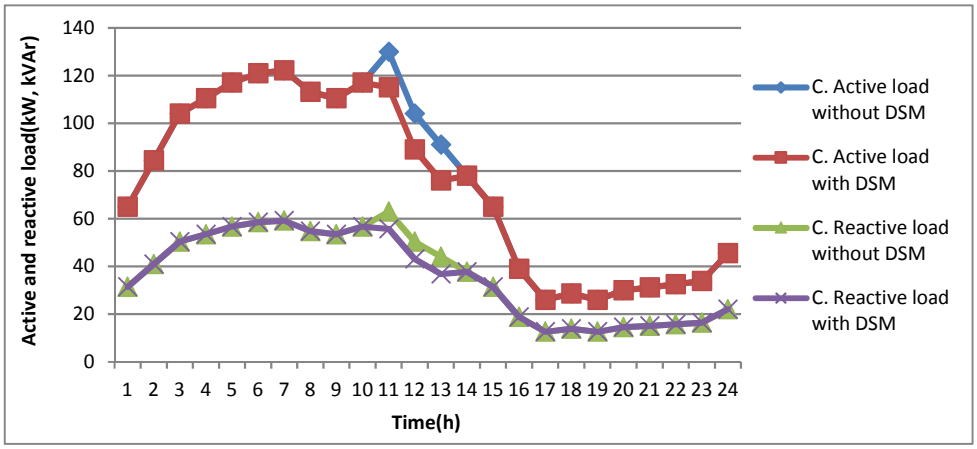

Figure 4-46 Impacts of the DSM on the active and reactive commercial loads

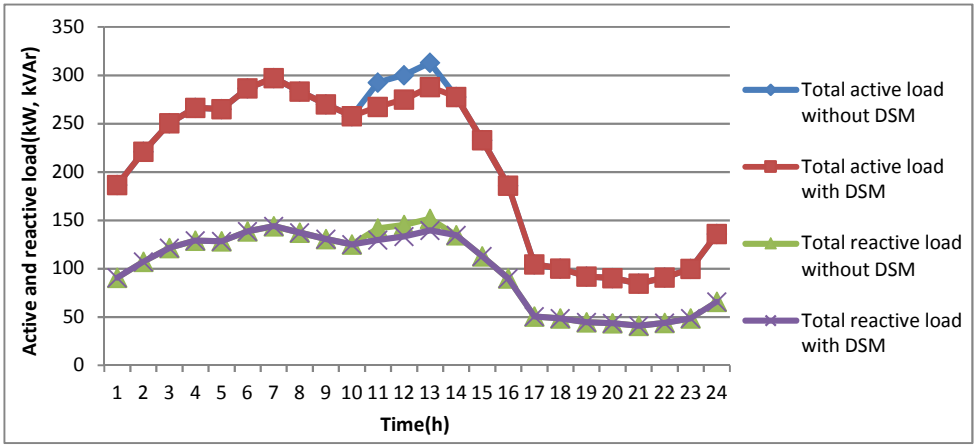

Figure 4-47 Impacts of the DSM on the active and reactive total loads

Figures 4-48 and 4-49 reveal that the MG sells more active and reactive power to the utility grid at hours 11, 12 and 13 with the same amount of the curtailed loads than in the base case because at these hours the total active and reactive loads are shed. In addition, the DGs on/off state are the same of the base case, which is shown in Table 4-2. The total operating cost is 405 € which is reduced by 2.8 €.

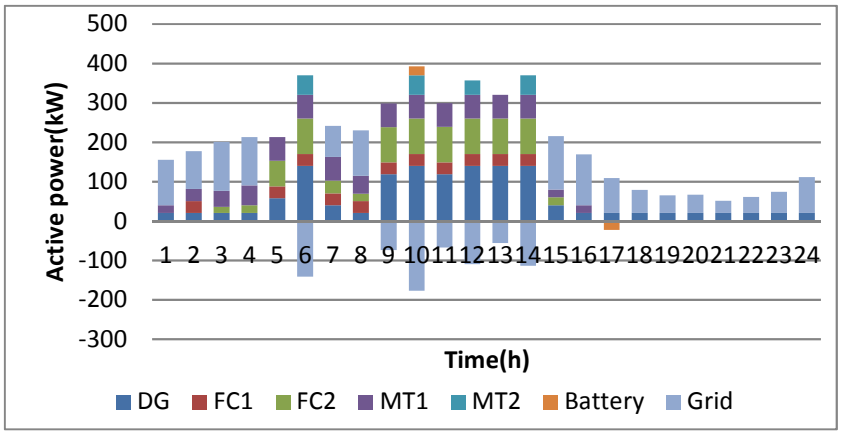

Figure 4-48 Optimal active power scheduling of the DGs and exchanging power with the battery and the utility grid

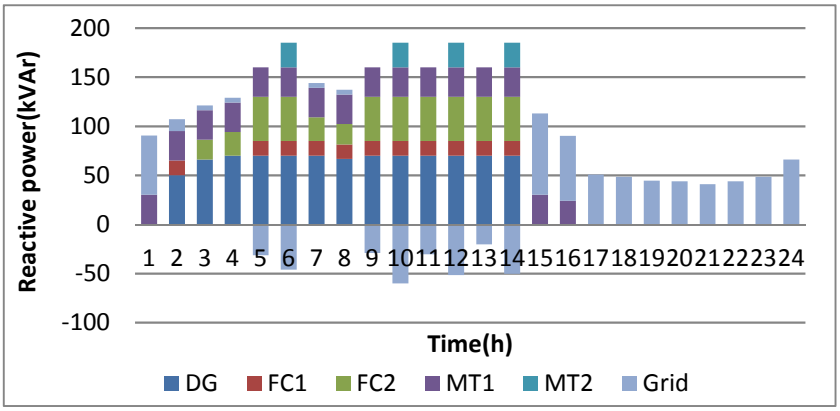

Figure 4-49 Optimal reactive power scheduling of the DGs and exchanging power with the utility grid

B. Isolated MG

Figures 4-50 and 4-51 reveal that the MG accepts the load shedding bids of the commercial consumers for the three hours, while it accepts the offer for industrial consumers for solely at hour 13 when the loads reach to the highest values. This is because the prices of cutting the active and reactive industrial loads are higher than the prices of cutting the active and reactive commercial loads and there is no connection with the utility grid. Moreover, the peak of the active and reactive total loads is reduced as shown in Figure 5-52 by 25 kW and 12.12 kVAr respectively, wherein the peak load is displaced to hour 7. The reduction of the peak of the active and reactive total loads improves the active and reactive power reserve.

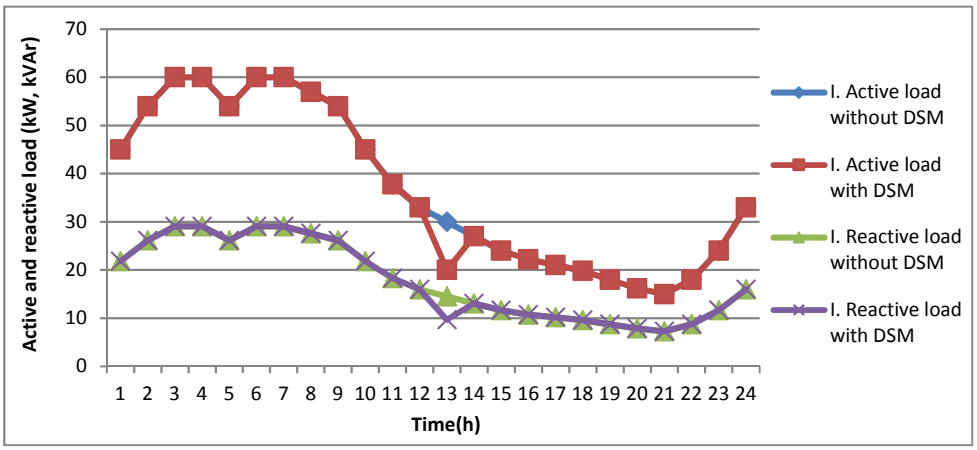

Figure 4-50 Impacts of the DSM on the active and reactive Industrial loads

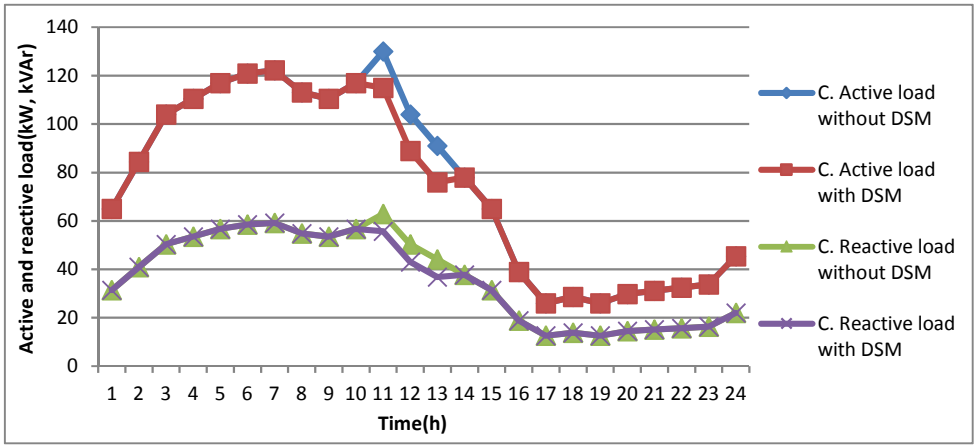

Figure 4-51 Impacts of the DSM on the active and reactive commercial loads

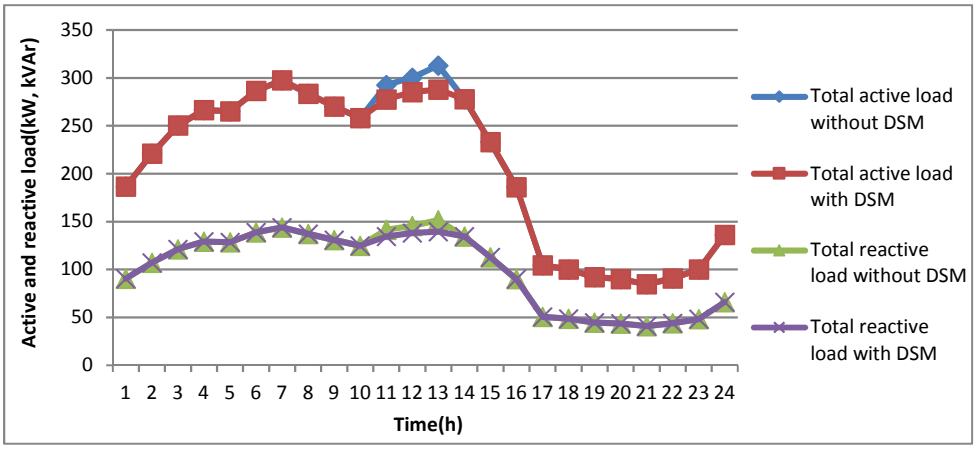

Figure 4-52 Impacts of the DSM on the active and reactive total loads

Figures 4-53, 4-54 and Table 4-13 show that the MG turns off the MT2 at hours 11, 12 and 13 because the active and reactive loads are curtailed at these hours; therefore, the other DGs can satisfy the SRCs and supply loads in comparison with the base case. It is found that the total operating cost is 546.1 € and it is reduced by 3.6 € per scheduling day.

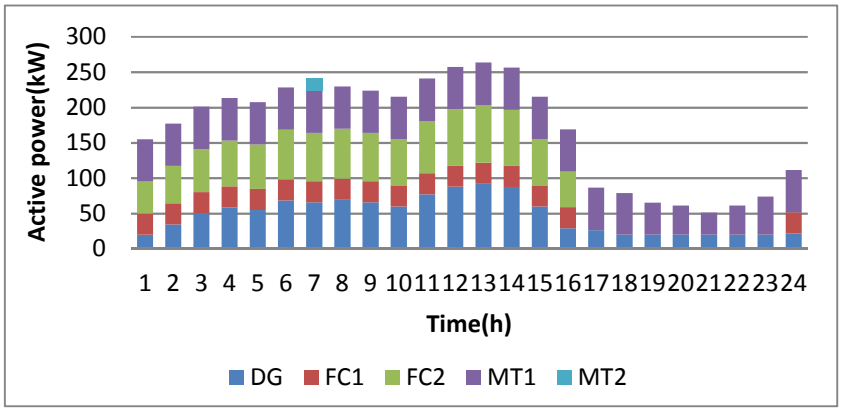

Figure 4-53 Optimal active power scheduling of the DGs

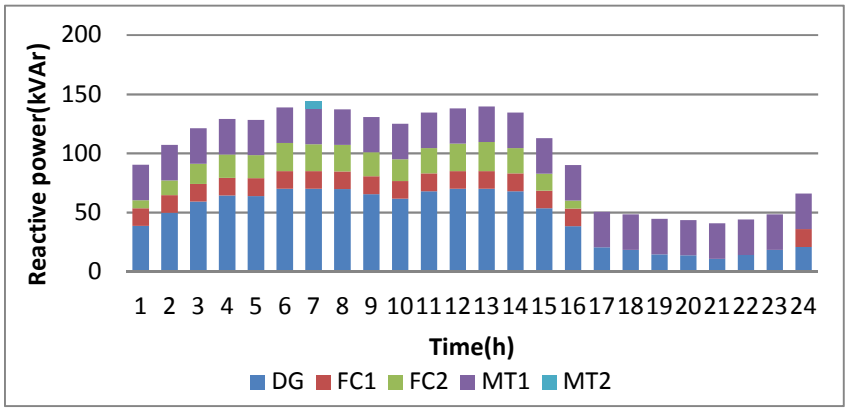

Figure 4-54 Optimal reactive power scheduling of the DGs

Table 4-13 Optimal on/off state of the DG

T(h)	1	2	3	4	5	6	7	8	9	10	11	12	13	14	15	16	17	18	19	20	21	22	23	24
DE	1	1	1	1	1	1	1	1	1	1	1	1	1	1	1	1	1	1	1	1	1	1	1	1
FC1	1	1	1	1	1	1	1	1	1	1	1	1	1	1	1	1	0	0	0	0	0	0	0	1
FC2	1	1	1	1	1	1	1	1	1	1	1	1	1	1	1	1	0	0	0	0	0	0	0	0
MT1	1	1	1	1	1	1	1	1	1	1	1	1	1	1	1	1	0	0	0	0	0	0	0	0
MT2	0	0	0	0	0	0	1	0	0	0	0	0	0	0	0	0	0	0	0	0	0	0	0	0

1 On state of the DG 0 Off state of the DG Different state from the previous state

Table 4-14 shows that the cost reduction is insignificant for both the connected and isolated MG because the MG should pay for the load shedding by the price consumers agree. It also can be seen that the peak load reduction is the same of the connected and isolated MG.

Table 4-14 Results of the connected and isolated MGs

	Cost without DSM (€/day)	Cost with DSM (€/ day)	Cost percentage Reduction %	Peak load reduction with DSM (kW)	Percentage reduction %
Connected MG	407.8	405	0.69	25	8
Isolated MG	549.7	546.1	0.65	25	8

4.14.2 Maximising the MG Profit

In case of the maximising the MG profit of the connected and isolated MG, there are no curtailments for the industrial or commercial loads and the results are the same of the base case.

It can be concluded from the aforementioned results that the applying of the DSM as load shedding is not preferable when formulating and solving the optimisation problem to maximise the profit because the load shedding results in reducing the MG profit.

4.15 Results of Applying the DSM as Shifting and DBP Simultaneously

The same control possibilities of the smart appliances are considered for the shifting techniques of the residential loads and simultaneously the DB technique is applied to the commercial and industrial loads.

4.15.1 Minimising the Total Operating Cost

A. Connected MG

Scenario 1

It can be observed from Figure 4-55 that the peak of the active total load is reduced by 45.1 kW. Similarly, the peak of the reactive total load is reduced by 21.8 kVAr. The peak of the total active and reactive loads is displaced to hour 7. The proposed DSM strategies reduce the peak of the active and reactive residential and commercial loads because their peaks coincide with the peak of the active and reactive total loads. In addition, the peak of the active and reactive industrial loads is not changed because the peak of the industrial load occurs at different hours of the peak of the total load, where the DSM strategies

are designed to reduce the peak of the active and reactive total loads. Furthermore, the reduction of the peak of the active and reactive total loads has resulted from the both shifting and shedding techniques. The proposed DSM improves the grid security by reducing the peak load.

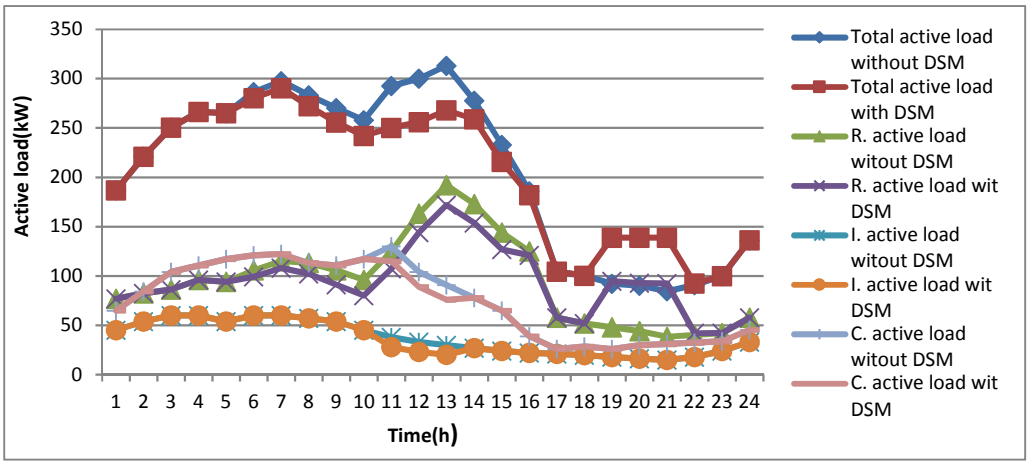

Figure 4-55 Impacts of the DSM on the active residential, industrial, commercial and total loads

Figures 4-56 and 4-57 illustrate that the MG sells more active and reactive power than the base case at hours 6, 9 to 14 by an equal amount to the shifted and curtailed loads, while the MG purchases more active and reactive power from the utility grid by an equal amount to the recovered load at hours 19 to 21 because the active and reactive loads are recovered at these hours because the OMPs have the lowest values at these hours. The on/off state of the DGs is the same in the case of applying the shifting DSM only and it is as in Table 4-4. In addition, the total operating cost is 379.6 € per scheduling day, where the proposed DSM reduces the total operating cost by 28.2 € or by 6.9 % per scheduling day.

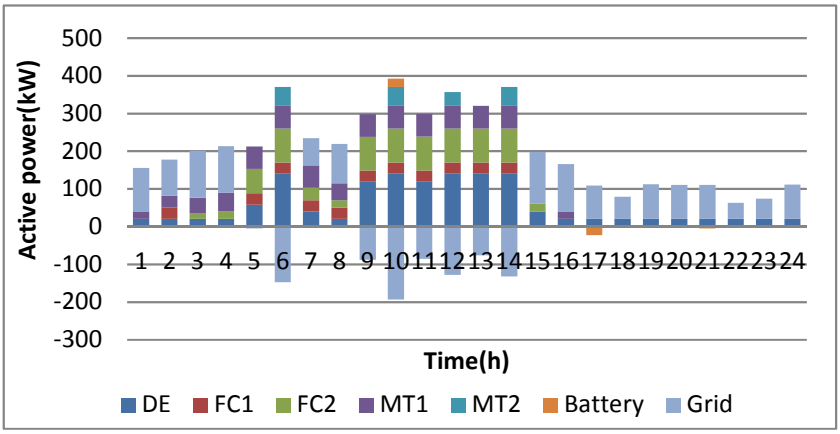

Figure 4-56 Optimal active power scheduling of the DGs and exchanging power with the battery and the utility grid

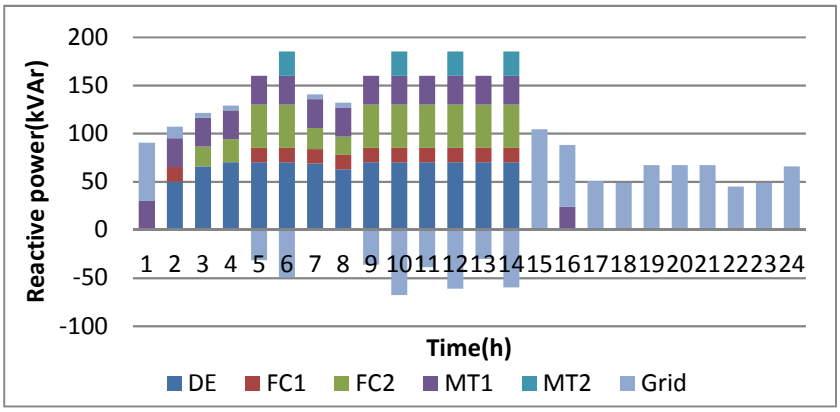

Figure 4-57 Optimal reactive power scheduling of the DGs and exchanging power with the utility grid

Scenario 2

Figure 4-58 shows that the peak of the total active load is reduced by 25 kW. Similarly, the peak of the reactive total load is reduced by 12.1 kVAr. The reductions of the peak of the active and reactive loads is resulted from DBP solely, where the MG accepted both the industrial and commercial bids. The system security is improved in this scenario as well.

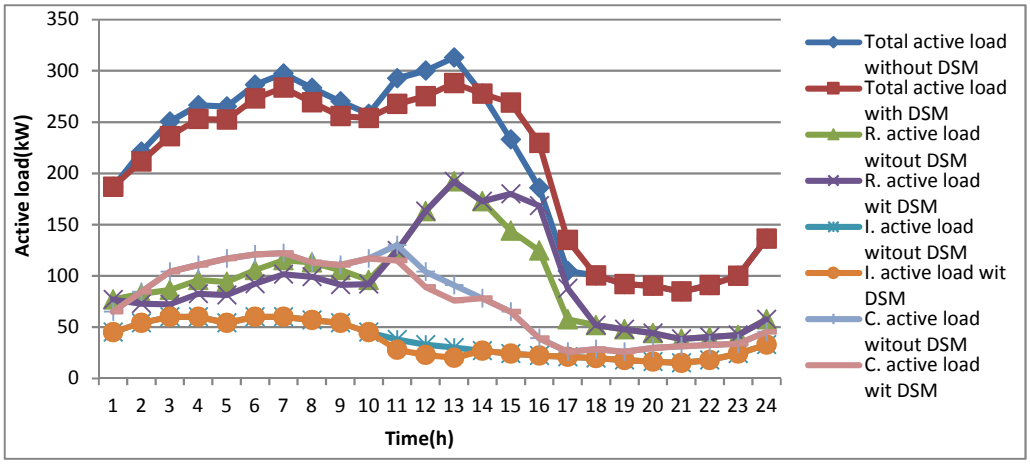

Figure 4-58 Impacts of the DSM on the active residential, industrial, commercial and total loads

It can be shown from Figures 4-59 and 4-60 that the MG purchases less active power than in the base case at hours 2, 3, 4, 7 and 8 by an equal amount to the shifting loads. Whereas, the MG purchases more active and reactive power at hours 15, 16, 17 by equal amount to the recovered active and reactive loads. In addition, the MG sells more active and reactive power than in the base case at hour 6 and hours 9 to 13 by equal amount to the shifted and shedding active and reactive loads because the loads are shifted at hours 6, 9 and 10 and shed at hours 11, 12 and 13. The on/off state of the DGs is the same as in case of applying the shifting DSM only as in Table 4-5.

It is found that the total cost is 395.8 € per scheduling day. It can be noticed that the proposed DSM reduces the total operating cost by 12 € or by 2.9 % per scheduling day.

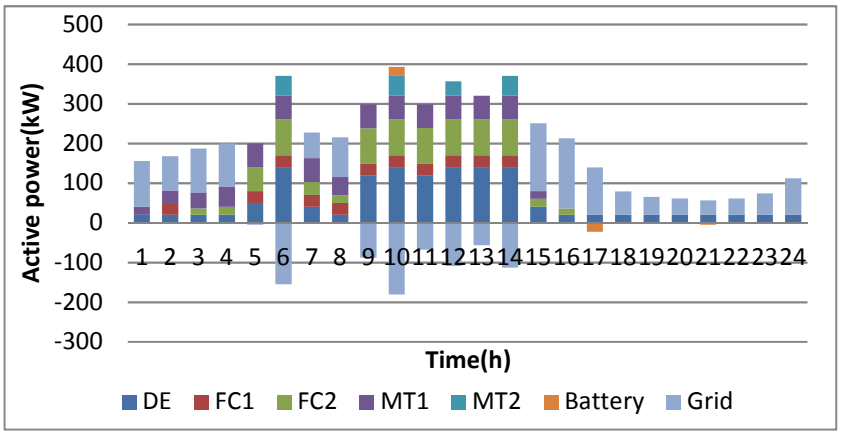

Figure 4-59 Optimal active power scheduling of the DGs and exchanging power with the battery and the utility grid

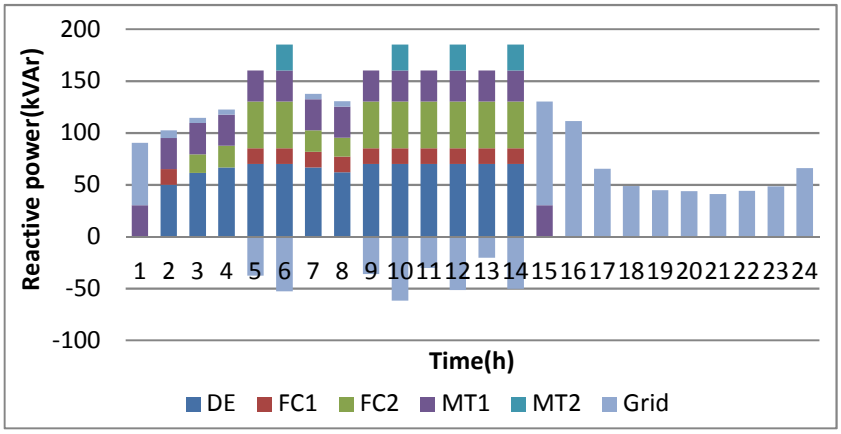

Figure 4-60 Optimal reactive power scheduling of the DGs and exchanging power with the utility grid

Scenario 3

It can be observed from Figure 4-61 that the peak of the active total load is reduced by 32.6 kW. Similarly, the peak of the reactive total load is reduced by 15.8 kVAr. The peak of the active and reactive total loads is moved at hour 7. In addition, the reduction of the peak of the active and reactive total loads is resulted from both the shifting and shedding loads. The proposed DSM reduces the generation capacity required to satisfy the SSSCs, where this leads to improve the grid security.

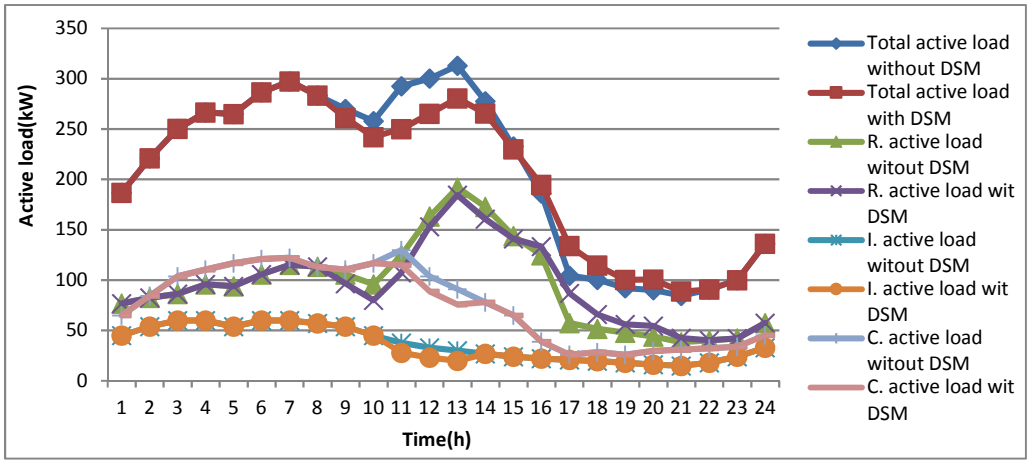

Figure 4-61 Impacts of the DSM on the active residential, industrial, commercial and total loads

Figures 4-62 and 4-63 reveal that the MG sells more active and reactive power than the base case at hours 9 to 14 by an equal amount to the shifted and shed loads. In addition, the MG purchases more active and reactive power from the utility grid at hours 16 to 21 because the loads are recovered at these hours. The on/off state of the DGs is as in Table 4-4. It is found that the total cost is 388 € per scheduling day, where the proposed DSM reduces the total operating cost by 19.8 € or by 4.9 % per scheduling day.

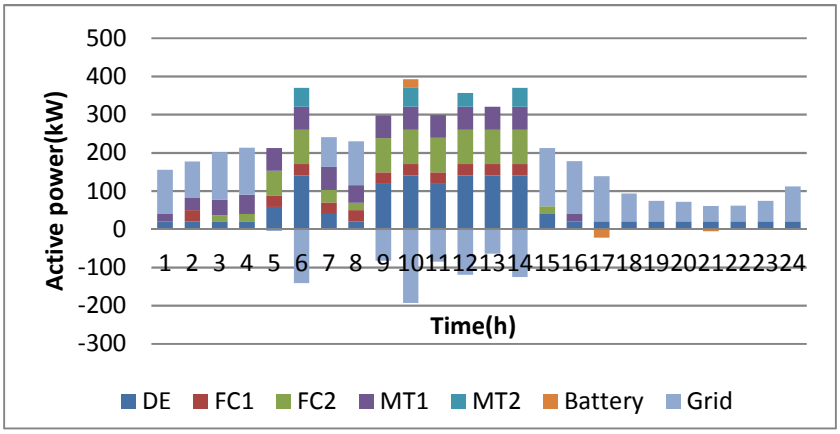

Figure 4-62 Optimal active power scheduling of the DGs and exchanging power with the battery and the utility grid

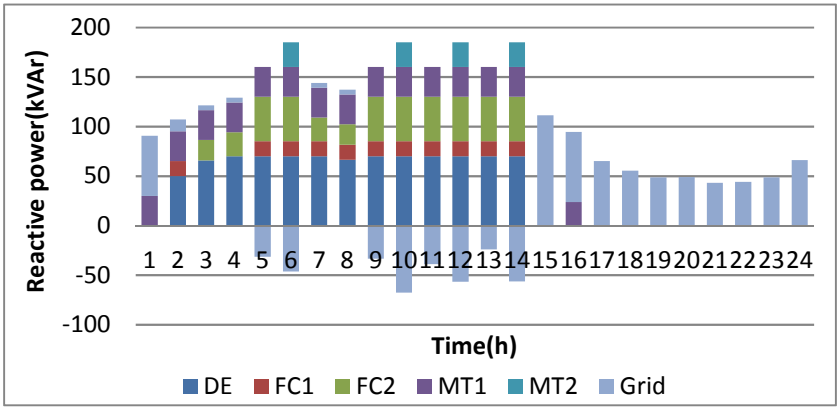

Figure 4-63 Optimal scheduling of the reactive power of the DGs and exchanging power with the utility grid

B. Isolated MG

Scenario1

The proposed DSM reduces the peak of the active and reactive total loads by 35.1 kW as shown in Figures 4-64. Similarly, the peak of the reactive total load is reduced by 17 kVAr, where the peak of the active and reactive total loads is moved to hour 7. The reduction of the peak total load is resulted from both the shifting of the residential load and the shedding of the commercial load. There is no reduction in active and reactive industrial loads because the prices of shedding the active and reactive industrial loads are higher than the prices of shedding the active and reactive commercial loads and there is no trading power with the utility grid. In addition, the proposed DSM improves the grid active and reactive spinning reserves.

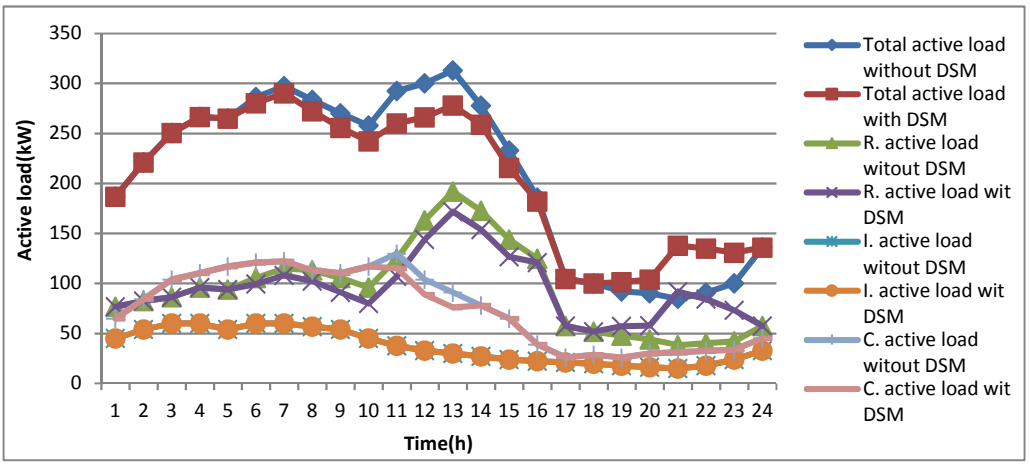

Figure 4-64 Impacts of the DSM on the active residential, industrial, commercial and total loads

Figures 4-65, 4-66, and Table 4-15 show that the MT2 uncommitted during the whole scheduling day in comparing with the base case because the loads are shifted and curtailed during these hours, so the MG does not need to switch on the MT2. The DGs also generate more active and reactive power at hours 19 to 23 than the base case to supply the recovered loads and the MG needs to switch on the FC1 at hours 21 to 23 to meet the load demand as shown in Table 4-15 because it is cheaper than increasing the generation of the DE. Furthermore, the DGs generate less active and reactive power at hours 6 to 16 by the same amount of the shifted load. It is found that the total cost is 538.7 € per scheduling day, where the proposed DSM reduces the total operating cost by 11 € or by 2 % per scheduling day.

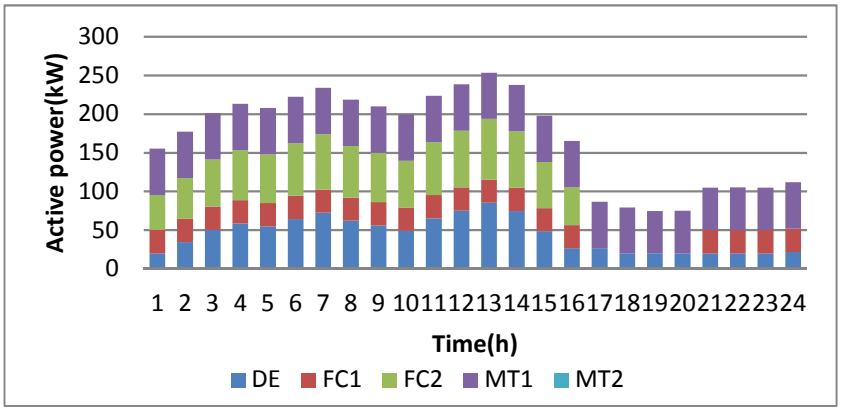

Figure 4-65 Optimal scheduling of the active power of the DGs

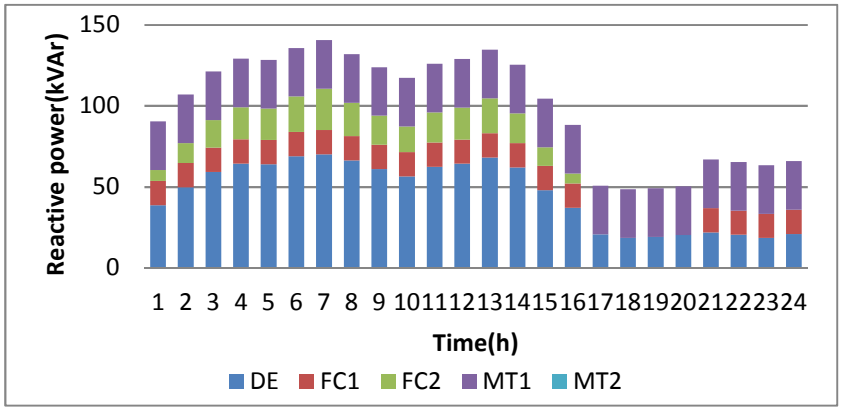

Figure 4-66 Optimal scheduling of the reactive power of the DGs

Table 4-15 Optimal on/off state of the DGs

T(h)	1	2	3	4	5	6	7	8	9	10	11	12	13	14	15	16	17	18	19	20	21	22	23	24
DE	1	1	1	1	1	1	1	1	1	1	1	1	1	1	1	1	1	1	1	1	1	1	1	1
FC1	1	1	1	1	1	1	1	1	1	1	1	1	1	1	1	1	0	0	0	0	1	1	1	1
FC2	1	1	1	1	1	1	1	1	1	1	1	1	1	1	1	1	0	0	0	0	0	0	0	0
MT1	1	1	1	1	1	1	1	1	1	1	1	1	1	1	1	1	1	1	1	1	1	1	1	1
MT2	0	0	0	0	0	0	0	0	0	0	0	0	0	0	0	0	0	0	0	0	0	0	0	0

1 On state of the DG 0 Off state of the DG Different state from the previous state

Scenario2

Figure 4-67 reveals that the peak of the active total load is reduced by 25 kW. Similarly, the peak of the reactive total load is reduced by 12.1 kVAr. The reduction of the peak of the active and reactive loads is resulted from DBP solely, where the MG accepts to shed the active and reactive industrial loads at hour 13 only when the load has the highest value and it accepts to shed the active and reactive commercial loads for the three hours.

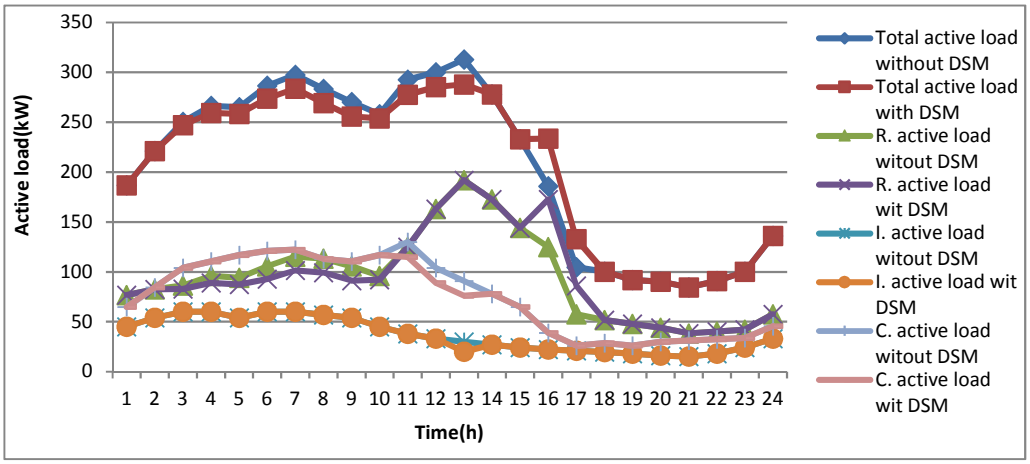

Figure 4-67 Impacts of the DSM on the active residential, industrial, commercial and total loads

It can be seen from Figures 4-68, 4-69, and Table 4-16 that the MG generates less active and reactive power by an equal amount to the shifted and shed loads than the base case at hours 3 to 13. This is because that the active and reactive loads are shifted and curtailed at these hours, while the MG generates more power than the base case at hours 16 and 17 because the active and reactive loads are recovered at these hours. In comparison with base case, the MG switches off the MT2 for the entire scheduling day because the peak of the active and reactive total loads is reduced at the hours of committing of the MT2. The MG also turns on the FC1 at hour 17 to meet the active and reactive recovered loads in comparison with the base case because it is more economical than increasing the generation of the DE. It is found that the total cost is 543.5 € per scheduling day, where the proposed DSM reduces the total operating cost by 6.2 € or by 1.1 %.

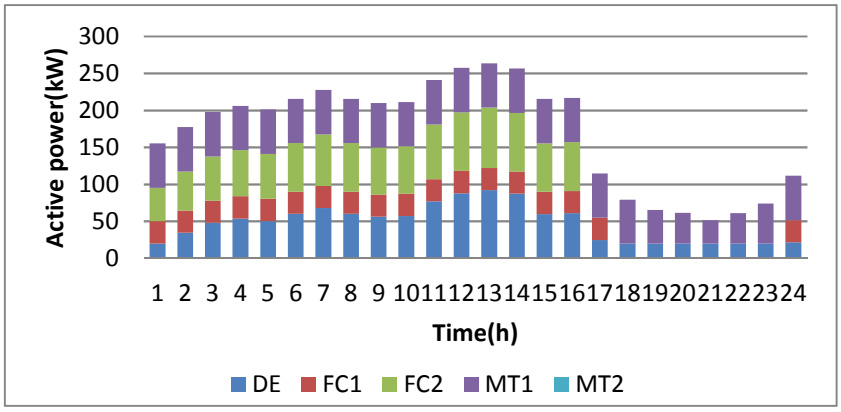

Figure 4-68 Optimal active power scheduling of the DGs with DSM

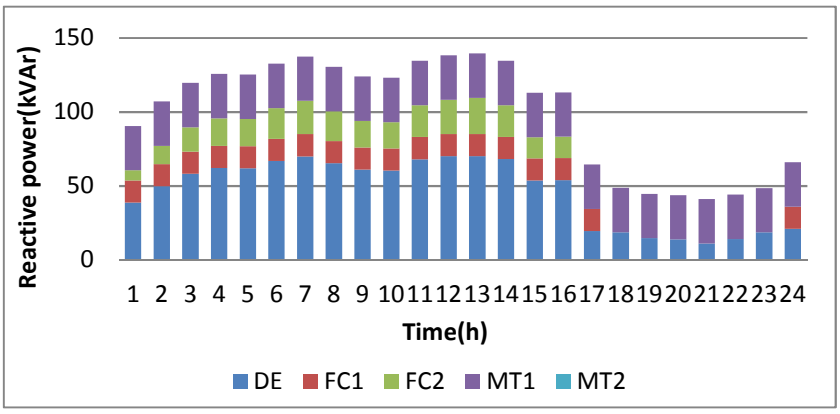

Figure 4-69 Optimal reactive power scheduling of the DGs with DSM

Table 4-16 Optimal on/off state of the DGs

T(h)	1	2	3	4	5	6	7	8	9	10	11	12	13	14	15	16	17	18	19	20	21	22	23	24
DE	1	1	1	1	1	1	1	1	1	1	1	1	1	1	1	1	1	1	1	1	1	1	1	1
FC1	1	1	1	1	1	1	1	1	1	1	1	1	1	1	1	1	1	0	0	0	0	0	0	1
FC2	1	1	1	1	1	1	1	1	1	1	1	1	1	1	1	1	0	0	0	0	0	0	0	0
MT1	1	1	1	1	1	1	1	1	1	1	1	1	1	1	1	1	1	1	1	1	1	1	1	1
MT2	0	0	0	0	0	0	0	0	0	0	0	0	0	0	0	0	0	0	0	0	0	0	0	0

1 On state of the DG 0 Off state of the DG Different state from the previous state

Scenario 3

The proposed DSM reduces the peak of the active total load by 34.7 kW as shown in Figures 4-70. Similarly, the peak of the reactive the total load is reduced by 16.8 kVAr, wherein the peak of the active and reactive total loads is moved to hour 7. The reduction of the peak of the active and reactive total loads

is resulted from both the shifting of the active and reactive residential loads and cutting the active and reactive commercial loads, where the MG rejects the industrial loads for the same reasons of Sc1. The proposed DSM reduces the generation capacity necessary to satisfy the active and reactive SRCs by reducing the peak of the active and reactive total loads.

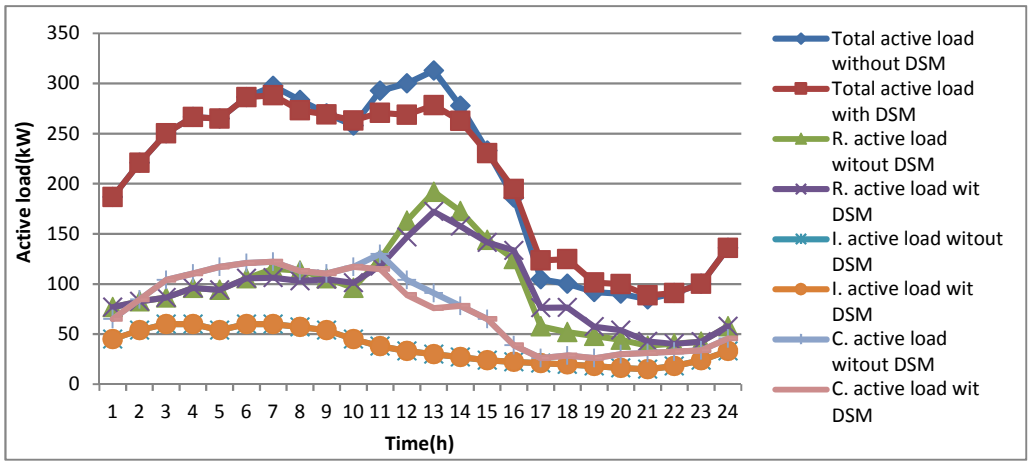

Figure 4-70 Impacts of the DSM on the active residential, industrial, commercial and total loads

Figures 4-71, 4-72, and Table 4-17 demonstrate that the DGs generate less active and reactive power than the base case at hours 7, 8, and 11 to 14 because the loads are shifted and curtailed at these hours. While, the DGs generate more active and reactive power than the base case at hours 16 to 21 by an equal amount to the recovered loads. The MG turns off the MT2 for the entire scheduling day in comparison with the base case for the same reasons of the Sc1 and the Sc2. The MG switches on the FC1 at hours 17 and 18 because the highest active and reactive loads are recovered at these hours. Overall, the total cost is 541.4 € per scheduling day, where the proposed DSM reduces the total operating and emission cost by 8.3 € or by 1.5 % per scheduling day.

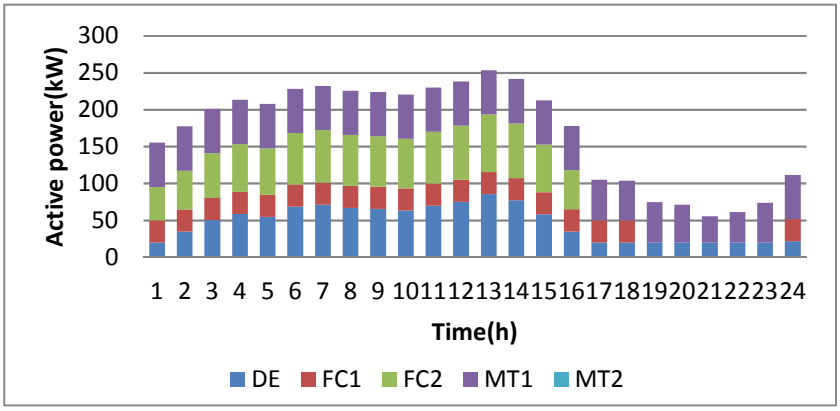

Figure 4-71 Optimal active power scheduling of the DGs

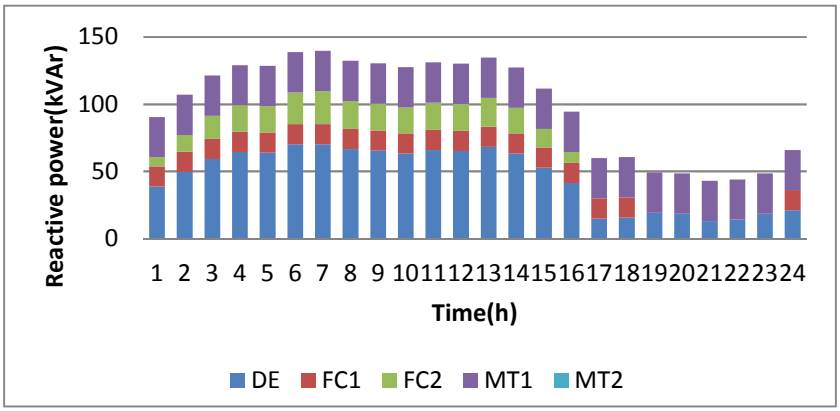

Figure 4-72 Optimal reactive power scheduling of the DGs

Table 4-17 Optimal hourly on/ off state of the DGs

T(h)	1	2	3	4	5	6	7	8	9	10	11	12	13	14	15	16	17	18	19	20	21	22	23	24
DE	1	1	1	1	1	1	1	1	1	1	1	1	1	1	1	1	1	1	1	1	1	1	1	1
FC1	1	1	1	1	1	1	1	1	1	1	1	1	1	1	1	1	1	1	0	0	0	0	0	1
FC2	1	1	1	1	1	1	1	1	1	1	1	1	1	1	1	1	0	0	0	0	0	0	0	0
MT1	1	1	1	1	1	1	1	1	1	1	1	1	1	1	1	1	1	1	1	1	1	1	1	1
MT2	0	0	0	0	0	0	0	0	0	0	0	0	0	0	0	0	0	0	0	0	0	0	0	0

1 On state of the DG 0 Off state of the DG Different state from the previous state

Tables 4-18 and 4-19 show that the highest reduction of the cost and the peak load for both the connected and isolated MG occur in the Sc1 because the load is shifted from peak to off-peak hours. The both connected and isolated MG in the Sc2 have the lowest reduction of the cost and peak loads among other scenarios.

Table 4-18 Results of the scenarios of the connected MG

	Cost with DSM (€/ day)	Percentage cost reduction %	Peak load reduction with DSM (kW)	Percentage load reduction %	No. shifting WMs	No. shifting DWs
Sc1	379.6	6.9	45.1	14.4	82	66
Sc2	395.8	2.9	25	8	62	46
Sc3	388	4.9	32.6	10.4	51	54

Table 4-19 Results of the scenarios of the isolated MG

	Cost with DSM (€/day)	Percentage cost reduction %	Peak load reduction with DSM (kW)	Percentage reduction %	No. shifting WMs	No. shifting DWs
Sc1	538.7	2	35.1	11.2	82	66
Sc2	543.5	1.1	25	8	32	40
Sc3	541.4	1.5	34.7	11.1	43	47

4.15.2 Maximising the MG Profit

The results in case of maximising the MG profit of the connected and isolated MG for all scenarios are the same as of the applying the shifting DSM technique only because in the case of the maximising the MG profit the MG dose not shed any active and reactive loads because the curtailed load leads to reduce the MG profit.

4.16 Chapter Conclusions

The integration of the DSM techniques with SCUC-UARDEED of the connected and isolated MG to minimise the total operating cost or maximise the profit is analysed. The results show that the DSM as load shifting reduces the total operating cost, improves the systems security and reserve for the connected and isolated MG, increases the profit for isolated MG, and it has an insignificant impact on the profit. In case of applying the DSM as DB, the DSM reduces the total operating cost, and improves the system security and reserve, while there is no curtailment to load in case of maximising the profit because the load cut increases the profit. In case of applying both the load shifting and DB strategies simultaneously, the results reveal that the DSM reduces the total operating cost, improves the system security and reserve. In case, when considering the DSM to maximise the profit, there is no curtailment for load for the connected and isolated MG and the results as in the case of applying the load shifting solely.

5 Integration of the DSM with Optimal Scheduling of the MG under Stochastic Environment

5.1 Chapter Summary

The number of the appliances that are connected to the grid at each time interval is obtained supposing that the diversified profile (Fig 4.2) is perfect. However, this is not true and it gives uncertainties. Therefore, the uncertainties occurring from the estimated number of the smart appliances are proposed and incorporated with an optimisation problem of the MG in the stochastic optimisation approach. A novel two-stage stochastic based-scenario optimisation approach is presented, where the uncertainties deriving from the estimation of the number of the smart appliance, the wind generation, and the solar generation are considered as the uncertain variables. The proposed stochastic approach is applied to the connected and isolated MG and many scenarios are conducted to verify the effectiveness of the proposed approach. Both the shifting and the DB techniques are applied simultaneously to the load and the control possibility of the smart appliances of the Sc1 in the previous chapter is considered in this chapter.

5.2 Literature review

The researchers pointed out the incorporating of the DSM techniques and uncertainties evolving from different resources with optimisation problems of the MG and investigated the impacts of the DSM with the uncertainties on the optimal operation of the MG. In [133], the DSM as a shifting technique and uncertainty that derived from wind generation were incorporated with optimisation problems of the isolated MG. Reference [94] presented the uncertainties that evolved from the intermittent nature of wind, solar generations, and the load forecasting with the DSM as a load shedding to minimise the operating cost of the MG. Reference [86] addressed the integration of the DSM and WT generation fluctuations with the optimisation problem of the LV MG to minimise the operating cost. Reference [97] presented a two-stage stochastic optimisation with the DSM as curtailing technique to

minimise the operating cost. The uncertainties that resulted from generations of the RDGs, load demands, and random outages of the DGs are considered as the sources of the uncertainties.

From above works, it would appear that the proposed stochastic optimisation approaches did not consider the DSM as a source of uncertainties. The DSM was treated as aggregated amount and the DSM was input to the optimisation algorithms. The DSM was proposed for active load only. In addition, it was not taken into consideration the models of the reactive power production cost, the environmental cost, the battery degradation cost, purchasing reactive power from the utility grid. Further, important constraints were ignored, such as active and reactive security constraints of the connected and isolated MG and emission limit of the greenhouse gases, constraints related to the reactive power, and the constraints related to the DSM techniques. Moreover, the optimisation problem was presented to minimise the operating cost solely. In case of maximising the profit, it appears no study has reported the stochastic optimisation with the DSM as source of the uncertainties to maximise the profit of the connected or isolated MG.

5.3 Stochastic Model of the MG Components

The stochastic models of the wind and solar generations have been done in chapter three, so solely the number of devices that are connected at each time intervals is needed to be modelled. The proposed models of the number of the connected WMs and DWs are as follows.

5.3.1 Stochastic Model of the Number of the WMs

The number of WMs that are connected to the MG at each time intervals is assumed to follow the normal distribution and the developed model as follows

$$X_{WM}(t) = X_{WM}(t)^{estim} + \mu(t)^{WM}.\sigma(t)^{WM} \quad \textbf{(5.1)}$$

where $X_{WM}{}^{estim}$ and $\sigma(t)^{WM}$ are the estimated number of the WMs at hour t and the standard deviation of WMs respectively, $\mu(t)^{WM}$ is a random variable

that is generated for number of the WMs at time t in Mote Carlo simulation by using normal probability with a mean of zero and a standard deviation is one. ${X_{WM}}^{estim}$ is obtained from Figure 4-4.

5.3.2 Stochastic Model of the Number of the DWs

The number of DWs that are connected to the MG at each time intervals is assumed to follow the normal distribution and the developed model of the number of the DWs as follows

$$X_{DW}(t) = {X_{DW}}^{estim} + \mu(t)^{DW}.\sigma(t)^{DW} \quad \textbf{(5.2)}$$

where ${X_{DW}}^{estim}$ and $\sigma(t)^{DW}$ are the estimated number of DWs at hour t and the standard deviation of the DWs respectively, $\mu(t)^{DW}$ is a random variable generated for the DWs at time t in Monte Carlo simulation by using normal probability with a mean of zero and a standard deviation is one. ${X_{DW}}^{estim}$ is obtained from Figure 4-4.

By following the same procedure in section 3.3 to determine the probability of the joint scenarios, the probability happening of each reduced scenario for the WMs and DWs is as follows.

$$\rho_{k2}^{WM} = [\rho_1^{WM}\ ,\ \rho_2^{WM}\ , \dots \rho_{m2}^{WM}]_{1\times m2} \quad \textbf{(5.3)}$$

$$\rho_{e1}^{DM} = [\rho_1^{DM}\ ,\ \rho_2^{DM}\ , \dots \rho_{r1}^{DM}]_{1\times r1} \quad \textbf{(5.4)}$$

where ρ^{WM}, ρ^{DW} are corresponding probability of the reduced scenarios for the WMs and the DWs respectively, where the summation probability of scenarios for each variable should equal 1.

$$\sum_{k2=1}^{m2} \rho_{k2}^{WM} = 1 \quad \textbf{(5.5)}$$

$$\sum_{e1=1}^{r1} \rho_{e1}^{DW} = 1 \quad \textbf{(5.6)}$$

The number of possible scenarios (S) is calculated as

$$S = n.q.m2.r1 \quad \textbf{(5.7)}$$

The summation probability of the joint scenarios is as follows:

$$\sum_{s=1}^{S} \lambda_s = \sum_{i3=1}^{n} \sum_{i4=1}^{q} \sum_{k2=1}^{m2} \sum_{e1=1}^{r1} \rho_{i3}^{W} \rho_{i4}^{PV} \rho_{k2}^{WM} \rho_{e1}^{DW} \quad \textbf{(5.8)}$$

5.4 Proposed Objective Functions

The proposed objective functions are a two-stage functions. In the first stage, the UC decision variables of each DG and the shedding of the active and reactive industrial and commercial loads decisions are taken before actual consideration the uncertainties. These decisions could not be change in the second stage. The decisions that are taken in the second stage after consideration the uncertainties are the active and reactive power scheduling of the DGs, the exchanging power with storage battery, the exchanging active and reactive power with the utility grid, and the active and reactive shifted and recovered loads. The decision variables are indexed by (s) for representing scenario.

5.4.1 Minimising the Total Operating Cost

A. Grid-connected mode

The optimisation problem is formulated as

$$\min(F) \quad \textbf{(5.9)}$$

where the objective function F is

$$\begin{aligned} F = \sum_{t=1}^{T}\{\sum_{i=1}^{N}[SU_{DG_i}(t) + SD_{DG_i}(t)] + C_{Pindshd}(t) + C_{Qindshd}(t) + \\ C_{Pcomshd}(t) + C_{Qcomshd}(t)\} + \sum_{s=1}^{S} \lambda_s \sum_{t=1}^{T}\{\sum_{i=1}^{N}[CP_{DG_i}(P_{DG_i}^{s}(t)) + \\ CQ_{DG_i}(Q_{DG_i}^{s}(t)) + COM_{DG_i}(P_{DG_i}^{s}(t))]\delta_{DG_i}(t) + C_e(P_{DG_i}^{s}(t)) + \\ C_{bo}^{s}(t) + c_{gP}^{s}(t) + c_{gQ}^{s}(t) + \sum_{i1=1}^{N1} CP_{W_{i1}}(P_{W_{i1}}^{s}(t)) + \\ \sum_{i2=1}^{N2} CP_{PV_{i2}}(P_{PV_{i2}}^{s}(t)) + c_{Pres}.P_{Drescut}^{s}(t) + c_{Qres}.Q_{Drescut}^{s}(t) + \\ c_{Pind}.P_{Dindcut}^{s}(t) + c_{Qind}.Q_{Dindcut}^{s}(t) + c_{Pcom}.P_{Dcomcut}^{s}(t) + \\ c_{Qcom}.Q_{Dcomcut}^{s}(t)\} \end{aligned} \quad \textbf{(5.10)}$$

This objective function is constructed using equations

(2.15), (2.16), (4.9), (4.10), (4.17), (4.18), (2.1), (2.2), (2.3), (2.14), (2.11), (2.12), (2.13), (2.5), (2.6), and the last six components which they represent the involuntary active and reactive loads cut for the residential, industrial, and commercial consumers.

B. Grid-isolated mode

The optimisation problem is formulated as

$$\min(F) \tag{5.11}$$

where the objective function F is

$$\begin{aligned} F = \sum_{t=1}^{T}\{\sum_{i=1}^{N}[SU_{DG_i}(t) + SD_{DG_i}(t)] + C_{Pindshd}(t) + C_{Qindshd}(t) + \\ C_{Pcomshd}(t) + C_{Qcomshd}(t)\} + \sum_{s=1}^{S}\lambda_s \sum_{t=1}^{T}\{\sum_{i=1}^{N}[CP_{DG_i}(P^s_{DG_i}(t)) + \\ CQ_{DG_i}(Q^s_{DG_i}(t)) + COM_{DG_i}(P^s_{DG_i}(t))]\delta_{DG_i}(t) + C_e(P^s_{DG_i}(t)) + C^s_{bo}(t) + \\ \sum_{i1=1}^{N1} CP_{W_{i1}}(P^s_{W_{i1}}(t)) + \sum_{i2=1}^{N2} CP_{PV_{i2}}(P^s_{PV_{i2}}(t)) + c_{Pres}.P^s_{Drescut}(t) + \\ c_{Qres}.Q^s_{Drescut}(t) + c_{Pind}.P^s_{Dindcut}(t) + c_{Qind}.Q^s_{Dindcut}(t) + \\ c_{Pcom}.P^s_{Dcomcut}(t) + c_{Qcom}.Q^s_{Dcomcut}(t) + \sum_{i=1}^{N} c_G.P^s_{DG_icut}(t) + \\ \sum_{i1=1}^{N1} c_{ren}.P^s_{W_{i1}cut}(t) + \sum_{i2=1}^{N2} c_{ren}.P^s_{PV_{i2}cut}(t)\} \end{aligned} \tag{5.12}$$

This objective function is constructed using equations

(2.15), (2.16), (4.9), (4.10), (4.17), (4.18), (2.1), (2.2), (2.3), (2.14), (2.11), (2.5), (2.6), and the last nine components which they represent the involuntary active and reactive loads cut for the residential, industrial, and commercial consumers and the generation cuts of the WT, PVs and the DGs.

5.4.2 The Proposed Maximising the MG Profit

A. Grid-connected mode

The optimisation problem is formulated as

$$\max(F) \tag{5.13}$$

where the objective function F is

$$\begin{aligned} F = &- \sum_{t=1}^{T}\{\sum_{i=1}^{N}[SU_{DG_i}(t) + SD_{DG_i}(t)] + C_{Pindshd}(t) + C_{Qindshd}(t) + \\ &C_{Pcomshd}(t) + C_{Qcomshd}(t)\} + \sum_{s=1}^{S}\lambda_s \sum_{t=1}^{T}\{\sum_{i=1}^{N}[c_{gP}(t).P^s_{DG_i}(t) + \\ &c_{gQ}(t).Q^s_{DG_i}(t)]\delta_{DG_i}(t) + c_{gP}(t).P^s_{bdis}(t).\Delta t + c_{gP}(t).\sum_{i2=1}^{N2}P^s_{PV_{i2}}(t) + \\ &c_{gP}(t).\sum_{i1=1}^{N1}P^s_W(t)\} - \sum_{s=1}^{S}\lambda_s \sum_{t=1}^{T}\{\sum_{i=1}^{N}[CP_{DG_i}(P^s_{DG_i}(t)) + \\ &CQ_{DG_i}(Q^s_{DG_i}(t)) + COM_{DG_i}(P^s_{DG_i}(t))]\delta_{DG_i}(t) + C_e(P^s_{DG_i}(t)) + C^s_{bo}(t) + \\ &c_{gP}(t).P^s_{bch}(t).\Delta t + \sum_{i1=1}^{N1}CP_{W_{i1}}(P^s_{W_{i1}}(t)) + \sum_{i2=1}^{N2}CP_{PV_{i2}}(P^s_{PV_{i2}}(t)) + \\ &c_{Pres}.P^s_{Drescut}(t) + c_{Qres}.Q^s_{Drescut}(t) + c_{Pind}.P^s_{Dindcut}(t) + \\ &c_{Qind}.Q^s_{Dindcut}(t) + c_{Pcom}.P^s_{Dcomcut}(t) + c_{Qcom}.Q^s_{Dcomcut}(t)\} \end{aligned} \tag{5.14}$$

The revenue of the MG comes from selling the active and reactive power from the DGs, the discharging power of the battery, the power from the RDGs. The cost is constructed using equations

(2.15), (2.16), (4.9), (4.10), (4.17), (4.18), (2.1), (2.2), (2.3), (2.14), (2.11), (2.5), (2.6), the battery charging cost, and the last six components which they represent the involuntary active and reactive loads cut for the residential, industrial, and commercial consumers.

B. Grid-isolated mode

The optimisation problem is formulated as

$$\max(F) \tag{5.15}$$

where the objective function F is

$$F = -\sum_{t=1}^{T}\{\sum_{i=1}^{N}[SU_{DG_i}(t) + SD_{DG_i}(t)] + C_{Pindshd}(t) + C_{Qindshd}(t) + C_{Pcomshd}(t) + C_{Qcomshd}(t)\} + \sum_{s=1}^{S}\lambda_s \sum_{t=1}^{T}\{\sum_{i=1}^{N}[c_{isoP}(t).P_{DG_i}^{s}(t) + c_{isoQ}(t).Q_{DG_i}^{s}(t)]\delta_{DG_i}(t) + c_{isoP}(t).P_{bdis}^{s}(t).\Delta t + c_{isoP}(t).\sum_{i2=1}^{N2}P_{PV_{i2}}^{s}(t) + c_{isoP}(t).\sum_{i1=1}^{N1}P_{W}^{s}(t)\} - \sum_{s=1}^{S}\lambda_s \sum_{i=1}^{T}\{\sum_{i=1}^{N}[CP_{DG_i}(P_{DG_i}^{s}(t)) + CQ_{DG_i}(Q_{DG_i}^{s}(t)) + COM_{DG_i}(P_{DG_i}^{s}(t))]\delta_{DG_i}(t) + C_e(P_{DG_i}^{s}(t)) + C_{bo}^{s}(t) + c_{isoP}(t).P_{bch}^{s}(t).\Delta t + \sum_{i1=1}^{N1}CP_{W_{i1}}(P_{W_{i1}}^{s}(t)) + \sum_{i2=1}^{N2}CP_{PV_{i2}}(P_{PV_{i2}}^{s}(t)) + c_{Pres}.P_{Drescut}^{s}(t) + c_{Qres}.Q_{Drescut}^{s}(t) + c_{Pind}.P_{Dindcut}^{s}(t) + c_{Qind}.Q_{Dindcut}^{s}(t) + c_{Pcom}.P_{Dcomcut}^{s}(t) + c_{Qcom}.Q_{Dcomcut}^{s}(t) + \sum_{i=1}^{N}c_G.P_{DG_icut}^{s}(t) + \sum_{i1=1}^{N1}c_{ren}.P_{W_{i1}cut}^{s}(t) + \sum_{i2=1}^{N2}c_{ren}.P_{PV_{i2}cut}^{s}(t)\} \quad \textbf{(5.16)}$$

The revenue of the MG comes from selling the active and reactive power from the DGs, the discharging power of the battery, the power from the RDGs. The cost is constructed using equations

(2.15), (2.16), (4.9), (4.10), (4.17), (4.18), (2.1), (2.2), (2.3), (2.14), (2.11), (2.5), (2.6), the battery charging cost, and the last nine components which they represent the involuntary active and reactive loads cut for the residential, industrial, and commercial consumers and the generation cuts of the WT, PVs and the DGs.

The first stage of these objective functions is subject to the constraints of equations (2.17) to (2.35) for the connected MG, whereas for the isolated MG, the first stage of the objective functions is subjected to the constraints of equations (2.17) to (2.25), (2.30) to (2.33), (2.36), and (2.37). All the above objective functions are subjected to the constraints of equations (4.5) to (4.8). The second stage of these objective functions is subjected to the same constraints of the first stage. However, the constraints of the equations (2.17), (2.18), (2.34), (2.35), (2.36), and (2.37) are modified in the second stage to involve the DSM techniques and the uncertainties as in the following equations:

A. Power balance constraints

The active and reactive power balance constraints are formulated as

For the connected MG

$$\sum_{t=1}^{T}\{\sum_{i=1}^{N}\delta_{DG_i}(t).P_{DG_i}^{S}(t)+\sum_{i1=1}^{N1}P_{W_{i1}}^{S}(t)+\sum_{i2=1}^{N2}P_{PV_{i2}}^{S}(t)+P_{b}^{S}(t)+ \quad (5.17)$$
$$P_{g}^{S}(t)=\left(P_{Dres}(t)-P_{Dres}^{shft,s}(t)+P_{Dres}^{reco,s}(t)-P_{Drescut}^{S}(t)\right)+(P_{Dind}(t)-$$
$$P_{Dindshd}(t)-P_{Dindcut}^{S}(t))+(P_{Dcom}(t)-P_{Dcomshd}(t)-P_{Dcomcut}^{S}(t))\}$$

$$\sum_{t=1}^{T}\{\sum_{i=1}^{N}\delta_{DG_i}(t).Q_{DG_i}^{S}(t)+Q_{g}^{S}(t)=(Q_{Dres}(t)-Q_{Dres}^{shft,s}(t)+Q_{Dres}^{reco,s}(t)- \quad (5.18)$$
$$Q_{Drescut}^{S}(t))+(Q_{Dind}(t)-Q_{Dindshd}(t)-Q_{Dindcut}^{S}(t))+(Q_{Dcom}(t)-$$
$$Q_{Dcomshd}(t)-Q_{Dcomcut}^{S}(t))\}$$

For the isolated MG

$$\sum_{t=1}^{T}\{\sum_{i=1}^{N}\delta_{DG_i}(t).P_{DG_i}^{S}(t)+\sum_{i1=1}^{N1}P_{W_{i1}}^{S}(t)+\sum_{i2=1}^{N2}P_{PV_{i2}}^{S}(t)+P_{b}^{S}(t)- \quad (5.19)$$
$$\sum_{i=1}^{N}P_{DG_icut}^{S}(t)-\sum_{i1=1}^{N1}P_{W_{i1}cut}^{S}(t)-\sum_{i2=1}^{N2}P_{PV_{i1}cut}^{S}(t)=\left(P_{Dres}(t)-\right.$$
$$\left.P_{Dres}^{shft,s}(t)+P_{Dres}^{reco,s}(t)-P_{Drescut}^{S}\right)+(P_{Dind}(t)-P_{Dindshd}(t)-$$
$$P_{Dindcut}^{S}(t))+(P_{Dcom}(t)-P_{Dcomshd}(t)-P_{Dcomcut}^{S}(t))\}$$

$$\sum_{t=1}^{T}\{\sum_{i=1}^{N}\delta_{DG_i}(t).Q_{DG_i}^{S}(t)=(Q_{Dres}(t)-Q_{Dres}^{shft,s}(t)+Q_{Dres}^{reco,s}(t)- \quad (5.20)$$
$$Q_{Drescut}^{S}(t))+(Q_{Dind}(t)-Q_{Dindshd}(t)-Q_{Dindcut}^{S}(t))+(Q_{Dcom}(t)-$$
$$Q_{Dcomshd}(t)-Q_{Dcomcut}^{S}(t))\}$$

B. SSSCs

The active and reactive SSSCs are modified as follows

$$\sum_{i=1}^{T}\{\sum_{i=1}^{N}\delta_{DG_i}(t).P_{DG_imax}^{S}(t)\geq\left(P_{Dres}(t)-P_{Dres}^{shft,s}(t)+\right. \quad (5.21)$$
$$\left.P_{Dres}^{reco,s}(t)-P_{Drescut}^{S}(t)\right)+(P_{Dind}(t)-P_{Dindshd}(t)-P_{Dindcut}^{S}(t))+$$
$$(P_{Dcom}(t)-P_{Dcomshd}(t)-P_{Dcomcut}^{S}(t))\}$$

$$\sum_{i=1}^{T}\{\sum_{i=1}^{N}\delta_{DG_i}(t).Q_{DG_imax}^{S}(t)\geq(Q_{Dres}(t)-Q_{Dres}^{shft,s}(t)+Q_{Dres}^{reco,s}(t)- \quad (5.22)$$
$$Q_{Drescut}^{S}(t))+(Q_{Dind}(t)-Q_{Dindshd}(t)-Q_{Dindcut}^{S}(t))+(Q_{Dcom}(t)-$$
$$Q_{Dcomshd}(t)-Q_{Dcomcut}^{S}(t))\}$$

C. SRCs

The active and reactive spinning reserve constraints are formulated as

$$\sum_{i=1}^{T}\{\sum_{i=1}^{N}\delta_{DG_i}(t).P^{S}_{DG_i max}(t) \geq \left(P_{Dres}(t) - P^{shft,s}_{Dres}(t) + P^{reco,s}_{Dres}(t) - P^{S}_{Drescut}\right) + \left(P_{Dind}(t) - P_{Dindshd}(t) - P^{S}_{Dindcut}(t)\right) + \left(P_{Dco}(t) - P_{Dcomshd}(t) - P^{S}_{Dcomcut}(t)\right) + R^{S}_{p}(t)\} \quad \textbf{(5.23)}$$

$$\sum_{i=1}^{T}\{\sum_{i=1}^{N}\delta_{DG_i}(t).Q^{S}_{DG_i max}(t) \geq (Q_{Dres}(t) - Q^{shft,s}_{Dres}(t) + Q^{reco,s}_{Dres}(t) - Q^{S}_{Drescut}(t)) + (Q_{Dind}(t) - Q_{Dindshd}(t) - Q^{S}_{Dindcut}(t)) + (Q_{Dcom}(t) - Q_{Dcomshd}(t) - Q^{S}_{Dcomcut}(t)) + R^{S}_{q}(t)\} \quad \textbf{(5.24)}$$

5.5 Results of the Stochastic Optimisation of the MG with Integration of the DSM

The proposed approaches are applied to the connected and isolated MG shown in Figure 2-3. The mean values of the WMs and DWs are depicted in Figure 4-4. Table D-1 and Table D-2 in Appendix D show the generated scenarios for 24 hours and reduced scenarios for MWs and DWs respectively. The case of the devices can be shifted every day at any time between hours 18 to 23 (Sc1) is considered as control possibilities of the smart appliance.

5.5.1 Minimising the Total Operating Cost

A. Connected MG

Figures 5-1 and 5-2 show the impacts of the uncertainties on the active residential and the total loads for the five highest probability scenarios and Det. Case, while the impacts of the DSM on the industrial and commercial loads are the same for all scenarios and are the same of the Det. Case (the results in the previous chapter). This is because the load shedding for the industrial and commercial consumers are taken in the first stage, which they could not be changed.

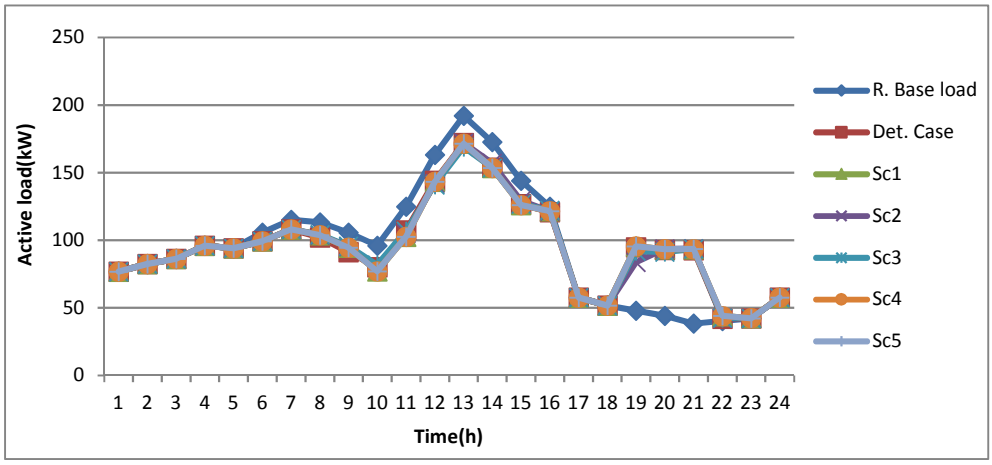

Figure 5-1 Active residential loads of the five highest probability scenarios and Det. Case of the connected MG

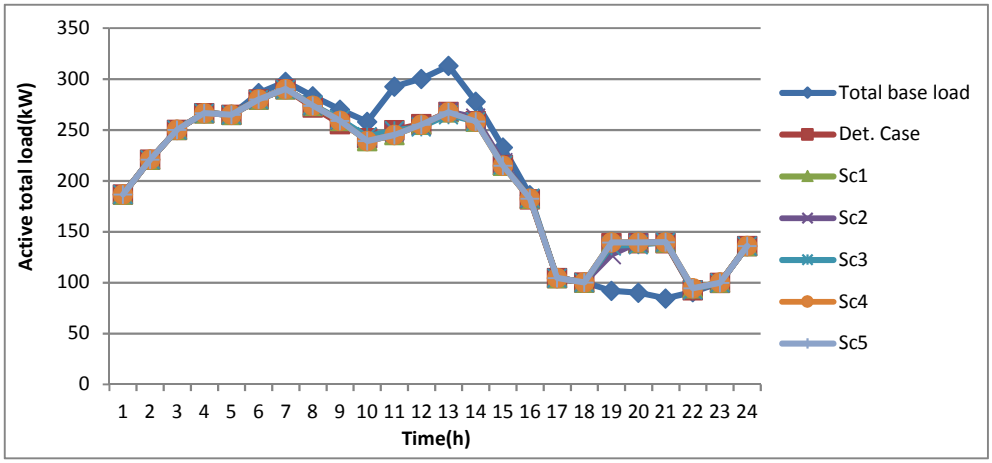

Figure 5-2 Active total loads of the five highest probability scenarios and Det. Case of the connected MG

Figures 5-3 and 5-4 show the optimal active and reactive power scheduling respectively. It can be seen from these figures and Table 5-1 that the uncertainties are compensated from the utility grid for the first three scenarios, wherein their active power generation are the same because they have the same RDGs profiles. Therefore, the difference in the exchanging active and reactive power with the utility grid is due to the uncertainties of the number of the connected appliances. In addition, Sc1, Sc4, and Sc5 have the same reactive power generation profile and the same exchanging reactive power with the utility grid because they have the same number of appliances and the shifted appliance are equal and there are not any stochastic reactive renewable

generation. Further, in all scenarios, the DGs generate the maximum possible active and reactive power to reduce its total cost at hour 6, 10, and 14 because at these hours the OMPs have the highest values. However, at hours 6 and 10 in the Sc4, the MG sells less active power than other scenarios because it has the lowest renewable generation among other scenarios, while the MG sells higher active power than other scenarios at hour 14 because the renewable generation is higher than the other scenarios. Furthermore, in the Sc4 at hours 21 and 22, the MG purchases higher active power than other scenarios to supply the base and recovered loads. This is because at these hours the renewable generations are equal to zero.

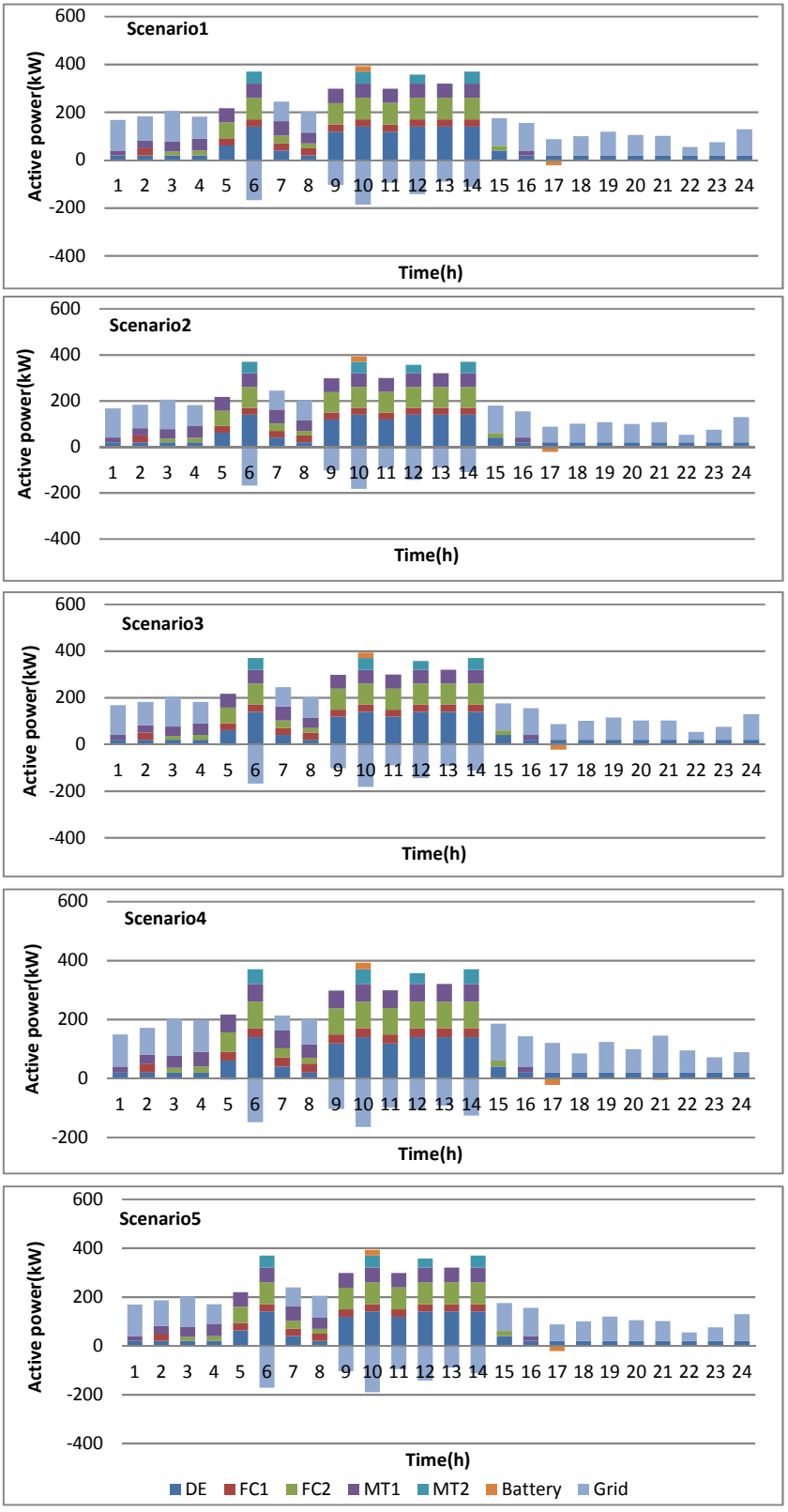

Figure 5-3 Optimal active power scheduling of the DGs for the five highest probability scenarios of the connected MG

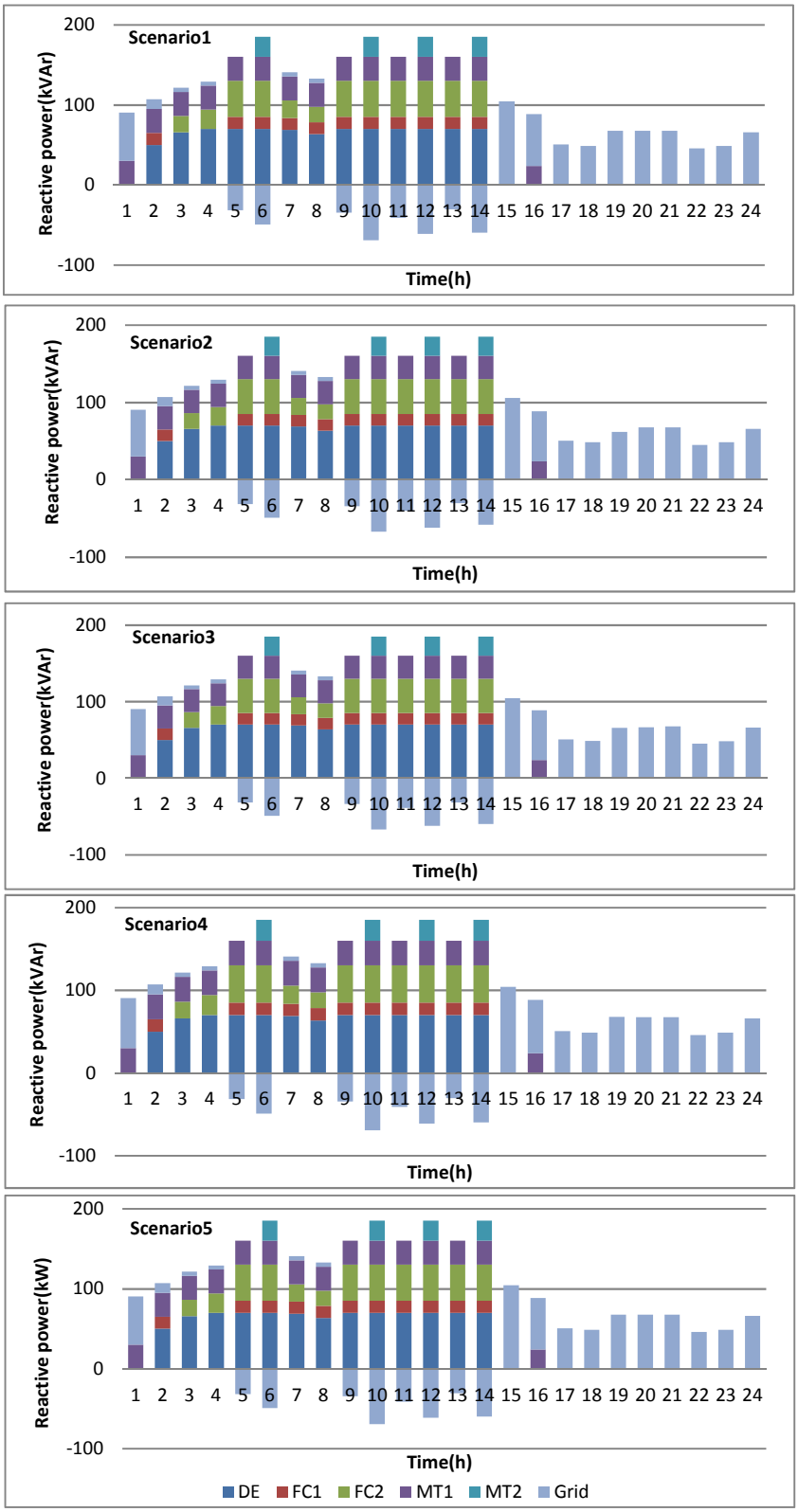

Figure 5-4 Optimal reactive power scheduling of the DGs for the five highest probability scenarios of the connected MG

Table 5-1 Results of the five highest probability scenarios and Det. Case per scheduling day of the connected MG

	Det. Case	Sc1	Sc2	Sc3	Sc4	Sc5
Total P_{DG} (kW)	3421.401	3425.856	3425.856	3425.856	3424.824	3428.556
Total Q_{DG} (kVAr)	2031.643	2032.399	2032.399	2032.675	2032.399	2032.399
Total P_{gb} (kW)	1505.994	1457.806	1447.801	1452.414	1466.881	1448.206
Total P_{gs} (kW)	857.199	903.291	893.286	897.898	844.868	911.761
Total Q_{gb} (kVAr)	721.522	723.591	718.745	720.703	723.591	723.591
Total Q_{gs} (kVAr)	374.536	377.360	372.514	374.748	377.360	377.360
Peak load reduction (kW)	45.07	45.535	44.965	48.025	45.353	45.353
Total cost (€)	379.6	382.7	385.8	384.8	388.6	381.1
No. WMs	82	76	76	76	76	76
No. DWs	66	74	63	68	74	74

B. Isolated MG

Figures 5-5 and 5-6 illustrate the impacts of the uncertainties on the active residential and total loads for the five highest probability scenarios and Det. Case, while the impacts of the DSM on the commercial and industrial loads are the same and they are the same of the Det. Case for the same reasons of the connected MG. These figures reveal that the time of the recovered loads of the Sc4 is different from other scenarios, where some of the shifted loads are recovered at hour 24 because the wind generation is abundant in comparison with the other scenarios. Moreover, the peak of the active and reactive loads is displaced to hour 7.

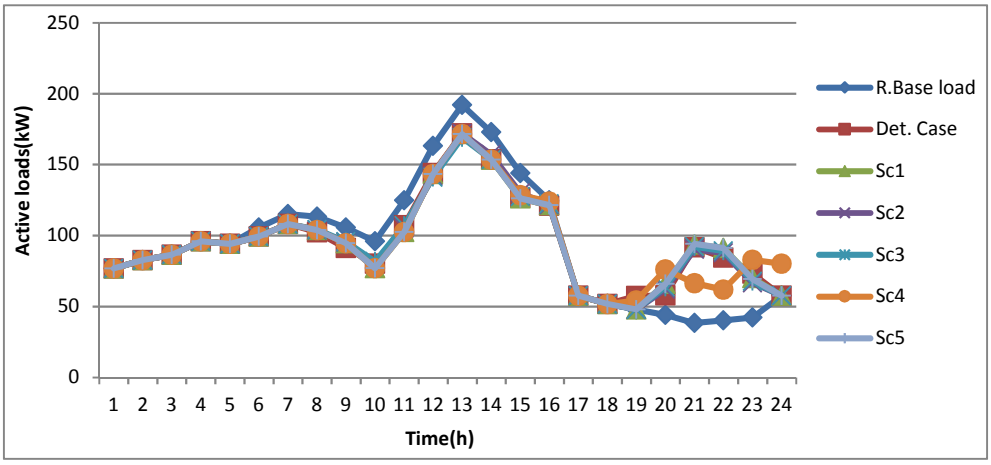

Figure 5-5 Active residential loads of the five highest probability scenarios and Det. Case of the isolated MG

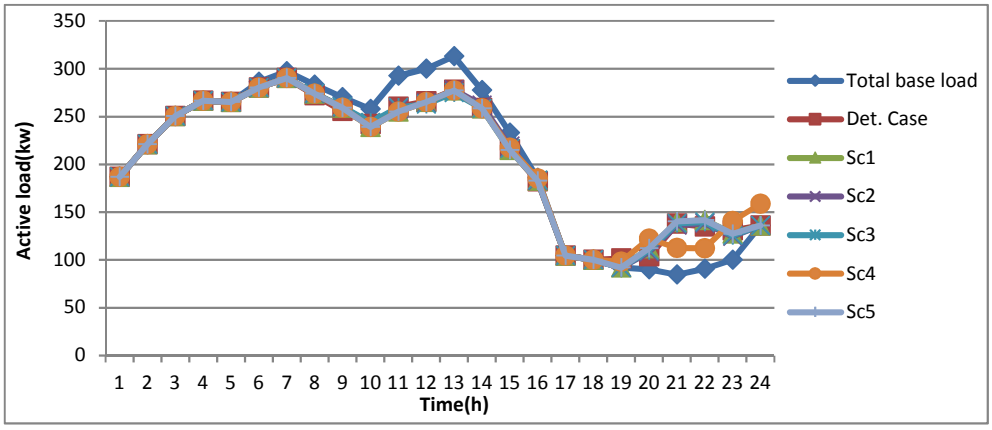

Figure 5-6 Active total loads of the five highest probability scenarios and Det. Case of the isolated MG

Figures 5-7 and 5-8 depict the optimal active and reactive power scheduling respectively. These figures and data in the Table 5-2 reveal that the DGs compensate the uncertainties for all the scenarios because there is no connection with the utility grid. The total reactive power generation of all the scenarios is equal because the DRGs generates only active power; however, they have different generation profiles because the uncertainties of the smart appliances. Further, the highest active power generation of the scenarios 1, 2, 3, and 5 is at hour 14 because they have the lowest renewable generation at this hour, while the highest generation in the Sc4 is at hour 12 because it has quite low wind and solar generation. The highest reactive power generation for all scenarios occurs at hour 7 because the RDGs supply only active power and the peak of the total load are displaced at hour 7. Furthermore, the Sc4 has the lowest active power generation at hour 24 because the wind generation has the maximum value at this hour, while other scenarios have zero wind generation at this hour. On the other hand, it can be seen that the reactive power generation at hours 21 and 22 for the scenarios 1, 2, 3, and 5 is higher than hours 23 and 24, although the base loads at hours 23 and 24 are higher than at hours 21 and 22. This is because the reactive recovered loads at hour 21 and 22 are higher than recovered loads at hours 23, where there is no recovered load at hour 24. While, for Sc4 is adverse because the recovered load at hour 23 and 24 is higher than recovered loads at hours 21 and 22.

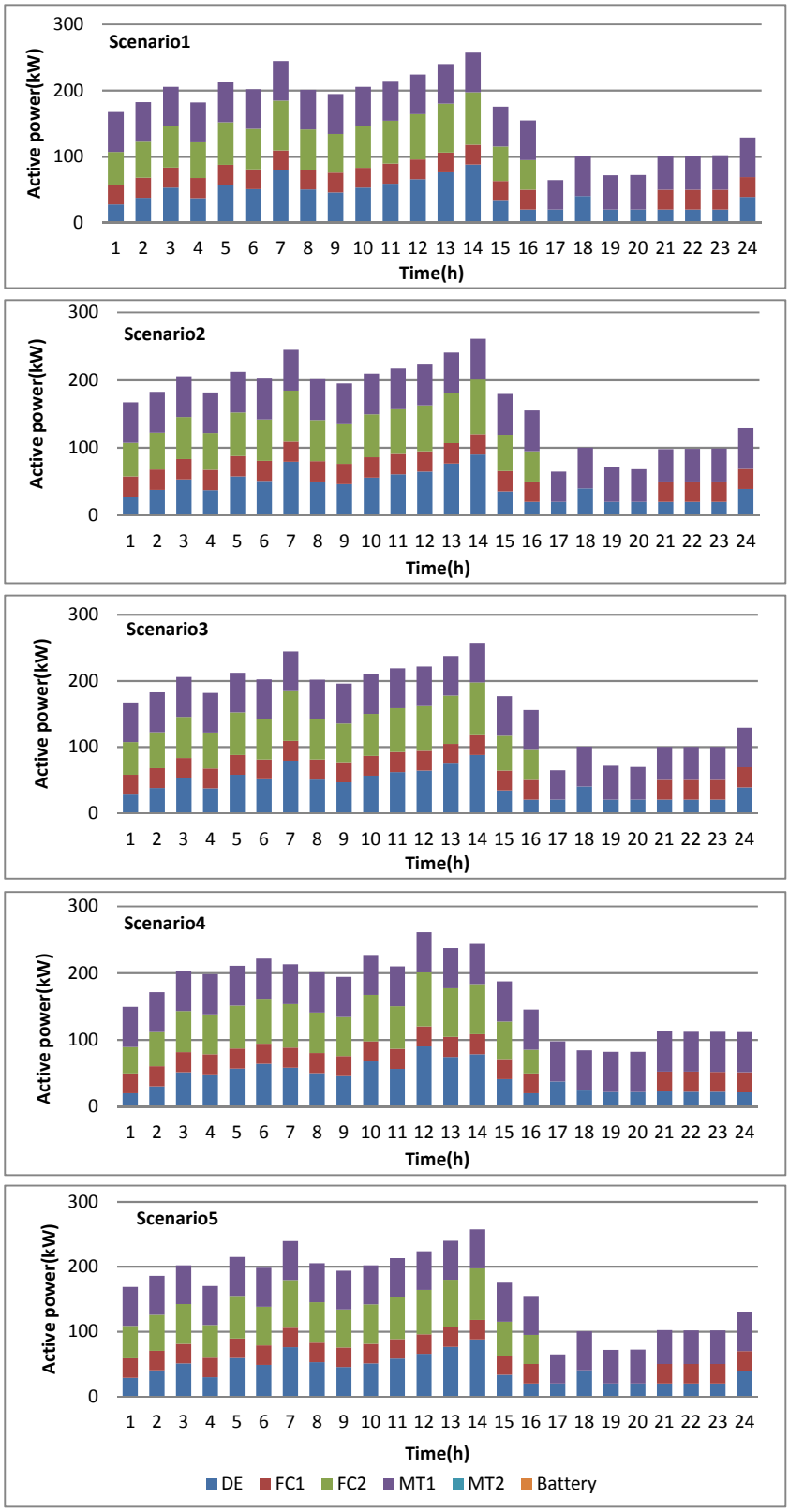

Figure 5-7 Optimal active power scheduling of the DGs of the five highest probability scenarios of the isolated MG

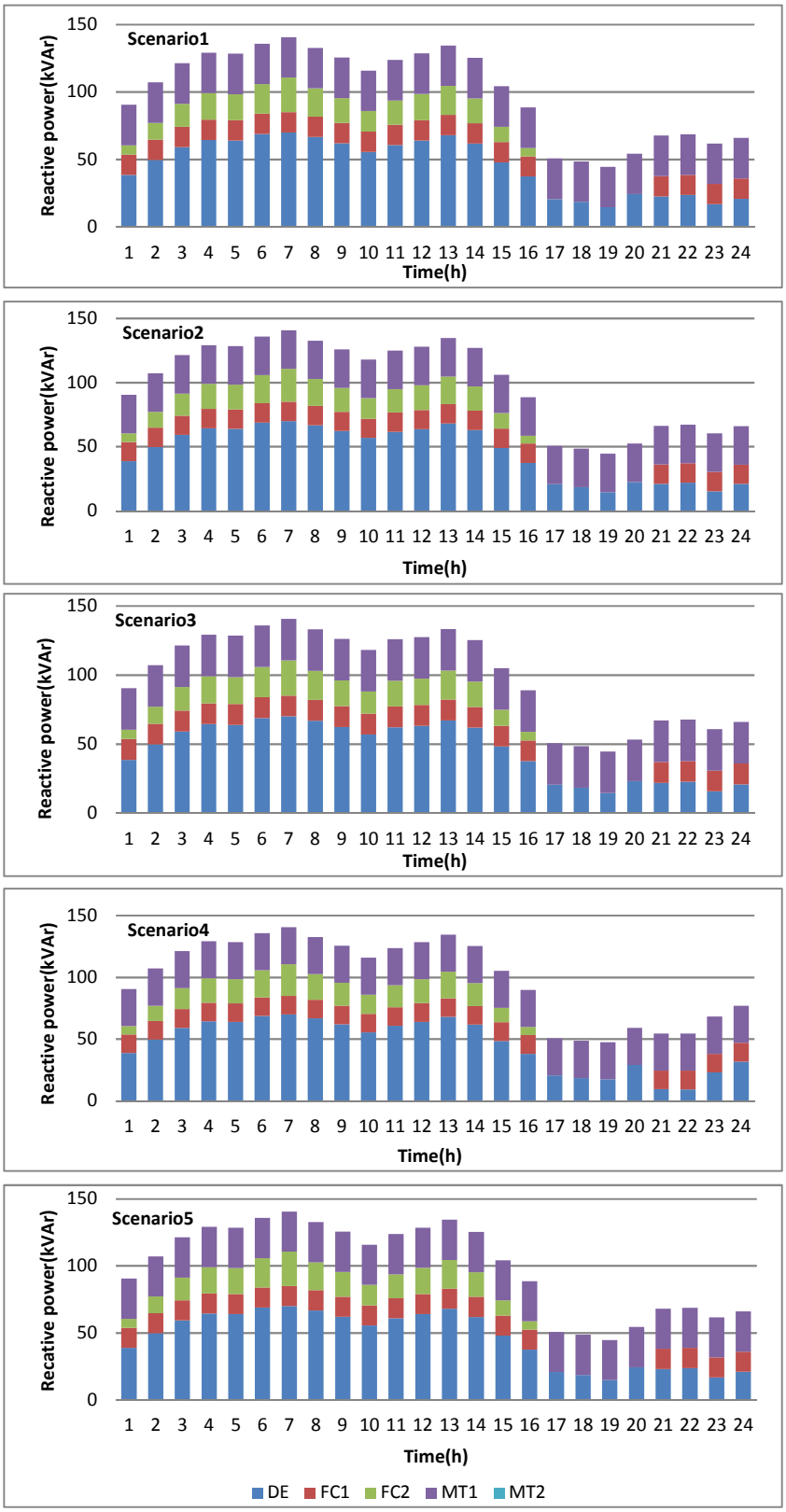

Figure 5-8 Optimal reactive power scheduling of the DGs of the five highest probability scenarios of the isolated MG

Table 5-2 Results of the five highest probability scenarios and Det. Case per scheduling day of the isolated MG

	Det. Case	Sc1	Sc2	Sc3	Sc4	Sc5
Total P_{DG} (kW)	4094.919	4005.094	4005.094	4005.094	4071.56	3989.723
Total Q_{DG} (kVAr)	2393.159	2393.159	2393.159	2393.159	2393.159	2393.159
Peak load reduction (kW)	35.1	35.535	34.965	38.025	35.535	35.535
Total cost (€)	538.7	537.8	538.4	538.1	537.8	537.6
No. WMs	82	76	75	75	76	76
No. DWs	66	74	63	68	70	74

5.5.2 Maximising the Profit of the MG

A. Connected MG

Figures 5-9 and 5-10 show the impacts of the uncertainties on the active residential and total loads of the five highest probability scenarios and Det. Case, where there is no cutting of industrial and commercial loads. It can be seen from these figures that the peak of the total and residential loads is not reduced for all scenarios for the same reason of the Det. Case.

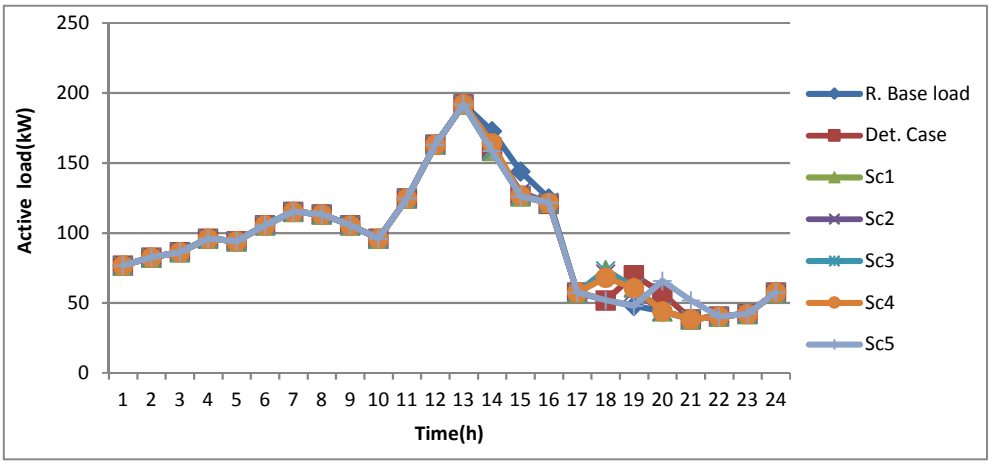

Figure 5-9 Active residential loads of the five highest probability scenarios and Det. Case of the connected MG

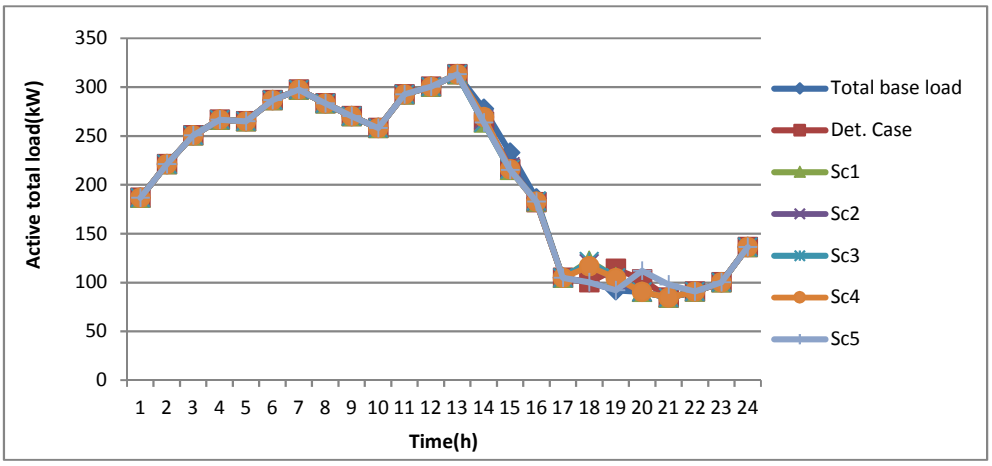

Figure 5-10 Active total loads of the five highest probability scenarios and Det. Case of the connected MG

Figures 5-11 and 5-12 depict the optimal active and reactive power scheduling. These figures show that in the Sc5 the MG at hour 20 purchases higher active and reactive power from the utility grid than other scenarios to satisfy the base and recovered loads because the recovered load has the highest value at this hour. In addition, the battery is charged with maximum power at hour 17 for all scenarios because the OMP has the lowest value of this hour and the battery is completed its charging at hours 20 or 21 depending on the renewable power availability and the recovered load because the OMPs are equal at these hours. Furthermore, at Sc4 the MG purchases lower active power than other scenarios at hour 24 because the wind generation has the maximum value at this hour in the Sc4.

Figure 5-12 reveals that all the scenarios have the same reactive power generation profiles because the uncertainties that come from the number of appliances are compensated from the utility grid and the renewable generations supply only active power.

Table 5-3 summarises the results of the five scenarios and Det. Case. This table reveals that the total generation of the reactive power are equal for all the scenarios because they have the same generation profile.

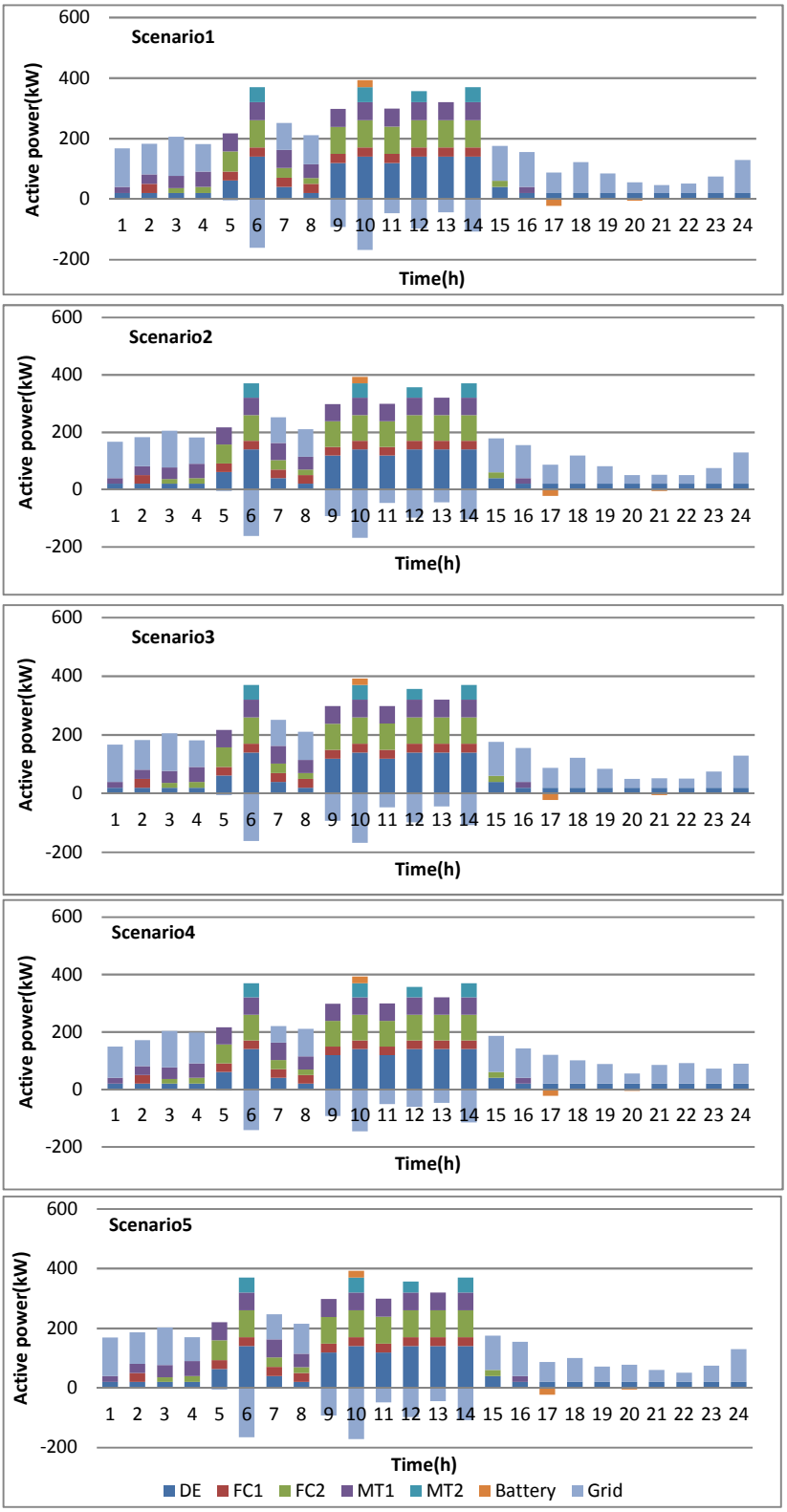

Figure 5-11 Optimal active power scheduling of the DGs of the five highest probability scenarios of the connected MG

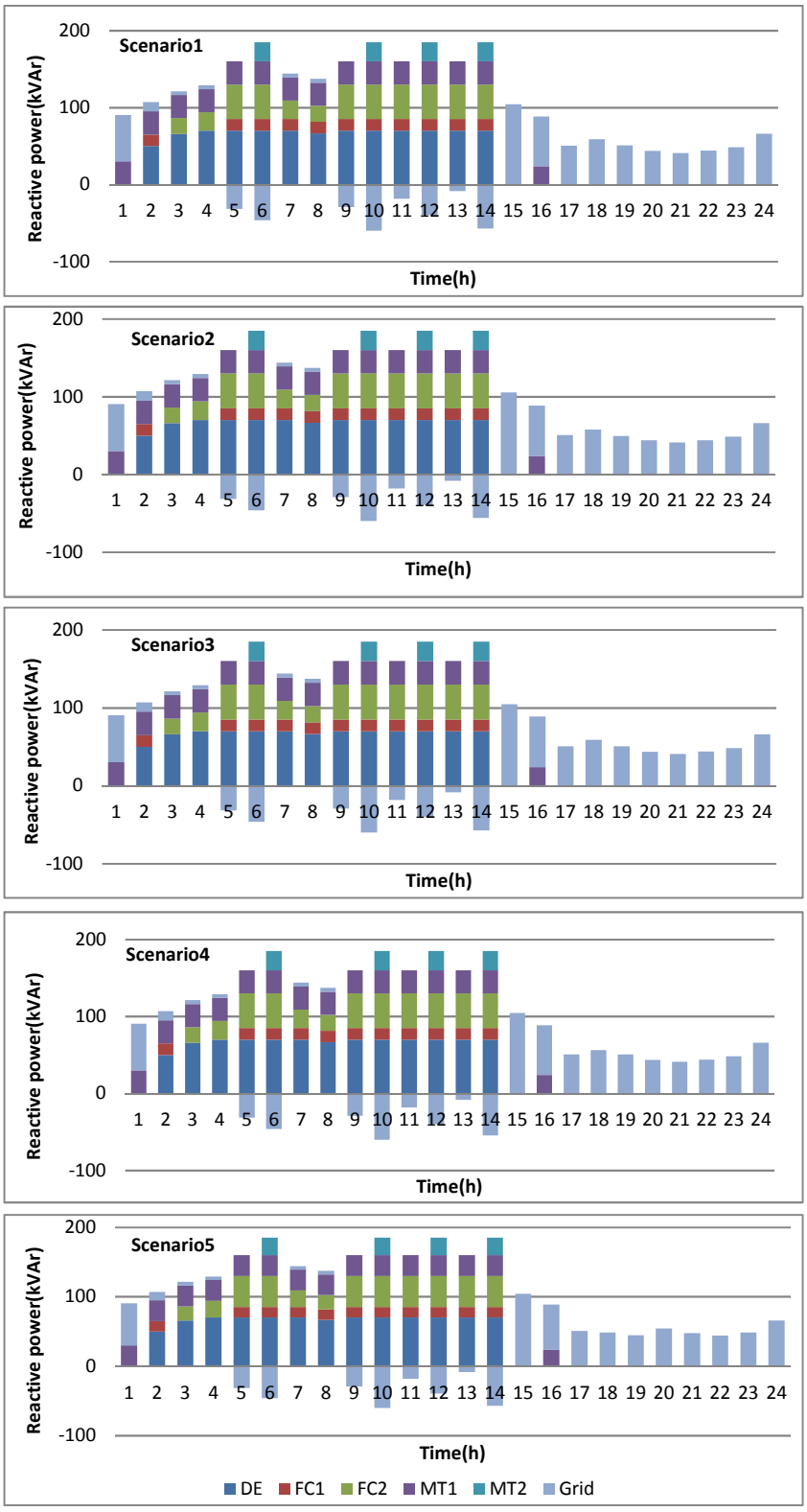

Figure 5-12 Optimal reactive power scheduling of the DGs of the five highest probability scenarios of the connected MG

Table 5-3 Results of the five highest probability scenarios and Det. Case per scheduling day of the connected MG

	Det. Case	Sc1	Sc2	Sc3	Sc4	Sc5
Total P_{DG} (kW)	3421.401	3425.856	3425.856	3425.856	3424.824	3428.556
Total Q_{DG} (kVAr)	2040.453	2040.453	2040.453	2040.453	2040.453	2040.453
Total P_{gb} (kW)	1407.482	1353.824	1350.974	1353.824	1357.438	1344.223
Total P_{gs} (kW)	683.687	724.308	721.458	724.308	660.425	732.779
Total Q_{gb} (kVAr)	665.004	665.178	663.798	665.178	662.534	665.178
Total Q_{gs} (kVAr)	290.504	290.679	289.298	290.679	288.034	290.679
Peak load reduction (kW)	0	0	0	0	0	0
Profit (€)	281.9	277.2	277.2	277.2	271.2	278.7
No. WMs	15	14	14	14	7	14
No. DWs	18	19	14	18	19	19

B. Isolated MG

Figures 5-13 and 5-14 show the impacts of the uncertainties on the active residential and total loads of the five highest probability scenarios and Det. Case, whereas the MG rejects the commercial and industrial loads cutting bids because the load cutting reduces the profit of the MG. These figures reveal that the recovered load of the Sc4 is different from other scenarios, where an amount of the shifted loads is recovered at hour 24 for the same reasons of the minimising the total cost.

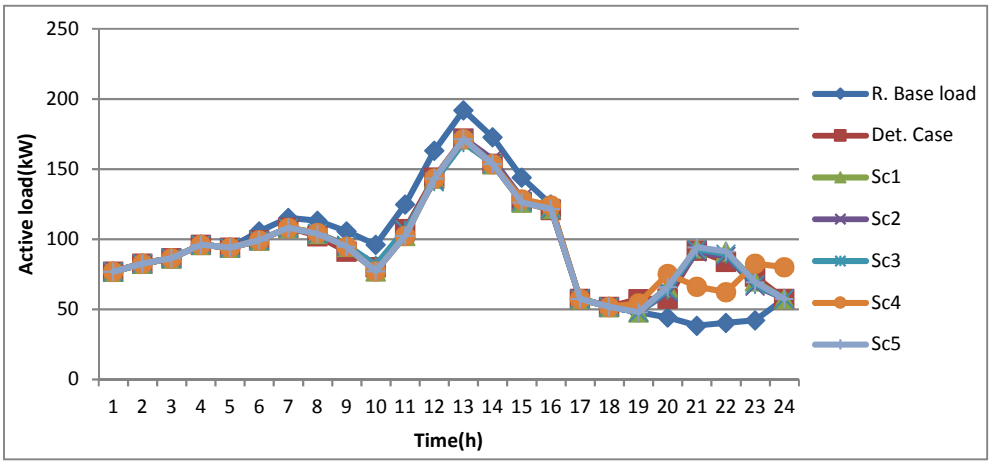

Figure 5-13 Active residential loads of the five highest probability scenarios and Det. Case of the isolated MG

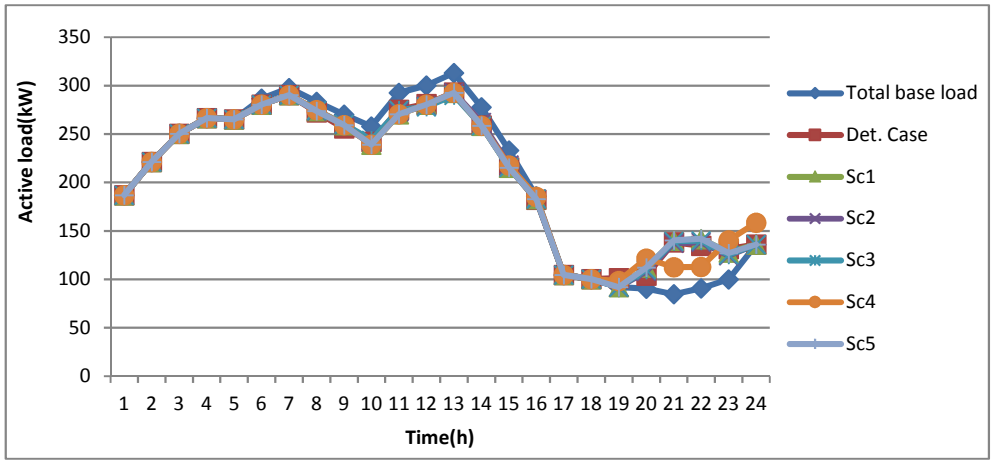

Figure 5-14 Active total loads of the five highest probability scenarios and Det. Case of the isolated MG

Figures 5-15 and 5-16 show the optimal active and reactive power scheduling. It can be observed that the storage battery is not operated during the entire scheduling horizon for all the scenarios because there is not economic incentive for operating the battery. In addition, the highest active power generation occurs at hour 14 for scenarios 1, 2, 3, and 5, while for Sc4 is at 12 for the same reason of the case of minimising the cost of the isolated MG. Further, the active power generation of the DGs at hour 18 in the scenarios 1, 2, 3, and 5 is higher than hour 17, although the active load at hour 17 higher than at hour 18. This is because the wind generation has the maximum value at hour 17 and solar generation is zero, while at hour 18 both the wind and solar generations have zero generation. Furthermore, in the Sc4 the active power generations of the DGs at hours 21, 22, and 23 are higher than other scenarios because the renewable generation at these hours is lower than other scenarios. Figure 5-16 reveals that the reactive power generation at hours 21 and 22 for Scenarios 1, 2, 3, and 5 are higher than hours 17 to 19, 23, and 24, although the reactive loads at hours 17 to 19, 23, and 24 are higher than 21 and 22. This is because the recovered loads at hours 21 and 22 have the highest values. Moreover, the reactive power generation at hour 24 for the Sc4 is higher than other scenarios because the load is recovered at hour 24, while the recovered load for other scenarios is equal to zero.

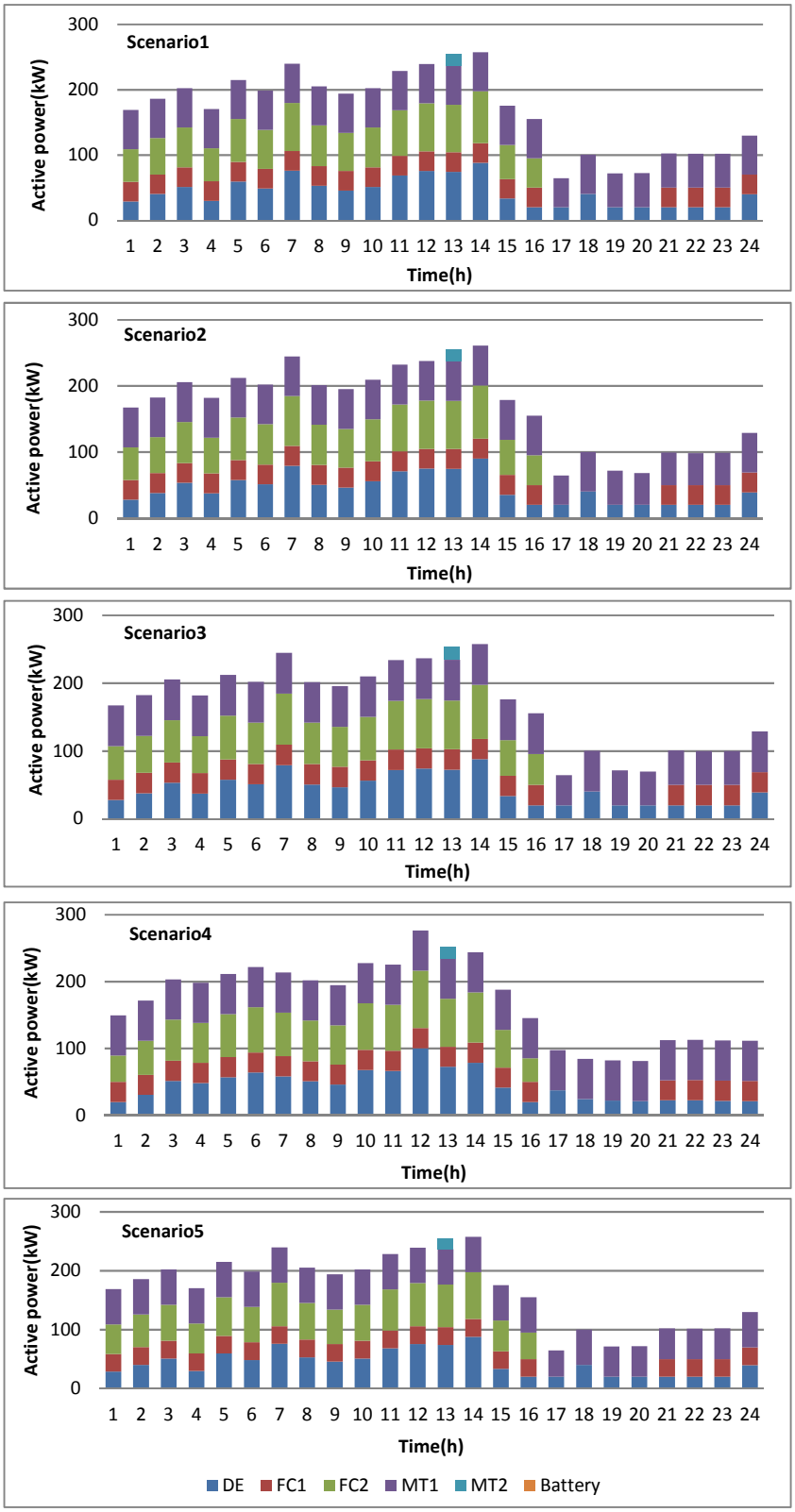

Figure 5-15 Optimal active power scheduling of the DGs of the five highest probability scenarios of the isolated MG

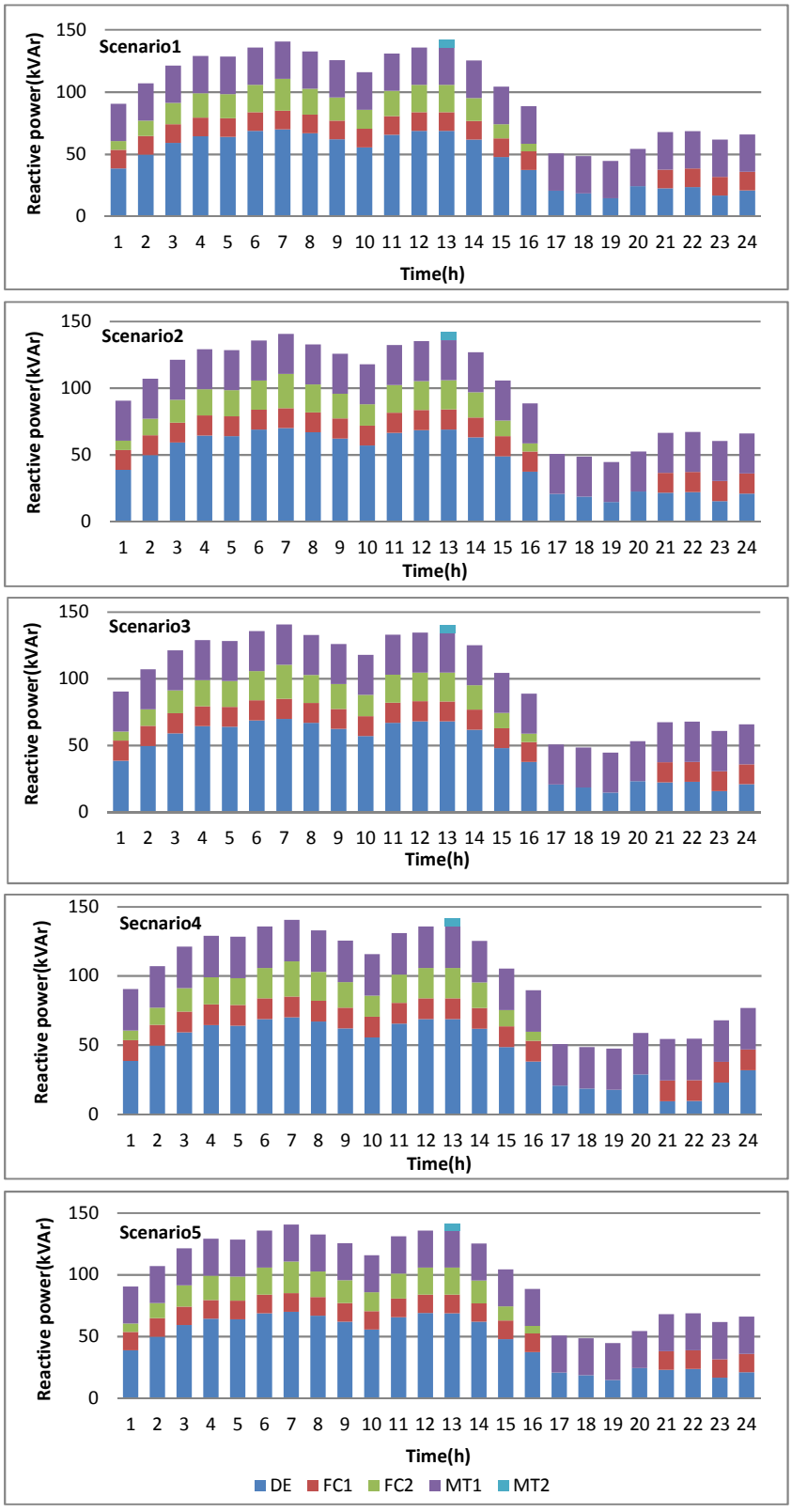

Figure 5-16 Optimal reactive power scheduling of the DGs of the five highest probability scenarios of the isolated MG

Table 5-4 reveals that the uncertainties are compensated by the changing the generation of the DGs because there is no connection with the utility grid. It also can be seen that the total reactive power generation for all scenarios are the same because the DRGs generate only active power, so solely the DGs supply the reactive load; however, they have different generation profiles.

Table 5-4 Results of the five highest probability scenarios and Det. Case per scheduling day of the isolated MG

	Det. Case	Sc1	Sc2	Sc3	Sc4	Sc5
Total P_{DG} (kW)	4139.919	4050.094	4050.094	4050.094	4116.560	4034.723
Total Q_{DG} (kVAr)	2414.952	2414.952	2414.952	2414.952	2414.952	2414.952
Peak load reduction (kW)	20.535	20.535	19.965	23.025	20.353	20.353
Profit (€)	243.9	244.7	244.3	244.5	244.7	245
No. WMs	82	76	76	76	75	76
No. DWs	66	74	63	68	70	74

5.6 Chapter Conclusions

The integration of the DSM with the two-stage stochastic optimisation of the connected and isolated MG to minimise the total operating cost or maximise the profit is analysed. The results show that the active and reactive OMPs have significant impacts on the shifted and recovered load for the connected MG. In addition, the stochastic generation of the RDGs affects the shifted and recovered loads for the isolated MG. Furthermore, the feasible solution is obtained for all scenarios for connected and isolated MG.

6 Dynamic Economic and Emission Dispatch of MG with Integration of Electric Vehicles

6.1 Chapter Summary

In this chapter, a novel multi-period SCUC-UARDEED with the bidirectional integration of the EVs and the environmental damage cost with a set of realistic constraints including security constraints is addressed. New scheduling strategy and optimisation approaches are proposed to formulate and solve the optimal scheduling with the integration of the EVs. The EVs with their constraints are modelled and incorporated with a novel SCUC-UARDEED two-stage scenario-based stochastic optimisation approach. The uncertainties related to the EVs behaviour and intermittence of the RDGs generation are considered as sources of uncertainties in this chapter. Multiple charging and discharging scenarios are conducted to analyse the impacts of the EVs on the optimal operation of the MG.

6.2 Electric Vehicles

The greenhouse gases have adverse impacts on the humans, environment, and natural resources. The electricity sector and transportation are the main sources of the emission of these gases [134]. Particularly, hybrid electric vehicles (HEVs) and pure electric vehicles (EVs) are the promising technology to reduce the emission of these greenhouse gases. However, the wider integration of the EVs may lead to negative impacts on the operation of the MG. Therefore, this integration should be controlled and managed to prevent the negative impacts on the operation of the MG.

The EVs in both types (HEVs) and (EVs) have many benefits for the MG operators, owners of the EVs and for the environment. For instance, the EVs are mobile storage devices, so it is transform surplus energy from one place to other. In addition, during working time the EVs are connected to the MG, therefore the EVs are saved the surplus energy when demand is low or discharge the stored energy when the demand is high. Further, the EVs are used as spinning reserve and regulation voltage and frequency because of its

bidirectional energy flow capabilities with grid [135], [136]. Furthermore, the EVs reduce the consumption of the oil and reduce the dependency on the oil. Generally, there are two ways to penetrate both EVs and HEVs with MGs either unidirectional power flow (charge mode as controllable load), (discharge mode as an energy source) or bidirectional energy flow (charging and discharging). The bidirectional integration of the EVs is considered in this thesis because its cover both the charging and discharging operation and it is more challenging than unidirectional.

6.3 Literature Review

The optimisation problem of the MG with the integration of the EVs was proposed in the previous works. Some of these works considered the integration of the EVs as V2G or G2V, and other considered the EVs as bidirectional. Reference [24] proposed a UC optimisation problem to reduce the cost and emission level of the conventional system with integration of EVs as V2G. it was found that the UC with EVs reduced operational cost and the emission level. Reference [26] presented an optimisation problem with EVs to minimise the cost and emission level for the system including renewable energy resources, the EVs were considered as bidirectional integration with the grid. The results of showed that the proposed integration of the EVs reduced the operating cost and emission level of greenhouse gases. Reference [137] addressed the optimisation problem of the distribution network to minimise the operating cost of the MG with the EVs as bidirectional integration. It was found that the integration of the aggregated EVs reduced the operating cost. In contrast, in [138], the mixed heat and electricity optimal scheduling of the connected and isolated MG with G2V integration are proposed. It was claimed that the charging of the EVs can manage to reduce the overall operation cost. Reference [139] presented a day-ahead EMS for a LV connected residential MG with the V2G and the aim of the optimisation problem was to minimise the operating cost. The results obtained demonstrated that the managing strategy reduced costs by 10 %. Reference [140] proposed EMS for low voltage MG which included PV, energy storage and V2G and G2V. It was found that the

proposed approach reduced the operation cost and improved the reliability of the system.

Reference [141] suggested the optimisation problem with integration of the EVs as G2V. Multi-charging regimes were conducted. The study showed that the off-peak charging was the best scenario in terms of using less fuel and releasing less emissions. It was pointed out in [142] that the UC optimisation problem of power system with the integration of the EVs and renewable energy resources. Multiple charging and discharging scenarios were conducted. The results showed that the off-peak charging and peak discharging reduced the economic cost significantly. Reference [143] presented an optimisation algorithm to minimise the operation cost and maximise the amount of the renewable energy resources by optimal scheduling of the DGs, the EVs and home appliances. It was found that controlling the EVs can result in penetration of 100 % renewable generation.

In contrast, some researchers proposed and formulated the optimisation problem with the integration of EVs to minimise the cost of charging of the EVs [144], [145] ,[146].

The above works formulated the optimisation problems with penetration of the EVs under the deterministic environment, while many researchers proposed the integration of EVs with an optimisation problem under stochastic environments. Reference [46] presented the stochastic UC optimisation problem of the power system with the integration of the EVs as bidirectional. The results revealed that the EVs reduced the operation cost. Reference [95] addressed a two-stage stochastic UC optimisation problem in the power system with the integration of EVs and large scale wind energy to minimise the operating cost, the fluctuation of the WT generation, and the EVs loads were taken as sources of uncertainties. The results demonstrated that the smart charging reduced the operating cost. Reference [147] proposed an optimal stochastic day-ahead EMS of a small electric system with the EVs and renewable energy resources. The EMS took into consideration the uncertainties that derived from the wind

generation and the number of the EVs as sources of the uncertainties, while it was established in [148] that a stochastic optimisation problem of the MG as office block with penetration of the EVs. The aim of the optimisation problem was to minimise the operating cost. The uncertainties evolved from the PV generation, load forecast, OMP, and the driven distance of the EVs were incorporated with the objective function. The results showed that the optimal integration of the EVs reduced the total cost.

In [75], the economic dispatch of the distribution system with the EVs as an uncertainty source is addressed. The uncertainties resulted from the integration of the EVs, such as charging time, initial battery state of charge and start/end time were considered as sources of uncertainties. It was found that the constrained charging had the lowest operating cost. Reference [149] a stochastic optimal scheduling of both the EVs and home appliances within MG to reduce the price of electricity to the consumer was pointed out. The fluctuations of the renewable generation and the arrival time of EVs to the MG were considered as stochastic variables in the optimisation algorithm. A stochastic multi-objective dynamic economic dispatch of the MG with consideration of the EVs was addressed in [150]. The daily mileage of EVs and the charging start time were adopted as stochastic variables. The results showed that the greater the load uncertainty the higher the operating cost. Reference [151] presented a two-stage stochastic EMS for commercial building with integration of the EVs, the uncertainties that resulted from PV generation, load forecasts and the number of the EVs were considered as sources of uncertainties. The results revealed that a moderate number of the EVs helped to reduce the overall operating cost. In [152], a scenario-based stochastic optimal scheduling to minimise the operating cost and enhance the reliability of reconfigurable of MG with integration of EVs was presented. It was claimed that penetration the EVs as V2G reduced the MG operating cost. Reference [153] proposed a two-stage stochastic simultaneous optimal scheduling of EVs and responsive load to reduce the operating cost and emission of the MG. The

fluctuations of WT and PV power generation were considered as stochastic variables. The proposed scheduling reduced the operation cost.

All the above papers presented the optimisation problem under deterministic and stochastic environments to minimise the operating cost or minimise the operating cost and emission level solely, while quite a few researchers addressed the maximising of the profit with integration of the EVs to the connected MG. Reference [154] presented a day-ahead probabilistic optimal operation of the MG to maximise the total profit of the MG and to investigate the impacts of the integration of the EVs on the economic operation of the MG. The load forecast error, wind generation fluctuation, and EVs were considered as source of uncertainties. It was concluded that the stochastic results outperformed of deterministic one.

The above literature review reveals that the majority of researchers focused on either the grid performance or preferences of the owners, while the proposed optimisation approach in this work considers both of them. It appears there is no study on the unified active and reactive power scheduling with consideration the integration of the EVs and other cost components in Chapter 2 and aims to minimise the total operating cost or maximise the profit and is subjected to a set of constraint in Chapter 2 and 6. In contrast, there is no publication on the maximising the isolated MG profit with the integration of the EVs under stochastic or deterministic optimisation. Furthermore, with regard to maximising the profit, there appears to be no study of the stochastic optimisation of the MG in the two-stage stochastic approach for connected or isolated MG.

6.4 Proposed Model of Electric Vehicles

The EVs are modelled as a storage battery in the economic operation of the power system and the focus is predominantly on the optimal scheduling of the exchanging power with grid in case of bidirectional integration. The modelling of the EV battery is as follows:

when the EV is charging G2V at hour t

$$E_{EV}(t) = E_{EV}(t-1) + P_{EVch}(t).\eta_{EVch}.\Delta t \quad \textbf{(6.1)}$$

when the EV is discharging V2G at hour t

$$E_{EV}(t) = E_{EV}(t-1) - (\frac{P_{EVdis}(t)}{\eta_{EVdis}}).\Delta t \quad \textbf{(6.2)}$$

when the EV is in bidirectional operation mode V2G and G2V, the energy exchange at hour t as:

$$E_{EV}(t) = E_{EV}(t-1) + P_{EVch}(t).\eta_{EVch}.\Delta t - (\frac{P_{EVdis}(t)}{\eta_{EVdis}}).\Delta t \quad \textbf{(6.3)}$$

where $E_{EV}(t)$, $E_{EV}(t-1)$ are the state charge of the battery at current and previous state respectively, $P_{EVch}(t)$, $P_{EVdis}(t)$ are the battery charging and discharging power respectively. η_{EVch}, η_{EVdis} are the corresponding charging and discharging efficiencies, Δt is the sampling time.

The following equations are used to determine the consumption energy by EV during the trip when it is driven.

$$E_{EV}(t) = E_{EV}(t-1) - E_{EV}^{Trip}(t) \quad \textbf{(6.4)}$$

$$E_{EV}^{Trip}(t) = C.D(t) \quad \textbf{(6.5)}$$

where $E_{EV}^{Trip}(t)$ is the energy consumption during the trip by EV at period t, C is the driving consumption energy per km, and $D(t)$ is the driving distance of the EV at hour t.

6.5 Proposed Electric Vehicle Operation Constraints

6.5.1 State of Charge Constraints

The state of charge should keep between maximum and minimum values when the battery operates. This constraint is represented in this equation

$$E_{EVmin} \leq E_{EV}(t) \leq E_{EVmax} \quad \textbf{(6.6)}$$

where E_{EVmax} and E_{EVmin} are the maximum and minimum values of the battery state of charge.

6.5.2 Charging and Discharging Power Constraints

To prevent the simultaneous charging and discharging operations of batteries of the EVs at each time interval two binary variables, $\delta_{EVch}(t) \in \{0,1\}$ and $\delta_{EVdis}(t) \in \{0,1\}$, are assigned to formulate the status of battery operation and $\delta_{EVch}(t) + \delta_{EVdis}(t) \leq 1$ is set to prevent the battery of the EV charging and discharging simultaneously during the optimisation. The charging and discharging power is performed at the maximum power that the charger provides. These constraints for the EVs are accordingly formulated as

$$\delta_{EVch}(t).P_{EVchmin} \leq P_{EVch}(t) \leq \delta_{EVch}.P_{EVchmax} \quad \textbf{(6.7)}$$

$$\delta_{EVdis}(t).P_{EVdismin} \leq P_{EVdis}(t) \leq \delta_{EVdis}.P_{EVcdismax} \quad \textbf{(6.8)}$$

where $P_{EVchmin}$ and $P_{EVdismin}$ are the minimum charging and discharging power of the charger respectively, $P_{EVchmax}$ and $P_{EVdismax}$ are the respective maximum charging and discharging power of the charger. $\delta_{EVch}(t)$ and $\delta_{EVdis}(t)$ are binary variables to prevent simultaneous charging and discharging operations.

6.5.3 The Owner of the EV Requirements

The economic integration of the EVs with MG should satisfy the needs of the owner of the EV as well. The minimum stored energy of the batteries of the EVs at last period when the EVs disconnected from grid should be higher than the energy required for the next trip of the owner of the vehicles. This constraint is formulated as

$$E_{EV}(t_{last}) \geq E_{EV}^{Trip,q1}(t) \quad \textbf{(6.9)}$$

where t_{last} is the last connected time of the EV with grid before start $q1$ trip, $E_{EV}^{Trip,q1}(t)$ is the required energy for the EV $q1$ trip.

6.6 Model of the Cost of the Integration of the EVs with the MG

The MG under study includes three different loads areas, namely: residential, industrial and commercial, wherein the EVs are connected to the MG at different areas and times, where the cost of the bidirectional integration of the EVs as follows:

The cost of the EVs that are connected to the residential area

$$C_{EV}^{Res}(t) = \sum_{t=1}^{T} N_{EV}^{Res}(t)\{c_{EVdis}(t).P_{EVdis}^{Res}(t) - c_{EVch}(t).P_{EVch}^{Res}(t)\}.\Delta t \quad \textbf{(6.10)}$$

The cost of the EVs that are connected to the industrial area

$$C_{EV}^{Ind}(t) = \sum_{t=1}^{T} N_{EV}^{Ind}(t)\{c_{EVdis}(t).P_{EVdis}^{Ind}(t) - c_{EVch}(t).P_{EVch}^{Ind}(t)\}.\Delta t \quad \textbf{(6.11)}$$

The EVs that are connected to the commercial area

$$C_{EV}^{Com}(t) = \sum_{t=1}^{T} N_{EV}^{Com}(t)\{c_{EVdis}(t).P_{EVdis}^{Com}(t) - c_{EVch}(t).P_{EVch}^{Com}(t)\}.\Delta t \quad \textbf{(6.12)}$$

where $c_{EVch}(t)$, $c_{EVdis}(t)$ are the prices of charging and discharging of the EVs in (€/kWh) respectively. $N_{EV}^{Res}(t)$, $N_{EV}^{Ind}(t)$, and $N_{EV}^{Com}(t)$ are the number of the EVs that are connected to the residential, industrial, and commercial areas respectively. P_{EVdis}^{Res}, P_{EVdis}^{Ind}, and P_{EVdis}^{Com} are the discharging power of the EVs in the residential, industrial and commercial areas respectively. P_{EVch}^{Res}, P_{EVch}^{Ind}, and P_{EVch}^{Com} are the charging power of the EVs in the residential, industrial and commercial areas respectively.

The discharging price $c_{EVdis}(t)$ determines the economic discharging operations of the EVs. It represents the kWh cost to the V2G battery owner for delivering power to the grid and it can be calculated by using the following equation [74]

$$c_{EVdis} = \frac{c_{EVch}}{\eta_{EVch}} + C_{EVd} = \frac{c_{EVch}}{\eta_{EVch}} + \frac{C_{EVb}}{L_c.E_{EV}.DOD} \quad \textbf{(6.13)}$$

where C_{EVd} is the battery degradation cost, C_{EVb} is the battery capital cost (€), L_c is the battery cycle life, E_{EV} is the rated energy capacity of the battery (kWh).

6.7 Proposed UC Optimal Operation of the MG with Integration of the EVs

The proposed SCUC-UARDEED of the connected and isolated MG with the integration of the EVs is formulated either to minimise the total operating cost or to maximise the profit of the MG. Two objective functions are proposed and developed for the connected and isolated MG and they are formulated as:

6.7.1 Proposed Objective Functions to Minimise the Total Operating Cost

The aim of this policy is to minimise the total operating cost of the connected and isolated MG with consideration the charging and discharging scheduling of the EVs.

A. Connected MG

The optimisation problem is formulated as

$$\min(F) \tag{6.14}$$

where the objective function F is

$$F = \sum_{t=1}^{T}\{\sum_{i=1}^{N}[[CP_{DG_i}(P_{DG_i}(t)) + CQ_{DG_i}(Q_{DG_i}(t)) + COM_{DG_i}(P_{DG_i}(t))]\delta_{DG_i}(t) + SU_{DG_i}(t) + SD_{DG_i}(t)] + C_e(P_{DG_i}(t)) + C_{bo}(t) + C_{gP}(t) + C_{gQ}(t) + \sum_{i1=1}^{N1} CP_{Wi1}(P_{Wi1}(t)) + \sum_{i2=1}^{N2} CP_{PVi2}(P_{PVi2}(t)) + C_{EV}^{Res}(t) + C_{EV}^{Ind}(t) + C_{EV}^{Com}(t) + c_{EVcut}.P_{EVcut}^{Res}(t).\Delta t + c_{EVcut}.P_{EVcut}^{Ind}(t).\Delta t + c_{EVcut}.P_{EVcut}^{Com}(t).\Delta t\} \tag{6.15}$$

where c_{EVcut} in (€/kWh) is the price of unserved the EVs charging power, $P_{EVcut}^{Res}(t)$, $P_{EVcut}^{Ind}(t)$, and $P_{EVcut}^{Com}(t)$ are unserved power to the EVs in the residential, industrial and commercial areas.

This objective function is constructed using equations

(2.1), (2.2), (2.3), (2.15), (2.16), (2.14), (2.11), (2.12), (2.13), (2.5), (2.6), (6.10), (6.11), (6.12), and the last three components which represents the cost of

unserved charging power to the EVs in the residential, industrial, and commercial areas.

B. Isolated MG

The optimisation problem is formulated as

$$\min(F) \tag{6.16}$$

where the objective function F is

$$F = \sum_{t=1}^{T}\{\sum_{i=1}^{N}[[CP_{DG_i}(P_{DG_i}(t)) + CQ_{DG_i}(Q_{DG_i}(t)) + COM_{DG_i}(P_{DG_i}(t))]\delta_{DG_i}(t) + SU_{DG_i}(t) + SD_{DG_i}(t)] + C_e(P_{DG_i}(t)) + C_{bo} + \sum_{i1=1}^{N1} CP_{Wi1}(P_{Wi1}(t)) + \sum_{i2=1}^{N2} CP_{PVi2}(P_{PVi2}(t)) + C_{EV}^{Res}(t) + C_{EV}^{Ind}(t) + C_{EV}^{Com}(t) + c_{EVcut}.P_{EVcut}^{Res}(t).\Delta t + c_{EVcut}.P_{EVcut}^{Ind}(t).\Delta t + c_{EVcut}.P_{EVcut}^{Com}(t).\Delta t\} \tag{6.17}$$

This is constructed using equations

(2.1), (2.2), (2.3), (2.15), (2.16), (2.14), (2.11), (2.5), (2.6), (6.10), (6.11), (6.12), and the last three components which represents the cost of unserved charging power to the EVs in the residential, industrial, and commercial areas.

6.7.2 Proposed Objective Functions to Maximise the MG Profit

For the connected MG, the MG sells the electricity to the consumers by the OMPs. Similarly, the MG sells and purchases electricity to/from the utility grid by OMP. The MG purchases the energy from the EVs by discharging price (c_{EVch}) and sells this energy to the consumers by the OMP. However, the MG sells the energy to the EVs by the charging price (c_{EVch}). For the isolated MG, the MG sells the electricity to the consumers with fixed price, while it sells the electricity to the EVs by the charging price and purchases the energy from the EVs by the discharging price.

A. Connected MG

The optimisation problem is formulated as

$$\max(F) \tag{6.18}$$

where

$$F = (Revenue - Expense) \tag{6.19}$$

where revenue is calculated as

$$\begin{aligned} Revenue = \sum_{t=1}^{T}\{\sum_{i=1}^{N}\left[c_{gP}(t).P_{DG_i}(t) + c_{gQ}(t).Q_{DG_i}(t)\right]\delta_{DGi}(t) + \\ c_{gP}(t).P_{bdis}(t).\Delta t + c_{gP}(t).\sum_{i2=1}^{N2}P_{PV_{i2}}(t) + c_{gP}(t).\sum_{i1=1}^{N1}P_{W_{i1}}(t) + \\ c_{gP}(t).P_{gp}(t) + c_{gQ}(t).Q_{gp}(t) + c_{gP}(t).[N_{EV}^{Res}(t).P_{EVdis}^{Res}(t) + \\ N_{EV}^{Ind}(t).P_{EVdis}^{Ind}(t) + N_{E}^{Com}(t).P_{EVdis}^{Com}(t)].\Delta t\} \end{aligned} \tag{6.20}$$

and expense is formulated as

$$\begin{aligned} Expense = \sum_{t=1}^{T}\{\sum_{i=1}^{N}[[CP_{DG_i}(P_{DG_i}(t)) + CQ_{DG_i}(Q_{DG_i}(t)) + \\ COM_{DG_i}(P_{DG_i}(t))]\delta_{DG_i}(t) + SU_{DG_i}(t) + SD_{DG_i}(t)] + C_e(P_{DG_i}(t)) + C_{bo}(t) + \\ c_{gP}.P_{bch}(t).\Delta t + c_{gP}(t).P_{gp}(t) + c_{gQ}(t).Q_{gp}(t) + \sum_{i1=1}^{N1}CP_{Wi1}(P_{Wi1}(t)) + \\ \sum_{i2=1}^{N2}CP_{PVi2}(P_{PVi2}(t)) + c_{EVcut}.P_{EVcut}^{Res}(t).\Delta t + c_{EVcut}.P_{EVcut}^{Ind}(t).\Delta t + \\ c_{EVcut}.P_{EVcut}^{Com}(t).\Delta t + c_{EVdis}.[N_{EV}^{Res}(t).P_{EVdis}^{Res}(t) + N_{EV}^{Ind}(t).P_{EVdis}^{Ind}(t) + \\ N_{EV}^{Com}(t).P_{EVdis}^{Com}(t)].\Delta t + (c_{gP}(t) - c_{EVch}).[N_{EV}^{Res}(t).P_{EVch}^{Res}(t) + \\ N_{EV}^{Ind}(t).P_{EVch}^{Ind}(t) + N_{EV}^{Com}(t).P_{EVch}^{Com}(t)].\Delta t\} \end{aligned} \tag{6.21}$$

giving

$$\begin{aligned} F = \sum_{t=1}^{T}\{\sum_{i=1}^{N}[c_{gP}(t).P_{DG_i}(t) + c_{gQ}(t).Q_{DG_i}(t)]\delta_{DG_i}(t) + \\ c_{gP}(t).P_{bdis}(t).\Delta t + c_{gP}(t).\sum_{i2=1}^{N2}P_{PV_{i2}}(t) + c_{gP}(t).\sum_{i1=1}^{N1}P_{W_{i1}}(t) + \\ c_{gP}(t).[N_{EV}^{Res}(t).P_{EVdis}^{Res}(t) + N_{EV}^{Ind}(t).P_{EVdis}^{Ind}(t) + N_{EV}^{Com}(t).P_{EVdis}^{Com}(t)].\Delta t\} - \\ \sum_{t=1}^{T}\{\sum_{i=1}^{N}[[CP_{DG_i}(P_{DG_i}(t)) + CQ_{DG_i}(Q_{DG_i}(t)) + COM_{DG_i}(P_{DG_i}(t))]\delta_{DG_i}(t) + \\ SU_{DG_i}(t) + SD_{DG_i}(t)] + C_e(P_{DG_i}(t)) + C_{bo} + c_{gP}.P_{bch}(t).\Delta t + \\ \sum_{i1=1}^{N1}CP_{Wi1}(P_{Wi1}(t)) + \sum_{i2=1}^{N2}CP_{PVi2}(P_{PVi2}(t)) + c_{EVcut}.P_{EVcut}^{Res}(t).\Delta t + \\ c_{EVcut}.P_{EVcut}^{Ind}(t).\Delta t + c_{EVcut}.P_{EVcut}^{Com}(t).\Delta t + c_{EVdis}.[N_{EV}^{Res}(t).P_{EVdis}^{Res}(t) + \\ N_{EV}^{Ind}(t).P_{EVdis}^{Ind}(t) + N_{EV}^{Com}(t).P_{EVdis}^{Com}(t)].\Delta t + (c_{gP}(t) - \\ c_{EVch}).[N_{EV}^{Res}(t).P_{EVch}^{Res}(t) + N_{EV}^{Ind}(t).P_{EVch}^{Ind}(t) + N_{EV}^{Com}(t).P_{EVch}^{Com}(t)].\Delta t\} \end{aligned} \tag{6.22}$$

The revenue of the MG comes from selling the active power from the DGs, the discharging power of the battery, the power from the RDGs, discharging power of the EVs. The cost is constructed using equations

(2.1), (2.3), (2.15), (2.16), (2.14), (2.11), (2.5), (2.6), the cost of charging the battery, the cost of unserved charging power to the EVs in the residential, industrial, and commercial areas, the cost of buying power from the EVs.

B. Isolated MG

The optimisation problem is formulated as

$$\max(F) \tag{6.23}$$

where the objective function F is

$$\begin{aligned} F = {} & \sum_{t=1}^{T}\{\sum_{i=1}^{N}[c_{isoP}(t).P_{DG_i}(t) + c_{isoQ}(t).Q_{DG_i}(t)]\delta_{DG_i}(t) + \\ & c_{isoP}(t).P_{bdis}(t).\Delta t + c_{isoP}(t).\sum_{i2=1}^{N2}P_{PV_{i2}}(t) + c_{isoP}(t).\sum_{i1=1}^{N1}P_{W_{i1}}(t) + \\ & c_{isoP}(t).[N_{EV}^{Res}(t).P_{EVdis}^{Res}(t) + N_{EV}^{Ind}(t).P_{EVdis}^{Ind}(t) + N_{EV}^{Com}(t).P_{EVdis}^{Com}(t)].\Delta t\} - \\ & \sum_{t=1}^{T}\{\sum_{i=1}^{N}[[CP_{DG_i}(P_{DG_i}(t)) + CQ_{DG_i}(Q_{DG_i}(t)) + COM_{DG_i}(P_{DG_i}(t))]\delta_{DG_i}(t) + \\ & SU_{DG_i}(t) + SD_{DG_i}(t)] + C_e(P_{DG_i}(t)) + C_{bo} + c_{isoP}.P_{bch}(t).\Delta t + \\ & \sum_{i1=1}^{N1}CP_{Wi1}(P_{Wi1}(t)) + \sum_{i2=1}^{N2}CP_{PVi2}(P_{PVi2}(t)) + c_{EVcut}.P_{EVcut}^{Res}(t).\Delta t + \\ & c_{EVcut}.P_{EVcut}^{Ind}(t).\Delta t + c_{EVcut}.P_{EVcut}^{Com}(t).\Delta t + c_{EVdis}.[N_{EV}^{Res}(t).P_{EVdis}^{Res}(t) + \\ & N_{EV}^{Ind}(t).P_{EVdis}^{Ind}(t) + N_{EV}^{Com}(t).P_{EVdis}^{Com}(t)].\Delta t + (c_{isoP}(t) - \\ & c_{EVch}).[N_{EV}^{Res}(t).P_{EVch}^{Res}(t) + N_{EV}^{Ind}(t).P_{EVch}^{Ind}(t) + N_{EV}^{Com}(t).P_{EVch}^{Com}(t)].\Delta t\} \end{aligned} \tag{6.24}$$

The revenue of the MG comes from selling the active power from the DGs, the discharging power of the battery, the power from the RDGs, discharging power of the EVs. The cost is constructed using equations

(2.1), (2.3), (2.15), (2.16), (2.14), (2.11), (2.5), (2.6), the cost of charging the battery, the cost of unserved charging power to the EVs in the residential, industrial, and commercial areas, the cost of buying power from the EVs.

The objective functions of equations (6.15) and (6.22) are subjected to the constraints of equations (2.17) to (2.35), whereas the objective functions of

equations (6.17) and (6.24) are subjected to the constraints of equations (2.17) to (2.25), (2.30) to (2.33), (2.36), and (2.37). These objective functions are subjected to the constraints of equations (6.6) to (6.9), and 6.26. However, the constraint of the equation (2.17) is modified to involve the EVs as in the following equations:

$$\sum_{t=1}^{T}\{\sum_{i=1}^{N}\delta_{DG_i}(t).P_{DG_i}(t)+\sum_{i1=1}^{N1}P_{W_{i1}}(t)+\sum_{i2=1}^{N2}P_{PV_{i2}}(t)+P_b(t)+ \quad \textbf{(6.25)}$$
$$P_g(t)+N_{EV}^{Res}(t).P_{EVdis}^{Res}(t)+N_{EV}^{Ind}(t).P_{EVdis}^{Ind}(t)+$$
$$N_{EV}^{Com}(t).P_{EVdis}^{Com}(t)=(P_{Dres}(t)+N_{EV}^{Res}(t).P_{EVch}^{Res}(t)-P_{EVcut}^{Res}(t))+$$
$$(P_{Dind}(t)+N_{EV}^{Ind}(t).P_{EVch}^{Ind}(t)-P_{EVcut}^{Ind}(t))+(P_{Dcom}(t)+$$
$$N_{EV}^{Com}(t).P_{EVch}^{Com}(t)-P_{EVcut}^{Com}(t))\}$$

For the isolated MG the same above equation is used with $P_g(t)=0$. The reactive power balance constraints do not change because the EVs provide active power solely.

To prevent the total load of the system from increasing higher than the grid capacity, this constraint is incorporated with optimisation approach and it is formulated as follows:

$$\sum_{t=1}^{T}\{P_{bch}(t)+(P_{Dres}(t)+N_{EV}^{Res}(t).P_{EVch}^{Res}(t)-P_{EVcut}^{Res}(t))+(P_{Dind}(t)+ \quad \textbf{(6.26)}$$
$$N_{EV}^{Ind}(t).P_{EVch}^{Ind}(t)-P_{EVcut}^{Ind}(t))+(P_{Dcom}(t)+N_{EV}^{Com}(t).P_{EVch}^{Com}(t)-$$
$$P_{EVcut}^{Com}(t))\leq S_{sys}.cos\theta\}$$

where S_{sys} is the rated kVA of the grid.

6.8 Electric Vehicles Parameters

The EVs being off road 90%-95% of the time [98], [155] and they can be connected to the MG at any area. The arriving time of the EVs to the MG, the driving distance, and the number of the EVs connected to the MG at each time interval are different and depend on the area where the EVs are connected. The EV that is driven 10 miles needs 2.8 kWh [95], [156], [157]. The approximate number of the drivers arriving their homes and works from the final trip of the residential and commercial areas for the UK are shown in Figures 6-1 and 6-2

respectively [158], [159], [160]. The EVs in the industrial area (IEVs) are assumed to be connected at hour 2. The IEVs and the EVs in the commercial area (CEVs) are assumed to be disconnected from the MG at the end of hour 9 after finishing work, while the EVs in the residential area (REVs) are assumed to be disconnected at the end of the scheduling day.

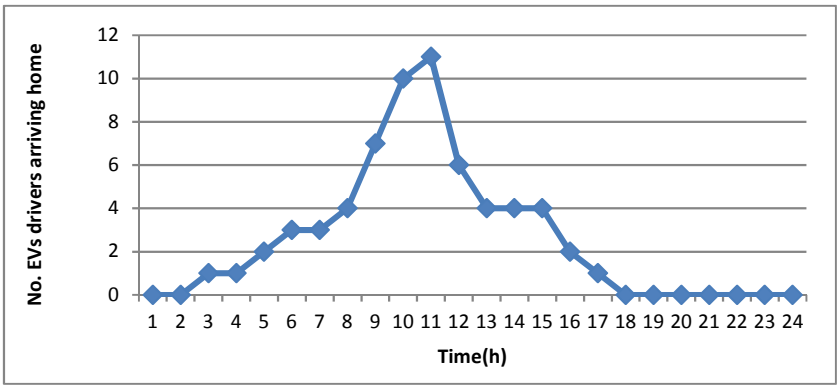

Figure 6-1 The EVs drivers arriving home from the final trip

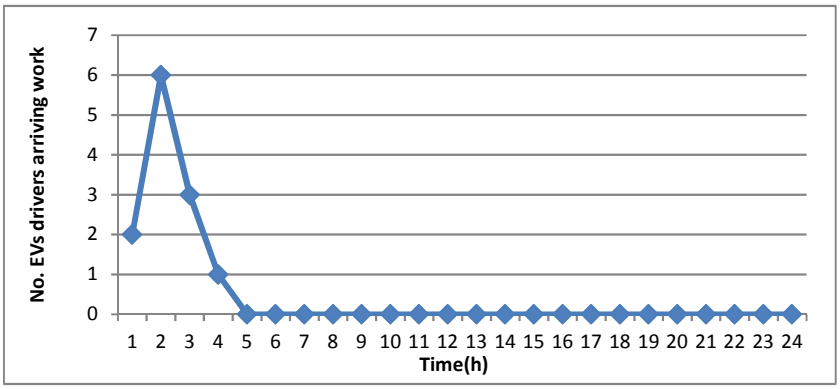

Figure 6-2 The EVs drivers arriving work from the final trip

The REVs are charged from the domestic charger at homes, where the main domestic charger characteristic of the UK is single phase (13 A, 230V) which it gives maximum possible charging and discharging power of 3 kW [161], [162], [163], [155] this value is used in this study with charging and discharging efficiencies of 90 %. The IEVs and CEVs are charged from the same characteristics of the domestic charger. The batteries of all the EVs are lithium ion and their capacities are 29.02 kWh for REVs and CEVs [159], while for IEVs are 15 kWh. The cycle life of the batteries and DoD are 2200 and 95%

respectively [148], [164]. It is considered that the 33 % of households have EVs [161], [165] and 3 EVs in the industrial area and 12 EVs in the commercial area.

6.9 Case Study

The proposed optimisation approach with the integration of EVs are applied to the connected and isolated proposed MG that is shown in Figure 6-3. The data of this grid are taken from [83], [84], [161] and this data is according to the real data of the UK distribution network. It is assumed that the scheduling day starts from 8:00 AM-8:00 AM next day. The hourly time series of the wind speed, PV generation, the OMPs, and the total active and reactive loads are illustrated in the Table D-1. The load of each area is illustrated in the Tables D-2. The charging and discharging prices of the EVs are shown in Table E-1. The charging and discharging prices are unchanged during the scheduling horizon, whether the EVs are charged or discharged. These prices are considered to encourage the EVs owners to participate in the MG operation.

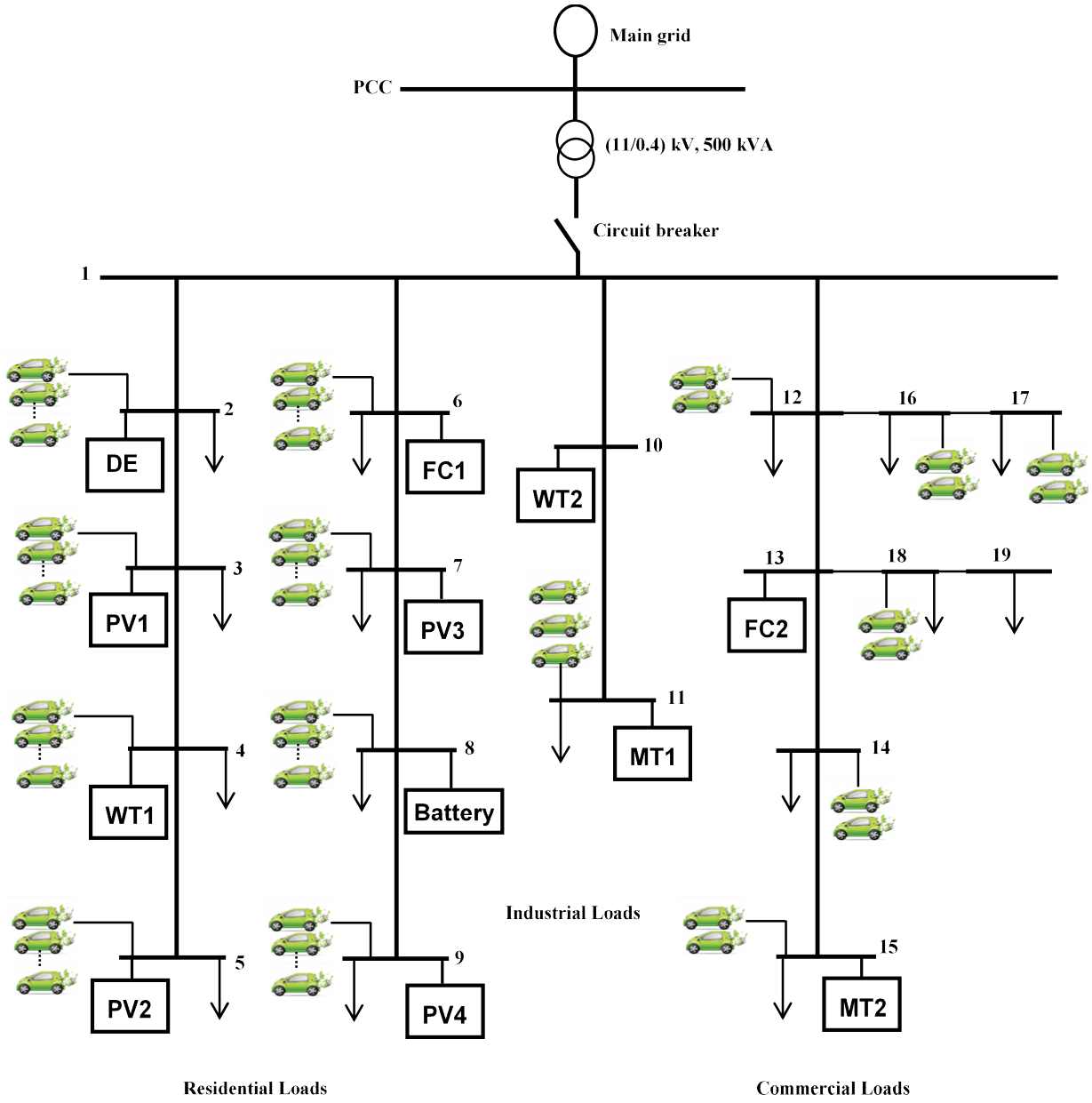

Figure 6-3 Structure of the MG test system

6.10 Results of the Economic Integration of the EVs with the Optimal Scheduling of the MG

The IEVs and CEVs are assumed charging and discharging during their connection to the grid, while multiple scenarios for charging and discharging of the REVS are considered and they are as follows:

Scenario 1: peak discharging/off-peak charging, where the discharging operations are allocated at peak hours (6-14), while charging allocates at hours (17-24 AM).

Scenario 2: off-peak discharging/peak and off-peak charging, where the discharging operations are allocated at off-peak hours (17-24), while charging allocates at hours (6-24).

Scenario 3: whole period charging and discharging, where the charging and discharging operations occur during the entire period of the connection of the REVs to the grid.

Scenario 4: the worst scenario, when the EVs start charging their vehicle to fully charge when they are connected to the grid in all areas during three hours.

Comparisons between these scenarios with the case of without EVs (base case) are carried out to reveal the impacts of the EVs on the optimal operation of the MG. In all scenarios, the charging and discharging decisions are made by the MG based on grid optimisation and owners of the EVs requirements. In order to meet the requirements of the consumers, the EVs are considered fully charged at the end of their connection to the grid and the charging and discharging prices are considered fixed. The base case results are illustrated in section 4.12.

6.10.1 Minimising the Operating Cost and Maximising the Profit

The optimisation approach is applied to the connected MG to investigate the impacts of the EVs on the optimal operation of the MG.

A. Connected MG

Scenario 1

Figure 6-4 depicts the charging and discharging operations of the all EVs. It can be observed that the IEVs and CEVs are charged when the OMP has low values and discharged when the OMP reaches the highest values. The ICEVs, CEVs, and REVs are discharged at hour 6 because the OMP has high value,

and higher than the discharging price. The highest charging power of IEVs and CEVs occurs at hour 8 because the OMP has low value and the owners should fully charge their vehicles before leaving the grid. In addition, the REVs are discharged when the OMP has high values at hours 6, 10, 11, 12, 13, and 14. The highest discharging power occurs at hour 14 because the OMP has high value and higher than hours 12 and 13. The discharging power at hours 14 is higher than at hour 10 as well, although the price at hour 10 is higher than at hour 14. This is because at hour 10 the EVs connected to the grid are lower than at hour 14.

In contrast, the REVs are charged over the entire charging period between hours 17 and 24 to prevent the base and EVs loads from increasing higher than the maximum capacity of the system. The highest charging power occurs at hour 21 because the OMP has the lowest value and the load has the lowest value as well.

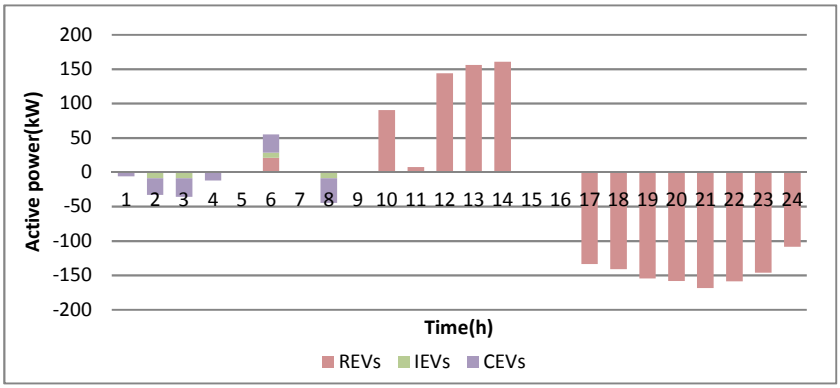

Figure 6-4 EVs optimal scheduling of the charging and discharging

Figures 6-5 and 6-6 show the optimal scheduling of the active and reactive power. These figures reveal that between hours 17 and 24 the base and REVs loads are provided from DE, renewable generations, and the utility grid. DE is committed to minimum output power at these hours to satisfy the active and reactive SSSCs and the utility grid is providing the maximum possible active power at these hours to supply the base and charging loads of the REVs because the OMP has the lowest values and lower than the charging price. Therefore, the MG purchases power from the utility grid and sells the power to

the REVs. The MG also sells the maximum permissible active power to the utility grid at hours 6, 10, and 14 to reduce its cost and increase its revenue, because the OMPs reach the highest values. Wherein, the MG buys active power from the EVs and sells it to the utility grid and to consumers at these hours because the active OMP has higher value than the discharging price. Further, the highest active power generation of the DGs is at hour 6 because the base load and the OMP have high values, where the MG sells maximum power to the utility grid. The number of EVs connected to the grid also is low at this hour, in comparison with hours 10 and 14; therefore, the MG generates higher power than at other hours. Furthermore, the battery is discharged at this hour as well. In comparison with the base case, the reactive power scheduling is changed, although the EVs are charged and discharge only active power. This is because the integration of the EVs changes the UC of the DGs, where the UC takes into consideration both the active and reactive power.

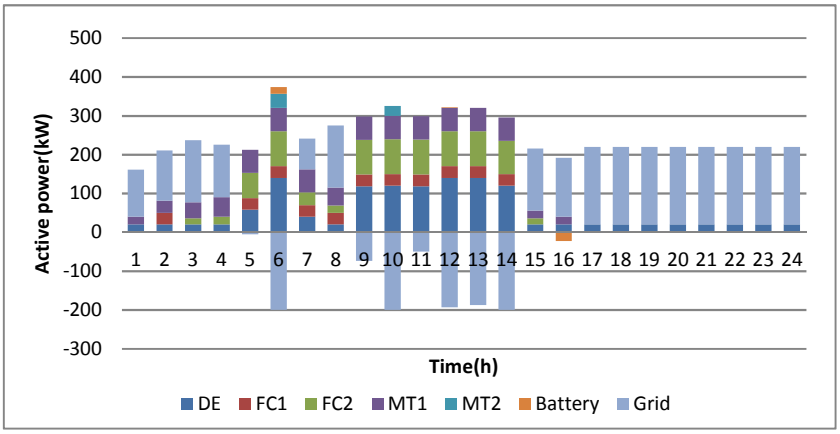

Figure 6-5 Optimal scheduling of the active power of the DGs and exchanging power with the battery and the utility grid

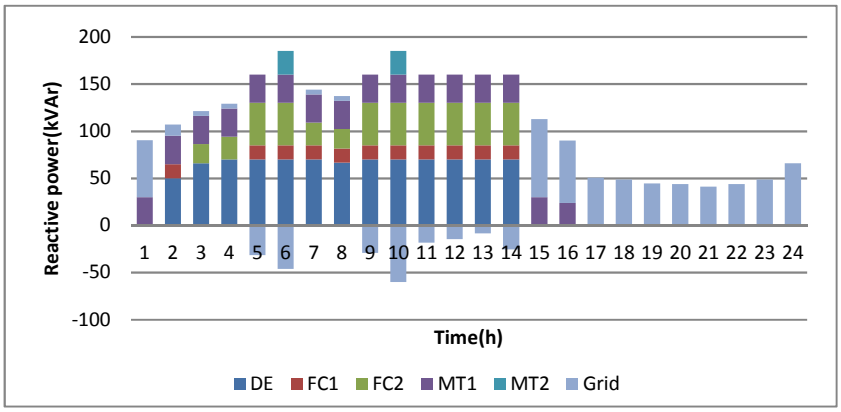

Figure 6-6 Optimal scheduling of the reactive power of the DGs and exchanging reactive power with the utility grid

Table 6-1 illustrates the optimal on/off state of the DGs per scheduling day. In comparison with the base case, the MG switches off the MT2 at hours 12 and 14 because the MT2 has the highest operating cost among the DGs and at these hours the REVs are discharged. Figure 6-7 shows that the EVs operations increase the load at hours 1, 2, 3, 4, and 8 due to the charging of the IEVs and CEVs, whereas the loads are increased significantly at hours 17 to 24 due to the charging of the REVs. It is obvious that the peak of the total active load is shifted to hour 8, while the peak of the reactive power does not change because the EVs are charged or discharged only active power. It is found that the total cost is 326.3 € per scheduling day, where the proposed economic integration of the EVs reduces the total cost by 81.5 € or by 20%, while the profit is 363 €, where the profit is increased by 81.5 € or by 29 %.

Table 6-1 Optimal on/off state of the DGs

T(h)	1	2	3	4	5	6	7	8	9	10	11	12	13	14	15	16	17	18	19	20	21	22	23	24
DE	1	1	1	1	1	1	1	1	1	1	1	1	1	1	1	1	1	1	1	1	1	1	1	1
FC1	0	1	0	0	1	1	1	1	1	1	1	1	1	1	0	0	0	0	0	0	0	0	0	0
FC2	0	0	1	1	1	1	1	1	1	1	1	1	1	1	1	0	0	0	0	0	0	0	0	0
MT1	1	1	1	1	1	1	1	1	1	1	1	1	1	1	1	1	0	0	0	0	0	0	0	0
MT2	0	0	0	0	0	1	0	0	0	1	0	0	0	0	0	0	0	0	0	0	0	0	0	0

1 On state of the DG 0 Off state of the DG Different state from the previous state

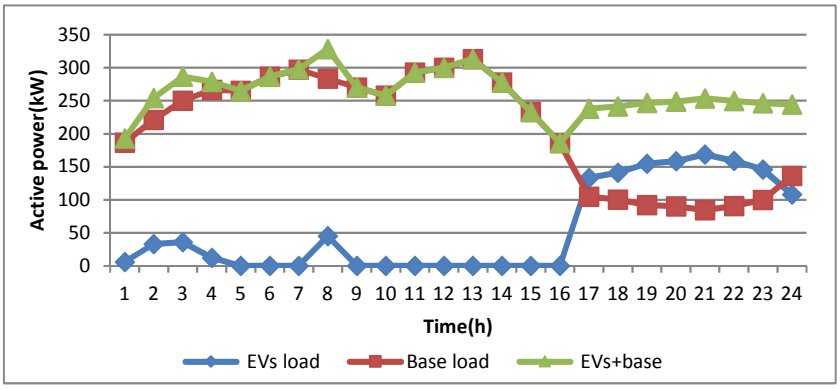

Figure 6-7 Modified load with the integration of the EVs

Scenario 2

Figure 6-8 shows the optimal scheduling of the EVs in the different areas. This figure reveals that the IEVs and CEVs are discharged at hour 6 for the same reason of the Sc1, where the discharging power is less than Sc1 because the REVs discharging time start at hour 17 in this scenario. It also can be observed that the highest charging power occurs at hours 2, 3, and 8 because the OMP has the lowest values at these hours. Therefore, the MG purchases power from the utility grid at these hour and sells this power to the EVs to reduce its cost or increase its profit. In addition, the REVs are charged during off-peak hours and when the OMP has low values, where the highest charging power is at hour 20 because the OMP price has the lowest price at these hours. The charging power at hour 20 is higher than 21 because the fixed battery charged at hour 21. Furthermore, there is no discharging operation in the period from 17 to 24 because the requirements of the owner of the EVs to fully charge their batteries

at the end of the scheduling day affect the discharging operation of EVs and there are no economic benefits for discharging during off-peak loads when the OMP has low values.

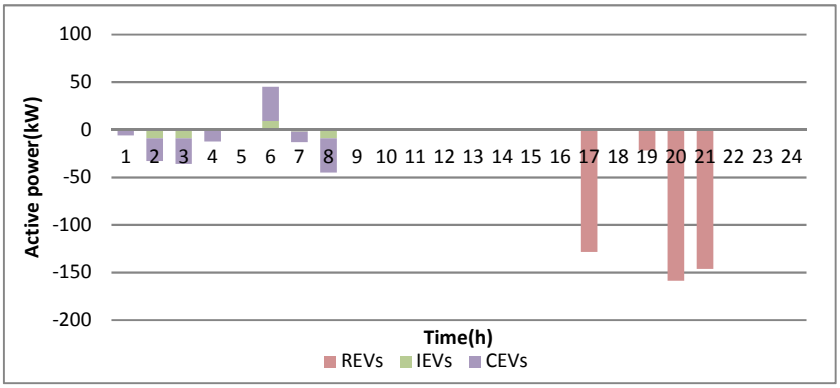

Figure 6-8 EVs optimal scheduling of the charging and discharging

Figure 6-9 shows the optimal scheduling of the active power of the DGs and exchanging power with the utility grid and the battery. This figure shows that the MG sells highest power to the utility grid at hour 6 because the OMP has high value and the IEVs and CEVs are discharged at this hour. The battery is discharged maximum permissible discharging power at hour 10 when the price has the highest value, while the battery is discharged at hour 6 in the Sc1 because in the Sc1 the REVs are discharged at hour 10, where there is not discharging power in the Sc2. The MG buys maximum permissible power from the utility grid at hours 17, 20, and 21 to meet its base load and charging loads of the REVs as shown in Figure 6-9 because the REVs are charged highest charging power at these hours.

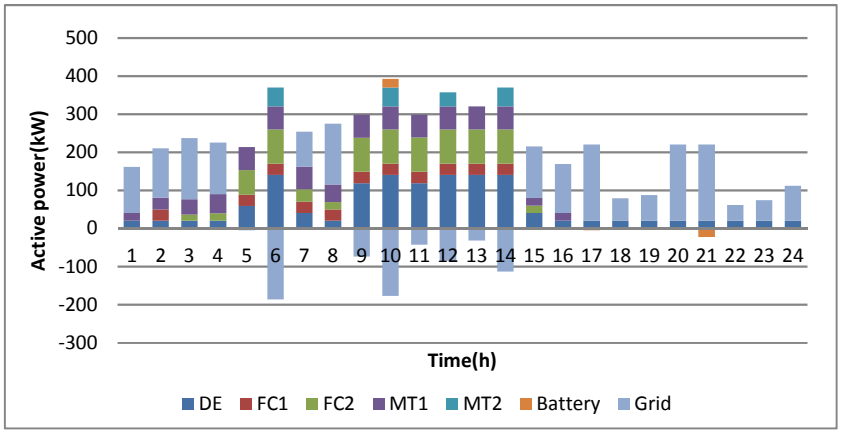

Figure 6-9 Optimal scheduling of the active power of the DGs and exchanging power with battery and the utility grid

The reactive power scheduling of the DGs and on/off state of the DGs are the same of the base case and on/off sate is depicted in Table 4-2. The reactive power is the same of the base case because the on/off state of the DGs are the same and the EVs are charged and discharged only active power.

Figure 6-10 shows that the integration of the EVs with MG increases the load at hours 1 to 8, 17, and 19 to 21 when the EVs are charged, where the total peak active load is shifted to hour 8, while the reactive power peak does not change for the same reason of the Sc1. It is found that the total operating cost is 381.8 €, where the cost is reduced by 26 € or by 6.4 % and the MG profit is 307.5 €, where the profit is increased by 26 € or by 9.2 %.

In comparison with Sc1, the MG switches on the MT2 at hour 12 and 14 because there is no discharging of the REVs at these hours. The MG turns on the MT2 at these hours to meet the loads and sells power to the utility grid because the OMPs have high values and higher than the cost of the generation of the MT2. The total charging power in the Sc2 is much lower than in the Sc1 because in the Sc2 there is no discharging of the REVs; therefore, the REVs need lower charging power than Sc1. However, the cost in the Sc1 is lower and the profit is higher than the Sc2.

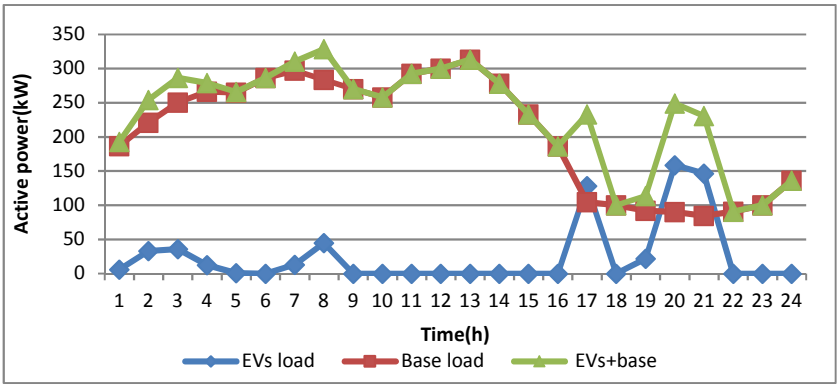

Figure 6-10 Modified load with the integration of the EVs

Scenario 3

Figure 6-11 shows the optimal charging and discharging scheduling of the EVs. This figure reveals that the REVs are discharged during the majority of the peak load hours. The REVs are discharged at hours 6, 9, to 14 because the active OMP has the highest values, whereas IEVs and CEVs are discharged at hour 6 for the same reasons of the Sc1. In addition, this figure shows that the REVs are charged at hours 15 to 24 because the OMP has the lowest values during the scheduling day and lower than charging price, where the highest charging power occurs at hour 21 for the same reasons of the Sc1.

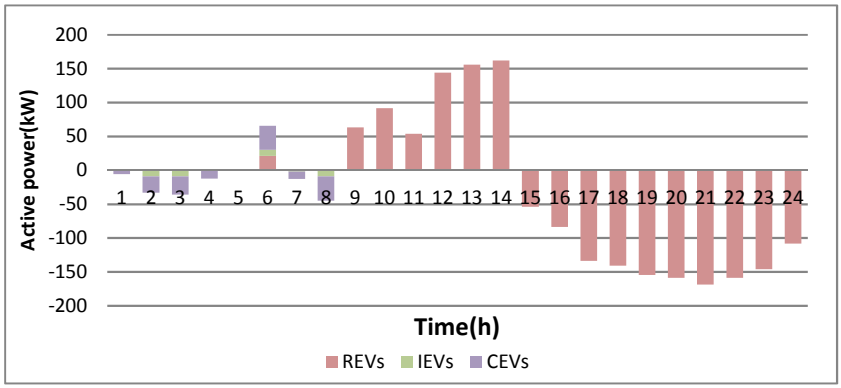

Figure 6-11 EVs optimal scheduling of the charging and discharging

Figure 6-12 reveals that the MG purchases active power from the EVs and sells power to the utility grid when the OMP has the highest values. The MG buys the maximum permissible active power from the utility grid at hours 15 to 24 to meet its base load and sells the active power to the REVs, wherein the charging price is higher than OMP at these hours. Further, the fixed battery is not operated for

the entire scheduling horizon because the EVs are discharged when the OMP reaches the highest values and the MG sells the maximum permissible active power to the utility grid at these hours. The MG incurs the cost of the charging and discharging power of the battery; therefore, there are not economic incentives from discharging the battery. The reactive power scheduling and the optimal on/off state of the DGs are the same of the Sc1. Figure 6-13 shows that the peak load is shifted to hour 8.

It is found that the total operating cost of the MG is 323.1 € per scheduling day, where the total cost is reduced by 84.7 € or by 20.8 %. Similarly, the profit is 366.2 € per scheduling day, where the profit is increased by 84.7 € or by 30.1 %.

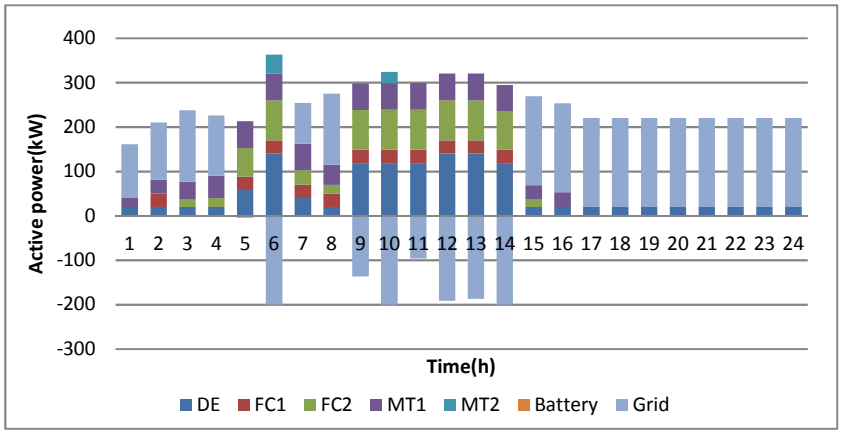

Figure 6-12 Optimal scheduling of the DGs active power and exchanging power with the battery and the utility grid

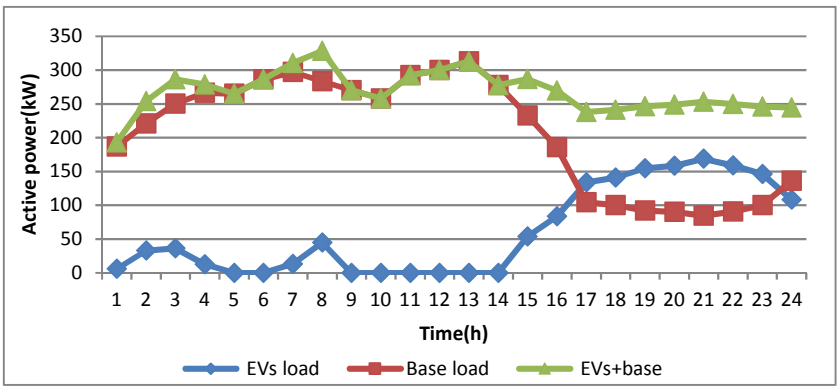

Figure 6-13 Modified load with integration of EVs

In comparison Sc3 with Sc1 and Sc2, it can be seen in the Sc3 the battery is not operated over the entire scheduling horizon because if the battery is operated, it will need to be charged and the charging should be at a low OMP time. Where, the MG buys the maximum permissible power from the utility grid at hours when the price reaches the low values to supply its base and EVs charging loads. Therefore, to be charged the battery, the MG needs to increase the generation of the committed DGs and this decision may be not economics. In addition, the MG incurs the charging cost of the battery.

Scenario 4

In this scenario, it is supposed that the owners of the EVs charge their vehicles to fully charge when they connect their vehicles to the gird directly during three hours. Figure 6-14 shows the charging schedule of the EVs. It can be seen from the figure that the highest charging power occurs at hour 11 because the highest number of the REVs are connected to the grid at this hour. The charging power at hour 10 is low in comparing with the number of connecting EVs at this hour. This is because the OMPs have the highest values and the MG sells the highest active and reactive power to the utility grid rather than to the REVs as shown in Figures 6-15 and 6-16, where the OMP is much higher than charging price at this hour.

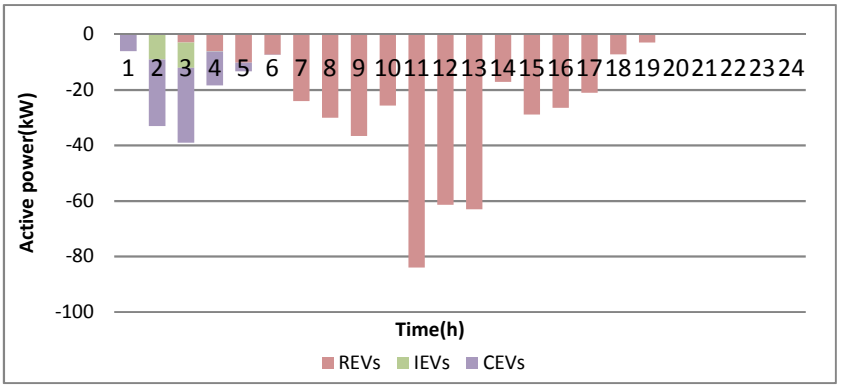

Figure 6-14 EVs optimal scheduling of charging and discharging

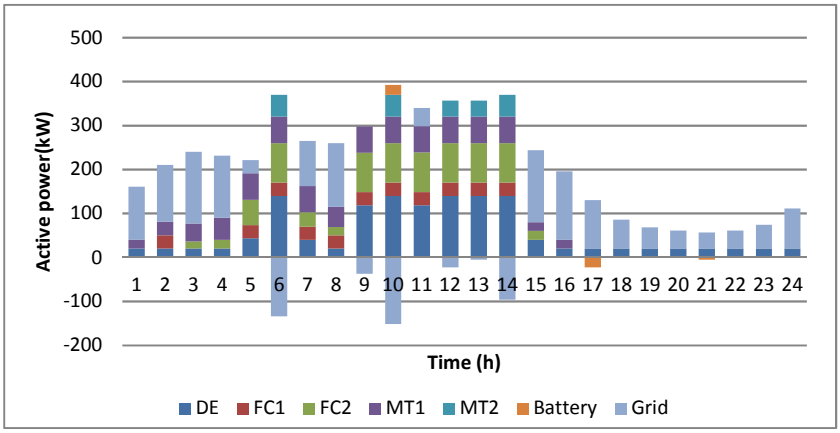

Figure 6-15 Optimal scheduling of the DGs active power and exchanging power with the battery and the utility grid

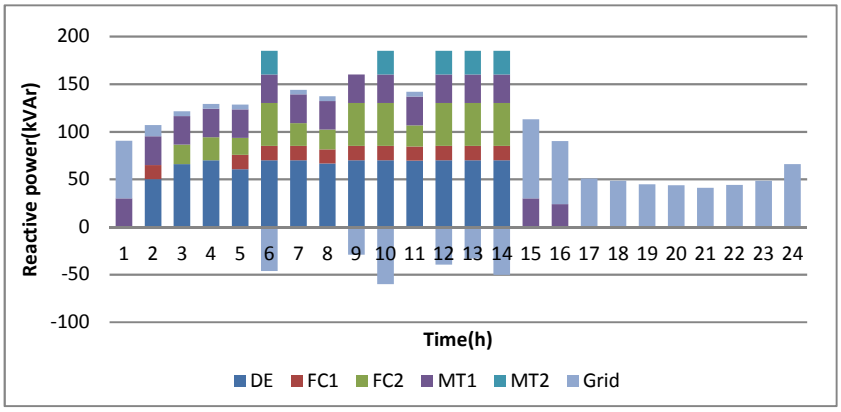

Figure 6-16 Optimal scheduling of the DGs reactive power and exchanging reactive power with the utility grid

Table 6-2 shows the optimal on/off state of the DGs. In comparison with the base case, this table reveals that the MG turns on the MT2 at hour 13 to meet the base and the EVs loads and sells active and reactive power to the utility grid because the OMPs have high value at this hour. Figure 6-17 shows the impacts of the charging of the EVs on the total load. This figure reveals that the total load is increased at hours 1 to 19 and the peak load is increased and shifted to hour 11. Overall, the total operating cost of the MG is 439.5 € per scheduling day, where the total cost is increased by 31.7 € or by 7.8 %, while the profit is 249.8 € per scheduling day, where the profit is reduced by 31.7 € or by 11.3 %. Increasing the total cost and decreasing the profit are due to the restriction of

the EVs to should be fully charged their batteries during three hours; therefore, the manage and control possibilities are restricted. The charging operation is coincided with the peak loads.

Table 6-2 Optimal on/off state of the DGs

T(h)	1	2	3	4	5	6	7	8	9	10	11	12	13	14	15	16	17	18	19	20	21	22	23	24
DE	1	1	1	1	1	1	1	1	1	1	1	1	1	1	1	1	1	1	1	1	1	1	1	1
FC1	0	1	0	0	1	1	1	1	1	1	1	1	1	1	0	0	0	0	0	0	0	0	0	0
FC2	0	0	1	1	1	1	1	1	1	1	1	1	1	1	1	0	0	0	0	0	0	0	0	0
MT1	1	1	1	1	1	1	1	1	1	1	1	1	1	1	1	1	0	0	0	0	0	0	0	0
MT2	0	0	0	0	0	1	0	0	0	1	0	1	1	1	0	0	0	0	0	0	0	0	0	0

1 On state of the DG 0 Off state of the DG Different state from the previous state

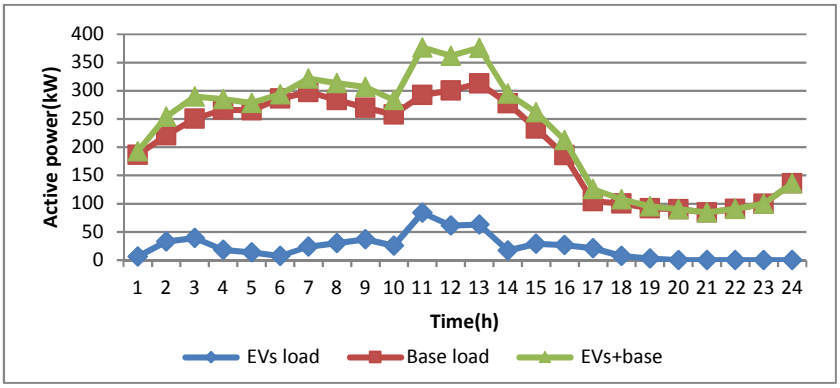

Figure 6-17 Modified load with the integration of EVs

Figures 6-18 and 6-19 show the optimal hourly cost and profit values for the connected MG for the four scenarios and case without the EVs and Table E-2 and Table E-3 illustrate the hourly values of these costs and profits. It can be seen that the lowest cost and the highest profit occur at hour 10 for all scenarios because the OMPs has by far the highest value at this hour. Therefore, the MG sells active and reactive power to the utility grid. The MG buys active power from the EVs and sells it to the utility grid and consumers in scenarios 1 and 3. The highest cost occurs at hour 13 for all scenarios because the load has the highest value at this hour. In addition, in the Sc1 and Sc3 the cost has low values (negative values) at hours 17 to 21 because the MG buys active power

from the utility grid and sells it to the EVs. Where, at these hours the OMP is lower than the charging price.

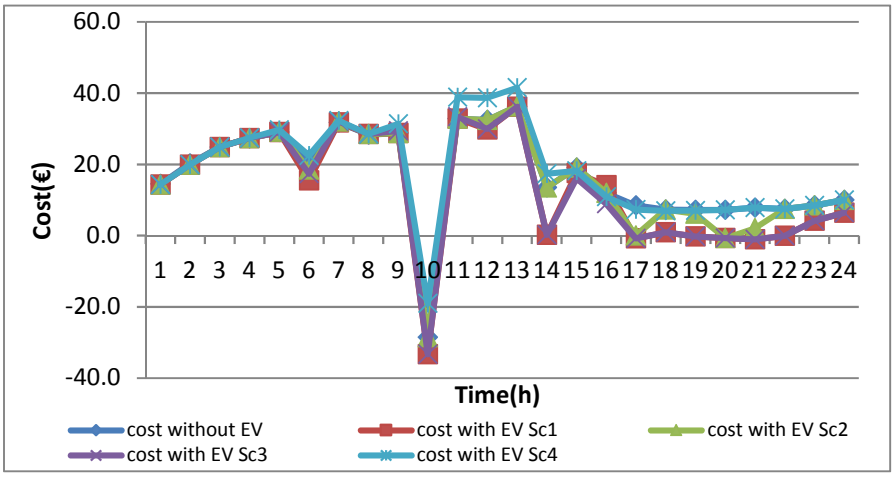

Figure 6-18 Optimal hourly cost with and without EVs for the connected MG

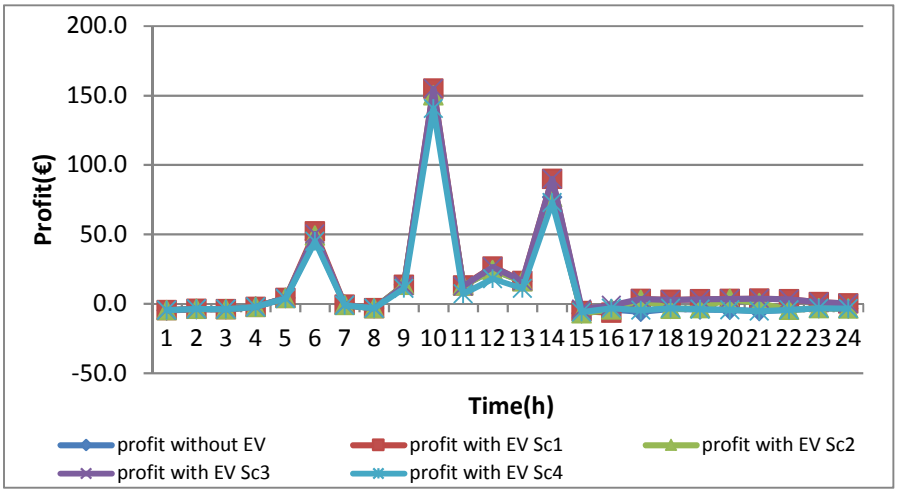

Figure 6-19 Optimal hourly profit with and without EVs for the connected MG

Table 6-3 summarises the results of the four scenarios, where this table reveals that the lowest operating cost occurs at Sc3 because the time of charging and discharging operations of the REVs are larger than other scenarios and there are no constraints to determine the certain period for charging or discharging. This means that the charging and discharging operations are more flexible, where this is employed to discharge the EVs when the OMP has high values and charge when the price has low values. The highest cost is at Sc4 because the EVs are charged only and the charging period for each vehicle is three

hours. The table also shows that the peak active load is increased in all scenarios; where the highest load is at Sc4 because the charging coincides with peak load. The negative sign in percentage of the cost and the profit of the Sc4 means that the cost increases and profit decreases.

Table 6-3 Results of four scenarios of the connected MG

	Cost with EVs (€/day)	Cost reduction %	Profit with EVs (€/day)	Profit increasing %	Charging cost (€)	Discharging cost (€)	Peak load(kW)
Sc1	326.3	20	363	29	104.2	98.1	328.38
Sc2	381.8	6.4	307.5	9.2	48.1	7.2	328.38
Sc3	323.1	20.8	366.2	30.1	116.2	117.6	328.38
Sc4	439.5	-7.8	249.8	-11.3	43.7	0	376

B. Isolated MG

In this case, the scheduling of the active and reactive power, the on/off states of the DGs, the charging of the EVs, the total cost, and the profit are the same for the first three scenarios because the EVs are operated in charge mode only. The REVs are charged at the off-peak load for all three scenarios to prevent the system load from increasing above the maximum capacity of the system and to make sure that the MG resources can meet the base and EVs loads.

Scenarios 1, 2, and 3

Figure 6-20 shows the optimal charging and discharging of the EVs in the different areas. This figure shows that the EVs in all sectors are operated in charge mode only because the discharging price is higher than the operating cost of the majority of the DGs and the price that the MG sells electricity to the consumers. The charging price is lower than the cost of the generation of the DGs; therefore, there are no economic incentives for discharging. The highest charging power of the IEVs and CEVs occurs at hour 2 because the highest number of the CEVs and the total number of the IEVs are connected to the grid at this hour.

The REVs are charged for the entire off-peak period to prevent the load from increasing higher than the system capacity and to make sure that the MG resources can meet the base and REVs charging loads, where the charging

power increases with decreasing the load and OMP as shown in the figure. The highest charging power of the REVs is at hour 21 because the load reaches to the lowest value and the OMP reach the lowest value during the scheduling horizon, while the lowest charging power occurs at hour 24 because the load has the highest value during off peak period.

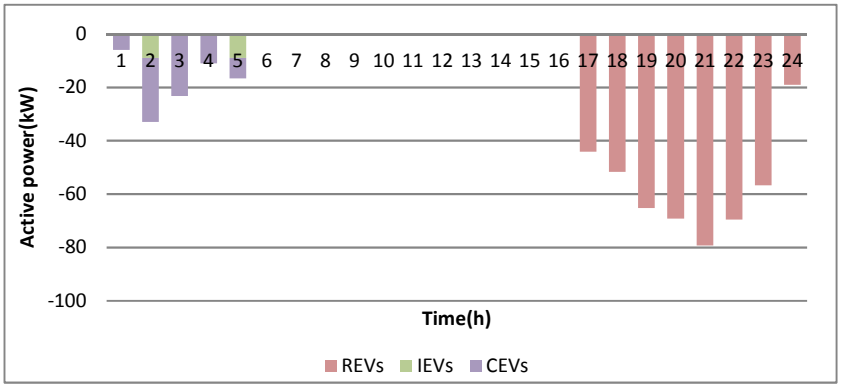

Figure 6-20 EVs optimal scheduling of charging and discharging

Figures 6-21 and 6-22 show the optimal scheduling of the active and reactive power of the DGs. In comparison with base case, it can be seen that the MG increases the generation of the DGs significantly at hours 1 to 5 and 17 to 24 to supply the EVs and base loads. The battery is not operated during the scheduling period. In addition, the highest generation is at hour 13 because the load has the highest value at this hour. Figure 6-22 shows that the reactive power generation follows the same pattern of the reactive load because the EVs are charged or discharged only active power and the REGs deliver only active power.

In comparison with the base case, Table 6-4 reveals that the MG switches on the FC1 and FC2 from hours 17 to 23 for FC1 and 17 to 24 for FC2 to cover base and EVs loads. Meantime, the MG turns off the DE at hours 18 to 24 because the FC1, FC2, and MT1 can meet the base and EVs loads and satisfy the SRCs. This also is more economical than increasing the generation of the DE. Figure 6-23 shows that the EVs operations do not affect the peak load, while the load at off-peak hours is increased significantly because the charging of the EVs is scheduled for the entire period. Overall, the total operating cost is

560.9 €, where the charging of the EVs increases the cost by 11.1 € or 2 %, while the profit is 223.3 €, while the profit is reduced by 11.2 € or 4.8 %.

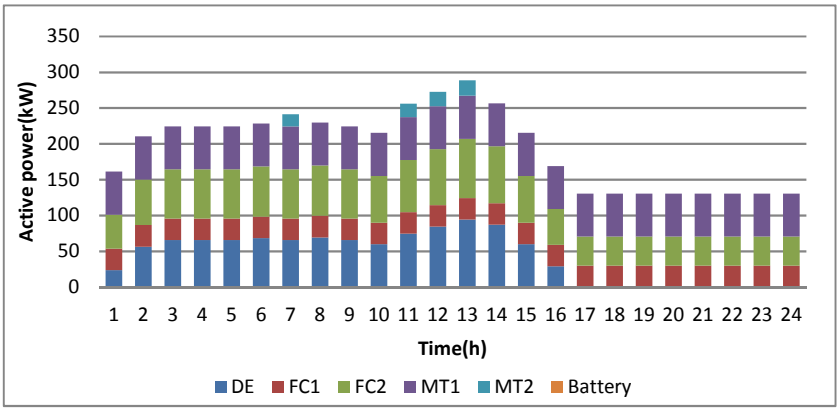

Figure 6-21 Optimal scheduling of the DGs active power and exchanging power with the battery

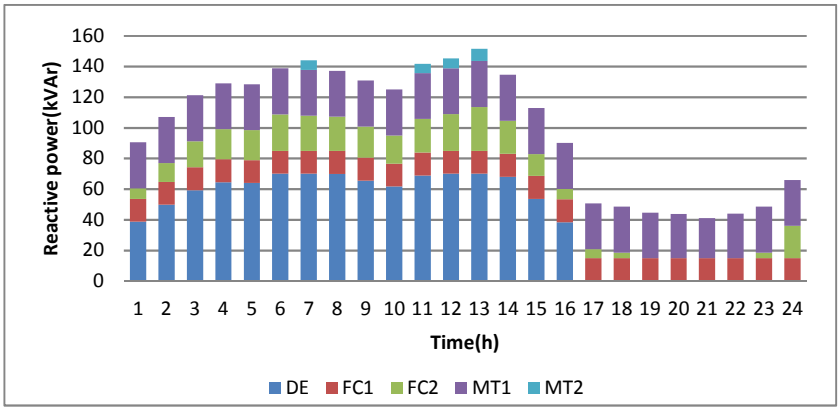

Figure 6-22 Optimal scheduling of the reactive power of the DGs

Table 6-4 Optimal on/off state of the DGs

T(h)	1	2	3	4	5	6	7	8	9	10	11	12	13	14	15	16	17	18	19	20	21	22	23	24
DE	1	1	1	1	1	1	1	1	1	1	1	1	1	1	1	1	0	0	0	0	0	0	0	0
FC1	1	1	1	1	1	1	1	1	1	1	1	1	1	1	1	1	1	1	1	1	1	1	1	1
FC2	1	1	1	1	1	1	1	1	1	1	1	1	1	1	1	1	1	1	1	1	1	1	1	1
MT1	1	1	1	1	1	1	1	1	1	1	1	1	1	1	1	1	1	1	1	1	1	1	1	1
MT2	0	0	0	0	0	0	1	0	0	0	1	1	1	0	0	0	0	0	0	0	0	0	0	0

1 On state of the DG 0 Off state of the DG Different state from the previous state

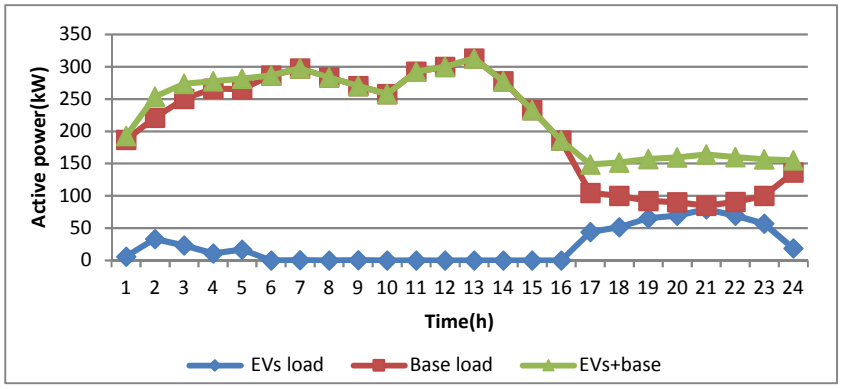

Figure 6-23 Modified load with the integration of the EVs

Scenario 4

Figure 6-24 shows the optimal charging schedule of the EVs in the different areas. This figure shows that the highest charging power is at hour 11 for the same reasons of the connected MG. In comparison with the scenario in the connected MG, it can be observed that in this scenario the charging load at hour 10 is higher because there is no connection with the utility grid to sell power at this time, where in the case of connected MG at hour 10 the OMP has the highest value and by far higher than charging price, so the MG sells power to the utility grid.

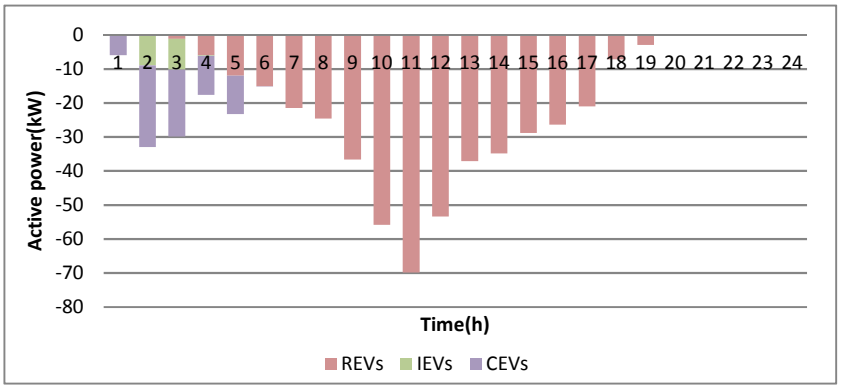

Figure 6-24 EVs optimal scheduling of charging and discharging

Figures 6-25 and 6-26 depict the optimal scheduling of the active and reactive power of the DGs. In comparison with base case, it is shown that the MG increases the generation of the DGs at hours 1 to 19 to satisfy the base and charging loads of the EVs. The MG generates the highest active power at hours

11, 12, and 13 because the load has the highest values at these hours and the charging of EVs is high as well. Furthermore, Figure 6-26 shows that the reactive power scheduling is different from the base case because the on/off state of the DGs is different from the base case.

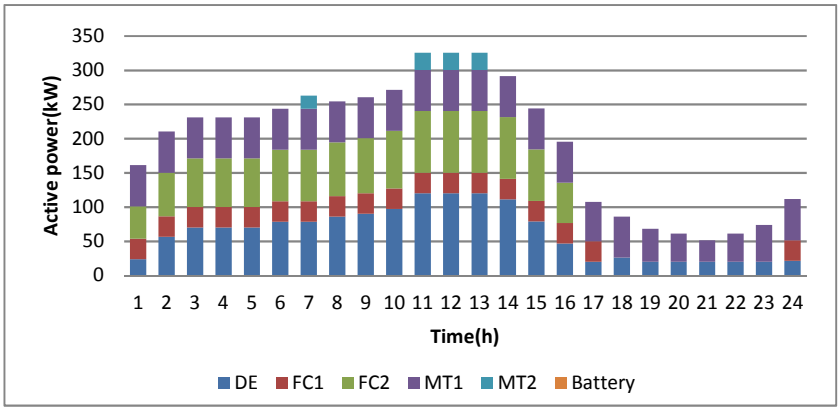

Figure 6-25 Optimal scheduling of the DGs active power and exchanging power with the battery

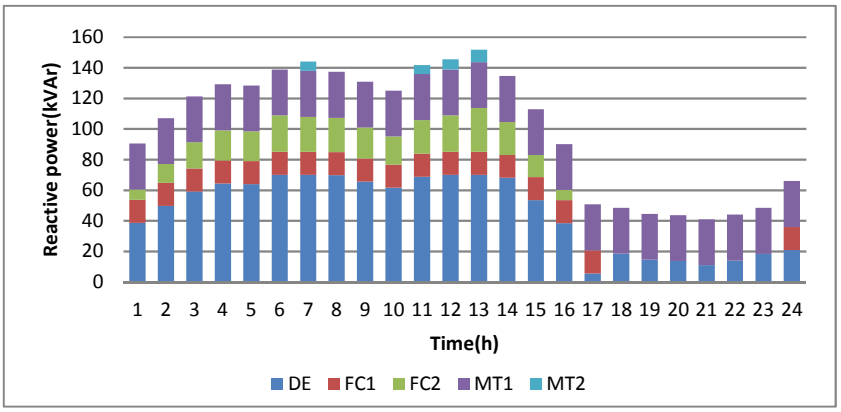

Figure 6-26 Optimal scheduling of the reactive power of the DGs

Table 6-5 illustrates the optimal on/off state of the DGs. In comparison with the base case, it can be seen that the MG turns on FC1 at hour 17 because it has lower operating cost than DE; therefore, it is more economical than increasing the generation of the DE. Figure 6-27 shows the impacts of the EVs on the total active load. It can be seen the peak load is shifted to hour 11.

It is found that the operating cost is 577.9 €, where the penetration of the EVs increases the cost by 28.1 € or 5.1 %, while the profit is 206.3 €, where the profit is reduced by 28.2 € or 12 %.

Table 6-5 Hourly optimal on/off state of the DGs

T(h)	1	2	3	4	5	6	7	8	9	10	11	12	13	14	15	16	17	18	19	20	21	22	23	24
DE	1	1	1	1	1	1	1	1	1	1	1	1	1	1	1	1	1	1	1	1	1	1	1	1
FC1	1	1	1	1	1	1	1	1	1	1	1	1	1	1	1	1	1	0	0	0	0	0	0	1
FC2	1	1	1	1	1	1	1	1	1	1	1	1	1	1	1	1	0	0	0	0	0	0	0	0
MT1	1	1	1	1	1	1	1	1	1	1	1	1	1	1	1	1	1	1	1	1	1	1	1	1
MT2	0	0	0	0	0	0	1	0	0	0	1	1	1	0	0	0	0	0	0	0	0	0	0	0

1 On state of the DG 0 Off state of the DG Different state from the previous state

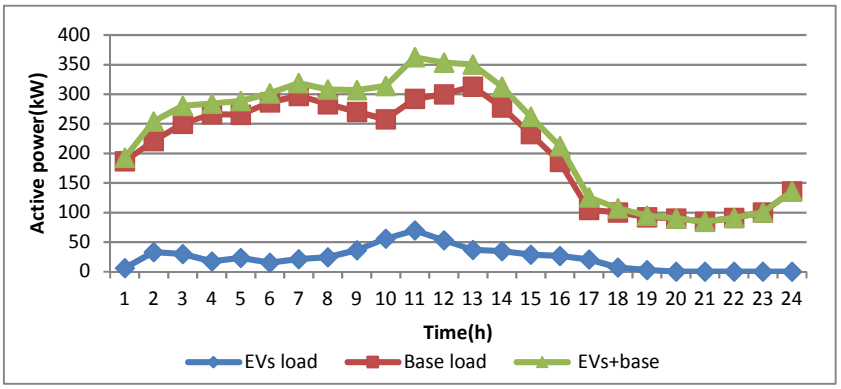

Figure 6-27 Modified load with the integration of the EVs

Figures 6-28 and 6-29 show the optimal hourly cost and profit for the isolated MG for the four scenarios and case without the EVs and Table E-4 and Table E-5 illustrate the hourly values of these costs and profits. It can be noticed that the majority of the day hours in the Sc1, 2, 3 the cost is lower and the profit is higher than the Sc4. This is because that the charging of the EVs coincides with the highest loads in the Sc4. These figures also reveal that in the Sc4 the cost is lower and profit is higher than the Sc1, 2, 3 at hours 17 to 24 because in the Sc1, 2, 3 all REVs are charged at these hours with much higher power than the Sc4. Furthermore, both the cost and profit have only positive values for the same reasons of the case without consideration of the EVs.

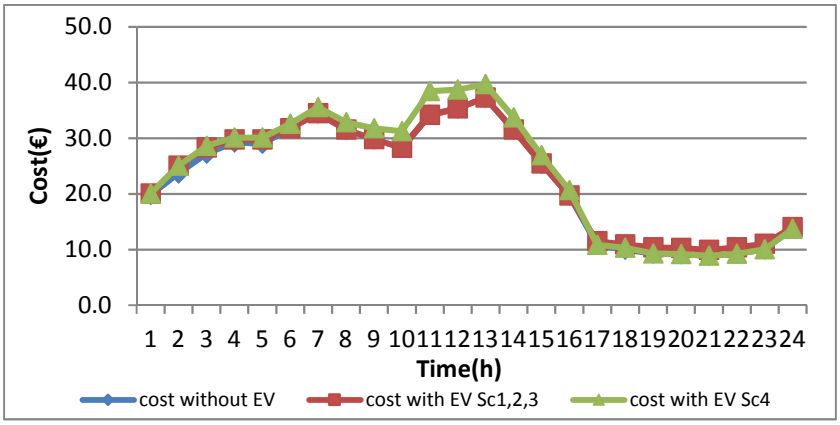

Figure 6-28 Optimal hourly cost with and without EVs for the isolated MG

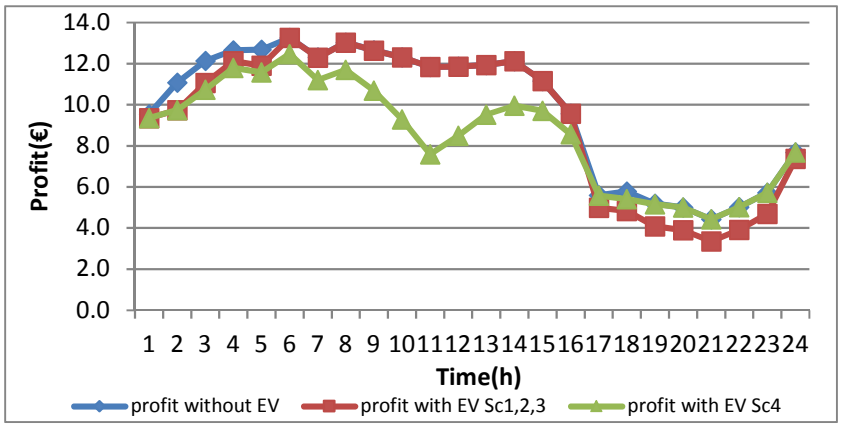

Figure 6-29 Optimal hourly profit with and without EVs for the isolated MG

Table 6-6 summarises the results of the four scenarios. This table reveals that the operating cost is increased for all scenarios because the charging price lower than the cost of power generation and there is no exchanging power with the utility grid. It also can be seen that the peak active load is increased in Sc4 because the charging of the REVs coincides with peak load. In addition, the charging cost is equal for all scenarios because there is no discharging operation and the charging price is fixed over the scheduling horizon and all the EVs should be fully charged before leaving the grid.

Table 6-6 Results of the four scenarios of the isolated MG

	Cost with EVs (€/day)	Cost reduction %	Profit with EVs (€/day)	Profit increasing %	Charging cost (€)	Discharging cost (€)	Peak load(kW)
Sc1 Sc2 Sc3	560.9	-2	223.3	-4.8	43.7	0	313
Sc4	577.9	-5.1	206.3	-12	43.7	0	362.482

To reduce the MG cost or increase the profit, it is assumed the charging price is increased to 0.11 (€/kWh) and the results are shown in Table 6-7. This table shows that the costs of the first three scenarios are decreased and the profits are increased in comparison with base case, while for the Sc4 the cost is reduced and the profit is increased in comparing with the previous case. However, the total cost is higher and the profit is lower than the base case because the restrictions on the charging of the EVs.

Table 6-7 Results of the four scenarios per scheduling day of the isolated MG

	Cost with EVs (€/day)	Cost reduction %	Profit with EVs (€/day)	Profit increasing %	Charging cost (€)	Discharging cost (€)	Peak load(kW)
Sc1 Sc2 Sc3	544.6	0.95	239.6	2.2	60	0	313
Sc4	561.5	-2.1	222.7	-5	60	0	362.482

6.11 Stochastic SCUC-UARDEED of the MG with Integration of the EVs

The integration of the EVs with the power grids creates new sources of uncertainties to the grid optimal operation. The EVs that are connected to each area of the grid at each time interval together with the uncertainties arising from the wind and solar generations are considered as uncertain variables in this section. These uncertainties are modelled and incorporated with an optimisation approach to address their impacts on the optimal scheduling of the MG.

6.11.1 The Stochastic Model of the EVs

The stochastic models of the wind and solar generations are conducted in chapter three. Wherein, the EVs that are connected to the residential and

commercial areas is assumed follows the normal distribution and the model of the number of the EVs as follows:

$$EV_{Res}(t) = {EV_{Res}}^{estim} + \mu(t)^{EV_{Res}}.\sigma(t)^{EV_{Res}} \quad \textbf{(6.27)}$$

$$EV_{Com}(t) = {EV_{Com}}^{estim} + \mu(t)^{EV_{Com}}.\sigma(t)^{EV_{Com}} \quad \textbf{(6.28)}$$

where ${EV_{Res}}^{estim}$ and ${EV_{Com}}^{estim}$ are the estimated number (mean values) of the EVs that are connected at hour t to the residential and commercial areas respectively. $\sigma(t)^{EV_{Res}}$ and $\sigma(t)^{EV_{Com}}$ are the standard deviation of the EVs in the residential and commercial areas respectively. $\mu(t)^{EV_{Res}}$ and $\mu(t)^{EV_{Com}}$ are the random variables generated for number of the EVs in the residential and commercial areas at time t in Mote Carlo simulation by using the normal probability density function with a mean of zero and a standard deviation is one.

By following the same procedure in section 3.3 to determine the probability of the joint scenarios, the probability of happening of each reduced scenario is as follows:

$$\rho_{k3}^{EV_{Res}} = [\rho_1^{EV_{Res}}, \ \rho_2^{EV_{Res}}, \dots \rho_{m3}^{EV_{Res}}]_{1\times m3} \quad \textbf{(6.29)}$$

$$\rho_{e2}^{EV_{Com}} = [\rho_1^{EV_{Com}}, \ \rho_2^{EV_{Com}}, \dots \rho_{r2}^{EV_{Com}}]_{1\times r2} \quad \textbf{(6.30)}$$

where $\rho^{EV_{Res}}$ and $\rho^{EV_{Com}}$ are the corresponding probability of scenario for the EVs at residential and commercial areas.

The summation probability of scenarios for each variable should equal 1 as follows.

$$\sum_{k3=1}^{m3} \rho_{k3}^{EV_{Res}} = 1 \quad \textbf{(6.31)}$$

$$\sum_{e2=1}^{r2} \rho_{e2}^{EV_{Com}} = 1 \quad \textbf{(6.32)}$$

The number of possible scenarios (S) is calculated as

$$S = n.q.m3.r2 \quad \textbf{(6.33)}$$

The summation of the probability of the joint scenarios is as follows

$$\sum_{s=1}^{S} \lambda_s = \sum_{i3=1}^{n} \sum_{i4=1}^{q} \sum_{k3=1}^{m3} \sum_{e2=1}^{r2} \rho_{i3}^{W} \rho_{i4}^{PV} \rho_{k3}^{EV_{Res}} \rho_{e2}^{EV_{Com}} \quad \textbf{(6.34)}$$

6.12 Proposed Objective Functions

Two objective functions are considered in this section. The first is the minimising the total operating cost and the second is the maximising the profit of the connected and isolated MG. The objective functions include two stages. In the first stage, the UC decision variables for each DG are taken before actual realisation the uncertainties. These decisions could not be changed in the second stage. In the second stage, the decisions of the output active and reactive power of the DGs, the on/off state of the DGs, the exchanging active and reactive power with the utility grid, and the exchanging power with the battery and the EVs are taken. The decisions that are taken in the first stage should ensure a feasible solution for all expected scenarios in the second stage. All the decision variables are denoted by (s) which representing scenario s.

6.12.1 Proposed Minimising the Total Operating Cost

The objective functions of the minimising the overall operating cost under stochastic environment are formulated as follows:

A. Connected MG

The optimisation problem is formulated as

$$\min(F) \quad \textbf{(6.35)}$$

where the objective function F is

$$F = \sum_{t=1}^{T}\sum_{i=1}^{N}[SU_{DG_i}(t) + SD_{DG_i}(t)] + \sum_{s=1}^{S}\lambda_s \sum_{t=1}^{T}\{\sum_{i=1}^{N}[CP_{DG_i}(P_{DG_i}^s(t)) + CQ_{DG_i}(Q_{DG_i}^s(t)) + COM_{DG_i}(P_{DG_i}^s(t))]\delta_{DG_i}(t) + C_e(P_{DG_i}^s(t)) + C_{bo}^s(t) + c_{gP}^s(t) + c_{gQ}^s(t) + \sum_{i1=1}^{N1} CP_{W_{i1}}(P_{W_{i1}}^s(t)) + \sum_{i2=1}^{N2} CP_{PV_{i2}}(P_{PV_{i2}}^s(t)) + C_{EV}^{Res,s}(t) + C_{EV}^{Ind,s}(t) + C_{EV}^{Com,s}(t) + c_{EVcut}.P_{EVcut}^{Res,s}(t).\Delta t + c_{EVcut}.P_{EVcut}^{Ind,s}(t).\Delta t + c_{EVcut}.P_{EVcut}^{Com,s}(t).\Delta t + c_{Pres}.P_{Drescut}^{s}(t) + c_{Qres}.Q_{Drescut}^{s}(t) + c_{Pcom}.P_{Dcomcut}^{s}(t) + c_{Qcom}.Q_{Dcomcut}^{s}(t) + c_{Pind}.P_{Dindcut}^{s}(t) + c_{Qind}.Q_{Dindcut}^{s}(t)\} \quad \textbf{(6.36)}$$

This is constructed from equations

(2.15), (2.16), (2.1), (2.2), (2.3), (2.14), (2.11), (2.12), (2.13), (2.5), (2.6), (6.10), (6.11), (6.12), and the last nine components are the cost of unserved power to the EVs and the cost of cut of the active and reactive residential, commercial, and industrial consumers.

B. Isolated MG

The optimisation problem is formulated as

$$\min(F) \quad \textbf{(6.37)}$$

where the objective function F is

$$F = \sum_{t=1}^{T}\sum_{i=1}^{N}[SU_{DG_i}(t) + SD_{DG_i}(t)] + \sum_{s=1}^{S}\lambda_s \sum_{t=1}^{T}\{\sum_{i=1}^{N}[CP_{DG_i}(P_{DG_i}^s(t)) + CQ_{DG_i}(Q_{DG_i}^s(t)) + COM_{DG_i}(P_{DG_i}^s(t))]\delta_{DG_i}(t) + C_e(P_{DG_i}^s(t)) + C_{bo}^s(t) + \sum_{i1=1}^{N1} CP_{W_{i1}}(P_{W_{i1}}^s(t)) + \sum_{i2=1}^{N2} CP_{PV_{i2}}(P_{PV_{i2}}^s(t)) + C_{EV}^{Res,s}(t) + C_{EV}^{Ind,s}(t) + C_{EV}^{Com,s}(t) + c_{EVcut}.P_{EVcut}^{Res,s}(t).\Delta t + c_{EVcut}.P_{EVcut}^{Ind,s}(t).\Delta t + c_{EVcut}.P_{EVcut}^{Com,s}(t).\Delta t + c_{Pres}.P_{Drescut}^{s}(t) + c_{Qres}.Q_{Drescut}^{s}(t) + c_{Pcom}.P_{Dcomcut}^{s}(t) + c_{Qcom}.Q_{Dcomcut}^{s}(t) + c_{Pind}.P_{Dindcut}^{s}(t) + c_{Qind}.Q_{Dindcut}^{s}(t) + \sum_{i=1}^{N} c_G.P_{DG_i cut}^{s}(t) + \sum_{i1=1}^{N1} c_{ren}.P_{W_{i1}cut}^{s}(t) + \sum_{i2=1}^{N2} c_{ren}.P_{PV_{i2}cut}^{s}(t)\} \quad \textbf{(6.38)}$$

This is constructed from equations
(2.15), (2.16), (2.1), (2.2), (2.3), (2.14), (2.11), (2.5), (2.6), (6.10), (6.11), (6.12), and the last twelve components are the cost of unserved power to the EVs, cost of cut of the active and reactive residential, commercial, and industrial loads, and the cost of renewable and DGs generation cut.

6.12.2 Proposed Maximising the MG Profit

The stochastic objective functions for maximising the MG profit are formulated as follows

A. Connected MG

The optimisation problem is formulated as

$$\max(F) \tag{6.39}$$

where the objective function F is

$$\begin{aligned} F = &- \sum_{t=1}^{T} \sum_{i=1}^{N} [SU_{DG_i}(t) + SD_{DG_i}(t)] + \\ &\sum_{s=1}^{S} \lambda_s \sum_{t=1}^{T} \{ \sum_{i=1}^{N} \left[c_{gP}(t).P_{DG_i}^{s}(t) + c_{gQ}(t).Q_{DG_i}^{s}(t) \right] \delta_{DG_i}(t) + \\ &c_{gP}(t).P_{bdis}^{s}(t).\Delta t + c_{gP}(t).\sum_{i2=1}^{N2} P_{PV_{i2}}^{s}(t) + \\ &c_{gP}(t).\sum_{i1=1}^{N1} P_{W}^{s}(t) + c_{gP}(t).[N_{EV}^{Res,s}(t).P_{EVdis}^{Res,s}(t) + N_{EV}^{Ind}(t).P_{EVdis}^{Ind,s}(t) + \\ &N_{EV}^{Com,s}(t).P_{EVdis}^{Com,s}(t)].\Delta t\} - \sum_{s=1}^{S} \lambda_s \sum_{t=1}^{T} \{ \sum_{i=1}^{N} [CP_{DG_i}(P_{DG_i}^{s}(t)) + \\ &CQ_{DG_i}(Q_{DG_i}^{s}(t)) + COM_{DG_i}(P_{DG_i}^{s}(t))] \delta_{DG_i}(t) + C_e(P_{DG_i}^{s}(t)) + C_{bo}^{s}(t) + \\ &c_{gP}(t).P_{bch}^{s}(t).\Delta t + \sum_{i1=1}^{N1} CP_{W_{i1}}(P_{W_{i1}}^{s}(t)) + \\ &\sum_{i2=1}^{N2} CP_{PV_{i2}}(P_{PV_{i2}}^{s}(t)) + c_{EVdis}.[N_{EV}^{Res,s}(t).P_{EVdis}^{Res,s}(t) + N_{EV}^{Ind}(t).P_{EVdis}^{Ind,s}(t) + \\ &N_{EV}^{Com,s}(t).P_{EVdis}^{Com,s}(t)].\Delta t + (c_{gP}(t) - c_{EVch}).[N_{EV}^{Res,s}(t).P_{EVch}^{Res,s}(t) + \\ &N_{EV}^{Ind}(t).P_{EVch}^{Ind,s}(t) + N_{EV}^{Com,s}(t).P_{EVch}^{Com,s}(t)].\Delta t + c_{EVcut}.P_{EVcut}^{Res,s}(t).\Delta t + \\ &c_{EVcut}.P_{EVcut}^{Ind,s}(t).\Delta t + c_{EVcut}.P_{EVcut}^{Com,s}(t).\Delta t + c_{Pres}.P_{Drescut}^{s}(t) + \\ &c_{Qres}.Q_{Drescut}^{s}(t) + c_{Pcom}.P_{Dcomcut}^{s}(t) + c_{Qcom}.Q_{Dcomcut}^{s}(t) + \\ &c_{Pind}.P_{Dindcut}^{s}(t) + c_{Qind}.Q_{Dindcut}^{s}(t)\} \end{aligned} \tag{6.40}$$

The revenue of the MG comes from selling the active power from the DGs, the discharging power of the battery, the power from the RDGs, discharging power of the EVs. The cost is constructed using equations

(2.15), (2.16), (2.1), (2.2), (2.3), (2.14), (2.11), (2.5), (2.6), , the cost of buying power from the EVs, and the last nine components are the cost of unserved power to the EVs and the cost of cut of the active and reactive residential, commercial, and industrial consumers..

B. Isolated MG

The optimisation problem is formulated as

$$\max(F) \tag{6.41}$$

where the objective function F is

$$F = Max\{-\sum_{t=1}^{T}\sum_{i=1}^{N}[SU_{DG_i}(t) + SD_{DG_i}(t)] + \tag{6.42}$$
$$\sum_{s=1}^{S}\lambda_s \sum_{t=1}^{T}\{\sum_{i=1}^{N}\left[c_{isoP}(t).P_{DG_i}^{s}(t) + c_{isoQ}(t).Q_{DG_i}^{s}(t)\right]\delta_{DG_i}(t) +$$
$$c_{isoP}(t).P_{bdis}^{s}(t).\Delta t + c_{isoP}(t).\sum_{i2=1}^{N2}P_{PV_{i2}}^{s}(t) +$$
$$c_{isoP}(t).\sum_{i1=1}^{N1}P_{W}^{s}(t) + c_{isoP}(t).[N_{EV}^{Res}(t).P_{EVdis}^{Res,s}(t) + N_{EV}^{Ind}(t).P_{EVdis}^{Ind,s}(t) +$$
$$N_{EV}^{Com}(t).P_{EVdis}^{Com,s}(t)].\Delta t\} - \sum_{s=1}^{S}\lambda_s \sum_{i=1}^{T}\{\sum_{i=1}^{N}\left[CP_{DG_i}\left(P_{DG_i}^{s}(t)\right) +$$
$$CQ_{DG_i}\left(Q_{DG_i}^{s}(t)\right) + COM_{DG_i}\left(P_{DG_i}^{s}(t)\right)\right]\delta_{DG_i}(t) + C_e(P_{DG_i}^{s}(t)) + C_{bo}^{s}(t) +$$
$$c_{isoP}(t).P_{bch}^{s}(t).\Delta t + \sum_{i1=1}^{N1}CP_{W_{i1}}(P_{W_{i1}}^{s}(t)) +$$
$$\sum_{i2=1}^{N2}CP_{PV_{i2}}(P_{PV_{i2}}^{s}(t)) + c_{EVdis}.[N_{EV}^{Res,s}(t).P_{EVdis}^{Res,s}(t) + N_{EV}^{Ind}(t).P_{EVdis}^{Ind,s}(t) +$$
$$N_{EV}^{Com,s}(t).P_{EVdis}^{Com,s}(t)].\Delta t + (c_{isoP}(t) - c_{EVch}).[N_{EV}^{Res,s}(t).P_{EVch}^{Res,s}(t) +$$
$$N_{EV}^{Ind}(t).P_{EVch}^{Ind,s}(t) + N_{EV}^{Com,s}(t).P_{EVch}^{Com,s}(t)].\Delta t + c_{EVcut}.P_{EVcut}^{Res,s}(t).\Delta t +$$
$$c_{EVcut}.P_{EVcut}^{Ind,s}(t).\Delta t + c_{EVcut}.P_{EVcut}^{Com,s}(t).\Delta t + c_{Pres}.P_{Drescut}^{s}(t) +$$
$$c_{Qres}.Q_{Drescut}^{s}(t) + c_{Pcom}.P_{Dcomcut}^{s}(t) + c_{Qcom}.Q_{Dcomcut}^{s}(t) +$$
$$c_{Pind}.P_{Dindcut}^{s}(t) + c_{Qind}.Q_{Dindcut}^{s}(t) + \sum_{i=1}^{N}c_G.P_{DG_icut}^{s}(t) +$$
$$\sum_{i1=1}^{N1}c_{ren}.P_{W_{i1}cut}^{s}(t) + \sum_{i2=1}^{N2}c_{ren}.P_{PV_{i2}cut}^{s}(t)\}\}$$

The revenue of the MG comes from selling the active power from the DGs, the discharging power of the battery, the power from the RDGs, discharging power of the EVs. The cost is constructed using equations

(2.15), (2.16), (2.1), (2.2), (2.3), (2.14), (2.11), (2.5), (2.6), and the last twelve components are the cost of unserved power to the EVs, cost of cut of the active and reactive residential, commercial, and industrial loads, and the cost of renewable and DGs generation cut.

The first stage of the objective functions of equations (6.36) and (6.40) is subjected to the constraints of equations (2.17) to (2.35), whereas the first stage of the objective functions of equations (6.38) and (6.42) is subjected to the constraints of equations (2.17) to (2.25), (2.30) to (2.33), (2.36), and (2.37). In addition, all the above objective functions are subjected to the constraints of equations (6.6) to (6.9), and (6.26). The second stage of these objective function is subjected to the same constraints of the first stage. However, the constraints of the equations (2.17), (6.26) are modified in the second stage to involve the uncertainties as in the following equations:

A. Active and reactive power balance constraints

These constraints are modified for the connected MG as follows

$$\sum_{t=1}^{T}\{\sum_{i=1}^{N}\delta_{DG_i}(t).P_{DG_i}{}^{s}(t)+\sum_{i1=1}^{N1}P_{W_{i1}}^{s}(t)+\sum_{i2=1}^{N2}P_{PV_{i2}}^{s}(t)+P_b{}^{s}(t)+ \quad \textbf{(6.43)}$$
$$P_g^s(t)+[N_{EV}^{Res,s}(t).P_{EVdis}^{Res,s}(t)+N_{EV}^{Ind}(t).P_{EVdis}^{Ind,s}(t)+$$
$$N_{EV}^{Com,s}(t).P_{EVdis}^{Com,s}(t)].\Delta t=\left(P_{Dres}(t)-P_{Drescut}^{s}(t)+\right.$$
$$N_{EV}^{Res,s}(t).P_{EVch}^{Res,s}(t).\Delta t-P_{EVcut}^{Res,s}(t).\Delta t\left.\right)+(P_{Dind}(t)-P_{Dindcut}^{s}(t)+$$
$$N_{EV}^{Ind}(t).P_{EVch}^{Ind,s}(t).\Delta t-P_{EVcut}^{Ind,s}(t).\Delta t)+(P_{Dcom}(t)-P_{Dcomcut}^{s}(t)+$$
$$N_{EV}^{Com,s}(t).P_{EVch}^{Com,s}(t).\Delta t-P_{EVcut}^{Com,s}(t).\Delta t)\}$$

The reactive power balance constraint as in equation (3.23)

For the isolated MG these constraints as follows

$$\sum_{t=1}^{T}\{\sum_{i=1}^{N}\delta_{DG_i}(t).{P_{DG_i}}^{s}(t)+\sum_{i1=1}^{N1}P_{W_{i1}}^{s}(t)+\sum_{i2=1}^{N2}P_{PV_{i2}}^{s}(t)+{P_b}^{s}(t)+ \quad \textbf{(6.44)}$$

$$[N_{EV}^{Res,s}(t).P_{EVdis}^{Res,s}(t)+N_{EV}^{Ind}(t).P_{EVdis}^{Ind,s}(t)+N_{EV}^{Com,s}(t).P_{EVdis}^{Com,s}(t)].\Delta t-$$

$$\sum_{i=1}^{N}c_G.P_{DG_icut}^{s}(t)-\sum_{i1=1}^{N1}c_{ren}.P_{W_{i1}cut}^{s}(t)-$$

$$\sum_{i2=1}^{N2}c_{ren}.P_{PV_{i2}cut}^{s}(t)=\big(P_{Dres}(t)-P_{Drescut}^{s}(t)+N_{EV}^{Res,s}(t).P_{EVch}^{Res,s}(t).\Delta t-$$

$$P_{EVcut}^{Res,s}(t).\Delta t\big)+(P_{Dind}(t)-P_{Dindcut}^{s}(t)+N_{EV}^{Ind}(t).P_{EVch}^{Ind,s}(t).\Delta t-$$

$$P_{EVcut}^{Ind,s}(t).\Delta t)+(P_{Dcom}(t)-P_{Dcomcut}^{s}(t)+N_{EV}^{Com,s}(t).P_{EVch}^{Com,s}(t).\Delta t-$$

$$-P_{EVcut}^{Com,s}(t).\Delta t)\}$$

The reactive power balance constraint of the isolated MG is as equation (3.25)

The constraint to prevent the system loads from exceeding the maximum capacity of the system is changed as follows

$$\sum_{t=1}^{T}\{P_{bch}^{s}(t)+((P_{Dres}(t)-P_{Drescut}^{s}+N_{EV}^{Res,s}(t).P_{EVch}^{Res,s}(t).\Delta t- \quad \textbf{(6.45)}$$

$$P_{EVcut}^{Res,s}(t).\Delta t)+(P_{Dind}(t)-P_{Dindcut}^{s}+N_{EV}^{Ind}(t).P_{EVch}^{Ind,s}(t).\Delta t-$$

$$P_{EVcut}^{Ind,s}(t).\Delta t)+((P_{Dcom}(t)-P_{Dcomcut}^{s}+N_{EV}^{Com,s}(t).P_{EVch}^{Com,s}(t).\Delta t-$$

$$P_{EVcut}^{Com,s}(t).\Delta t)\le S_{sys}.cos\theta\}$$

6.13 Results of the UC Stochastic Optimisation of the MG with Integration of the EVs

The proposed approaches are applied to the connected and isolated MG of the MG shown in Figure 6-3. The mean values of wind speed and PV power are listed in Table D-1 in appendix D, while the mean values of the number of the REVs and CEVs are connected to the grid are depicted in Figures 6-1 and 6-2. Figures E-1 and E-2 in appendix E show the generated scenarios for 24 hours ahead and final reduced scenarios for REVs and CEVs respectively. Two scenarios of the charging and discharging operations of the REVs are considered in this section. These two scenarios are the same of scenario 3 and scenario 4 that are considered in the deterministic case and they are as follows:

Scenario 1: whole period charging and discharging.

Scenario 2: the worst scenario.

6.13.1 Minimising the Total Operating Cost and Maximising the Profit

A. Connected MG

Scenario 1

Figures 6-30 and 6-31 show how the stochastic nature of the renewable generation and the EVs availability affect the optimal charging and discharging operations of the EVs. It can be noticed that for all scenarios the EVs are discharged at hour 6 because the OMP has high value at this hour and the OMP is higher than the discharging price. The IEVs and the REVs are charged when the price has low values during their connection to the grid. In addition, the highest charging power at hour 24 is in the Sc3 because it has abundant wind generation among other scenarios, whereas the Sc3 has the lowest charging power among other scenarios at hours 21 and 22 because at these hours it has zero renewable generation. Furthermore, the total load is increased significantly during off-peak load period for all the scenarios as shown in Figure 6-31because the REVs are charged at these hours.

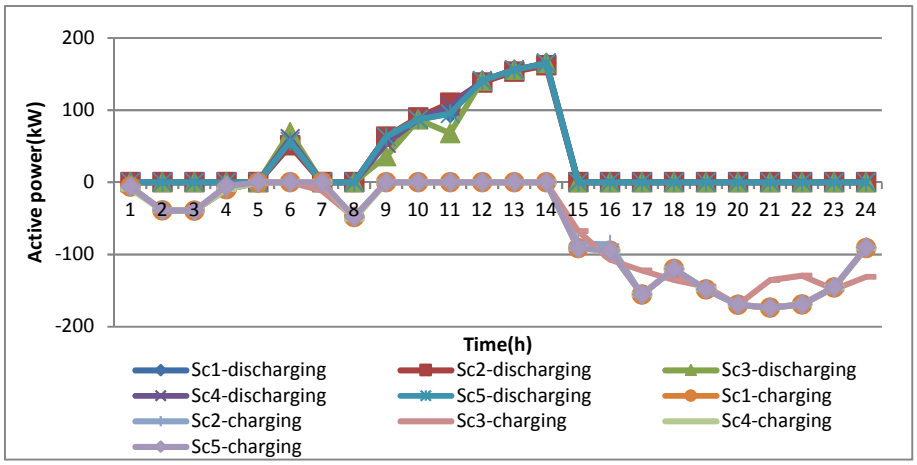

Figure 6-30 Optimal charging and discharging of the EVs of the five highest probability scenarios of the connected MG

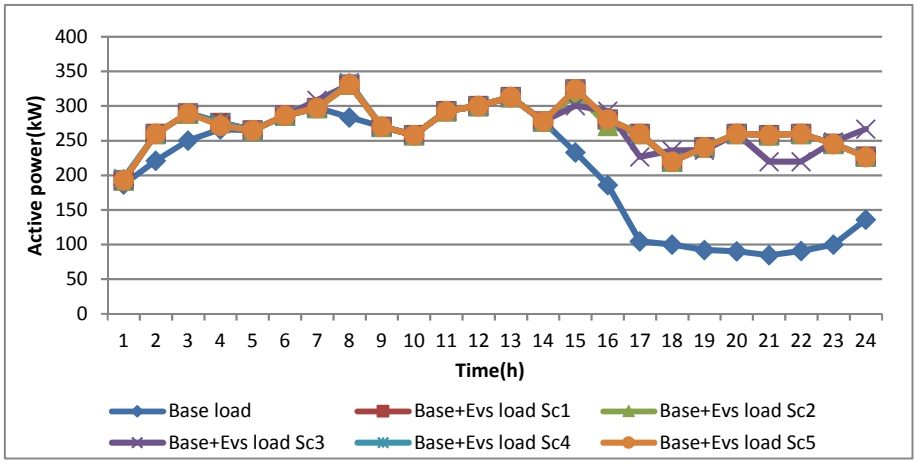

Figure 6-31 Modified load with the integration of the EVs of the five highest probability scenarios and base load of the connected MG

Figure 6-32 shows the impacts of the uncertainties on the optimal scheduling of the active power of the DGs and exchanging power with the storage battery and with the utility grid. It can be seen that the DE is committed to the whole scheduling day and some hours the DE is committed with minimum output power to satisfy the active and reactive SSSCs. The battery also is not operated for an entire scheduling period for all the scenarios for the same reasons of the Det. Case. In addition, the MG sells active power to the utility grid at hours 6 and 9 to 14 when the active OMP has the highest values, where the REVs are discharged at these hours and the IEVs and the CEVs are discharged at hour 6 as well because the values of the OMP are higher than the discharging price. Further, the Sc3 has the lowest selling power to the utility grid at hour 12 because it has the lowest wind generation among the other scenarios. In contrast, the reactive power scheduling is not changed when consideration the uncertainties because the UC of the DGs for all scenarios are the same of the Det. Case and the UC is determined before realisation the uncertainties. Furthermore, the EVs exchange solely active power with grid and the RDGs provide active power.

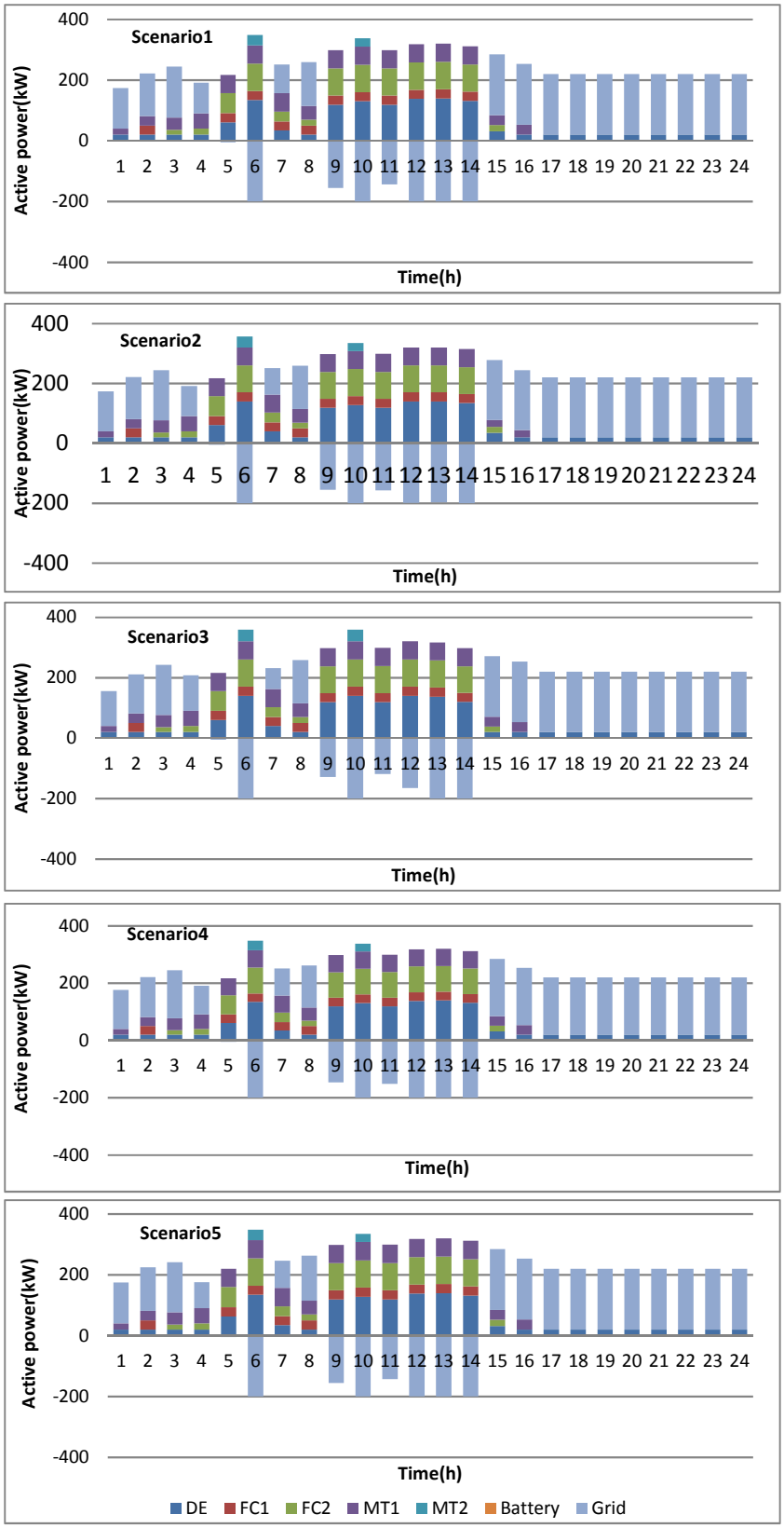

6-32 Optimal active power scheduling of the DGs and exchanging power with the utility grid and the battery of the five highest probability scenarios

Table 6-8 summarises the results of the five stochastic scenarios and Det. Case. This table reveals that the integration of the EVs with the MG reduces the total operating cost and increases the MG profit in comparison with the base case for all scenarios. The percentage of reducing the cost and increasing profit are in comparison with the base case. The total peak load is increased slightly for all the scenarios.

Table 6-8 Results of the five highest probability scenarios and Det. Case of the connected MG

	Cost with EVs (€/day)	Cost reduction %	Profit with EVs (€/day)	Profit increasing %	Charging cost (€)	Discharging cost (€)	Peak load(kW)
Det. case	323.1	20.8	366.2	30.1	116.3	117.6	328.38
Sc1	321.8	21.1	367.5	30.6	120	100.7	331.38
Sc2	322.5	20.9	366.8	30.3	118.8	100.7	331.38
Sc3	325.3	20.2	364	29.3	115.5	100.7	331.8
Sc4	321.8	21.1	367.5	30.6	120.5	100.7	334.38
Sc5	321.4	21.2	367.9	30.7	119.6	100.7	331.38

Scenario 2

Figure 6-33 shows the optimal charging behaviours of the EVs during their connection to the grid and Figure 6-34 shows the impacts of the EVs on the total load for the five highest probability scenarios. It can be noticed that for all the scenarios the lowest charging power occurs at hour 1 because solely the small number of the CEVs are connected to the grid at this hour. The charging power of the EVs also has low values at hour 6 because at this hour the OMP has high value and higher than the charging price; therefore, the MG sells power to the utility grid rather than to the EVs. In addition, the lowest charging power is in the Sc2 at hour 6 because it has the lowest number of the connecting EVs to the grid at this hour and the two hours before hour 6. By far the highest charging power is at hour 11 because the highest numbers of the REVs are connected to the grid for all scenarios and the highest one occurs in the Sc2 because it has the highest number of the EVs at hour 11 and the previous two hours.

Figure 6-35 shows the impacts of the uncertainties on the hourly optimal scheduling of the active power. The battery is discharged highest power at hour 10 because the OMP has the highest value and it is charged when the price has low values for all scenarios. The MG also sells active power to the utility grid when the OMP has high values, wherein the lowest selling power is at hour 12 for all scenarios and the lowest selling power occurs in the Sc3 because it has the lowest wind generation at this hour. In addition, in the Sc3 the MG purchases higher active power at hours 21 and 22 than other scenarios because the renewable generations at these hours equal to zero.

The reactive power scheduling of the DGs and exchanging reactive power with the utility grid are the same for the all five scenarios and they are the same of the Det. Case.

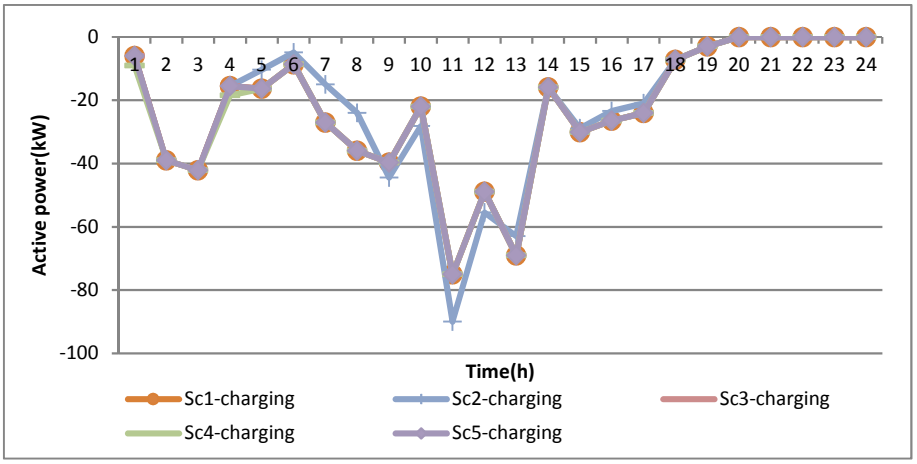

Figure 6-33 Optimal charging of the EVs of the five highest probability scenarios of the connected MG

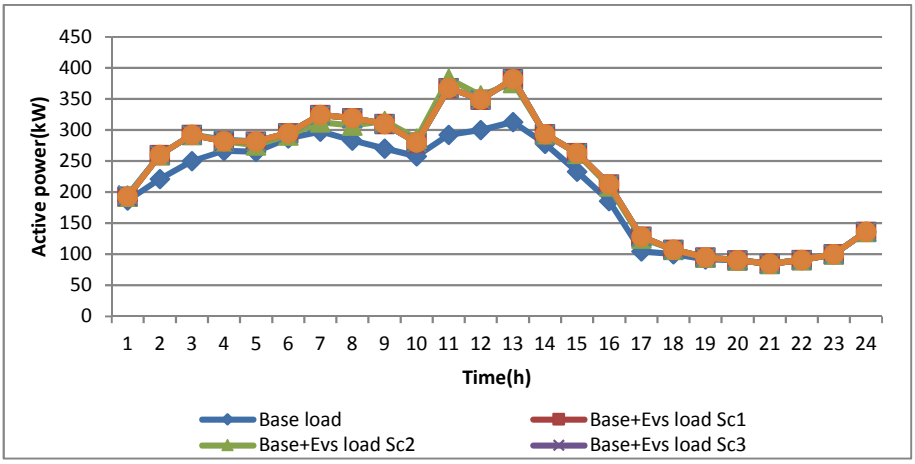

Figure 6-34 Modified load with integration of EVs of the five highest probability scenarios and base load of the connected MG

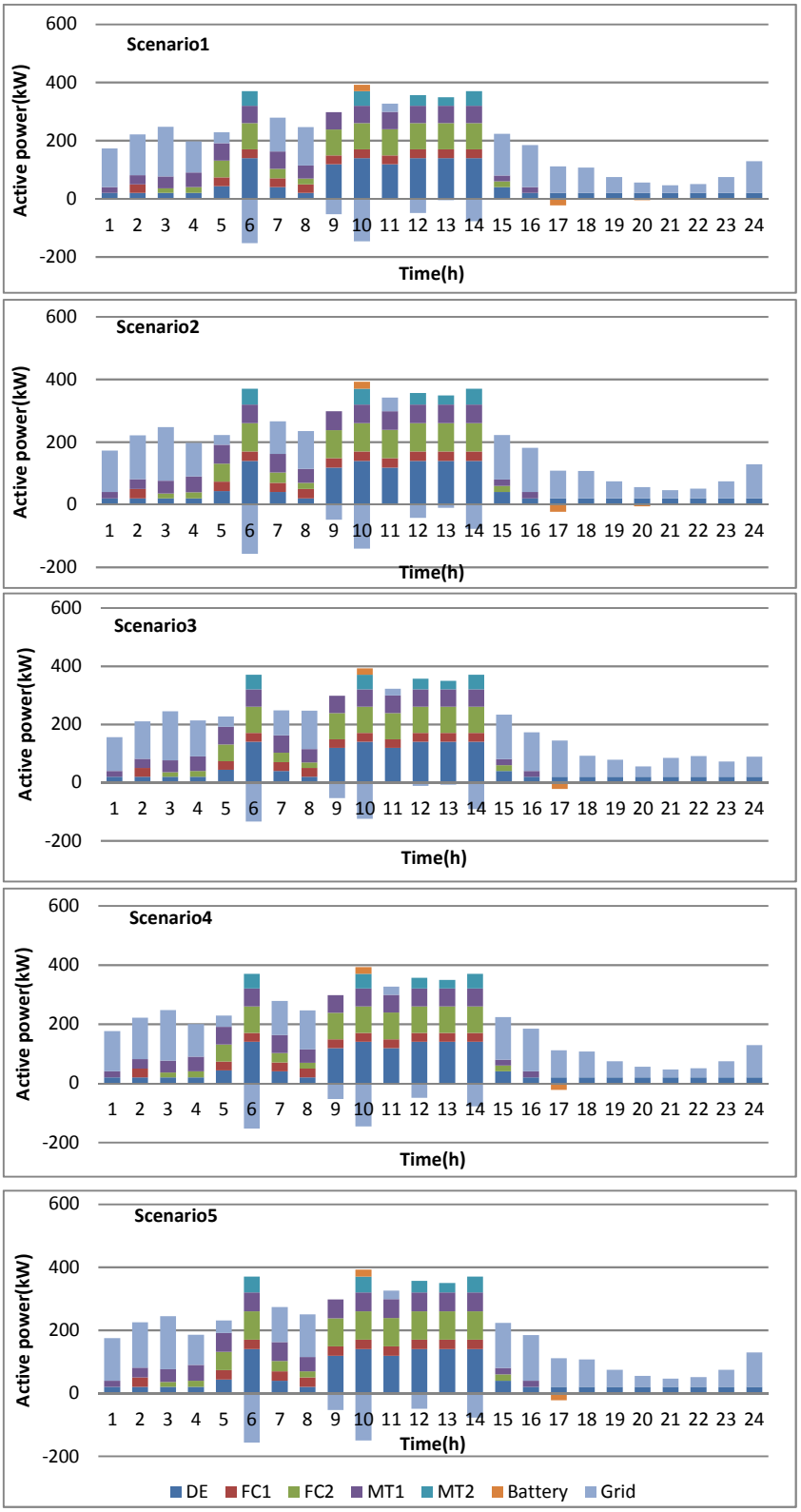

Figure 6-35 Optimal active power scheduling of the DGs and exchanging power with the utility grid and the battery of the five highest probability scenarios

Table 6-9 summarises the results of the five high probability scenarios and Det. Case. It can be seen that the total cost is increased and the profit is reduced for all scenarios in comparison with the base case. This is because the EVs are operated in the charge mode only and the charging power is lower than OMP in some hours and the charging power is lower than the generation of the DGs as well. The charging time for the EVs is restricted. Furthermore, the peak of the total load is increased because the time restriction of the charging of the EVs and the charging time coincides with peak load.

Table 6-9 Results of the five highest probability scenarios and Det. Case of the connected MG

	Cost with EVs (€/day)	Cost reduction %	Profit with EVs (€/day)	Profit increasing %	Charging cost (€)	Discharging cost (€)	Peak load(kW)
Det. case	439.5	-8	249.8	-11.3	43.7	0	376.6
Sc1	441.5	-8.3	247.9	-11.9	44.1	0	376.6
Sc2	444.5	-9	244.8	-13	43	0	382.6
Sc3	447.4	-9.7	241.9	-14.1	44.1	0	382
Sc4	441.4	8.2	247.9	-11.9	4.6	0	382
Sc5	439.9	7.9	249.5	-11.4	44.1	0	382

B. Isolated MG

Scenario 1

Figure 6-36 shows the optimal charging operations of the EVs of the five highest probability scenarios and Figure 6-37 shows the impacts of the EVs on the total load of the five highest probability scenarios. It can be noticed that the EVs in all sectors interact with the MG in the charge mode only for the same reasons of the Det. Case. The IEVs and CEVs have two peaks of charging power during their connection to the grid at hours 2 and 4 because at these two hours, the load has low values and the renewable generation is abundant. At hour 2, the highest charging power is in the Sc3 because it has the highest renewable generation among other scenarios, while Sc5 has the lowest charging power because it has the lowest renewable generation at this hour. For the same reasons, at hour 4 the highest charging power is in the Sc5, while the lowest charging power is in the Sc3. Further, the REVs are charged at off-

peak load hours for the same reasons of the Det. Case, where the highest charging power is at hour 21 for scenarios 1, 2, 4, and 5 because the wind generation is abundant for these scenarios and the load has the lowest value. While, for the Sc3 the highest charging power is at hour 20 because at hour 21 the renewable generation is zero, whereas at hour 20 the wind generation is abundant. Furthermore, the charging power at hour 24 for scenarios 1, 2, 4, and 5 is zero because the wind generation is zero and solar generation quite low, while the Sc3 has charging power at this hour because the wind generation has a maximum value. Figure 6-37 reveals that the peak load is not changed because there is no charging during on peak load.

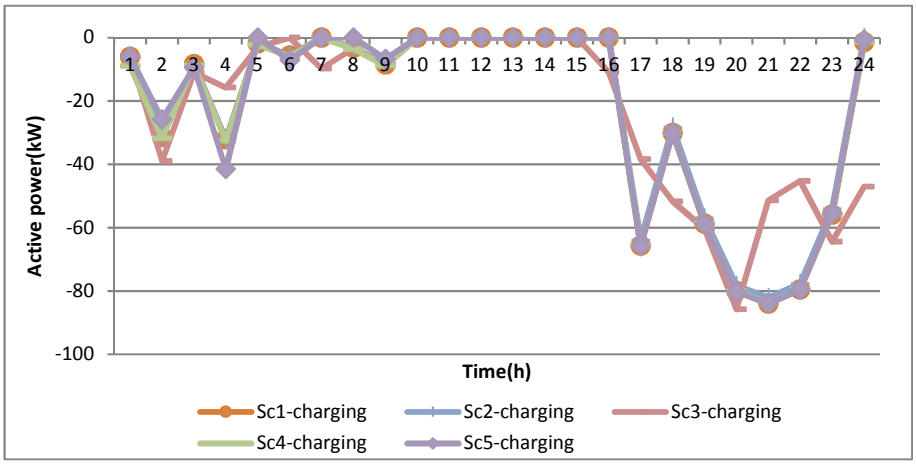

Figure 6-36 Optimal charging and discharging of the EVs of the five highest probability scenarios and Det. Case of the isolated MG

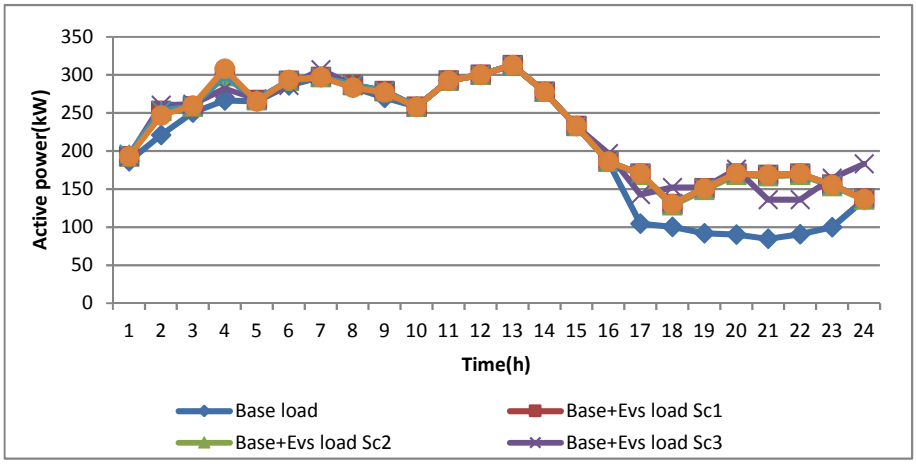

Figure 6-37 Modified load with the integration of the EVs of the five highest probability scenarios and base load of the isolated MG

Figure 6-38 shows the optimal scheduling of the active power of the DGs. The fluctuations of the renewable generation and availability of the EVs are compensated by changing the generation of the DGs as shown in the figure. The battery is not operated for all scenarios because there are no economic incentives for involving the battery in the active power scheduling. In addition, the highest generation occurs at hour 14 for scenarios 1, 2, 4, and 5, although the highest load is at hour 13 because at hour 14 the wind generation has the lowest value. For the Sc3, the highest generation is at hour 12, although the load has highest value at hour 13 because the wind and solar generation have the lowest value at hour12, while wind generation has the maximum value at hour 13. The optimal reactive power scheduling is the same for all five scenarios and they are the same of the Det. Case for the same reasons of the connected MG.

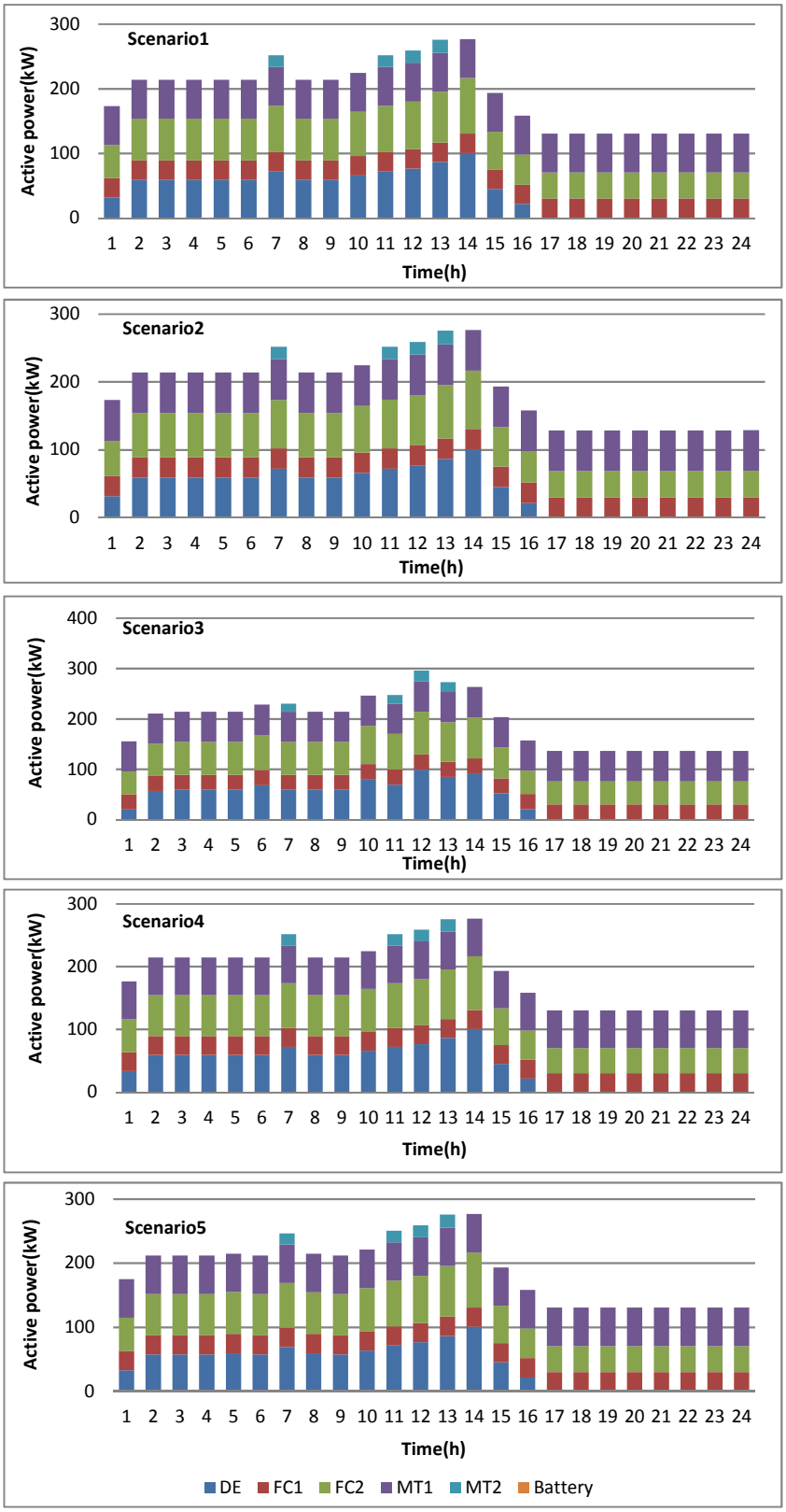

Figure 6-38 Optimal active power scheduling of the DGs and exchanging power with the battery of the five highest probability scenarios

Table 6-10 summarises the results of the five scenarios and Det. Case. It can be seen that the peak of the total load is not changed for all the scenarios because the charging of the EVs is for the whole period of the connection of the EVs. The operating cost is higher than the base case for all the scenarios and the profit is lower.

Table 6-10 Results of the five highest probability scenarios and Det. Case of the isolated MG

	Cost with EVs (€/day)	Cost reduction %	Profit with EVs (€/day)	Profit increasing %	Charging cost (€)	Discharging cost (€)	Peak load(kW)
Det. Case	560.9	-2	223.3	-4.8	43.7	0	313
Sc1	559.4	-1.8	224.8	-4.1	44.1	0	313
Sc2	559.1	-1.7	225.1	-4	43	0	313
Sc3	560.4	-1.9	223.8	4.6	44.1	0	313
Sc4	559.7	1.82	224.5	4.3	44.6	0	313
Sc5	559.1	-1.7	225.1	-4	44.1	0	313

Scenario 2

Figure 6-39 shows the optimal charging of the EVs for the five highest probability scenarios, whereas Figure 6-40 shows the base load and the base load with EVs charging load for the five highest probability scenarios. It can be noticed that there are two peak periods at hour 2 and hour 4 for the same reasons of the previous scenario. The lowest charging power occurs at hours 5 and 7 in the Sc2 because it has low renewable generation and the number of connected IEVs and CEVs to the grid at these hours and the two hours before these two hours is lower than the other scenarios. Furthermore, the highest charging power for all scenarios is at hour 11 because the highest number of the REVs is connected to the MG. Figure 6-40 shows that the total load is increased throughout the charging period of the EVs because the EVs are operated with charge mode only, where the Sc3 has the highest peak load at hour 13 because the Sc3 has the highest charging power at this hour. The reactive load is still not changing and it is the same of the base case.

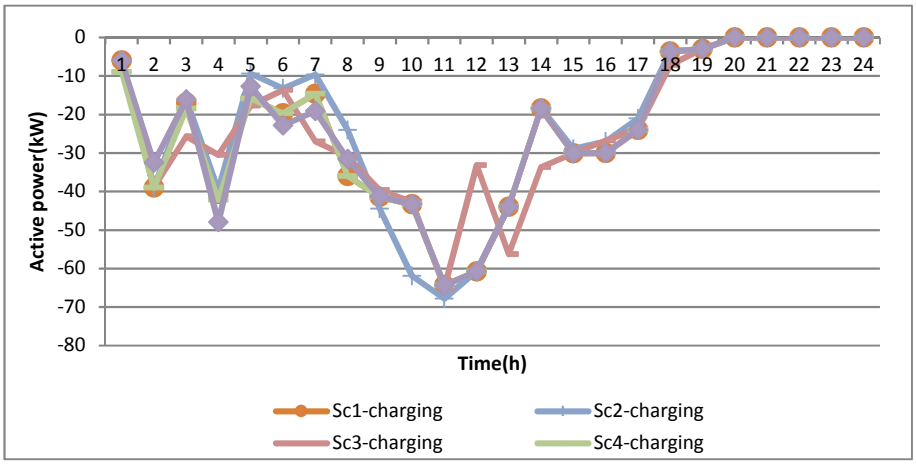

Figure 6-39 Optimal charging of the EVs of the five highest probability scenarios of the isolated MG

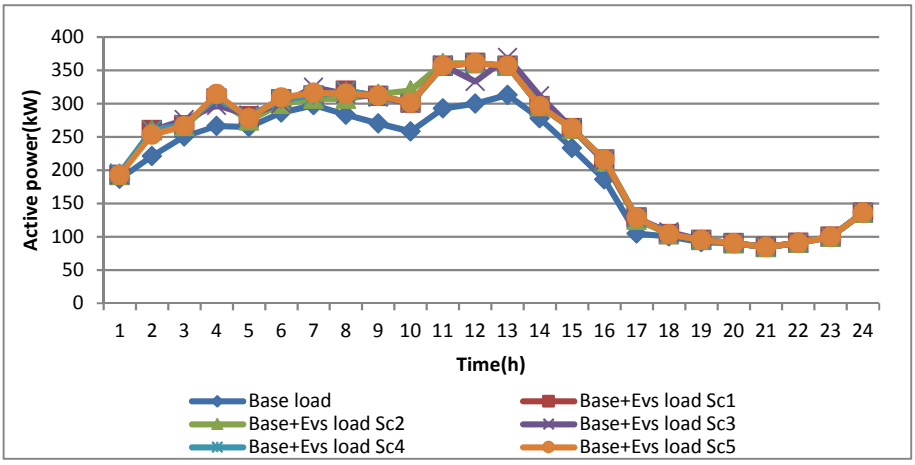

Figure 6-40 Modified load with the integration of the EVs of the five highest probability scenarios and base load of the isolated MG

Figure 6-41 shows the optimal scheduling of the active power of the DGs. This figure shows the impacts of the uncertainties on the optimal scheduling of the DGs. It can be seen that the highest generation occurs at hours 11, 12, and 13 for the all scenarios because the total load has the highest values at these hours and the charging power is high as well. However, the Sc3 has the lowest generation at hour 11 among other scenarios because at hour 11 the Sc3 has the highest renewable generation. The Sc3 has the higher generation at hours 21 and 22 than other scenarios because the renewable generations are equal to zero, While the Sc2 has lower generation than other scenarios at hour 24

because the wind generation has the maximum value. The optimal reactive power is the same for all five scenarios and they are the same of the Det. Case.

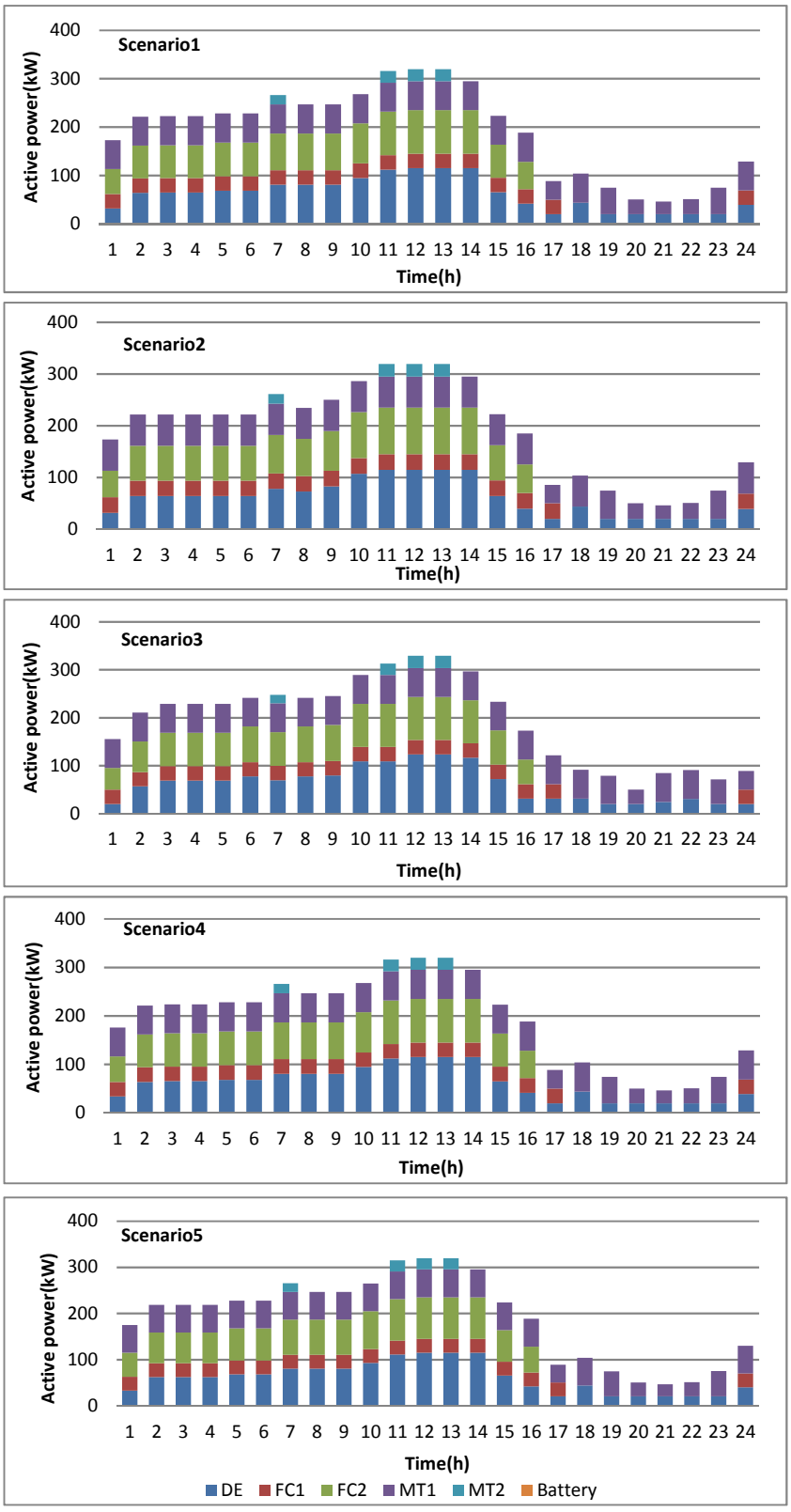

Figure 6-41 Optimal active power scheduling of the DGs and exchanging power the battery of the five highest probability scenarios

Table 6-11 summarises the results of the five scenarios and Det. Case. This table reveals that the total cost for all scenarios is increased and the profit is decreased. The peak of the total load is increased for all the scenarios because the charging power of the EVs coincides with the peak load.

Table 6-11 Results of the five highest probability scenarios and Det. Case of the isolated MG

	Cost with EVs (€/day)	Cost reduction %	Profit with EVs (€/day)	Profit increasing %	Charging cost (€)	Discharging cost (€)	Peak load (kW)
Det. Case	577.9	-5.1	206.3	-12	43.7	0	362.481
Sc1	576.8	-4.9	207.4	-11.6	44.1	0	360.923
Sc2	576.5	-4.87	207.7	-11.4	43	0	360.786
Sc3	576.5	-4.87	207.7	-11.4	44.1	0	369.261
Sc4	577.1	-5	207.1	-11.7	44.6	0	360.923
Sc5	576.4	-4.85	207.8	-11.38	44.1	0	360.935

6.14 Chapter Conclusion

In this chapter, the bidirectional integration of the EVs with the SCUC-UARDEED of the connected and isolated MG is analysed under deterministic and stochastic environments. The results reveal that the EVs decrease the total operating cost and increase the profit of the connected MG. The OMP affects significantly the charging and discharging operations of the connected MGs. In addition, the reactive power scheduling is changed, although the EVs charge and discharge active power because the EVs changes the results of the UC and it is formulated based on the active and reactive power. In case of isolated MG, the EVs increase the total operating cost and decrease the profit. the uncertainties affect the charging and discharging operations of the EVs. Feasible solution is obtained for all scenarios.

7 Conclusions and Future Work

7.1 Chapter Summary

This chapter contains the discussions and conclusions in relation to the three core areas of this thesis. Firstly, the SCUC-UARDEED of the MG discussions and conclusions are presented under deterministic and stochastic environments; second the discussions and conclusions of the integration of the DSM with optimisation problems of the MG under deterministic and stochastic environments are introduced; and third the integration of EVs with the optimal scheduling of the MG discussions and conclusions are presented. Furthermore, this chapter also recommends the future works related to the area of the thesis.

7.2 Discussions and Conclusions

7.2.1 Unified Active and Reactive Dynamic Economic and Emission Dispatch of the MG

A SCUC-UARDEED to minimise the total operating and emission costs or maximise the MG profit is proposed. One of the goals of this research is to formulate and solve the unified active and reactive optimisation problem and determine the active reactive power scheduling of the MG resources. The models for the emission of the greenhouse gases are included in the formulation of the optimisation problem to reduce the negative impacts to the environment. To involve the battery in the scheduling of the MG, the model of its degradation cost is considered. The model of the UC is developed to involve both the active and reactive power. In addition, the models of the exchanging active and reactive power with the utility grid are incorporated in the scheduling of the connected MG. Furthermore, the production cost of renewable generation is included in the proposed optimisation approach. The scheduling problem of the MG is subjected to a set of constraints, including active and reactive power SSSCs, active and reactive power SRCs, and limit of emission of the greenhouse gases. These models of the different cost function components and the constraints are combined in a unified optimisation approach, which can be

solved in real-time. Literature has shown that no work has been done in analysing the models of reactive power management, emission cost, and battery degradation cost with emission and security constraints in the modelling of the optimisation problem to minimise the operating cost or maximise the profit for the connected and isolated MG. New approaches and strategies are proposed to model all these cost parameters and constraints and they are incorporated with the DEED problem of the MG. The optimisation problem is validated by testing the proposed approaches on the LV multi-feeder connected and isolated MG. The MG includes various types of loads, such as residential, commercial and industrials. Each load type has a different profile, where the active and reactive total loads are aggregated of these loads. The MG includes different types of the DGs technology, such as DE, MTs, FCs, WTs, and PV units. This combination presents a good renewable mix likely to be found in the future grid. The overall optimisation problems are formulated by using MIQP, which can be solved efficiently by using the efficient software platform CPLEX. It is based on the branch and bond method, and if a solution is obtained from this method, it is known as a globally optimal solution.

The importance of the DGs to generate reactive power is quantified in Chapter 2. The obtained results reveal that the total operating cost is reduced and the profit is increased when the DGs generate reactive power is compared with the reactive power from the utility grid. The impacts of the storage battery on the optimal scheduling of the MG are determined, where different scenarios for the state of charge of the battery are conducted to determine the ultimate impacts of the storage battery on the economic operation of the MG. The results show that the charging and discharging operations of the battery typically reduce the total operating cost and increase the MG profit in all scenarios for the connected MG, despite the degradation cost of the battery. The impacts of the active and reactive power SSSCs for full and critical loads on the optimal scheduling of the MG are determined. It is found that consideration given to the SSSCs makes the MG operate securely throughout the entire schedule. Consideration of the SSSCs also helps the system operator to avoid resorting to the costly

involuntary load shedding when the connection with the utility grid is lost. Furthermore, the SSSCs guarantee a continuous operation when the MG loses the connection with the utility grid. However, consideration of the active and reactive power SSSCs increases the total operating cost and reduces the profit. In contrast, the reduction of the technical minimum of the active output power of the DGs with consideration given to the active and reactive power SSSCs, leads to a reduction in the total operating cost, increases the MG profit, and reduces the emission of the greenhouse gases.

In particular, the results of the proposed connected MG demonstrate that the lowest cost occurs at the same time with the highest profit and both occur when the OMPs have the highest value because at this hour MG sells the highest active and reactive power to the utility grid to reduce the cost or increase the profit. The revenue and the profit patterns also have the same shape of the OMPs. In addition, the total cost has a negative value when the OMPs have the highest value during the scheduling day. In the isolated MG, the profit and the cost profiles have a similarity to the power generation, where the pattern shapes of the active and reactive power generation are close to the pattern of the total load. The profit and the total cost have only positive values during the entire scheduling horizon.

Chapter 3 presents a developed stochastic optimisation scenario-based approach, based on the same models of the cost components and constraints in Chapter 2 with the uncertainties arising from the fluctuations of the generation of the renewable resources and the OMPs. This increases the complexity of the scheduling problem of the MG. Therefore, a new scheduling strategy to model and incorporate these uncertainties with SCUC-UARDEED of the MG is proposed, which involves a stochastic optimisation problem with a two-stage approach. The first stage involving the decision variables are the UC results before taking into account the uncertainties, and the second stage is the scheduling of the MG resources by considering the uncertainties where the UC results are not changed in the second stage. The second stage of the objective functions includes the penalty cost of the involuntary load cutting for the

connected MG, while the objective function of the isolated MG contains the involuntary load and generation cutting. The load and generation cutting are considered to prevent the system from outages and to insure feasible solution in the second stage, therefore, the penalty costs of the load and generation cutting are taken significantly high to avoid the system from resorting to load or generation cutting when it is not necessary.

The results obtained demonstrate that the proposed optimisation approaches can accommodate the uncertainties. In addition, a feasible solution for all scenarios and for the connected and isolated MG of the system under study are obtained. The OMP significantly impacts on the charging and discharging operations of the battery.

7.2.2 Integration of the DSM with Dynamic Economic and Emission Dispatch of the MG

A novel approach and methodology are proposed to integrate the DSM with SCUC-UARDEED of the connected and isolated MG. This is presented in Chapter 4. The DSM techniques are developed to consider both active and reactive load demands. All load types that are considered in Chapter 2 participate in the active and reactive DSM techniques, wherein different strategies of the DSM are applied to the different types of load simultaneously. The shifting technique is applied to the residential loads, where the start times of connecting the WMs and DWs are shifted based on the optimisation algorithm as to whether minimise the operating cost or to maximise the profit of the connected and isolated MG. The impacts of the DSM as a shifting technique on the profit of the isolated MG have not been analysed yet. Similarly, the active and reactive DB strategy is applied to the industrial and commercial loads, where the consumers in the industrial and commercial sectors offer the load cutting with the specific price. The MG should accept or reject the bids of the consumers according to the objective function. The DSM is considered as a decision variable in the optimisation approach and it is treated as a separate load with an operation cycle. The overall formulation of the optimisation problem

of the MG with DSM involves the same models of the cost components and constraints in Chapter 2 with integrating the models of the DSM techniques with their constraints. Three key scenarios based on deterministic environment are conducted to analyse the impacts of the DSM on the optimal scheduling of the MG.

Firstly, the DSM as a shifting technique is applied to active and reactive residential loads. The results demonstrate that the proposed DSM reduces the total operating cost and reduces the peak of the active and reactive total loads of both the connected and isolated MG. In addition, the grid security and the reserve of the active and reactive generations are improved. Moreover, the OMPs significantly impact on the time and the amount of the recovered load with regard the operating cost of the connected MG. In contrast, in the case of maximising the profit, the obtained results reveal that the proposed DSM of the connected MG insignificantly impacts on the profit, while for the isolated MG the profit is increased. The profit is increased in the isolated MG because the MG sells active and reactive power to the consumers with fixed prices for the entire scheduling horizon, and there is no connection to the utility grid. Therefore, the loads can be shifted and recovered, regardless of the price. This means that the revenue is not affected when the loads are shifted and only the expense is affected. The shifting load of the isolated MG reduces the expense and this leads to increase the MG profit.

Secondly, the DSM as a shedding load technique is applied to the active and reactive industrial and commercial loads. It is found that the proposed DSM reduces the total operating cost and the peak of the active and reactive total loads are reduced for both the connected and isolated MG. In the case of maximising the MG profit, the results reveal that the MG does not accept the consume bids to cut the loads in both the connected and isolated MG because the load cutting costs are incurred by the MG, which leads to a reduction the profit. This means that applying the DSM as a curtailed load is not recommended to maximise the profit.

Thirdly, both the shifting and DB techniques are applied to the all types of loads simultaneously. The results reveal that the operating cost and the peak of the total active and reactive load is reduced more than when applying the shifting or DBP technique individually. In contrast, to maximise the MG profit and for the connected and isolated MG, the results are the same as applying the shifting technique because the curtailed load is not preferable.

Furthermore, a two-stage stochastic optimisation of the MG with the integration of the DSM is presented in Chapter 5. The estimated number of WMs and DWs at each time interval are determined from the diversified curve, which is considered as perfect. However, in reality, it is not perfect and it produces new uncertainty to the optimisation problem. The fluctuations generated from the renewable resources and the number of the WMs and DWs are considered as stochastic variables. According to the open literature, the DSM as a stochastic variable has never been investigated in the previous work. The same constraints and cost components' models of Chapters 2 and 4 with the uncertainties are considered into proposed stochastic optimisation approach. In the first stage, the decision of the UC and the bids of the industrial and commercial consumers to cut their loads are taken, where these decisions are not changed in the second stage. The second stage includes the scheduling of the MGs resources and demand side while considering the uncertainties. The optimisation approach is applied to the connected and isolated MG. In addition, the obtained results through different scenarios demonstrate that the proposed approach can accommodate the uncertainties from both the generation and demand side. The obtained results also reveal that a feasible solution can be obtained for all scenarios and for the connected and isolated MG under study.

7.2.3 Integration of the EVs with Security-Constrained Dynamic Economic and Emission Dispatch of the MG

A novel multi-period optimal scheduling of the MG with bidirectional integration of the EVs to minimise the total operating cost or maximise the profit of the connected and isolated MG is presented in Chapter 6. The bidirectional

integration of the EVs is more challenging than unidirectional integration (charging or discharging) and the bidirectional integration covers both the charging and discharging operations of the EVs. Therefore, the modelling of bidirectional integration needs new optimisation approaches and strategies to integrate the EV with optimal scheduling of the MG. The EVs are modelled with their constraints and the EVs are incorporated with optimisation problems of the MG together with the models of the cost function components and constraints in Chapter 2. The charging and discharging prices are unchanged whether the EVs charge or discharge. This is to encourage the EVs to involve in the scheduling resources of the MG. Multiple charging and discharging scenarios are conducted to inspect the impacts of the EVs on the optimal scheduling of the MG.

The results show that the proposed economic integration of the EVs with connected MG reduces the total operating cost and increases the profit. Furthermore, the OMP significantly impacts to determine the charging and discharging operations of the EVs. In contrast, in the case of the isolated MG, the integration of the EVs increases the total operating cost and decreases the profit because the discharging price is higher than the generation cost of the of the DGs, and the charging price is lower than the cost of generating the DGs. In particular, the integration of the EVs changes the reactive power scheduling, although the EVs are charged and discharged only active power because the integration the EVs change the UC results of the DGs and the UC is formulated based on both the active and reactive power.

A two-stage scenario-based optimisation problem with the integration of the EVs is introduced. The number of EVs are connected to the MG at each time interval in different areas with the fluctuations of the generation of the renewable generation are considered as sources of the uncertainties. These uncertainties are modelled and incorporated with stochastic scheduling problem of the MG with including the models of cost components and constraints in chapters 2 and 6. The first stage involves the UC results of the DGs before consideration the uncertainties, while the second stage is the scheduling of the

MG resources and the charging and discharging operation of the EVs. The results show that the proposed approach can accommodate the uncertainties and it can obtain a feasible solution for all scenarios for connected and isolated MG. The uncertainties also affect the charging and discharging behaviours of the EVs in the connected and isolated MG.

7.3 Recommendations for Future Works

In this section, recommendations for future works relating to the subject of this thesis are addressed. The following recommendations all equally weighted and important:

A. The future MGs can provide both the heat and the electricity. Therefore, the optimisation problem can be extended to involve combined heat and electrical power (CHP) with modelling of the active and reactive economic and emission dispatch of the MG under deterministic and stochastic environments. The heat recovery boiler can be considered as a heat generator to supply the heat load. This needs to develop scheduling strategy to accommodate the scheduling both the electricity and the heat.

B. New demand management strategies to manage both the heat and electric loads are needed to quantify the impacts of these management strategies on the economic operation of the MG.

C. The time-based programming, such as time of use and real-time prices can be used as the DSM techniques, wherein the load management or reduction has to be accomplished by consumers in response to the price. These DSM techniques can incorporate an optimisation problem of the MG under deterministic and stochastic environments.

D. New sources of uncertainties related to the grid and to the DGs such as outages of generation or losing lines can be modelled and incorporated with optimisation algorithms of the MG. These increase complexity of the scheduling

strategy in term of formulation and solution. This needs to develop scheduling strategy to accommodate these uncertainties.

E. The EVs can be integrated with optimisation problems as demand response appliances to manage the network congestion and to increase the network capability in accommodating the renewable energy.

F. The huge developments of the battery technologies need to develop new models of the batteries and consider new pricing scheme to involve the EVs in the scheduling operation of the MG.

G. The proposed optimisation approaches in this work can be analysed with respect of the sensitivity of the system to change in the MG parameters.

REFERENCES

[1] M. K. Al-saadi, Patrick C. K. Luk, W. Fei, and A. Bati, “Security Constrained Active and Reactive Optimal Power Management of Microgrid in Different Market Policies,” in *UKACC 11th International Conference on Control (CONTROL), Belfast, UK, 31st August-2nd September, 2016*.

[2] L. I. Dulău, M. Abrudean, and D. Bică, “Effects of Distributed Generation on Electric Power Systems,” *Procedia Technol.*, vol. 12, pp. 681–686, 2014.

[3] P. P. Padhi, R. K. Pati, and A. A. Nimje, “Distributed generation : Impacts and cost analysis,” *Int. J. Power Syst. Oper. Energy Manag.*, vol. 1, no. 3, pp. 91–96.

[4] A. M. Elaiw, X. Xia, and A. M. Shehata, “Application of model predictive control to optimal dynamic dispatch of generation with emission limitations,” *Electr. Power Syst. Res.*, vol. 84, no. 1, pp. 31–44, 2012.

[5] X. S. Han, H. B. Gooi, and D. S. Kirschen, “Dynamic economic dispatch: feasible and optimal solutions,” *IEEE Trans. Power Syst.*, vol. 16, no. 1, pp. 22–28, 2001.

[6] X. P. Liu, M. Ding, J. H. Han, and P. P. Han, “Dynamic Economic Dispatch for Microgrids Including Battery Energy Storage,” in *Power Electronics for Distributed Generation Systems (PEDG), 2nd IEEE International Symposium, Hefei, China, 16-18 June, 2010*.

[7] X. Xia and A. M. Elaiw, “Optimal dynamic economic dispatch of generation: A review,” *Electr. Power Syst. Res.*, vol. 80, no. 8, pp. 975–986, 2010.

[8] A. Parisio, E. Rikos, and L. Glielmo, “A model predictive control approach to microgrid operation optimization,” *IEEE Trans. Control Syst. Technol.*, vol. 22, no. 5, pp. 1813–1827, 2014.

[9] W. Su. and J. Wang, “Energy Management Systems in Microgrid Operations,” *Electr. J.*, vol. 25, no. 8, pp. 45–60, 2012.

[10] Antonis G. Tsikalakis and Nikos D. Hatziargyriou, “Operation of microgrids with demand side bidding and continuity of supply for critical loads,” *Eur. Trans. Electr. POWER*, vol. 21, pp. 1238–1254, 2011.

[11] N. L. Dıaz, A. C. Luna, J. C. Vasquez, and J. M. Guerrero, “Centralized Control Architecture for Coordination of Distributed Renewable Generation and Energy Storage in Islanded AC Microgrids,” *IEEE Trans. Power Electron.*, vol. 32, no. 7, pp. 5202–5213, 2017.

[12] M. Gavrilas, “Heuristic and metaheuristic optimization techniques with application to power systems,” in *international conference on Mathematical methods and computational techniques in electrical engineering, Timisora, Romania, 21-23 October, 2010*, pp. 95–103.

[13] A. A. HAMISU, “Petroleum Refinery Scheduling With Consideration for Uncertainty,” PhD Thesis, Cranfield University, 2015.

[14] Mostafa M. Delshad, Sam K. Kamali, Ehsan. Taslimi, S. HR. A. Kaboli, and N. A. Rahim, “Economic dispatch in a microgrid through an iterated-based algorithm,” in *IEEE Conference on Clean Energy and Technology, CEAT , Langkawi, Malaysia, 18-20 November, 2013*, pp. 82–87.

[15] J. P. Fossati, “Unit Commitment and Econmoic Dispatch in Microgrid,” *Mem. Trab. Difusión Científica y Técnica, núm*, vol. 10, pp. 83–96, 2012.

[16] A. Parisio, E. Rikos, G. Tzamalis, and L. Glielmo, “Use of model predictive control for experimental microgrid optimization,” *Appl. Energy*, vol. 115, pp. 37–46, 2014.

[17] R. Palma-Behnke, C. Benavides, F. Lanas, B. Severino, L. Reyes, J. Llanos, and D. Saez, “A microgrid energy management system based on the rolling horizon strategy,” *IEEE Trans. Smart Grid*, vol. 4, no. 2, pp. 996–1006, 2013.

[18] H. Kanchev, B. F. S. Member, and V. Lazarov, “Unit commitment by dynamic programming for microgrid operational planning optimization and emission reduction,” in *International Aegean Conference on Electrical Machines and Power Electronics, ACEMP, Joint Conference, Istanbul, Turkey, 8 -10 September, 2011*.

[19] M. A. Abido, “Multiobjective evolutionary algorithms for electric power dispatch problem,” *IEEE Trans. Evol. Comput.*, vol. 10, no. 3, pp. 315–329, 2006.

[20] S. Agrawal, B. K. Panigrahi, and M. K. Tiwari, “Multiobjective Particle Swarm Algorithm With Fuzzy Clustering for Electrical Power Dispatch,” *Evol. Comput. IEEE Trans.*, vol. 12, no. 5, pp. 529–541, 2008.

[21] V. Vahidinasab and S. Jadid, “Joint economic and emission dispatch in energy markets: A multiobjective mathematical programming approach,” *Energy*, vol. 35, no. 3, pp. 1497–1504, 2010.

[22] B. Hadji, B. Mahdad, K. Srairi, and N. Mancer, “Multi-objective PSO-TVAC for Environmental/Economic Dispatch Problem,” *Energy Procedia*, vol. 74, pp. 102–111, 2015.

[23] M. A. Abido, “Environmental/economic power dispatch using

multiobjective evolutionary algorithms," *IEEE Trans. Power Syst.*, vol. 18, no. 4, pp. 1529–1537, 2003.

[24] A. Y. Saber and G. K. Venayagamoorthy, "Intelligent unit commitment with vehicle-to-grid -A cost-emission optimization," *J. Power Sources*, vol. 195, no. 3, pp. 898–911, 2010.

[25] A. Y. Saber and G. K. Venayagamoorthy, "Plug-in Vehicles and Renewable Energy Sources for Cost and Emission Reductions," *IEEE Trans. Ind. Electron.*, vol. 58, no. 4, pp. 1229–1238, 2011.

[26] A. Zakariazadeh, S. Jadid, and P. Siano, "Multi-objective scheduling of electric vehicles in smart distribution system," *Energy Convers. Manag.*, vol. 79, pp. 43–53, 2014.

[27] A. Parisio and L. Glielmo, "Multi-objective Optimization for Environmental / Economic Microgrid Scheduling," in *IEEE International Conference on Cyber Technology in Automation, Control and Intelligent Systems, Bangkok, Thailand, 27-31 May, 2012*, pp. 17–22.

[28] X. Wang, A. Palazoglu, and N. H. El-Farra, "Operational optimization and demand response of hybrid renewable energy systems," *Appl. Energy*, vol. 143, pp. 324–335, 2015.

[29] M. A. Jirdehi, V. S. Tabar, R. Hemmati, and P. Siano, "Multi objective stochastic microgrid scheduling incorporating dynamic voltage restorer," *Int. J. Electr. Power Energy Syst.*, vol. 93, pp. 316–327, 2017.

[30] L. Wang, Q. Li, R. Ding, M. Sun, and G. Wang, "Integrated scheduling of energy supply and demand in microgrids under uncertainty: A robust multi-objective optimization approach," *Energy*, vol. 130, pp. 1–14, 2017.

[31] S. M. V. Pandian, "An Efficient Particle Swarm Optimization Technique to Solve Combined Economic Emission Dispatch Problem," *Eur. J. Sci. Res.*, vol. 54, no. 2, pp. 187–192, 2011.

[32] S. Krishnamurthy and R. Tzoneva, "Impact of price penalty factors on the solution of the combined economic emission dispatch problem using cubic criterion functions," in *IEEE Power and Energy Society General Meeting, San Diego, USA, 22-26 July, 2012*, pp. 1–9.

[33] H. Hamedi, "Solving the combined economic load and emission dispatch problems using new heuristic algorithm," *Int. J. Electr. Power Energy Syst.*, vol. 46, no. 1, pp. 10–16, 2013.

[34] G. C. Liao, "Solve environmental economic dispatch of Smart MicroGrid containing distributed generation system - Using chaotic quantum genetic algorithm," *Int. J. Electr. Power Energy Syst.*, vol. 43, no. 1, pp. 779–787,

2012.

[35] S. X. Chen, H. B. Gooi, and M. Q. Wang, “Sizing of energy storage for microgrids,” *IEEE Trans. Smart Grid*, vol. 3, no. 1, pp. 142–151, 2012.

[36] Z. Zhao, S., E. B. Makram, and Y. Tong, “Impact Study of Energy Storage for Optimal Energy Scheduling in Microgrid,” in *IEEE Power and Energy Society General Meeting, PES , San Diego, USA, 22 -26 July , 2012*, pp. 1–7.

[37] Z. Wang and J. Zhong, “A multi-period optimal power flow model including battery energy storage,” in *IEEE Power and Energy Society General Meeting, PES ,Vancouver, Canada, 21-25 July, 2013*.

[38] P. Mahat, J. Escribano Jimenez, E. Rodriguez Moldes, S. I. Haug, I. G. Szczesny, K. E. Pollestad, and L. C. Totu, “A micro-grid battery storage management,” in *PIEEE Power and Energy Society General Meeting, PES ,Vancouver, Canada, 21-25 July, 2013*, pp. 1–5.

[39] T. A. Nguyen, M. L. Crow, and A. C. Elmore, “Optimal Sizing of a Vanadium Redox Battery System for Microgrid Systems,” *IEEE Trans. Sustain. Energy*, vol. 6, no. 3, pp. 729–737, 2015.

[40] E. E. Sfikas, Y. A. Katsigiannis, and P. S. Georgilakis, “Simultaneous capacity optimization of distributed generation and storage in medium voltage microgrids,” *Int. J. Electr. Power Energy Syst.*, vol. 67, pp. 101–113, 2015.

[41] E. Mayhorn, K. Kalsi, M. Elizondo, W. Zhang, S. Lu, and N. Samaan, “Optimal Control of Distributed Energy Resources using Model Predictive Control,” in *IEEE Power and Energy Society General Meeting, PES, San Diego, USA, 22-26 July, 2012*, pp. 1–8.

[42] Y. Riffonneau, S. Bacha, F. Barruel, and S. Ploix, “Optimal Power Flow Management for Grid Connected PV Systems With Batteries,” *IEEE Trans. Sustain. Energy*, vol. 2, no. 3, pp. 309–320, Jul. 2011.

[43] Y. Levron, J. M. Guerrero, and Y. Beck, “Optimal Power Flow in Microgrids With Energy Storage,” *IEEE Trans. Power Syst.*, vol. 28, no. 3, pp. 3226–3234, Aug. 2013.

[44] M. Marzband, H. Alavi, S. S. Ghazimirsaeid, H. Uppal, and T. Fernando, “Optimal energy management system based on stochastic approach for a home Microgrid with integrated responsive load demand and energy storage,” *Sustain. Cities Soc.*, vol. 28, pp. 256–264, 2017.

[45] W. Bingying, Z. Buhan, M. Biao, and Z. Jiajun, “Optimal capacity of flow battery and economic dispatch used in peak load shifting,” in *4th*

International Conference on Electric Utility Deregulation and Restructuring and Power Technologies, DRPT , Weihai, Shandong, China, 6-9 July, 2011.

[46] M. E. Khodayar, L. Wu, and M. Shahidehpour, “Hourly coordination of electric vehicle operation and volatile wind power generation in SCUC,” *IEEE Trans. Smart Grid*, vol. 3, no. 3, pp. 1271–1279, 2012.

[47] W. Su, J. Wang, and J. Roh, “Stochastic energy scheduling in microgrids with intermittent renewable energy resources,” *IEEE Trans. Smart Grid*, vol. 5, no. 4, pp. 1876–1883, 2014.

[48] T. A. Nguyen and M. L. Crow, “Stochastic Optimization of Renewable-Based Microgrid Operation Incorporating Battery Operating Cost,” *IEEE Trans. Power Syst.*, vol. 31, no. 3, pp. 2289–2296, 2016.

[49] Y. Cao, C. Li, X. Liu, B. Zhou, C. Y. Chung, and K. W. Chan, “Optimal scheduling of virtual power plant with battery degradation cost,” *IET Gener. Transm. Distrib.*, vol. 10, no. 3, pp. 712–725, 2016.

[50] A. G. Tsikalakis and N. D. Hatziargyriou, “Centralized Control for Optimizing Microgrids Operation,” *IEEE Trans. Energy Convers.*, vol. 23, no. 1, pp. 241–248, 2008.

[51] A. Bagherian and S. M. Moghaddas Tafreshi, “A developed energy management system for a microgrid in the competitive electricity market,” in *IEEE Bucharest Power Tech Conference, Bucharest, Romania, June28th-2nd July, 2009*, pp. 1–6.

[52] N. M. Muhamad Razali and A. H. Hashim, “Profit-based optimal generation scheduling of a microgrid,” in *4th International Power Engineering and Optimization Conference, PEOCO, Shah Alam, Malaysia, 23 -24 June, 2010*, pp. 232–237.

[53] D. Zhang, S. Li, P. Zeng, and C. Zang, “Optimal microgrid control and power-flow study with different bidding policies by using powerworld simulator,” *IEEE Trans. Sustain. Energy*, vol. 5, no. 1, pp. 282–292, 2014.

[54] V. Mohan, J. G. Singh, W. Ongsakul, and S. G. Nair, “Online benefit optimization in a liberalized/free microgrid market model,” in *IEEE International Conference on Technological Advancements in Power and Energy, TAP Energy , Kollam, India, 24 -26 June, 2015*.

[55] V. Mohan, J. G. Singh, W. Ongsakul, A. C. Unni, and N. Sasidharan, “Stochastic Effects of Renewable Energy and Loads on Optimizing Microgrid Market Benefits,” *Procedia Technol.*, vol. 21, pp. 15–23, 2015.

[56] D. T. Nguyen and L. B. Le, “Risk-constrained profit maximization for

microgrid aggregators with demand response," *IEEE Trans. Smart Grid*, vol. 6, no. 1, pp. 135–146, 2015.

[57] T. Logenthiran, D. Srinivasan, A. M. Khambadkone, and H. N. Aung, "Multiagent system for real-time operation of a microgrid in real-time digital simulator," *IEEE Trans. Smart Grid*, vol. 3, no. 2, pp. 925–933, 2012.

[58] S. W. Kim, J. Kim, Y. G. Jin, and Y. T. Yoon, "Optimal bidding strategy for renewable microgrid with active network management," *Energies*, vol. 9, no. 1, pp. 1–15, 2016.

[59] J. Silvente, G. M. Kopanos, E. N. Pistikopoulos, and A. Espuña, "A rolling horizon optimization framework for the simultaneous energy supply and demand planning in microgrids," *Appl. Energy*, vol. 155, pp. 485–501, 2015.

[60] D. T. Nguyen and L. B. Le, "Optimal Bidding Strategy for Microgrids Considering Renewable Energy and Building Thermal Dynamics," *IEEE Trans. Smart Grid*, vol. 5, no. 4, pp. 1608–1620, 2014.

[61] A. Bonfiglio, S. Bracco, M. Brignone, F. Delfino, F. Pampararo, R. Procopio, M. Robba, and M. Rossi, "A receding-horizon approach for active and reactive power flows optimization in microgrids," in *IEEE Conference on Control Applications,CCA , Juan Les Antibes, France, 8-10 October, 2014*.

[62] K. Zou, A. P. Agalgaonkar, K. M. Muttaqi, and S. Perera, "Distribution system planning with incorporating DG reactive capability and system uncertainties," *IEEE Trans. Sustain. Energy*, vol. 3, no. 1, pp. 112–123, 2012.

[63] M. Khodayar, M. Barati, and M. Shahidehpour, "Integration of High Reliability Distribution Systems in Microgrids operation," *Comput. Eng.*, vol. 3, no. 4, pp. 1–10, 2012.

[64] J. P. Fossati, A. Galarza, A. Martín-villate, and L. Font, "A method for optimal sizing energy storage systems for microgrids," *Renew. Energy*, vol. 77, pp. 539–549, 2015.

[65] M. Govardhan and R. Roy, "Economic analysis of unit commitment with distributed energy resources," *Int. J. Electr. Power Energy Syst.*, vol. 71, pp. 1–14, 2015.

[66] K. Xie, Y. H. Song, D. Zhang, Y. Nakanishi, and C. Nakazawa, "Calculation and decomposition of spot price using interior point nonlinear optimisation methods," *Int. J. Electr. Power Energy Syst.*, vol. 26, no. 5, pp. 349–356, 2004.

[67] P. Siano, C. Cecati, H. Yu, and J. Kolbusz, “Real time operation of smart grids via FCN networks and optimal power flow,” *IEEE Trans. Ind. Informatics*, vol. 8, no. 4, pp. 944–952, 2012.

[68] M. Braun, “Reactive power supply by distributed generators,” in *2008 IEEE Power and Energy Society General Meeting-Conversion and Delivery of Electrical Energy in the 21st Century, Pittsburgh, PA, USA, 20-24 July, 2008*, pp. 1–8.

[69] A. H. Fathima and K. Palanisamy, “Optimization in microgrids with hybrid energy systems - A review,” *Renew. Sustain. Energy Rev.*, vol. 45, pp. 431–446, 2015.

[70] S. Singh, M. Singh, and S. C. Kaushik, “Optimal power scheduling of renewable energy systems in microgrids using distributed energy storage system,” *IET Renew. Power Gener.*, vol. 10, no. 9, pp. 1328–1339, 2016.

[71] H. Wu, X. Liu, and M. Ding, “Dynamic economic dispatch of a microgrid: Mathematical models and solution algorithm,” *Int. J. Electr. Power Energy Syst.*, vol. 63, pp. 336–346, 2014.

[72] H. Farzin, M. Fotuhi-Firuzabad, and M. Moeini-Aghtaie, “Stochastic Energy Management of Microgrids during Unscheduled Islanding Period,” *IEEE Trans. Ind. Informatics*, vol. 13, no. 3, pp. 1079–1087, 2017.

[73] W. Kempton and J. Tomić, “Vehicle-to-grid power fundamentals: Calculating capacity and net revenue,” *J. Power Sources*, vol. 144, no. 1, pp. 268–279, 2005.

[74] J. Tomić and W. Kempton, “Using fleets of electric-drive vehicles for grid support,” *J. Power Sources*, vol. 168, no. 2, pp. 459–468, 2007.

[75] W. Su, J. Wang, K. Zhang, and A. Q. Huang, “Model predictive control-based power dispatch for distribution system considering plug-in electric vehicle uncertainty,” *Electr. Power Syst. Res.*, vol. 106, pp. 29–35, 2014.

[76] J. R. Santos, A. T. Lora, A. G. Expósito, and J. L. M. Ramos, “Finding improved local minima of power system optimization problems by interior-point methods,” *IEEE Trans. Power Syst.*, vol. 18, no. 1, pp. 238–244, 2003.

[77] “IBM ILOG CPLEX Optimization Studio CPLEX User’s Manual,” *Version 12 Release 6*, 2014.

[78] “IBM ILOG CPLEX for Microsoft Excel User ’ s Manual,” 2009.

[79] C. Bliek, P. Bonami, and A. Lodi, “Solving Mixed-Integer Quadratic Programming problems with IBM-CPLEX : a progress report,” in *Proceedings of the Twenty-Sixth RAMP Symposium, Hosei University,*

Tokto, 16-17 October, 2014, pp. 171–180.

[80] R. C. Dugan and T. E. Mcdermott, “An Open Source Platform for Collaborating on Smart Grid Research,” in *IEEE PES General Meeting: The Electrification of Transportation and the Grid of the Future, Detroit, MI, USA, 24 - 28 July, 2011*, pp. 1–7.

[81] R. C. Dugan, “Reference Guide: The Open Distribution System Simulator (OpenDSS),” in *Electric Power Research Institute, Inc.*, 2013, pp. 1–177.

[82] J. Ma, F. Yang, Z. Li, and S. J. Qin, “A renewable energy integration application in a MicroGrid based on model predictive control,” in *IEEE Power and Energy Society General Meeting, PES ,San Diego, USA, 22 - 26 July, 2012*, pp. 1–6.

[83] S. Papthanassious, N. Hatziargyriou, K. Strunz, “A Benchmark Low Voltage Microgrid Network,” in *CIGRE Symp, Power Systems with Dispersed Generation, Athens, Greece, 2005*.

[84] P. Trichakis, P. C. Taylor, P. F. Lyons, R. Hair, “Predicting the technical impacts of high levels of small-scale embedded generators on low-voltage networks,” *Renew. Power Gener. IET*, vol. 2, no. 2, pp. 249–262, 2008.

[85] M. Neaimeh, R. Wardle, A. M. Jenkins, J. Yi, G. Hill, P. F. Lyons, Y. Hübner, P. T. Blythe, and P. C. Taylor, “A probabilistic approach to combining smart meter and electric vehicle charging data to investigate distribution network impacts,” *Appl. Energy*, vol. 157, pp. 688–698, 2015.

[86] A. Zakariazadeh, S. Jadid, and P. Siano, “Smart microgrid energy and reserve scheduling with demand response using stochastic optimization,” *Electr. Power Energy Syst.*, vol. 63, pp. 523–533, 2014.

[87] “MICROGRIDS Large Scale Integration of Micro-Generation to Low Voltage Grids,” in *Eu contract ENK5-CT-2002-00610, Tech. Annex*, 2004.

[88] Faisl A. Mohammed, Heikki N. Koivo, “Online Management of MicroGrid with Battery Storage Using Multiobjective Optimization,” in *International Conference on Power Engineering, Energy and Electrical Drives, POWERENG, Setubal, Portugal, 12-14 April , 2007*, pp. 231–236.

[89] R. M. Kamel, A. Chaouachi, and K. Nagasaka, “Carbon Emissions Reduction and Power Losses Saving besides Voltage Profiles Improvement Using Micro Grids,” *Low Carbon Econ.*, vol. 1, no. 1, pp. 1–7, 2010.

[90] D. R. di Valdalbero, “External costs and their integration in energy costs,” in *Europen Sustain Energy Policy Seminar*, 2006.

[91] ATSE, “The Hidden Costs of Electricity: Externalities of Power Generation

in Australia," in *Australian academy of technology science engineering, Australia*, 2009.

[92] D. García-Gusano, H. Cabal, and Y. Lechón, "Evolution of NOx and SO2 emissions in Spain: Ceilings versus taxes," *Clean Technol. Environ. Policy*, vol. 17, no. 7, pp. 1997–2011, 2015.

[93] A. Daniel E. Olivares, Jose D. Lara, Claudio A. Cañizares and M. Kazerani, "Stochastic-Predictive Energy Management System for Isolated Microgrids," *IEEE Trans. Smart Grid*, vol. 6, no. 6, pp. 2681–2692, 2015.

[94] A. Parisio, E. Rikos, and L. Glielmo, "Stochastic model predictive control for economic / environmental operation management of microgrids : An experimental case study," *J. Process Control*, vol. 43, pp. 24–37, 2016.

[95] C. Liu, J. Wang, A. Botterud, Y. Zhou, and A. Vyas, "Assessment of impacts of PHEV charging patterns on wind-thermal scheduling by stochastic unit commitment," *IEEE Trans. Smart Grid*, vol. 3, no. 2, pp. 675–683, 2012.

[96] Z. Li, C. Zang, P. Zeng, and H. Yu, "Combined Two-Stage Stochastic Programming and Receding Horizon Control Strategy for Microgrid Energy Management Considering Uncertainty," *Energies*, vol. 9, no. 7, pp. 1–16, 2016.

[97] S. Talari, M.-R. Haghifam, and M. Yazdaninejad, "Stochastic-based scheduling of the microgrid operation including wind turbines, photovoltaic cells, energy storages and responsive loads," *IET Gener. Transm. Distrib.*, vol. 9, no. 12, pp. 1498–1509, 2015.

[98] A. Y. Saber, G. K. Venayagamoorthy, "Resource Scheduling Under Uncertainty in a Smart Grid with Renewables and Plug-in Vehicles," *IEEE Syst. J.*, vol. 6, no. 1, pp. 103–109, 2012.

[99] S. Mohammadi, S. Soleymani, and B. Mozafari, "Scenario-based stochastic operation management of MicroGrid including Wind, Photovoltaic, Micro-Turbine, Fuel Cell and Energy Storage Devices," *Int. J. Electr. Power Energy Syst.*, vol. 54, pp. 525–535, 2014.

[100] T. Niknam, R. Azizipanah-Abarghooee, and M. R. Narimani, "An efficient scenario-based stochastic programming framework for multi-objective optimal micro-grid operation," *Appl. Energy*, vol. 99, pp. 455–470, 2012.

[101] W. Alharbi and K. Raahemifar, "Probabilistic coordination of microgrid energy resources operation considering uncertainties," *Electr. Power Syst. Res.*, vol. 128, pp. 1–10, 2015.

[102] Y. Li and E. Zio, "Uncertainty analysis of the adequacy assessment model

of a distributed generation system," *Renew. Energy*, vol. 41, pp. 235–244, 2012.

[103] J. Sumaili, H. Keko, V. Miranda, A. Botterud, and J. Wang, "Clustering-Based Wind Power Scenario Reduction Technique," in *17th Power Systems Computation Conference, PSCC, Stockholm, Sweden, 22-26 August, 2011*.

[104] J. Sumaili, H. Keko, V. Miranda, Z. Zhou, A. Botterud, and J. Wang, "Finding representative wind power scenarios and their probabilities for stochastic models," in *16th International Conference on Intelligent System Applications to Power Systems, ISAP , Hersonisos, Crete, Greece, 25 -28 September, 2011*.

[105] B. A, "Use of Wind Power Forecasting in Operational Decisions," in *Argona National Labortary*, 2011.

[106] A. Sinha and M. De, "Load Shifting Technique for Reduction of Peak Generation Capacity Requirement in Smart Grid," in *International Conference on Power Electronics, Intelligent Control and Energy Systems (ICPEICES), Delhi, India, 4-6 July ,2016*, pp. 1–5.

[107] P. Siano, "Demand response and smart grids - A survey," *Renew. Sustain. Energy Rev.*, vol. 30, pp. 461–478, 2014.

[108] V. Hamidi, "Domestic Demand Response to Increase the Value of Wind Power," PhD thesis, Bath University, 2009.

[109] I. Cobelo, "Active control of Distribution Networks," PhD thesis , Manchester University, 2005.

[110] M. Zhou, G. Li, and P. Zhang, "Impact of demand side management on composite generation and transmission system reliability," in *IEEE PES Power Systems Conference and Exposition, PSCE, Atlanta, USA ,29 October-1 November, 2006*, pp. 819–824.

[111] M. Fotuhi-Firuzabad and R. Billinton, "Impact of load management on composite system reliability evaluation short-term operating benefits," *IEEE Trans. Power Syst.*, vol. 15, no. 2, pp. 858–864, 2000.

[112] C. M. Affonso, L. C. P. Da Silva, and W. Freitas, "Demand-Side Management to Improve Power System Security," in *IEEE Power Engineering Society Transmission and Distribution Conference, PES, TD, 21-24 May, 2006*, pp. 1–6.

[113] M. Govardhan and R. Roy, "Impact of Demand Side Management On Unit Commitment Problem," in *International Conference on Control, Instrumentation, Energy and Communication, CIEC, Department of*

Applied Physics, University of CalcuttaKolkata, India, 31 January -2 February, 2014, pp. 446–450.

[114] G. Stanojevic, V., Bilton, M., Dragovic, J., Schofield, J., Strbac, "Application of demand side response and energy storage to enhance the utilization of the existing distribution network capacity," in *22nd International Conference and Exhibition on Electricity Distribution, CIRED , Stockholm, Sweden, 10 - 13 June, 2013*.

[115] V. Hamidi, F. Li, L. Yao, and M. Bazargan, "Domestic demand side management for increasing the value of wind," in *China International Conference on Electricity Distribution, CICED , Guangzhou, China, 10-13 December, 2008*, pp. 1–10.

[116] M. P. Marietta, M. Graells, and J. M. Guerrero, "A rolling horizon rescheduling strategy for flexible energy in a microgrid," in *IEEE International Energy Conference, ENERGYCON , Dubrovnik, Croatia, 13 -16 May, 2014*, pp. 1297–1303.

[117] T. Logenthiran, D. Srinivasan, and T. Z. Shun, "Demand side management in smart grid using heuristic optimization," *IEEE Trans. Smart Grid*, vol. 3, no. 3, pp. 1244–1252, 2012.

[118] N. Kinhekar, N. P. Padhy, F. Li, and H. O. Gupta, "Utility Oriented Demand Side Management Using Smart AC and Micro DC Grid Cooperative," *IEEE Trans. Power Syst.*, vol. 31, no. 2, pp. 1151–1160, 2016.

[119] G. Tsagarakis, R. Camilla Thomson, A. J. Collin, G. P. Harrison, A. E. Kiprakis, and S. McLaughlin, "Assessment of the Cost and Environmental Impact of Residential Demand-Side Management," *IEEE Trans. Ind. Appl.*, vol. 52, no. 3, pp. 2486–2495, 2016.

[120] P. Faria and Z. Vale, "Demand response in electrical energy supply: An optimal real time pricing approach," *Energy*, vol. 36, no. 8, pp. 5374–5384, 2011.

[121] H. A. Aalami, M. P. Moghaddam, and G. R. Yousefi, "Demand response modeling considering Interruptible/Curtailable loads and capacity market programs," *Appl. Energy*, vol. 87, no. 1, pp. 243–250, 2010.

[122] P. Palensky and D. Dietrich, "Demand Side Management: Demand Response, Intelligent Energy Systems, and Smart Loads," *Ind. Informatics, IEEE Trans.*, vol. 7, no. 3, pp. 381–388, 2011.

[123] "Demand Response in Liberalised Electricity Markets," in *internation energy agency*, 2003.

[124] Federal Energy Regulatory Commission, “Assessment of demand response and advanced metering,” in *staff report Docket Number AD-06-2-00*, 2006.

[125] L. Gelazanskas and K. A. A. Gamage, “Demand side management in smart grid: A review and proposals for future direction,” *Sustain. Cities Soc.*, vol. 11, pp. 22–30, 2014.

[126] G. T. Bellarmine. P. E, “Load management techniques,” in *Southeastcon . Proceedings of the IEEE, Nashville, TN, USA, 9-9 April ,2000*, pp. 139–145.

[127] H. Jang, “The Development , Implementation , and Application of Demand Side Management and control (DSM+c) Algorithm for Integrating Micro-generation System within Built Environment,” PhD thesis,University of Strathclyde, 2009.

[128] P. D. Mark Bilton, Matt Woolf and G. S. Marko Aunedi, Richard Carmichael, “Impact of energy efficient appliances on network utilisation,” in *Low Carbon London Learning Lab, Imperial College London*, 2014.

[129] G. S. Mark Bilton, Marko Aunedi, Matt Woolf, “Smart appliances for residential demand response,” in *Low Carbon London Learning Lab, Imperial College London*, 2014.

[130] W. Mert, J. Suschek-Berger, and W. Tritthart, “Consumer Acceptance of Smart Appliances,” in *European Communities, Brussels*, 2008.

[131] R. Stamminger, “Synergy Potential of Smart Appliances,” in *report for EIE project (Smart Domestic Appliances in Sustainable Energy Sysytem), University of Bonn,* 2008.

[132] T. Gönen, *Electric Power Distribution System Engineering*, Second edi. Boca Raton: Taylor and Francis, 2008.

[133] J. Olamaei and S. Ashouri, “Demand response in the day-ahead operation of an isolated microgrid in the presence of uncertainty of wind power,” *Turkish J. Electr. Eng. Comput. Sci.*, vol. 23, no. 2, pp. 491–504, 2015.

[134] Department of Energy & Climate Change, “2014 UK Greenhouse Gas Emissions,” 2015.

[135] L. Meiqin, M., Shujuan, S., Chang, “Economic analysis of the microgrid with multi-energy and electric vehicles,” in *8th International Conference on Power Electronics-ECCE Asia: “Green World with Power Electronics”, ICPE-ECCE Asia, Jeju, South Korea, 30 May-3 June, 2011*.

[136] J. W. Whitefoot, “Optimal co-design of microgrids and electric vehicles :

synergies , simplifications and the effects of uncertainty," PhD thesis, University of Michigan, 2012.

[137] H. Z. Lan-xiang, Change-nian, Yu-kai, "optimal operation of complicated distribution networks," in *5th IEEE International Conference on Electric Utility Deregulation, Restructuring and Power Technologies, DRPT , Changsha, China, 26 -29 November, 2015*, pp. 667–672.

[138] S. Y. Derakhshandeh, A. S. Masoum, S. Deilami, M. A. S. Masoum, and M. E. H. Golshan, "Coordination of Generation Scheduling with PEVs Charging in Industrial Microgrids," *IEEE Trans. Power Syst.*, vol. 28, no. 3, pp. 3451–3461, 2013.

[139] L. Igualada, C. Corchero, M. Cruz-Zambrano, and F. J. Heredia, "Optimal energy management for a residential microgrid including a vehicle-to-grid system," *IEEE Trans. Smart Grid*, vol. 5, no. 4, pp. 2163–2172, 2014.

[140] W. Wang, X. Jiang, S. Su, J. Kong, J. Geng, and W. Cui, "Energy management strategy for microgrids considering photovoltaic-energy storage system and electric vehicles," in *IEEE Transportation Electrification Conference and Expo, ITEC Asia-Pacific, Beijing International Convention CenterBeijing, China, 31 August - 3 September, 2014*, pp. 1–6.

[141] Z. Yang, K. Li, Q. Niu, C. Zhang, and A. Foley, "Non-convex dynamic economic/environmental dispatch with plug-in electric vehicle loads," in *Computational Intelligence Applications in Smart Grid (CIASG), Orlando, FL, USA, 9-12 December. 2014*.

[142] Z. Yang, K. Li, Q. Niu, and A. Foley, "Unit Commitment Considering Multiple Charging and Discharging Scenarios of Plug-in Electric Vehicles," in *International Joint Conference on Neural Networks, IJCNN , Killarney, Ireland, 12 - 17 July, 2015*.

[143] P. Mesarić and S. Krajcar, "Home demand side management integrated with electric vehicles and renewable energy sources," *Energy Build.*, vol. 108, pp. 1–9, 2015.

[144] W. Hu, C. Su, Z. Chen, and B. Bak-Jensen, "Optimal operation of plug-in electric vehicles in power systems with high wind power penetrations," *IEEE Trans. Sustain. Energy*, vol. 4, no. 3, pp. 577–585, 2013.

[145] R. A. Verzijlbergh, L. J. De Vries, and Z. Lukszo, "Renewable Energy Sources and Responsive Demand. Do We Need Congestion Management in the Distribution Grid?," *Power Syst. IEEE Trans.*, vol. 29, no. 5, pp. 2119–2128, 2014.

[146] M. Zhang and J. Chen, "The energy management and optimized

operation of electric vehicles based on microgrid," *IEEE Trans. Power Deliv.*, vol. 29, no. 3, pp. 1427–1435, 2014.

[147] C. Battistelli, L. Baringo, and A. J. Conejo, "Optimal energy management of small electric energy systems including V2G facilities and renewable energy sources," *Electr. Power Syst. Res.*, vol. 92, pp. 50–59, 2012.

[148] C. Chen and S. Duan, "Optimal Integration of Plug-In Hybrid Electric Vehicles in Microgrids," *IEEE Trans. Ind. Informatics*, vol. 10, no. 3, pp. 1917–1926, 2014.

[149] M. H. K. Tushar, C. Assi, M. Maier, and M. F. Uddin, "Smart microgrids: Optimal joint scheduling for electric vehicles and home appliances," *IEEE Trans. Smart Grid*, vol. 5, no. 1, pp. 239–250, 2014.

[150] H. Liu, Y. Ji, H. Zhuang, and H. Wu, "Multi-objective dynamic economic dispatch of microgrid systems including vehicle-to-grid," *Energies*, vol. 8, no. 5, pp. 4476–4495, 2015.

[151] Y. Wang, B. Wang, C. C. Chu, H. Pota, and R. Gadh, "Energy management for a commercial building microgrid with stationary and mobile battery storage," *Energy Build.*, vol. 116, pp. 141–150, 2016.

[152] A. Kavousi-fard and A. Khodaei, "Efficient integration of plug-in electric vehicles via reconfi gurable microgrids," *Energy*, vol. 111, pp. 653–663, 2016.

[153] A. Rabiee, M. Sadeghi, J. Aghaeic, and A. Heidari, "Optimal operation of microgrids through simultaneous scheduling of electrical vehicles and responsive loads considering wind and PV units uncertainties," *Renew. Sustain. Energy Rev.*, vol. 57, pp. 721–739, 2016.

[154] S. Masoud, M. Tafreshi, H. Ranjbarzadeh, and M. Jafari, "A probabilistic unit commitment model for optimal operation of plug-in electric vehicles in microgrid," *Renew. Sustain. Energy Rev.*, vol. 66, pp. 934–947, 2016.

[155] V. Stanojevid, "Enhancing Performance of Electricity Networks through Application of Demand Side Response and Storage Technologies," Imperial College London, PhD Thesis, 2012.

[156] W. Su, "Smart Grid Operations Integrated with Plug-in Electric Vehicles and Renewable Energy Resources," PhD thesis, North Carolina State University, 2013.

[157] H. Lund and W. Kempton, "Integration of renewable energy into the transport and electricity sectors through V2G," *Energy Policy*, vol. 36, no. 9, pp. 3578–3587, 2008.

[158] "Electric vehicles in the UK and Republic of Ireland : Greenhouse gas

emission infrastructure needs," in *Final Report for WWF UK*, 2010.

[159] M. Aunedi, M. Woolf, M. Bilton, and G. Strbac, "Impact & opportunities for wide-scale EV deployment," in *Report B1 for the, Low Carbon London Learning Lab, Imperial College London*, 2014.

[160] UK Power Networks, "Impact of Electric Vehicle and Heat Pump Loads on Network Demand Profiles," in *Low Carpon Londodn Energising change*, 2014.

[161] P. Papadopoulos, "Integration of electric vehicles into distribution networks," PhD Thesis, Cardiff University, 2012.

[162] "Guidance for implementation of electric vehicle charging infrastructure," in *Transport for London*, 2010.

[163] I. Grau, "Management of electric vehicle battery charging in distribution networks," PhD Thesis, Cardiff University, 2012.

[164] C. Zhou, K. Qian, M. Allan, and W. Zhou, "Modeling of the cost of EV battery wear due to V2G application in power systems," *IEEE Trans. Energy Convers.*, vol. 26, no. 4, pp. 1041–1050, 2011.

[165] "Investigation into the Scope for the Transport Sector to Switch to Electric Vehicles and Plug- in Hybrid Vehicles," in *Department for Transport*, 2008.

Appendix A Line Impedances of the Test System

Table A-1 Line impedances of the test system

Line buses		Lines resistance and reactance						
From	to	R(Ω/km)	X(Ω/km)	R_o(Ω/km)	X_o(Ω/km)	R_n(Ω/km)	I_Z(A)	CSA (m^2)
Residential feeders								
1	2	0.284	0.083	1.136	0.417	0.284	355	185
2	3	0.284	0.083	1.136	0.417	0.284	355	185
3	4	0.284	0.083	1.136	0.417	0.284	241	95
4	5	0.284	0.083	1.136	0.417	0.284	241	95
1	6	0.284	0.083	1.136	0.417	0.284	355	185
6	7	0.497	0.086	2.387	0.447	0.63	355	185
7	8	0.497	0.086	2.387	0.447	0.63	241	95
8	9	0.497	0.086	2.387	0.447	0.63	241	95
Industrial feeder								
1	10	0.264	0.071	0	0	0.387	280	120
10	11	0.264	0.071	0	0	0.387	280	120
Commercial feeders								
1	12	0.397	0.279	0	0	0.397	355	185
12	13	0.397	0.279	0	0	0.397	355	185
13	14	0.397	0.279	0	0	0.397	241	95
14	15	0.397	0.294	0	0	0.397	241	95
12	16	0.574	0.294	0	0	0.574	205	70
16	17	0.574	0.294	0	0	0.574	120	35
13	18	0.574	0.294	0	0	0.574	205	70
18	19	0.574	0.294	0	0	0.574	120	35

I_z= the conductor current -carrying capacity

CSA= Cross section area of the conductor

Appendix B Characteristics Parameters of the DGs

Table B-1 Technical characteristics parameters of the DGs

	DE	FC1	FC2	MT1	MT2
P_{min}(Kw)	20	1	16	20	6
P_{max}(Kw)	140	30	90	60	50
Q_{min}(kVAr)	0	0	0	0	0
Q_{max}(kVAr)	70	15	45	30	25
d (€/h)	0.6	1.3	1.14	0.65	1.34
e (€/Kwh)	0.05	0.031	0.06	0.0152	0.062
f (€/Kw^2 h)	0.0002	0.0001	0.0004	0.00052	0.0013
dr(€/h)	0.06	0.13	0.114	0.065	0.134
er (€/kVAr)	0.005	0.0031	0.006	0.00152	0.0062
fr (€/$kVAr^2$)	0.00002	0.00001	0.00004	0.000052	0.00013
K_{Omi} (€/Kw^2)	0.01258	0.00419	0.00419	0.00587	0.00587
T_{up}(h)	1.5	0.5	1	0.5	0.5
T_{down}(h)	1.5	0.5	1	0.5	0.5
Sc_i(€)	0.25	0.16	0.2	0.1	0.1
Sd_i(€)	0.25	0.16	0.2	0.1	0.1
UR_i(kW)	100	30	70	60	50
DR_i(kW)	100	30	70	60	50

Table B-2 Emission rate of greenhouse gases for the DGs

Unit	CO_2 (kg/kWh)	NO_X (kg/kWh)	SO_2 (kg/kWh)	PM(kg/kWh)
DE	0.848	0.0013	0.00125	0.00036
FC1	0.489	0.00001	0.000003	0.000001
FC2	0.489	0.00001	0.000003	0.000001
MT1	0.725	0.0002	0.000004	0.000041
MT2	0.725	0.0002	0.000004	0.000041

Table B-3 Cost of emission of greenhouse gases

E_{CO2}	0.02 (€/kg)
E_{NO_X}	5 (€/kg)
E_{SO2}	6 (€/kg)
E_{PM}	25 (€/kg)

Table B-4 Wind turbines data

$\boldsymbol{P_{W-r}}$(kW)	$\boldsymbol{v_{ci}}$(m/s)	$\boldsymbol{v_{co}}$(m/s)	$\boldsymbol{v_r}$(m/s)
20	3	25	12

Table B-5Storage battery data

E_b(kWh)	E_{bmin}(kWh)	E_{bmax}(kWh)	η_{bch}	η_{bdis}	DOD%
50	25	50	0.9	0.9	50

Table B-6 Hourly profiles of the wind, PV generation, active and reactive open market prices, and the total active and reactive loads

Time(h)	Wind speed (m/s)	PV power generation (kW)	Active power price(€/kWh)	Reactive power price(€/Kw)	Total active load (kW)	Total reactive load (kVAr)
1	7.8	0	0.035	0.004	100.240	48.546
2	9	0	0.032	0.003	92.000	44.556
3	9.5	0	0.030	0.003	90.260	43.713
4	10.5	0	0.030	0.003	84.600	40.972
5	9.7	0	0.033	0.003	90.820	43.984
6	8.6	0.335	0.050	0.005	100.040	48.449
7	7	1.693	0.047	0.005	136.100	65.913
8	6.6	3.916	0.050	0.005	186.800	90.467
9	6.8	6.721	0.070	0.007	221.060	107.059
10	6	9.014	0.080	0.008	250.400	121.269
11	5.3	10.760	0.090	0.009	266.500	129.066
12	5.5	11.589	0.120	0.012	265.080	128.378
13	5.8	11.431	0.225	0.023	286.500	138.752
14	6.3	10.408	0.100	0.010	297.400	144.031
15	7.5	8.414	0.085	0.009	283.380	137.241
16	8	5.962	0.150	0.015	270.100	130.809
17	9.6	3.352	0.450	0.045	258.000	124.949
18	10	1.411	0.150	0.015	292.600	141.706
19	9	0.3	0.180	0.018	300.200	145.387
20	8.5	0	0.160	0.016	313.000	151.586
21	7.8	0	0.310	0.031	277.800	134.539
22	7	0	0.050	0.005	233.000	112.842
23	6.8	0	0.040	0.004	186.000	90.080
24	7.1	0	0.025	0.003	104.600	50.658

Appendix C the Stochastic Scenarios of Wind, PV Generation and Open Market Price

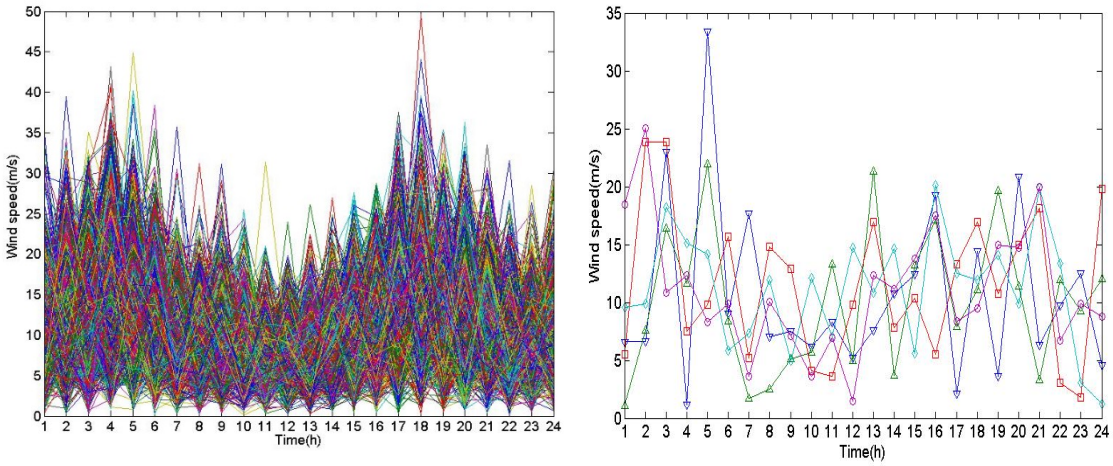

(a) (b)

Figure C-1 Scenarios generation and reduction of wind speed (a) generated 1000 scenarios of wind speed (b) reduced the scenarios to 5

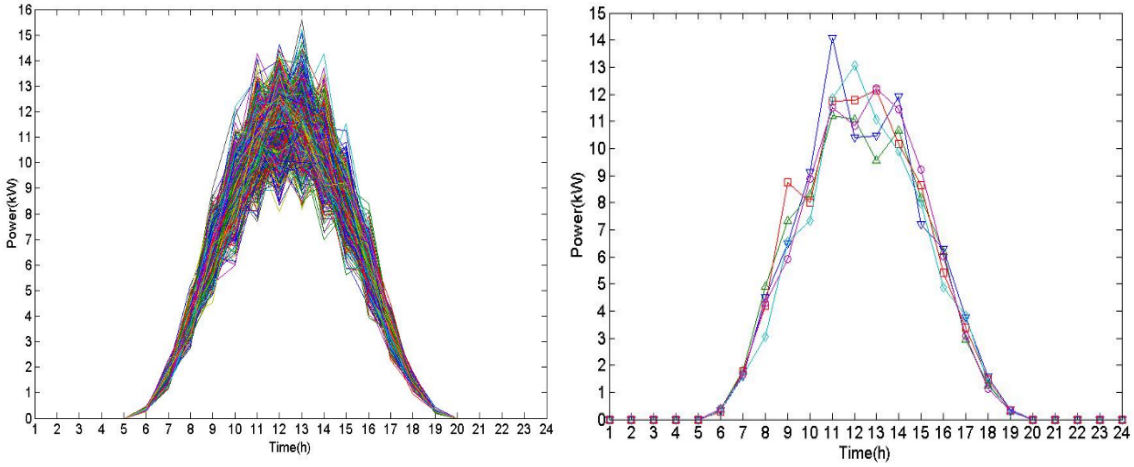

(a) (b)

Figure C-2 Scenarios generation and reduction PV generation (a) generated 1000 scenarios of the PV power (b) reduced the scenarios to 5

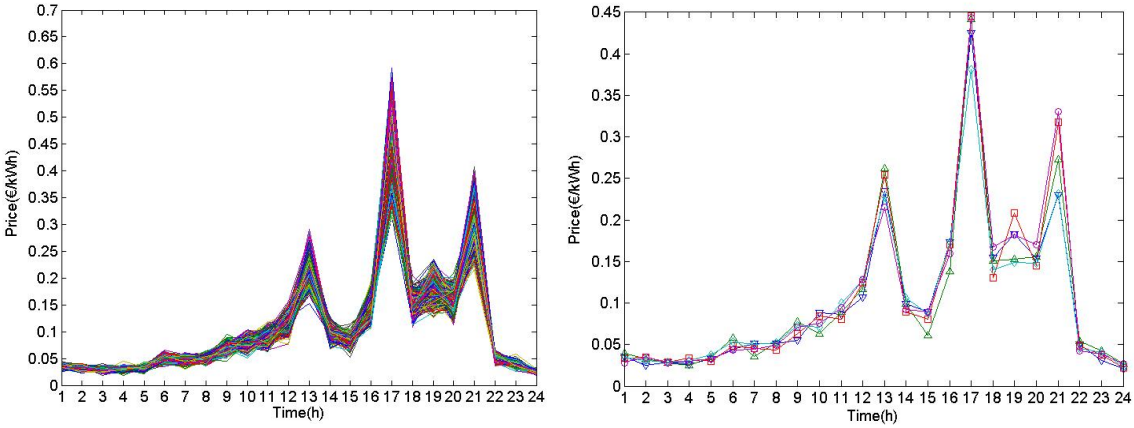

(a) (b)

Figure C-3 Scenarios generation and reduction of the OMP (a) generated 1000 scenarios of OMP (b) reduced the scenarios to 5

Table C-1 Hourly cost values of the five highest probability scenarios and Det. Case for the connected MG

Time(h)	Cost(€/h) Sc1	Cost(€/h) Sc2	Cost(€/h) Sc3	Cost(€/h) Sc4	Cost(€/h) Sc5	Cost(€/h) Det. Case
1	6.8	6.4	7.8	6.8	7.5	7.9
2	6.8	6.4	6.5	6.8	6.0	7.2
3	8.0	8.0	8.0	8.0	8.0	7.2
4	7.6	7.7	4.5	7.6	4.6	7.4
5	8.3	8.2	5.4	8.3	5.2	7.5
6	9.0	8.1	9.1	9.0	8.3	8.5
7	7.7	9.5	10.5	7.6	11.7	10.0
8	13.8	13.6	14.7	13.7	14.6	14.1
9	20.8	18.4	21.1	20.7	18.9	20.2
10	22.3	25.7	22.4	22.5	25.8	24.8
11	27.7	27.4	27.4	27.9	27.1	27.2
12	29.1	28.8	29.1	29.1	28.8	29.1
13	8.2	17.3	11.3	7.7	19.9	21.4
14	32.5	31.7	32.7	32.5	31.9	31.8
15	28.8	29.1	28.8	28.6	29.1	28.3
16	28.9	25.7	28.9	28.9	25.6	28.8
17	-23.9	-21.0	-16.6	-25.0	-14.0	-28.5
18	32.6	32.4	32.4	32.5	32.2	32.8
19	34.1	31.1	35.8	34.1	34.0	32.5
20	35.7	35.9	35.6	35.8	35.7	36.3
21	21.3	25.5	19.0	21.3	23.8	13.5
22	20.7	20.3	20.3	20.7	19.8	19.1
23	13.5	12.0	14.3	13.5	12.9	12.5
24	10.4	9.8	7.9	10.4	7.1	8.5

Table C-2 Hourly profit values of the five highest probability scenarios and Det. Case for the connected MG

Time(h)	Profit (€/h) Sc1	Profit (€/h) Sc2	Profit (€/h) Sc3	Profit (€/h) Sc4	Profit (€/h) Sc5	Profit (€/h) Det. Case
1	-2.6	-2.6	-3.6	-2.6	-3.8	-4.2
2	-3.6	-4.1	-3.3	-3.6	-3.6	-4.1
3	-5.4	-5.3	-5.4	-5.4	-5.3	-4.4
4	-5.4	-5.3	-2.3	-5.4	-2.3	-4.7
5	-5.0	-5.1	-2.1	-5.0	-2.1	-4.3
6	-2.8	-3.5	-3.0	-2.8	-3.7	-3.3
7	-2.6	-2.2	-5.5	-2.6	-4.4	-3.3
8	-3.5	-3.6	-4.5	-3.4	-4.6	-4.3
9	-2.8	-5.6	-3.1	-2.7	-6.1	-4.0
10	-5.7	-2.5	-5.9	-5.9	-2.6	-3.8
11	-2.7	-3.2	-2.4	-2.9	-2.9	-2.1
12	3.2	0.9	3.2	3.2	0.9	4.3
13	70.5	53.3	67.5	71.1	50.7	46.1
14	-1.5	-0.6	-1.7	-1.6	-0.8	-0.6
15	-10.5	-2.7	-10.5	-10.3	-2.7	-3.1
16	10.0	23.4	10.0	10.0	23.4	13.7
17	143.3	135.9	136.0	144.4	128.8	150.3
18	13.5	15.0	13.7	13.6	15.2	13.2
19	14.0	26.6	12.3	14.0	23.7	24.2
20	15.4	14.5	15.5	15.4	14.7	16.2
21	58.2	41.5	60.5	58.2	43.2	76.7
22	-7.5	-8.1	-7.0	-7.5	-7.5	-6.9
23	-5.3	-6.0	-6.0	-5.3	-6.9	-4.7
24	-7.4	-7.7	-4.8	-7.4	-4.8	-5.7

Table C-3 Hourly cost values of the five highest probability scenarios and Det. Case for the isolated MG

Time(h)	Cost(€/h) Sc1	Cost(€/h) Sc2	Cost(€/h) Sc3	Cost(€/h) Sc4	Cost(€/h) Sc5	Cost(€/h) Det. Case
1	10.6	10.5	10.6	10.6	10.5	10.4
2	9.2	9.1	9.2	9.2	9.7	9.3
3	9.5	9.5	9.5	9.5	9.5	9.2
4	9.1	8.3	9.1	9.1	8.5	8.9
5	9.6	9.0	9.6	9.6	9.3	9.3
6	10.0	10.1	10.0	10.0	10.3	10.0
7	13.9	14.1	13.9	13.9	13.8	13.7
8	20.0	19.6	20.1	20.1	19.3	19.7
9	24.0	23.8	24.0	23.9	23.7	23.9
10	27.3	27.3	27.3	27.3	27.4	27.3
11	28.8	29.0	28.7	28.8	29.4	29.3
12	29.1	29.1	29.1	29.0	28.7	29.0
13	31.4	31.8	31.3	31.2	31.4	31.8
14	34.7	34.1	34.6	34.8	34.3	34.5
15	31.1	31.1	31.2	31.1	31.3	31.5
16	29.5	29.5	29.4	29.5	30.1	29.8
17	28.5	29.0	28.4	28.4	28.1	28.3
18	34.1	34.0	34.0	34.1	34.0	34.2
19	35.0	36.1	35.0	35.0	35.1	35.4
20	36.9	36.8	36.9	36.9	36.8	37.3
21	32.2	31.8	32.2	32.2	31.0	31.6

Time(h)	Cost(€/h) Sc1	Cost(€/h) Sc2	Cost(€/h) Sc3	Cost(€/h) Sc4	Cost(€/h) Sc5	Cost(€/h) Det. Case
22	25.1	25.3	25.1	25.1	25.9	25.5
23	19.5	19.5	19.6	19.6	19.8	19.7
24	11.6	10.4	11.7	11.7	11.7	10.6

Table C-4 Hourly profit values of the five highest probability scenarios and Det. Case for the isolated MG

Time(h)	Profit (€/h) Sc1	Profit (€/h) Sc2	Profit (€/h) Sc3	Profit (€/h) Sc4	Profit (€/h) Sc5	Profit (€/h) Det. Case
1	5.2	5.3	5.2	5.2	5.3	5.3
2	5.3	5.4	5.3	5.3	4.8	5.2
3	4.7	4.7	4.7	4.7	4.7	5.0
4	4.2	5.0	4.2	4.2	4.8	4.4
5	4.7	5.3	4.7	4.7	5.0	5.0
6	5.7	5.7	5.7	5.7	5.4	5.7
7	7.5	7.3	7.5	7.5	7.6	7.7
8	9.3	9.8	9.3	9.3	10.1	9.6
9	10.8	10.9	10.8	10.9	11.0	10.9
10	12.2	12.1	12.1	12.0	11.9	12.1
11	13.1	12.9	13.2	13.1	12.5	12.6
12	12.6	12.6	12.6	12.6	13.0	12.7
13	13.7	13.3	13.8	13.8	13.7	13.3
14	12.1	12.7	12.2	12.0	12.5	12.3
15	13.4	13.4	13.4	13.5	13.3	13.0
16	13.0	13.0	13.0	13.0	12.4	12.7
17	12.1	11.6	12.2	12.1	12.5	12.3
18	12.0	12.1	12.0	12.0	12.1	11.8
19	12.2	11.1	12.2	12.2	12.1	11.9
20	12.4	12.4	12.4	12.5	12.4	11.9
21	11.4	11.9	11.4	11.4	12.6	12.1
22	11.5	11.4	11.5	11.5	10.8	11.2
23	9.6	9.5	9.6	9.6	9.4	9.6
24	4.8	6.0	4.7	4.8	4.7	5.7

Appendix D Input Data of Integration of the DSM with Optimisation Problems

Table D-1 Hourly profiles of the wind weather, PV power, active and reactive OMPs, and the total active and reactive loads

	Time(h)	Wind speed(m/s)	PV power generation (kW)	Active power Price(€/kW)	Reactive power Price (€/kVAr)	Total active load (kW)	Total reactive load (kVAr)
1	8am-9am	6.6	3.916	0.050	0.005	186.800	90.467
2	9am-10am	6.8	6.721	0.070	0.007	221.060	107.059
3	10am-11am	6	9.014	0.080	0.008	250.400	121.269
4	11am-12am	5.3	10.760	0.090	0.009	266.500	129.066
5	12am-1pm	5.5	11.589	0.120	0.012	265.080	128.378
6	1pm-2pm	5.8	11.431	0.225	0.023	286.500	138.752
7	2pm-3pm	6.3	10.408	0.100	0.010	297.400	144.031
8	3pm-4pm	7.5	8.414	0.085	0.009	283.380	137.241
9	4pm-5pm	8	5.962	0.150	0.015	270.100	130.809
10	5pm-6pm	9.6	3.352	0.450	0.045	258.000	124.949
11	6pm-7pm	10	1.411	0.150	0.015	292.600	141.706
12	7pm-8pm	9	0.3	0.180	0.018	300.200	145.387
13	8pm-9pm	8.5	0	0.160	0.016	313.000	151.586
14	9pm-10pm	7.8	0	0.310	0.031	277.800	134.539
15	10pm-11pm	7	0	0.050	0.005	233.000	112.842
16	11pm-12pm	6.8	0	0.040	0.004	186.000	90.080
17	12pm-1am	7.1	0	0.025	0.003	104.600	50.658
18	1am-2am	7.8	0	0.035	0.004	100.240	48.546
19	2am-3am	9	0	0.032	0.003	92.000	44.556
20	3am-4am	9.5	0	0.030	0.003	90.260	43.713
21	4am-5am	10.5	0	0.030	0.003	84.600	40.972
22	5am-6am	9.7	0	0.033	0.003	90.820	43.984
23	6am-7am	8.6	0.335	0.050	0.005	100.040	48.449
24	7am-8am	7	1.693	0.047	0.005	136.100	65.913

Table D-2 Hourly time series of residential, industrial, commercial and total loads

	Time(h)	Residential active load (kW)	Industrial active load (kW)	Commercial active load (kW)	Total active load (kW)
1	8am-9am	76.800	45.000	65.000	186.800
2	9am-10am	82.560	54.000	84.500	221.060
3	10am-11am	86.400	60.000	104.000	250.400
4	11am-12am	96.000	60.000	110.500	266.500
5	12am-1pm	94.080	54.000	117.000	265.080
6	1pm-2pm	105.600	60.000	120.900	286.500
7	2pm-3pm	115.200	60.000	122.200	297.400
8	3pm-4pm	113.280	57.000	113.100	283.380
9	4pm-5pm	105.600	54.000	110.500	270.100
10	5pm-6pm	96.000	45.000	117.000	258.000
11	6pm-7pm	124.800	37.800	130.000	292.600
12	7pm-8pm	163.200	33.000	104.000	300.200
13	8pm-9pm	192.000	30.000	91.000	313.000
14	9pm-10pm	172.800	27.000	78.000	277.800
15	10pm-11pm	144.000	24.000	65.000	233.000
16	11pm-12pm	124.800	22.200	39.000	186.000
17	12pm-1am	57.600	21.000	26.000	104.600
18	1am-2am	51.840	19.800	28.600	100.240
19	2am-3am	48.000	18.000	26.000	92.000
20	3am-4am	44.160	16.200	29.900	90.260
21	4am-5am	38.400	15.000	31.200	84.600
22	5am-6am	40.320	18.000	32.500	90.820
23	6am-7am	42.240	24.000	33.800	100.040
24	7am-8am	57.600	33.000	45.500	136.100

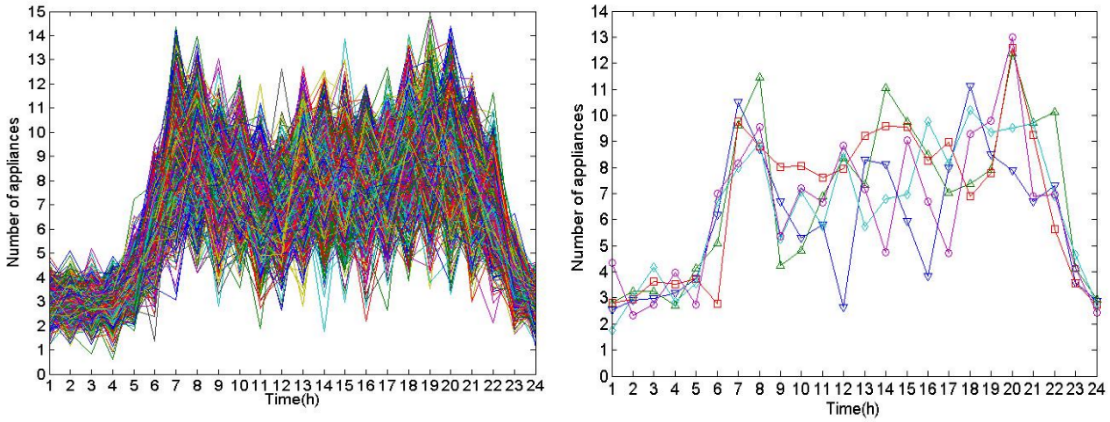

(a) (b)

Figure D-1 Scenarios generation and reduction of WM (a) generated 1000 scenarios of WM (b) reduced the scenarios to 5

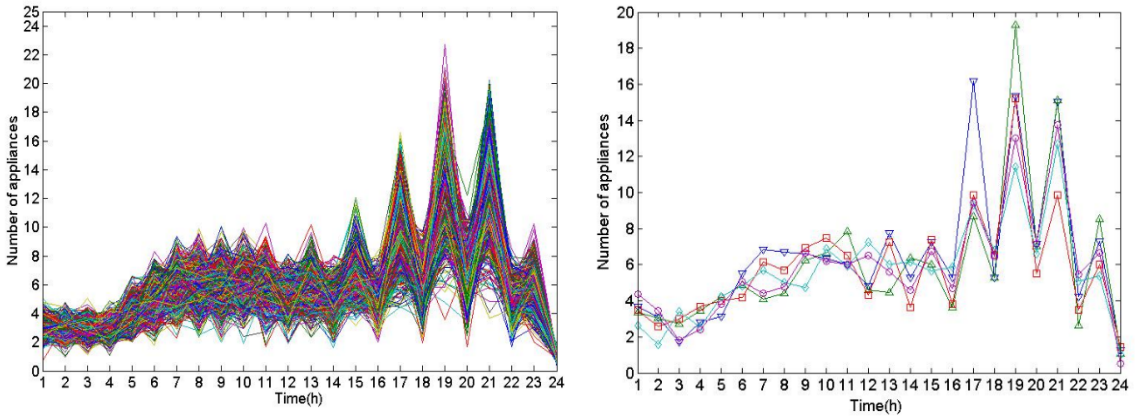

(a) (b)

FigureD-2 Scenarios generation and reduction of DW (a) generated 1000 scenarios of DW (b) reduced the scenarios to 5

Appendix E The EVs Data

Table E-1The charging and discharging prices of the EVs

	Time (h)	Charging price (€)	Discharging price (€)
1	8am-9am	0.08	0.16
2	9am-10am	0.08	0.16
3	10am-11am	0.08	0.16
4	11am-12am	0.08	0.16
5	12am-1pm	0.08	0.16
6	1pm-2pm	0.08	0.16
7	2pm-3pm	0.08	0.16
8	3pm-4pm	0.08	0.16
9	4pm-5pm	0.08	0.16
10	5pm-6pm	0.08	0.16
11	6pm-7pm	0.08	0.16
12	7pm-8pm	0.08	0.16
13	8pm-9pm	0.08	0.16
14	9pm-10pm	0.08	0.16
15	10pm-11pm	0.08	0.16
16	11pm-12pm	0.08	0.16
17	12pm-1am	0.08	0.16
18	1am-2am	0.08	0.16
19	2am-3am	0.08	0.16
20	3am-4am	0.08	0.16
21	4am-5am	0.08	0.16
22	5am-6am	0.08	0.16
23	6am-7am	0.08	0.16
24	7am-8am	0.08	0.16

Table E-2 Hourly cost with and without the EVs for the connected MG

Time(h)	Cost without EV	Cost with EV Sc1	Cost with EV Sc2	Cost with EV Sc3	Cost with EV Sc4
1	14.5	14.3	14.3	14.3	14.3
2	20.2	19.9	19.9	19.9	19.9
3	24.8	24.8	24.8	24.8	24.8
4	27.2	27.3	27.3	27.3	27.4
5	29.1	29.1	29.1	29.1	29.7
6	21.4	15.5	18.5	17.3	22.5
7	31.8	31.8	32.0	32.0	32.2
8	28.3	28.5	28.5	28.5	28.5
9	28.8	28.8	28.8	29.4	31.4
10	-28.5	-33.3	-28.5	-33.3	-19.0
11	32.8	32.9	32.8	33.3	38.8
12	32.5	29.8	32.5	30.0	38.6
13	36.3	36.2	36.3	36.2	41.5
14	13.5	0.2	13.5	0.2	17.4
15	19.1	17.5	19.1	16.1	18.2
16	12.0	14.2	12.0	8.9	10.9
17	8.5	-0.7	0.0	-0.7	7.3
18	7.3	0.9	7.3	0.9	7.0
19	7.2	-0.2	6.2	-0.2	7.1
20	7.2	-0.7	-0.7	-0.7	7.2
21	7.9	-1.0	2.1	-1.0	7.9
22	7.5	0.0	7.5	0.0	7.5
23	8.5	4.1	8.5	4.1	8.5
24	10.0	6.5	10.0	6.5	10.0
Total	407.8	326.3	381.8	323.1	439.5

Table E-3 Hourly profit with and without the EVs for the connected MG

Time(h)	Profit without EV	Profit with EV Sc1	Profit with EV Sc2	Profit with EV Sc3	Profit with EV Sc4
1	-4.7	-4.5	-4.5	-4.5	-4.5
2	-4.0	-3.7	-3.7	-3.7	-3.7
3	-3.8	-3.8	-3.8	-3.8	-3.8
4	-2.1	-2.2	-2.2	-2.2	-2.3
5	4.3	4.3	4.2	4.3	3.7
6	46.1	52.1	49.1	50.2	45.1
7	-0.6	-0.6	-0.8	-0.8	-1.1
8	-3.1	-3.3	-3.3	-3.3	-3.2
9	13.7	13.7	13.7	13.0	11.1
10	150.3	155.0	150.3	155.0	140.8
11	13.2	13.2	13.2	12.7	7.2
12	24.2	26.8	24.2	26.7	18.0
13	16.2	16.3	16.2	16.3	11.0
14	76.7	90.0	76.7	90.0	72.9
15	-6.9	-5.3	-6.9	-3.9	-6.0
16	-4.2	-6.4	-4.2	-1.1	-3.1

Time(h)	Profit without EV	Profit with EV Sc1	Profit with EV Sc2	Profit with EV Sc3	Profit with EV Sc4
17	-5.7	3.5	2.7	3.5	-4.6
18	-3.6	2.7	-3.6	2.7	-3.3
19	-4.1	3.3	-3.1	3.3	-4.0
20	-4.4	3.5	3.5	3.5	-4.4
21	-5.2	3.7	0.6	3.7	-5.2
22	-4.3	3.2	-4.3	3.2	-4.3
23	-3.3	1.1	-3.3	1.1	-3.3
24	-3.3	0.3	-3.3	0.3	-3.3
Total	281.5	363.0	307.5	366.2	249.8

Table E-4 Hourly cost with and without the EVs for the isolated MG

Time(h)	Cost without EV	Cost with EV Sc1,2,3	Cost with EV Sc4
1	19.8	20.0	20.0
2	23.7	25.0	25.0
3	27.3	28.3	28.6
4	29.3	29.8	30.1
5	29.0	29.8	30.1
6	31.8	31.8	32.6
7	34.5	34.5	35.6
8	31.5	31.5	32.9
9	29.8	29.8	31.8
10	28.3	28.3	31.3
11	34.2	34.2	38.4
12	35.4	35.4	38.7
13	37.3	37.3	39.7
14	31.6	31.6	33.7
15	25.5	25.5	26.9
16	19.7	19.7	20.7
17	10.8	11.5	10.9
18	10.0	10.9	10.4
19	9.3	10.4	9.3
20	9.2	10.3	9.2
21	8.9	10.0	8.9
22	9.3	10.4	9.3
23	10.0	11.0	10.0
24	13.7	14.0	13.7
Total	549.7	560.9	577.9

Table E-5 Hourly profit with and without the EVs for the isolated MG

Time(h)	profit without EV	profit with EV Sc1,2,3	profit with EV Sc4
1	9.5	9.3	9.3
2	11.1	9.7	9.7
3	12.1	11.1	10.7
4	12.6	12.1	11.8
5	12.7	11.9	11.6
6	13.3	13.3	12.5
7	12.3	12.3	11.2
8	13.0	13.0	11.7
9	12.7	12.6	10.7
10	12.3	12.3	9.3
11	11.8	11.8	7.6
12	11.9	11.9	8.5
13	11.9	11.9	9.5
14	12.1	12.1	10.0
15	11.2	11.2	9.7
16	9.6	9.6	8.6
17	5.6	5.0	5.6
18	5.8	4.8	5.4
19	5.2	4.1	5.2
20	5.0	3.9	5.0
21	4.4	3.3	4.4
22	5.0	3.9	5.0
23	5.7	4.7	5.7
24	7.7	7.4	7.7
Total	234.5	223.3	206.3

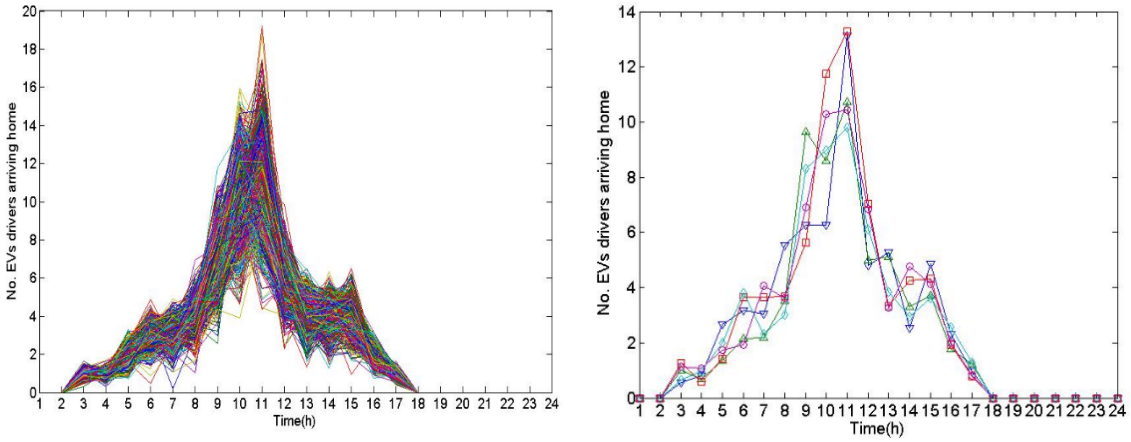

(a) (b)

Figure E-1 Scenarios generation and reduction of REVs (a) generated 1000 scenarios of REVs (b) reduced the scenarios to 5

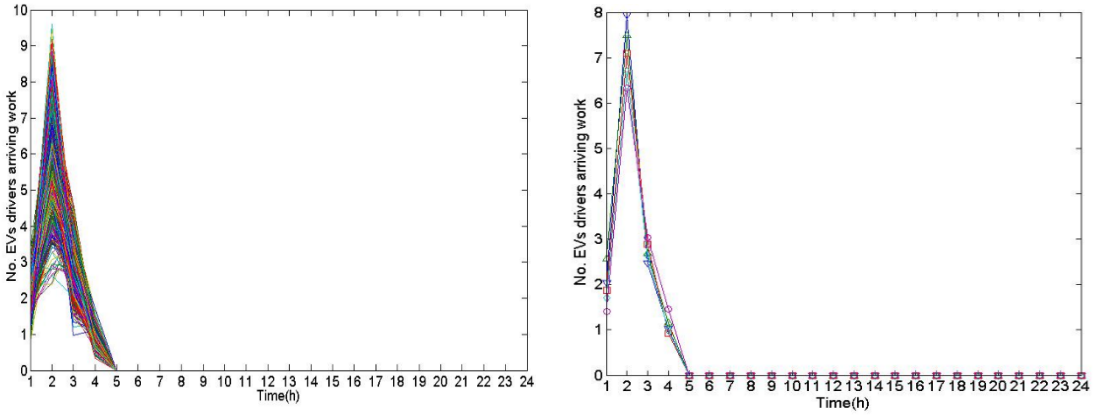

(a) (b)

Figure E-2 Scenarios generation and reduction of CEVs (a) generated 1000 scenarios of CEVs (b) reduced the scenarios to 5